

MECHANISMS OF RAPID REACTIONS

INVOLVING METAL-ION COMPLEXES.

by

A. GRAHAM LAPPIN

A thesis submitted to the University of Glasgow for
the degree of Doctor of Philosophy.

August, 1975.

ProQuest Number: 11018043

All rights reserved

INFORMATION TO ALL USERS

The quality of this reproduction is dependent upon the quality of the copy submitted.

In the unlikely event that the author did not send a complete manuscript and there are missing pages, these will be noted. Also, if material had to be removed, a note will indicate the deletion.



ProQuest 11018043

Published by ProQuest LLC (2018). Copyright of the Dissertation is held by the Author.

All rights reserved.

This work is protected against unauthorized copying under Title 17, United States Code
Microform Edition © ProQuest LLC.

ProQuest LLC.
789 East Eisenhower Parkway
P.O. Box 1346
Ann Arbor, MI 48106 – 1346

ACKNOWLEDGEMENTS

The work described in this thesis was carried out in the Department of Chemistry, University of Glasgow, under the direction of Professor D.W.A. Sharp.

I would like to express my sincere thanks to my supervisor, Dr. A. McAuley for his help and encouragement over the past three years.

I would like to acknowledge the help and advice of the supervisory and technical staff of the glassblowing, mechanical engineering and electronic workshops in the above Department. Technical services of Mr. A. Sharp, Miss S. Maxwell, Miss L. McKechnie and Miss H. McMahon are also gratefully acknowledged.

The helpful discussion of my friends and colleagues, in particular Mr. Z. Amjad, Mr. A. Olatunji, Dr. R. Shanker, Dr. U. Gomwalk and Dr. J.P. McCann is also much appreciated. The useful comments on this work by Dr. K.J. Ellis, Professor W.C.E. Higginson and Professor P. Hemmerich are also acknowledged.

I would also like to thank my sister for typing this work.

Lastly I would like to acknowledge the receipt of a Scholarship from the Carnegie Trust to the Universities of Scotland.

TABLE OF CONTENTS

Chapter 1	
Introduction to metal-ligand substitution and reduction-oxidation reactions	1
Ligand substitution reactions	2
Metal ion-ligand redox reactions	10
The chemistry of metal ion intermediates in the oxidation of non-metallic substrates by a one electron oxidant M^{III}	12
Chapter 2	
Experimental details; the stopped-flow apparatus	16
Rapid mixing methods and the study of intermediates in irreversible reactions	16
Description of apparatus	18
Measurement of absorbance	31
Chapter 3	
Experimental details; preparation of materials	40
Chapter 4	
Substitution reactions of iron III	47
Introduction	47
Substitution reactions of iron III with 2-mercaptocarboxylic acids.	71
Kinetics and mechanism of complex formation	82
Substitution reactions of iron III with phenolic ligands	105
General discussion	116
The solution composition	118
Chapter 5	
Oxidation of mercaptocarboxylic acids	127
Oxidation of non-metallic substrates by iron III	127
Reaction between iron III and mercaptocarboxylic acids	131
Kinetics and mechanism of the redox reaction between iron III and mercaptocarboxylic acids in aqueous acidic media	138

Chapter 5 cont'd.

Reaction between copper II and 2-mercapto- succinic acid	159
---	-----

Chapter 6

Acid dissociation constants of mercaptocarboxylic acids	167
Introduction	167
Experimental	172
Results and discussion	183

SUMMARY

Reactions of iron(III) and copper(II) with organic substrates have been studied using stopped-flow spectrophotometry. Two forms of stopped-flow apparatus have been constructed and are described.

The transient blue colour formed when aqueous acidic solutions of iron(III) and mercaptocarboxylic acids are mixed has been shown to be due to the rapid formation and subsequent slower disappearance of a sulphur-oxygen bonded monochelate. Visible absorption spectra, extinction coefficients and equilibrium constants have been obtained in the case of mercaptoacetic acid, 2-mercaptopropionic acid and 2-mercaptoisobutyric acid. The effect of ligand structure on these parameters is interpreted in terms of solvation of the free substrate.

Complex formation reactions have been shown to proceed by a mechanism involving reaction of the first hydrolysis product of hexaquo-iron(III), $\text{Fe}(\text{H}_2\text{O})_5\text{OH}^{2+}$, with the unprotonated form of the acid. Data are consistent with an I_d mechanism in which the effects of solvation of the mercaptocarboxylic acids are again important. Comparable reactions with phenolic ligands are also consistent with this hypothesis. Other mechanisms are discussed. Medium effects are attributed to the variation of activity coefficients on changing the reaction conditions.

The rates of disappearance of the blue complexes have been shown to follow a rate law which is second order in complex suggesting a dimerisation mechanism. Reaction products are iron(II) and the corresponding disulphide and it is argued that such a process reflects the high energy of formation of a mercaptide radical ion species. A bimolecular reaction affords the possibility of simultaneous two electron transfer leading to direct formation of the disulphide product. The implications of such a mechanism are outlined.

Methyl substituents have been shown to retard the overall rate of disulphide formation. A detailed analysis of the rate parameters reveals that this may be ascribed more to a reduction in the thermodynamic stability of the monocomplex than to an overall reduction in the rate

of dimerisation.

Consideration of the mechanism of the reaction with iron(III) has afforded a means of interpreting the kinetically more complex reaction of 2-mercaptosuccinic acid with copper(II). Similarities in the two systems are outlined. The reactions are directly comparable and, under suitable conditions, both monomeric and dimeric copper(II)-mercaptosuccinate complexes are observed.

The first acid dissociation constants of the mercaptocarboxylic acids used, have been determined to enable elucidation of the mechanism and evaluation of the kinetic parameters. Thermodynamic quantities associated with the ionisation constants have been shown to reflect solvation effects similar to those observed in the complex formation reactions.

It is apparent that the substantial effects occurring in the systems described in this thesis may be ascribed to the solvating nature of the reaction medium. Such an interpretation may have wider applications in other reactions involving ionic and neutral reactants in solution.

CHAPTER 1

Introduction to Metal-ligand Substitution and
Reduction-Oxidation Reactions.

The investigation of a reaction mechanism is an attempt to establish and identify the elementary steps in a particular chemical process.¹ Kinetic studies yield information only on the slowest of these steps, those prior to this rate determining step appear as pre-equilibria while those at a later stage are not included in the rate law. Two types of information may be obtained;²

- (1) the stoichiometric composition of the reaction transition state, and
- (2) the rate at which the overall process occurs.

Application of transition state theory³ allows this latter quantity to be evaluated in terms of thermodynamic parameters relating to the transition state. The transition state is the point of highest energy reached as reactants proceed to products. Kinetically distinct steps relate to different maxima separated by minima which correspond to intermediate species. The identification and characterisation of intermediates in reactions is of major interest in the elucidation of the mechanism. To be distinguishable from a transition state, an intermediate must be amenable to detection either by direct observation or by its effect on the reaction kinetics and products.⁴ Thus, although the presence of a common intermediate may be inferred by comparison of the activation parameters of related reactions, in isolation, modification of the reaction stoichiometry in predictable ways is required.^{2,4}

In this thesis, two types of transition metal-ligand interactions are considered, substitution and oxidation-reduction. While both of these may occur as distinct processes, it has been found that in many instances, ligand substitution is a prerequisite to redox with a metal ion complex as intermediate.^{5,6}

It is reasonable to expect that the kinetic properties of the species participating in these reactions will be explicable in terms of their basic chemistry. Although the situation is complex,⁷ certain general trends have emerged. In transition metal ions of the same charge and geometry, the electronic structure is an important factor in determining the rate of reaction. No matter the mode of activation of substitution

processes, going from the ground state to the transition state involves a loss of ligand field stabilisation energy.⁷ Ions with a large ligand field stabilisation such as octahedral d^3 , d^8 and low spin d^6 are relatively inert with respect to substitution while those with little or no stabilisation such as d^9 and high spin d^5 are labile.⁷

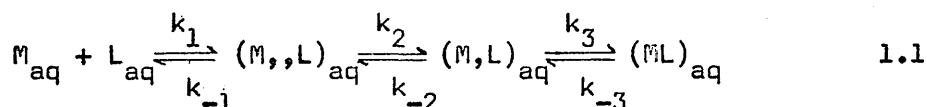
This is also of importance in redox reactions. Labile transition metal ions may undergo a redox process in which the first step is the formation of a metal ion complex while inert transition metal ions favour a pathway which involves no substitution and in which electron transfer takes place by a long range interaction.⁸

In aqueous solution, all species interact with water molecules. The extent of this interaction is determined by both the charge and size of the species. Small highly charged metal ions are surrounded by at least two distinct zones of solvent molecules,⁹ strongly bound in the inner coordination sphere and less tightly in the outer coordination sphere. Large uncharged species on the other hand are hydrophobic, tending to be desolvated and promoting a strengthening of the bulk water structure.¹⁰ In dealing with any reaction mechanism therefore, a contribution from solvation effects might be expected.

Ligand Substitution Reactions.^{2,4,7,11-15}

Only metal ions having an inner coordination sphere which is approximately octahedral are considered in this thesis and consequently discussion is restricted to this geometry although some consideration is given to square planar complexes as the limiting case of tetragonally distorted octahedra.

Unless reaction results from a long range interaction, direct contact between the reactant molecules is required. This is usually achieved in a multi-step process.^{2,16}



where M and L are the metal ion and ligand respectively and the subscript aq refers to solvation. Charges and water molecules are omitted for the sake of clarity.

The first step is the diffusion of the reactants together to form an encounter complex⁴ $(M, L)_{aq}$ in which separation to free solvated species is prevented by the solvent structure. The limiting rate of diffusion¹⁷ k_1 is about $10^{10} M^{-1} s^{-1}$. This is followed by the formation of an outer sphere complex $(M, L)_{aq}$ in which the ligand has penetrated the outer coordination sphere of the metal ion allowing more intimate interaction. Rate constants for this process have been found to be in the region $k_2 \sim 10^8 s^{-1}$, $k_{-2} \sim 10^7 s^{-1}$ for the reaction of sulphate with divalent metal ions.¹⁸ Finally, the inner sphere complex is formed in a step which is generally much slower.¹⁶

Study of the first two processes is beyond the capabilities of the techniques employed in this work, and thus, these are treated in terms of pre-equilibria to the third step where appropriate. The most useful and flexible classification of this latter process is that proposed by Langford and Gray,⁴ later modified by Swaddle.¹³ They describe three categories of substitution reactions based on the stoichiometry of the rate process.

Associative, A, in which the incoming ligand enters the inner coordination sphere before loss of the outgoing species to form an intermediate complex of higher coordination number.

Dissociative, D, in which the outgoing ligand is lost to form an intermediate of reduced coordination number. Relaxation of the outer coordination sphere must occur before bond formation to the incoming ligand is initiated.

Interchange, I, in which the incoming ligand enters the inner coordination sphere before the metal ion can discriminate as to the loss of the outgoing ligand. A further subdivision based on the energetics of activation of this process is also necessary. If the entering group participates in the activation step then the mechanism is I_a while if this process is independent of the incoming ligand, and thus determined by breaking the bond with

the outgoing ligand, the mechanism is I_d .

If it is assumed that the role of the ligand is of secondary importance in determining the reaction mechanism and further that a given metal ion will exhibit the same activation mode (a or d) in differing circumstances, then this activation mode may be determined readily by studying a number of reactions with different ligands.^{2,4} Proof of a D or A mechanism however demands direct evidence for an intermediate complex.^{2,4}

The simplest substitution reaction is the replacement of one monodentate ligand by another



The rates and activation parameters of reactions which are associatively activated (A or I_a) show a marked dependence on the nature of the incoming ligand.^{2,7,19} Steric crowding causes a decrease in the rate²⁰ while increasing the nucleophilicity or affinity for a particular cationic centre, of the incoming ligand has an accelerating effect.^{2,7} Absolute values for the activation parameters may be misleading. While it is pleasing to argue⁷ that in associative reactions, the enthalpy of activation will be small since bond making compensates bond breaking and the entropy of activation will be large and negative reflecting the aggregation of particles, in practice the release of solvent molecules and the possibility of pre-equilibria prevent a meaningful interpretation.^{2,4,7,13} Comparison of the parameters for related reactions may however reveal indicative trends.²

Distinction of an A process from an I_a process may be made on a kinetic basis if the intermediate of higher coordination number is stable enough to accumulate in significant quantity during the reactions.^{2,21}



Other criteria which have been employed utilise the ability of the intermediate to discriminate between different chemical entities and the rationalisation of stereochemical data in terms of pseudorotation.^{2,22}

An A mechanism has not yet been identified in a reaction of any octahedral complex since steric crowding prevents the formation of the necessary intermediate.⁴ On these grounds, dissociative (D or I_d) reactions should be favoured.⁴ Dissociative reactions show rate constants which are essentially independent of the incoming ligand¹⁶ and which are characteristic of the metal ion.⁴ They are subject to steric acceleration²³ and would be expected to have large enthalpies and positive entropies of activation,⁷ although again solvation effects mask the significant values.⁴ A linear free energy relationship based on the reactions

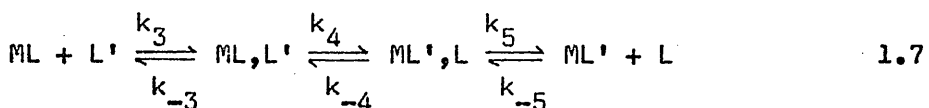
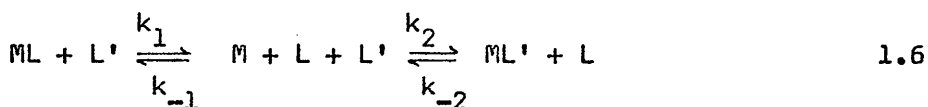


and



has been suggested.^{4,24} A plot of ΔG^* against ΔG should be linear with a slope equal to unity since both equations 1.4 and 1.5 reflect the strength of the M-L' bond, the former with respect to that of M-L which is held constant for the reactions of a particular complex ML. If the reaction exhibits some associative character then the relationship should no longer be exactly linear¹³ and the slope less than unity, most probably in the region of 0.5 for a mainly associative process.²⁵

The kinetic behaviour of dissociative reactions may be treated in terms of the following equations.²⁶



In which both 1.6 the D process and 1.7 the I_d process show a similar rate law dependence on the ligand L'; first order at low concentration tending to zero order at high concentration. Kinetic distinction between an I_d and a D process cannot thus be made from consideration of the rate law itself but from the value of the limiting rate.² For the D mechanism the limiting rate is k₁,

the rate of exchange of L in ML^2 corresponding to selective reaction of M with L'. For the I_D mechanism however, the limiting rate corresponds to saturation of the complex ML in the form of the outer sphere complex (ML, L') yielding a rate constant $k_3 k_4 / k_{-3}$ which may differ significantly from the rate of L exchange in the complex ML .^{2,13} The rate of exchange of ligand L from an outer sphere complex is usually considered to be similar to that in the free metal ion complex²⁷ although there is evidence for acceleration in some instances.^{28,29} As was noted previously, the step



involving outer sphere complex formation is outwith the scope of this thesis and may be treated as a pre-equilibrium. A satisfactory estimate of the ratio $k_3/k_{-3} = K_{os}$ ³⁰ may be made when L' is ionic using the Fuoss relationship. The equation exists in a modified form³¹ for dipolar L' and values of K_{os} calculated under specific conditions are given in table 1.1. These values are in satisfactory agreement with the few outer sphere association constants determined experimentally.^{33,34}

A further reduction in the observed limiting rate for I_D reactions is noted in the case where L is solvent. The statistical predominance of solvent in the outer coordination sphere of a metal ion coupled by a lack of selectivity should markedly reduce the probability of reaction taking place.^{2,15} On the other hand if L and L' are both anionic then since the probability of ion triplet formation is low owing to repulsion between L and L' in the outer coordination sphere, a solvation reaction might be favoured.^{2,13,15}

Evidence for a D process may also be provided by examination of the stereochemistry³⁵ and product distribution.^{4,7,13} This is possible only where the products are inert. Detection of intermediate species in reactions of labile complexes is difficult due to the rapid reorganisation of the inner coordination spheres. Further, a restriction is placed on the range of ligand concentrations available for study due to the occurrence of more highly substituted complexes thereby preventing kinetic

TABLE 1.1Aqueous outer-sphere formation constants.^a

$z_M z_L$	$K_{os} M^{-1}$
6	87
4	13
3	8
2	2
1	1
0 ^b	0.3

a Calculated from Fuoss equation $T = 298^{\circ}K$, $I = 0.1$, minimum approach distance 5\AA

b $z_M = +1, +2$ or $+3$, $z_L = 0$

characterisation. It has also been suggested¹³ that aquated metal cations of charge greater than or equal to two should fail to produce detectable intermediates in substitution reactions due to their tendency to form outer sphere associations.

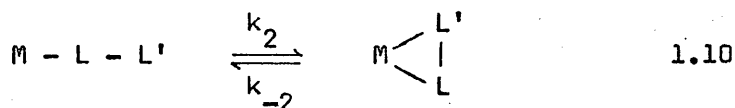
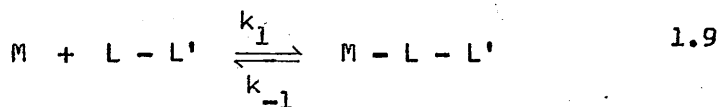
The substitution reactions of first row transition hexaquo cations in oxidation states II and III provide a wide range of rates and mechanisms. All the octahedral complexes of divalent ions react at rates which are generally insensitive to the nature of the entering group once outer sphere association phenomena have been taken into account.^{16,32,36} Such reactions are typically dissociative in nature, probably proceeding via an I_D mechanism since k_4 is significantly smaller than the rate of solvent exchange.⁴² For copper (II) which forms complexes of tetragonally distorted octahedral geometry,³⁷ associative substitutions as found with inert square planer complexes⁴ might be expected.³⁸ The available information however gives no indication of this.^{39,40} Rapid rates of copper (II) substitution reactions ($\sim 10^7 \text{ s}^{-1}$) have been ascribed to Jahn-Teller distortion in which the two axial ligands, being less tightly bound, can exchange much more rapidly than the equatorial ligands. The fact that all six ligands undergo solvent exchange at the same rate is explained by a pseudorotational process involving change of the coordinate axes.⁴¹ There is evidence however that if this pseudorotation is prevented by complexation, the rate of solvent exchange is considerably reduced.^{42,43}

Assignment of mechanisms to trivalent ions is less clear cut due to the problems of hydrolysis and a lack of accurate data.¹⁶ At one point, the inert low spin cobalt (III) complexes were considered² paradigmatic of all trivalent octahedral metal ions, reacting by an I_D mechanism. Although Eigen¹⁶ proposed an associative process for reactions of iron (III), an alternative interpretation of the data led to the opposite conclusion⁴⁴ as in the case of chromium (III).⁷ The current view is that a significant amount of associative character is prevalent in all reactions of trivalent metal ions except cobalt (III).^{2,13,15,32} Experimental studies reveal a rate variation of several orders of magnitude³⁹ with differing ligand in reactions of $\text{Cr}(\text{H}_2\text{O})_6^{3+}$ ^{13,25} $\text{Fe}(\text{H}_2\text{O})_6^{3+}$ ⁴⁴, $\text{Ti}(\text{H}_2\text{O})_6^{3+}$ ^{39,46} and $\text{Mo}(\text{H}_2\text{O})_6^{3+}$.⁴⁵

more consistent with an I_a mechanism than an I_d . The evidence for an I_a process in reactions of hexaquo chromium (III) is particularly strong in the light of data obtained from the determination of volumes of activation which reveal cobalt(III) reactions as being anomalous among trivalent metal ions.⁴⁷

Although trivalent metal ions appear to react by an I_a mechanism, the reactions of their hydrolysis products MOH^{2+} show a smaller variation of rate constant with entering ligand^{48,49} possibly implying stabilisation of the transition state in an I_d process.¹³ Complications in the interpretation of hydrogen ion dependent data however lead to uncertainties in the reported rate constants. This matter is discussed in chapter 4.

Although in most instances, effects attributable to properties of the ligand may be ignored, in a few important cases they become the dominant feature of the reaction. One such case of relevance to the work contained in this thesis arises when a metal ion reacts with a multi-dentate ligand. Consider the case of a bidentate ligand $L-L'$.



The rate of chelate formation is $k_1 k_2 / (k_{-1} + k_2)$ and is dominated by the ratio k_2 / k_{-1} . If $k_2 \gg k_{-1}$ then the rate of formation is k_1 and the process is normal, being controlled by the rate at which the unidentate species is formed. Rate determining ring closure⁵⁰ however results when $k_2 \ll k_{-1}$ corresponding to an intermediate containing a weakly bound unidentate ligand.¹⁵ This situation may arise when chelate formation involves steric hindrance or strain,^{51,52} or when ring closure is inhibited by a blocking group, for example, if the ligand to be replaced is strongly bound⁵³ or if the closing arm is protonated.³⁸ Rate determining ring closure may be detected kinetically and direct observation of the intermediate has been possible in favourable circumstances.⁵⁴

Metal Ion-Ligand Redox Reactions.^{5,6,55}

Redox reactions involve a change in the formal oxidation levels of at least two of the participants. This may be accomplished either by an exchange of electrons or by the transfer of an atom or radical group from one reactant to another.⁶ In the absence of evidence to the contrary, the occurrence of the former process will be assumed.

While transition metal ions generally have available to them several oxidation states differing only by one equivalent of charge, most non-metallic elements require a two electron change on altering from one thermodynamically stable state to another. If reaction takes place with a metal ion which has no readily accessible oxidation levels differing by two equivalents, the process is non-complimentary and may lead to complex rate law dependences with the formation of unstable intermediate species.⁵⁶

In discussing metal ion-ligand redox reactions, two categories may be envisaged.⁵⁷

(1) Outer-sphere in which the inner coordination sphere of the metal ion remains intact although not necessarily undisturbed and,

(2) Inner-sphere in which the inner coordination sphere of the metal ion is penetrated by its reaction partner.

There are no rules of general application to distinguish between these two possibilities. Most assignments of outer sphere mechanisms have been made on the basis of reaction rate and activation parameters. If the redox rate is greater than the rate at which the metal ion undergoes substitution, then the reaction is very probably outer-sphere. This type is prevalent when the metal ion is inert to substitution.⁸ The rates may also conform to the Marcus free energy relationship^{58,59} although again, this is not conclusive since similar relationships have been found with inner sphere mechanisms.⁶⁰ Outer-sphere reactions have been reported in many cases including⁶¹ the oxidation of hydrazine by IrCl_6^{2-} and $\text{Fe}(\text{CN})_6^{3-}$.

In both these instances, unstable radical species are produced leading to further reactions which are discussed later in this section.

Inner-sphere reactions might be expected when the rate of electron transfer is less than the rate of substitution and, as a result, examples are common among substitution labile reactants. Unambiguous assignment of an inner-sphere mechanism from analysis of the immediate reaction products is rarely possible due to the need to invoke multi-step electron transfer and the possible substitution lability of the metal ion in an intermediate oxidation state. Most information on inner-sphere mechanisms is derived from the detection of metal-ion complexes as intermediates⁵ in the redox process. The complex may however be detectable yet play no part in the mechanism.^{6,62} There is no reason why the transition state for redox should resemble the products of the substitution reaction.⁵⁵ Establishing the role of the "intermediate" may thus be a major problem.

An intermediate complex may contribute to the kinetics in one of several ways.^{63,64}



(a) If the rate of complex formation is the rate determining step then the rate law and activation parameters for redox and substitution processes will be similar. This behaviour has been observed in a number of cases.⁶⁵

(b) If, on the other hand, the redox step is the rate determining process, then the rate constant and activation parameters will be composite, reflecting a pre-equilibrium contribution from the substitution reaction.

(c) When however the dominant decomposition pathway for the intermediate involves dissociation to the free ligand and metal ion, both complex formation and the redox step may be observed. Although kinetic analysis of the first two situations may lead to ambiguity in determining the role of the intermediate,⁶ in the third case, proof of a sequential process may be obtained by the observation of induction periods and isosbestic points. Kinetic treatment of these reactions is complicated by the fact

that differential equations of high order and degree are often involved.^{66,67} Numerical analysis by computer may provide a means of evaluating the rate constants.⁶⁸⁻⁷⁰

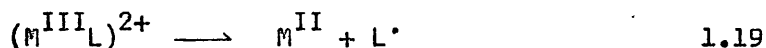
The Chemistry of Metal Ion Intermediates in the Oxidation of Non-metallic Substrates by a One Electron Oxidant M^{III} .

In ascertaining the chemical role of the intermediate, it is convenient to consider two types of ligand redox equilibria involving two electron changes



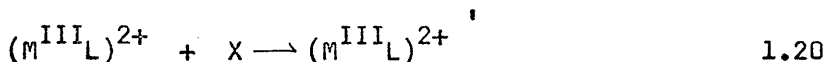
The charges are not significant and merely serve to denote the oxidation level of the ligand.

On complex formation, the redox potential of a metal ion may be altered substantially.^{71,72} Spontaneous redox within the complex will result if the activation energy of the process



is small enough. It might be expected⁷³ that this value will be determined by the free energy difference between the complex and the immediate products of step 1.19, and hence on the stability of the radical $L \cdot$.

Further decomposition pathways are available to complexes which are not inherently unstable. They involve modification by interaction with some other species X in solution.⁷⁴⁻⁷⁶



In this way the complex acts as a template for the formation of species which are more stable than the products of reaction 1.19. Although solvent molecules and the supporting electrolyte may be incorporated in the step 1.20, the nature of X in further discussion will be limited to M^{III} , L^- or the complex $(ML)^{2+}$

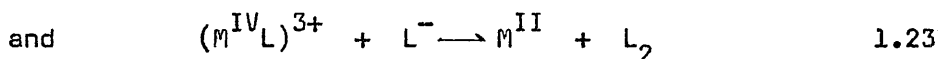
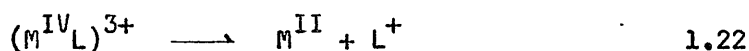
itself.

Higginson⁶¹ suggests that the complex ML provides a means of preserving an otherwise unstable free radical. In other words, the complex is in a state of indeterminate valency.



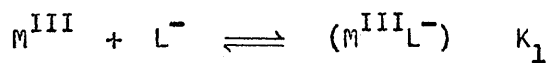
Subsequent reaction with a metal ion oxidant would yield the monomeric product L^+ while reaction with L^{-} would produce the generally more stable^{77,78} radical ion $L_2^{\cdot-}$ leading, after further oxidation, to dimeric L_2 . Indeed the fate of any radical species is generally determined either by dimerisation or further oxidation by M^{III} . The interaction of two molecules of complex may lead to the direct formation of the dimeric product without recourse to the energetically unfavourable radical mechanism.

Oxidants which are capable of a two electron exchange may also function in a similar fashion although certain possibilities will be favoured, namely



The probability of simultaneous two⁷⁹ or even three⁸⁰ electron transfer is only slightly less favourable than one electron transfer,⁵⁶ requiring a correspondingly larger structural change between the reactants and products.⁸¹

While this discussion has been limited to metal ion oxidation reactions, similar arguments could be used for the reduction processes. Possible reaction pathways in the oxidation reactions and the corresponding product types are shown in scheme 1.1. Clearly the preferred pathway in any reaction will be determined by the thermodynamic stability of the radical species and the nature of the product as well as the redox properties of the metal ion, ligand and the association constant K_1 for the intermediate complex formation.

SCHEME 1.1

<u>Reaction</u>	<u>Product</u>
A. Spontaneous $(M^{III}L^-) \longrightarrow M^{II} + L^\bullet$	L^+, L_2
B. Ligand Catalysed $(M^{III}L^-) + L^- \longrightarrow M^{II} + L_2^-$	L_2
C. Metal-ion Catalysed $(M^{III}L^-) + M^{III} \longrightarrow 2M^{II} + L^+$	L^+
D. Complex Catalysed $2(M^{III}L^-) \longrightarrow 2M^{II} + L_2$	L_2
E. Subsequent rapid steps	
$M^{III} + L^\bullet \longrightarrow M^{II} + L^+$	
$M^{III} + L_2^- \longrightarrow M^{II} + L_2$	
$2L^\bullet \longrightarrow L_2$	
$(2L_2^- \longrightarrow L_4^{2-})$	

There are numerous examples of these reaction types tabulated in the literature; ^{63,82-85} spontaneous, ^{65,86,87} ligand, ⁸⁸ metal ⁸⁹ ion and complex ⁹⁰ catalysed processes occurring with various oxidants. Further examples and discussion relating to iron (III) chemistry will be given in chapter 5.

The reactions examined in this thesis fall conveniently into two categories. In chapter 4, substitution reactions of the hexaquo-iron (III) ion with mercaptocarboxylic acids and phenolic derivatives are discussed. In chapter 5, data on oxidations of mercaptocarboxylic acids by iron (III) and copper (II) are presented. Chapter 6 is devoted to a study of the acid dissociation constants of the mercaptocarboxylic acids and the relevant introduction may be found on page 167. The remaining chapters contain experimental details.

CHAPTER 2

Experimental Details; The Stopped-flow Apparatus

In the study of chemical processes in solution taking place in the millisecond timescale, two fundamental difficulties arise;

- (1) initiating the reaction
- and
- (2) monitoring its time course.

To obtain significant information, both of these procedures must be completed within a time which is virtually instantaneous compared with the reaction half life. The main methods in use at present to overcome both problems have been reviewed extensively^{1,91-96} and a comprehensive discourse on each individual technique is beyond the scope of this work. Since many of the reactions in this thesis are irreversible, relaxation techniques⁹⁷ are inappropriate and stopped-flow spectrophotometry has been used exclusively. Discussion will therefore be restricted solely to this technique.

Rapid Mixing Methods and the Study of Intermediates in Irreversible Reactions.

The problem of extending conventional mixing methods for initiating chemical reactions into the millisecond range has been tackled with considerable ingenuity.^{91,95} A classification of mixing can be made on the basis of whether the reactants are in motion (flow methods) or stationary (baffle methods). The criterion for application of these methods depends upon the minimum time required to obtain a homogeneous solution for observation. This gives an indication of the shortest half lives available for a particular system.

Flow methods have a common feature in that the reactants are driven at high speed through separate jets into a special chamber where mixing occurs. In the continuous flow mode⁹⁸ the resulting homogeneous solution is allowed to flow along an observation tube of uniform cross-sectional area. If the flow velocity is maintained constant, a steady state between the fluid flow and reaction progress is obtained. The composition of the solution at any point may thus be determined by conventional monitoring methods. Moreover the distance between the mixing chamber and point of observation is a measure of the time into the reaction.

This "time clamp" aspect is the major advantage of the continuous flow method and, while mixing times of the order of tenths of milliseconds are now readily accessible,^{98,99} large fluid requirements and the need for uniform flow characteristics have led to its demise.

The accelerated flow mode^{100,101} accommodates many of the advantages of continuous flow and reduces greatly the volumes of reactants required. In this method, the distance from mixing to observation is maintained constant and the flow rate varied continuously. Complex monitoring devices are however required to enable instantaneous evaluation of both the flow rate and the composition of the solution. An adaptation of accelerated flow is stopped flow¹⁰⁰⁻¹⁰⁴ in which, after mixing, the flow is abruptly arrested and the progress of the reaction monitored in a particular element of solution usually close to the point of mixing. Although the combined mixing-stopping of the stopped flow technique leads to a slightly longer time requirement than in the previously mentioned methods, low fluid requirements and the ease of design and operation render it superior to them in the study of processes taking place in some tens of milliseconds as in this work. Also, the timescale is conveniently extended into the classical range, the upper limit being determined by the rate of diffusion of the unmixed reactants into the observation tube.¹ In this respect, the baffle method¹⁰⁵⁻¹⁰⁷ where the reactant solutions are initially separated by a barrier which is suddenly removed and the ensuing agitation aids the mixing process, has advantages. The mixing time for this technique is however usually of the order of tens of milliseconds. A further flow method with a time requirement of around one second is capacity flow.^{108,109} The operation in this case is on roughly the same principle as continuous flow but with a steady state invariant in both time and space between the reaction progress and the inflow-outflow of material to a combined reaction-observation chamber, mixing being achieved in the chamber itself by mechanical stirring.

The evolution of these techniques has largely been determined by the criterion of monitoring rapid reactions. Thus the

development of the continuous flow with its compatibility with standard reaction analysis techniques preceded that of the other methods which depend on rapid response detection. To date, many means of monitoring these reactions have been employed; spectrophotometry, fluorimetry, magnetic resonance, thermal and electrochemical methods having the widest application.

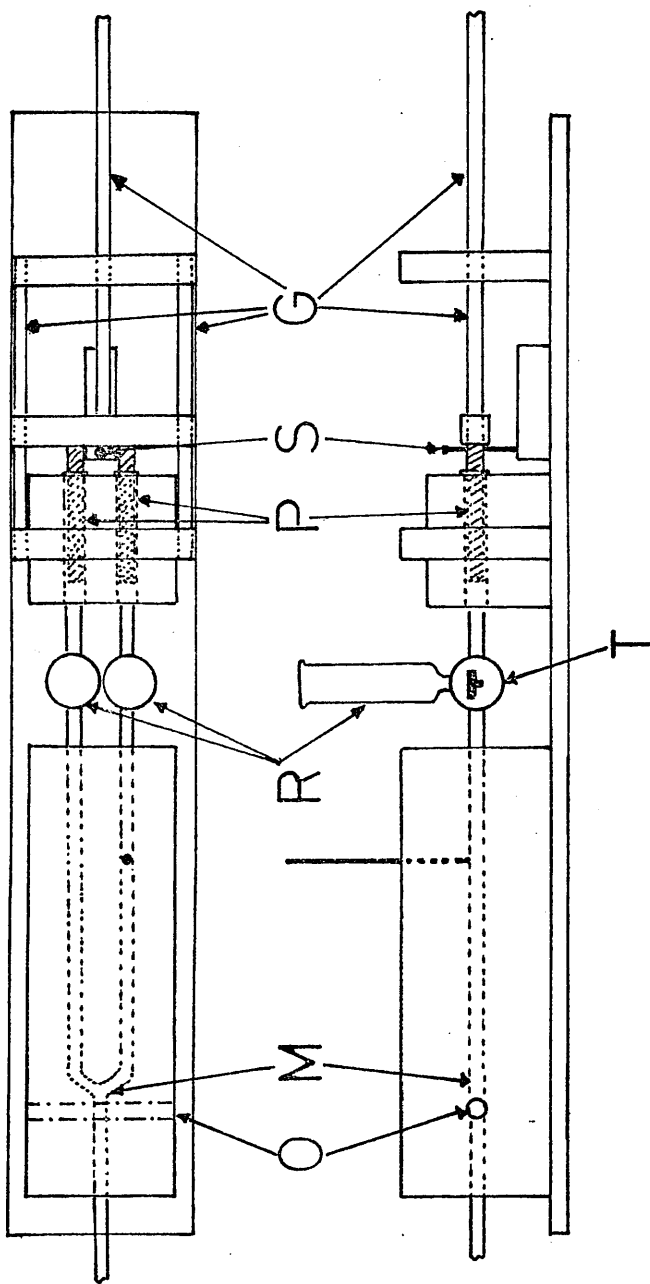
By using a specific and precise detection system in conjunction with rapid mixing techniques, intermediates with lifetimes greater than the time resolution of the instrument may be identified in irreversible reactions. Spectrophotometric detection is well suited to problems of this type.

Description of the Apparatus.

Two stopped flow systems, A and B, were used in the course of this work. Both were of similar design, the former being a modification of the type described by McAuley and others^{110,111} and the latter based on the design of Sturtevant.¹¹²

Stopped Flow Apparatus A

The apparatus is illustrated in figure 2.1. It was mounted on an aluminium base 30 inches by 5 inches screwed to a laboratory bench. The flow system was positioned parallel to the base and was constructed entirely in materials which showed no chemical reaction with the reagents used. Two 2 millilitre pushing syringes P (Jencons, Zippette) containing the reactants were arranged side by side and were attached by glass blowing to glass 3-way taps, T, through which they could be filled from 10 millilitre reservoir syringes, R (Jencons, Zippette) attached by polypropylene tubing (Portex Surgical Tubing, Hythe, Kent) at right angles to the flow. The nozzles of these syringes were specially widened to avoid constriction of the fluid motion during the filling operation. Plungers for the pushing syringes were constructed in teflon with neoprene rubber o-rings (Edwards, Vacuum Products Ltd., Crawley) to ensure no leakage, and 1:1 delivery was made possible by attaching the plungers to a rigid pushing block supported freely on greased steel guide rods, G.



STOPPED FLOW APPARATUS A

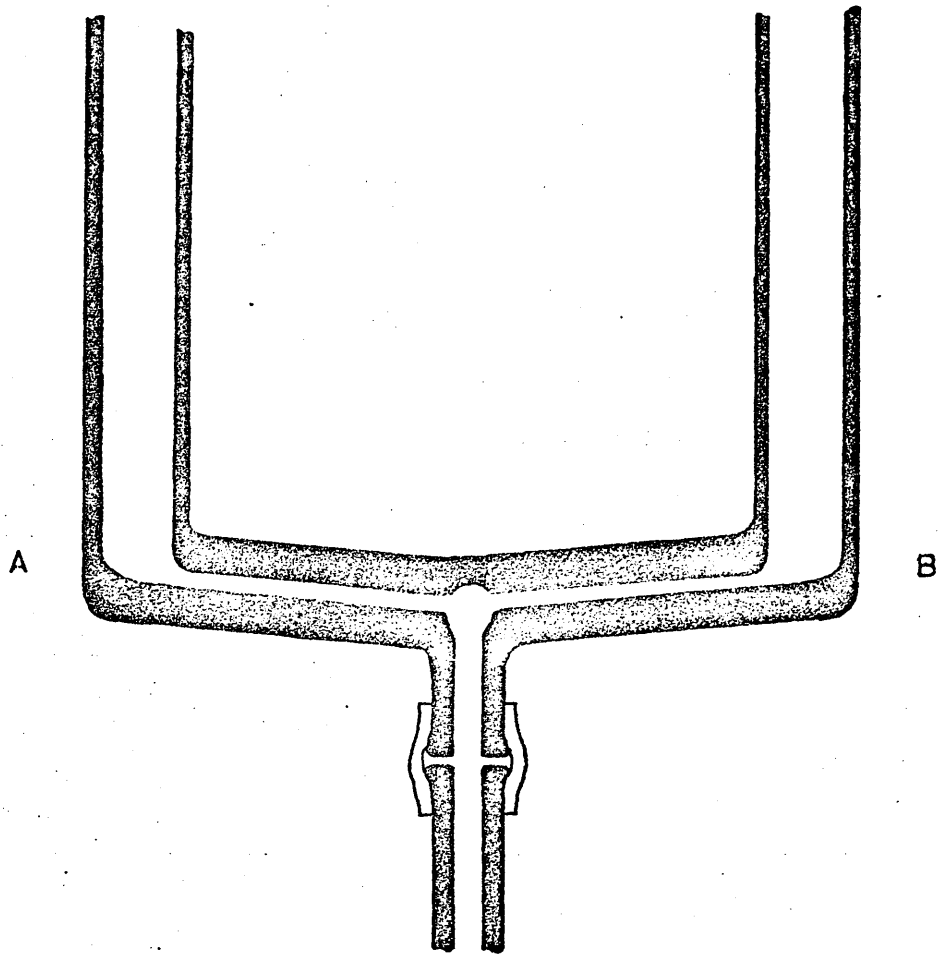
FIGURE 2.1

Lengths of glass tubing (5mm internal diameter, 7mm external) were connected to the remaining outlet of the three way taps either by glass blowing or, in a later design by a short length of polypropylene tubing wired at each end and enclosed in a matrix of copper wire and cellulose filler (Polycell Products Ltd., Welwyn Garden City, Herts.) to prevent expansion during flow. The join was constructed in such a way that the copper wire could not come into contact with the liquid in the tubes. These tubes terminated at the mixing chamber M.

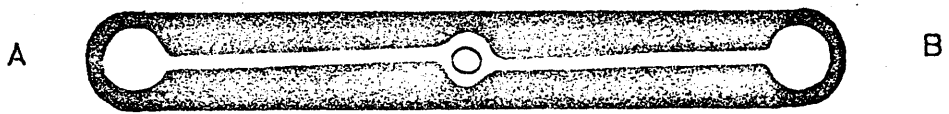
Over the period of study, two designs of mixing chamber were employed. The first was an eight-jet tangential mixer of the type described by Dulz and Sutin¹¹³ constructed in teflon. In this case, each reagent tube was divided into two at a Y-junction, attached to the mixer by short lengths of wired polypropylene tubing and encased in cellulose filler as described above. The arrangement of the tubing caused radial alternation of the reagent jets in the mixer. Despite the fact that the gap between the Y-pieces and the mixer inlets was very small, recurring problems of leakage at these joints led to the adoption of a simpler design.

This was a two jet all glass tangential mixer (figure 2.2) which was constructed by glass blowing and could be attached by the same method directly to the glass reagent tubes. The specifications were as follows; inlet capillary 1mm. diameter, outlet 2mm. diameter, with jets off set centre to centre 1mm. and inclined at an angle of 92° to the direction of the flow.⁹² A mixer of this sort is considered adequate for the study of reactions with half lives greater than ten milliseconds⁹³ provided the flow rate and stopping are adequate.

In both cases, the mixing chambers were attached directly to a rectangular quartz optical cell of 5mm. path length (Hellma Instruments, Southend on Sea, Type 134 QS) either by a screwed joint sealed by o-rings in the case of the Dulz-Sutin mixer or by wired polypropylene tubing as described above, with the two jet mixer. The effluent tube was carried to a point several inches above the level of flow to provide a gravity back pressure.



PLAN



SECTION

ALL GLASS TWO JET TANGENTIAL MIXER

FIGURE 2.2

Anchoring of the whole flow system was achieved by clamping the pushing syringes in a perspex block and applying cellulose filler around the mixing chamber, optical cell and three-way taps.

The mixing chamber, observation chamber and the glass feed lengths were enclosed in a light tight thermostatted aluminium block and good thermal contact between the glass and block was assured by packing any air spaces with brass filings. Temperature control was achieved by circulating water from a constant temperature bath of twenty-four litres capacity through this block using a Circotherm Mk. II Thermomix Series 769 (Shandon Southern, Camberley) fitted with a 27559-E contact thermometer (B. Braun, Melsungen) to regulate the temperature. A Tekam dip-cooler refrigeration unit (Techne Ltd., Cambridge) was used to obtain temperatures lower than room temperature and to increase the sensitivity of control. The aluminium block and tubing connecting the flow apparatus with the constant temperature bath were lagged with expanded plastic. The temperature of the thermostating solution was measured using a Zecol 0° - 50° C mercury thermometer (Baird and Tatlock Ltd., (London)) placed through the aluminium block in contact with the glass tubing.

At the point of observation approximately 1cm. from the mixing chamber, a beam of light from an Unicam SP 500 monochromator was passed at right angles through an aperture roughly 2mm. square in the optical face of the observation tube. The monochromator was mounted on a surface independent of any vibrations caused by the flow device to which it was connected by a flexible light tight tube. In the visible region of the spectrum, a 36 watt, 6 amp tungsten source powered by a Unicam 1150 tungsten lamp power supply was employed. At shorter wavelengths however, use was made of a deuterium lamp connected to a Unicam deuterium lamp supply (0.3 amps, 220 watts.)

Transmitted light was detected by an E.M.I. type 6256S photomultiplier tube enclosed in a copper casing which was bolted to the aluminium block and made light tight using dark adhesive tape. The high tension voltage was supplied by an A.E.I. photomultiplier power unit type R 1184. Voltage signals from the photo-tube were then amplified by the

photomultiplier head amplifier, figure 2.3, and could be displayed on a Tektronix 564 storage oscilloscope fitted with a 2A 63 differential amplifier and a 2B 67 time base. The "back off", a known variable voltage, also incorporated in the photo-tube head amplifier could be applied simultaneously to the differential amplifier. Random noise in the light input signal was partially filtered by a variable series of capacitors in the amplification circuit. Care, however, was required in selecting the correct magnitude of capacitance which had a decay time much shorter than the reaction half-life otherwise the oscilloscope trace showed the exponential decay curve of the capacitor. Oscilloscope traces were photographed using a Shackman Supper 7 Mk. II oscilloscope camera with a Polaroid model CB-40 back. The trace was recorded on Polaroid 47 black and white film.

The line voltage to all the electronic equipment was stabilised by an A.C. automatic voltage stabilised power supply type BTR-5 (Claude Lyons Ltd.) with an output of 240 volts at 50 Hz.

The flow was driven pneumatically by a 50ml. nylon syringe (Altas, Charles Thackray, Leeds) connected via a 3-way tap to a cylinder of compressed air. The plunger of the syringe was placed in contact with a moving rod attached to the pushing block and the 3-way tap opened rapidly to allow compressed air to enter the syringe barrel thereby pushing the block forward. Rapid stopping, essential for efficient mixing, was achieved by means of a steel pin S rigidly fixed in a hole in the aluminium base plate. Several holes were provided so that a number of pushes could be had from each thermostatted solution. It was found that a push of 1.5 mls. was sufficient to flush out the observation tube completely and thus three thermostatted pushes were safely obtained from the volume of solution enclosed in the aluminium block (~7.5mls.).

Recording of the reaction trace was accomplished by attaching a roller miniature microswitch (Radiospares Ltd.) to the pushing block. The roller striking the steel pin activated the trigger circuit on the oscilloscope fractionally before the pushing block came to rest thereby providing a complete record of the reaction.

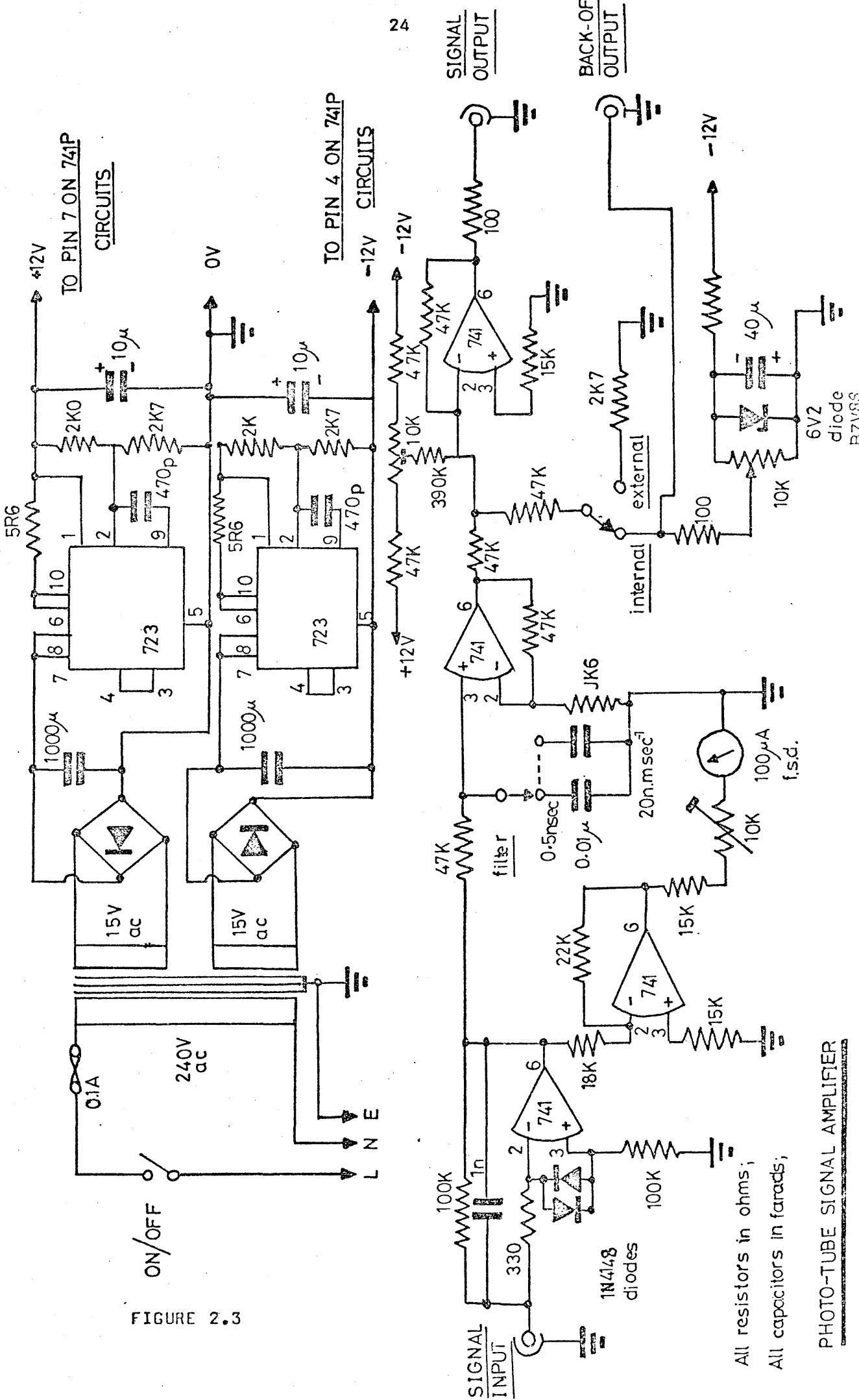


FIGURE 2.3

All resistors in ohms;
All capacitors in farads;

PHOTO-TUBE SIGNAL AMPLIFIER

SIGNAL
OUTPUT

BACK-OF
OUTPUT

TO PIN 7 ON 741P
CIRCUITS

TO PIN 4 ON 741P
-12V CIRCUITS

5R6

1000µ

15V ac

15V ac

240V ac

ON/OFF

0.1A

2K0

10µ

2K7

470p

723

5

1000µ

15V ac

15V ac

240V ac

ON/OFF

0.1A

2K7

10µ

2K7

470p

723

5

1000µ

15V ac

15V ac

240V ac

ON/OFF

0.1A

2K7

10µ

2K7

470p

723

5

1000µ

15V ac

15V ac

240V ac

ON/OFF

0.1A

2K7

10µ

2K7

470p

723

5

1000µ

15V ac

15V ac

240V ac

ON/OFF

0.1A

2K7

10µ

2K7

470p

723

5

1000µ

15V ac

15V ac

240V ac

ON/OFF

0.1A

2K7

10µ

2K7

470p

723

5

1000µ

15V ac

15V ac

240V ac

ON/OFF

0.1A

2K7

10µ

2K7

470p

723

5

1000µ

15V ac

15V ac

240V ac

ON/OFF

0.1A

2K7

10µ

2K7

470p

723

5

1000µ

15V ac

15V ac

240V ac

ON/OFF

0.1A

10K

47K

47K

100

741

15K

2K7

external

internal

10K

40µ

6V2 diode B7V88

100

100µA f.s.d.

47K

47K

100

741

15K

2K7

external

internal

10K

40µ

6V2 diode B7V88

100

100µA f.s.d.

47K

47K

100

741

15K

2K7

external

internal

10K

40µ

6V2 diode B7V88

100

100µA f.s.d.

47K

47K

100

741

15K

2K7

external

internal

10K

40µ

6V2 diode B7V88

100

100µA f.s.d.

47K

47K

100

741

15K

2K7

external

internal

10K

40µ

6V2 diode B7V88

100

100µA f.s.d.

47K

47K

100

741

15K

2K7

external

internal

10K

40µ

6V2 diode B7V88

100

100µA f.s.d.

47K

47K

100

741

15K

2K7

external

internal

10K

40µ

6V2 diode B7V88

100

100µA f.s.d.

47K

47K

100

741

15K

2K7

external

internal

10K

40µ

6V2 diode B7V88

100

100µA f.s.d.

47K

47K

100

741

15K

2K7

external

internal

10K

40µ

6V2 diode B7V88

100

100µA f.s.d.

47K

47K

100

741

15K

2K7

external

internal

10K

40µ

6V2 diode B7V88

100

100µA f.s.d.

47K

47K

100

741

15K

2K7

external

internal

10K

40µ

6V2 diode B7V88

100

100µA f.s.d.

47K

47K

100

741

15K

2K7

external

internal

10K

40µ

6V2 diode B7V88

100

100µA f.s.d.

47K

47K

100

741

15K

2K7

external

internal

10K

40µ

6V2 diode B7V88

100

100µA f.s.d.

47K

47K

100

741

15K

2K7

external

internal

10K

40µ

6V2 diode B7V88

100

Stopped Flow Apparatus B

The flow system in this apparatus is almost identical to that described by Sturtevant,¹¹² figure 2.4, and is similar to the system outlined above. Apart from the reservoir and pushing syringes and the observation tube, the entire apparatus was constructed in teflon. Instead of in glass tubes, the flow was confined in passages machined in the teflon. The mixing chamber was attached to the block containing the three-way taps by teflon plugs sealed by o-rings. These plugs inserted into a layer of teflon providing the inlet ports of the mixer as shown in figure 2.5. The mixer itself is of a four-jet tangential type milled in a similar layer and placed above the inlets. Situated on top of this was the quartz observation cell (Thermal Syndicate Ltd.) of 2 mm. pathlength and the complete assembly was clamped by two brass plates held by six screws. As in the previous device, the effluent tube, screwed to the end of the observation tube, was raised several inches above the level of the apparatus.

Teflon is a curious material. It is chemically inert, self lubricating and self sealing. Unfortunately, it is also difficult to machine precisely and flows under even the slightest pressure. While a few of the joints were threaded to give a good seal, the majority were smoothly machined and reliance was made on the self sealing properties. Early attempts to bring this flow system to operational standard were thwarted by fluid leaks at almost every conceivable position (and there are many)! This problem was however solved by tightly clamping the joints together and leaving them for several days in a warm room. After this period, it was found that the leaks had sealed.

The pushing syringes, mixing laminae and observation assembly were totally enclosed in a hollow brass jacket through which water was pumped as described above. Again the temperature was recorded using a Zecol 0^o - 50^o C thermometer placed adjacent to the effluent from the observation tube.

The spectrophotometric monitoring and electronic equipment were similar to those described previously. Exceptions included a Farnell stabilised E.H.T. supply type EHT 1 and the

FLUORESCENCE
OUTPUT

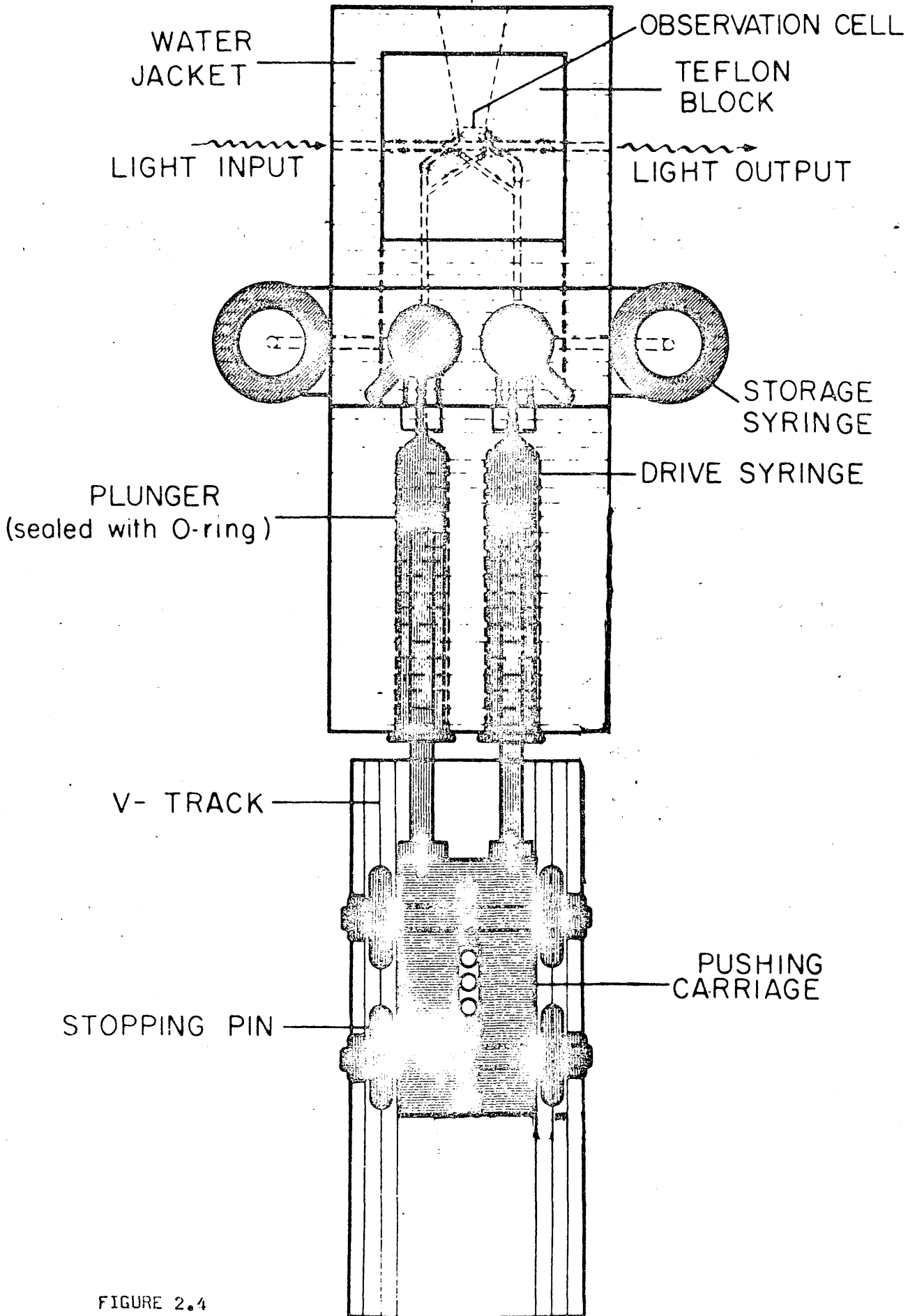


FIGURE 2.4

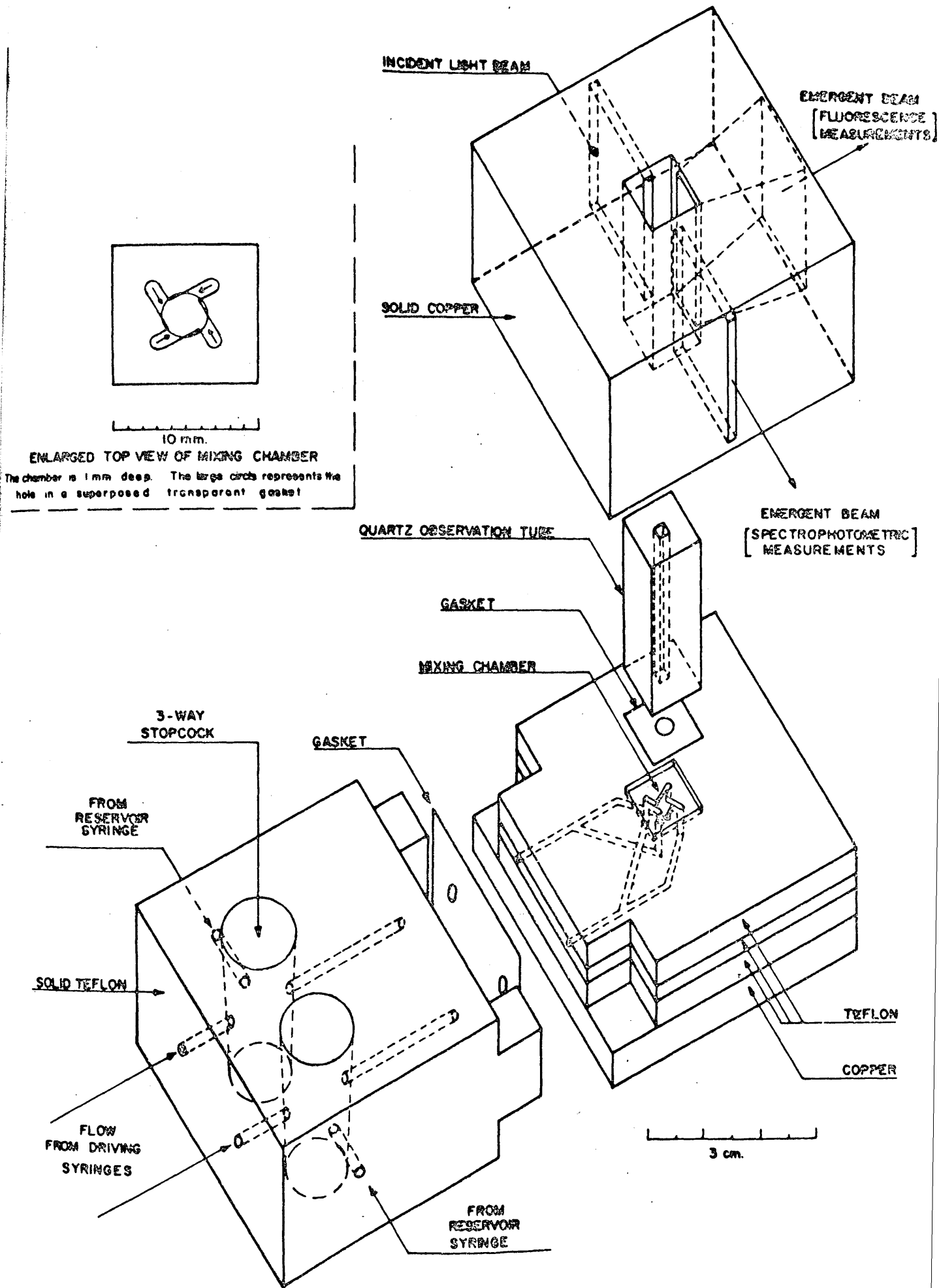


FIGURE 2.5

use of a Tektronix 5103N single beam storage oscilloscope incorporating a 5A20N differential amplifier and 5E10N time base. Traces were photographed on Polaroid 107 black and white film using a Tektronix C-5 oscilloscope camera.

Calibration and Performance.

A rigorous assesment of the capabilities of each device was made before use and routine calibration checks on the electronic equipment and flow characteristics were made at frequent intervals during operation. Oscilloscopes were calibrated at weekly intervals during operation and were serviced annually. Monochromators were serviced at six month intervals. Throughout this work, a slit width of 0.3mm. was used giving uncertainties in the wavelength of $\pm 5\text{nm.}$ at 600nm., $\pm 1\text{nm.}$ at 400nm. The variable voltage output from the back-off circuit was calibrated against known voltages on the oscilloscope screen. Plots of back-off units against voltage were shown to be linear over the range used (0-4 volts) with one back-off unit being equal to $5.55 \pm 0.02 \times 10^{-3}$ volts in both cases. The specifications of the 6256S photomultiplier tube include a spectro-sil quartz window with a small cathode area giving a low dark current. The output voltage was shown to exhibit a response linear to the light intensity up to an amplified voltage of 5 volts (see later for details). In the case of apparatus B, a spurious but constant voltage of 0.042V. arising from an untraced source in the amplification circuit was taken into account in the evaluation of the data.

The resolution of the monitoring system was found to be independent of the photomultiplier tube which is reported to have a rise time of 10ns. and a transit time over thirteen venetian blind dynodes of 55ns, clearly negligible compared with half lives of the order of milliseconds. Linear amplification of the signal was possible on a micro-second timescale and the time limit was found to depend only on the rise time of capacitors in the noise filtering circuit of the amplifier. Throughout this work the highest capacitance employed registered a rising half life of five milliseconds

and this was used only when the reaction half life exceeded one hundred milliseconds. In other cases, minimum capacitance was used giving a time resolution for the monitoring system of less than half a millisecond.

The performance of the flow system was checked by four independent means, each supplying a specific piece of information. Before these characteristics can be determined however, a leak proof bubble free system is required. Preliminary tests for leakage involved subjecting the flow system to a larger hydrostatic pressure than might be experienced under use. Persistent air bubbles were removed by using degassed water.

A more satisfactory check on both leakage and the mixing stoichiometry involved the use of the iron (III)- thiocyanate reaction. By choosing conditions to produce a solution of suitable optical density, with iron (III) in excess, both the reaction rate and optical density are sensitive to the iron (III) concentration. Comparison of the reaction traces obtained with iron (III) in first one then the other reservoir allows the mixing ratio to be determined. In both devices described above, this was found to be 1:1 within a 1% error after repeated determinations. Any leakage in the system while under pressure is revealed by lack of reproducibility in either configuration. Both machines were found to give identical traces to within 2% even with the simple two-jet mixer. A further use for this test was to assess the absolute performance of the flow device by comparison of the rate and absorbance data with literature values.

Schlieren gradients¹¹⁴ were used to determine the efficiency of mixing. When two colourless solutions of widely differing refractive index are mixed, there is the appearance of turbidity due to multiple refractions of the illuminating light and hence reduction in the intensity of the transmitted light. The approach to homogeneity is directly related to the approach to perfect mixing. In this case, degassed solution of 3 M sodium perchlorate and distilled water were employed and after the flow was brought to rest, the decrease in transmittance was less than 0.6% disappearing after 50 ms. in the case of apparatus A while the

corresponding figures for apparatus B were 0.2% and 10 ms. respectively. These were considered acceptable mixing characteristics in both cases.

The dead space of a stopped-flow apparatus is the distance between the mixing chamber and the point of observation. The dead time, or time taken by the mixed solution to travel this distance, may be found using the iron III - thiocyanate reaction described above with the addition of a trace corresponding to the transmittance of an unreacted solution. Since, in the visible region, the optical density of this solution is zero within experimental error, this may be obtained by flushing the observation tube with distilled water and recording the voltage corresponding to this transmission. Extrapolation of the initial rate of the iron III - thiocyanate reaction to this voltage permits the determination of the dead time (figure 2.6f). A more convenient method utilises the iron III - thiol reaction (chapters 4,5) since in this case, at wavelengths around 600nm the initial and final optical densities are identical thus dispensing with the flushing procedure.

With the dependence of mixing rate and efficiency and dead time on the character and rate of flow and stopping, it is essential that these be reproducible if absolute measurements are to be made. For this reason, a pneumatic drive and pin stop was preferred to other configurations. Pin stopping is however not without its disadvantages, the most important of which is the problem of cavitation.¹¹⁵⁻¹¹⁷

Cavitation is caused by a local reduction in the hydrostatic pressure of the fluid resulting in the formation of water vapour¹¹⁵ and a fine stream of bubbles and consequent turbidity of the solution. If optical measurements are employed, a large sharp decrease in transmission is observed.¹¹⁷ Unfortunately local reductions in pressure occur when the kinetic energy of the solution is dissipated and so cavitation is associated with the optimum conditions for mixing.¹¹⁶

The prevention of cavitation has provoked much interest¹¹⁵⁻¹¹⁷ and the results may be summarised under four headings;

- (1) degassing to remove nuclei for the formation of gas bubbles.
- (2) mixing without sharp edges and protusions.

- (3) application of a back pressure whether in the form of a constriction at the exit of the observation tube or by working at high pressure.
- (4) reduction of the flow rate.

Obviously a compromise situation must be reached.

The dead times of the instruments were found to vary with the flow rate and since an accurate knowledge of the former parameter was required for the calculations, it was determined daily. Sturtevant claims¹¹² a dead time of 3 ms. for his apparatus and the modified version described above was tested to a dead time of 2 ms. For most purposes, however, less severe conditions were used to minimise wear and tear and typically, with a flow rate of 8 cc.s^{-1} , the dead time was around 6 ms. Flow device A had a larger time requirement with a dead time of around 10 ms. with the Dulz-Sutin mixer and 15 ms. with the two-jet mixer at a flow rate of 15 cc.s^{-1} .

Solutions of ferroin of known optical density were used to determine the path length of the instrument. Comparison of the absorbance of these solutions relative to water, obtained from the stopped flow apparatus with those obtained using a Unicam S.P. 800 spectrophotometer at the same slit width and wavelength and known path length afforded a direct measurement of the pathlengths of the instruments. That of the apparatus A was found to be $0.5 \pm 0.01 \text{ mm.}$ while that of system B was $0.21 \pm 0.01 \text{ mm.}$ in good agreement with the manufacturers specifications. The optical density of these solutions determined at various values of the back-off also served to calibrate the linearity of the photomultiplier tube.

Measurement of Absorbance

The principles involved in the calculation of optical density from data acquired from a stopped-flow trace are relatively simple. The optical density or absorbance of a test solution is given by the expression

$$\text{O.D.} = \log_{10} \frac{I_0}{I} \quad 2.1$$

where I_0 and I are the intensity of transmitted light when a

reference solution (in this case water) and test solution respectively are placed in the beam of light.

Assuming that the intensity of light falling on the photocathode produces a linear response in the photomultiplier tube, then the anode currents

$$i_o \propto I_o$$

and

$$i \propto I \quad 2.2$$

or if the voltage drop over a constant resistance is measured,

$$V_o \propto I_o$$

and

$$V \propto I \quad 2.3$$

Hence,

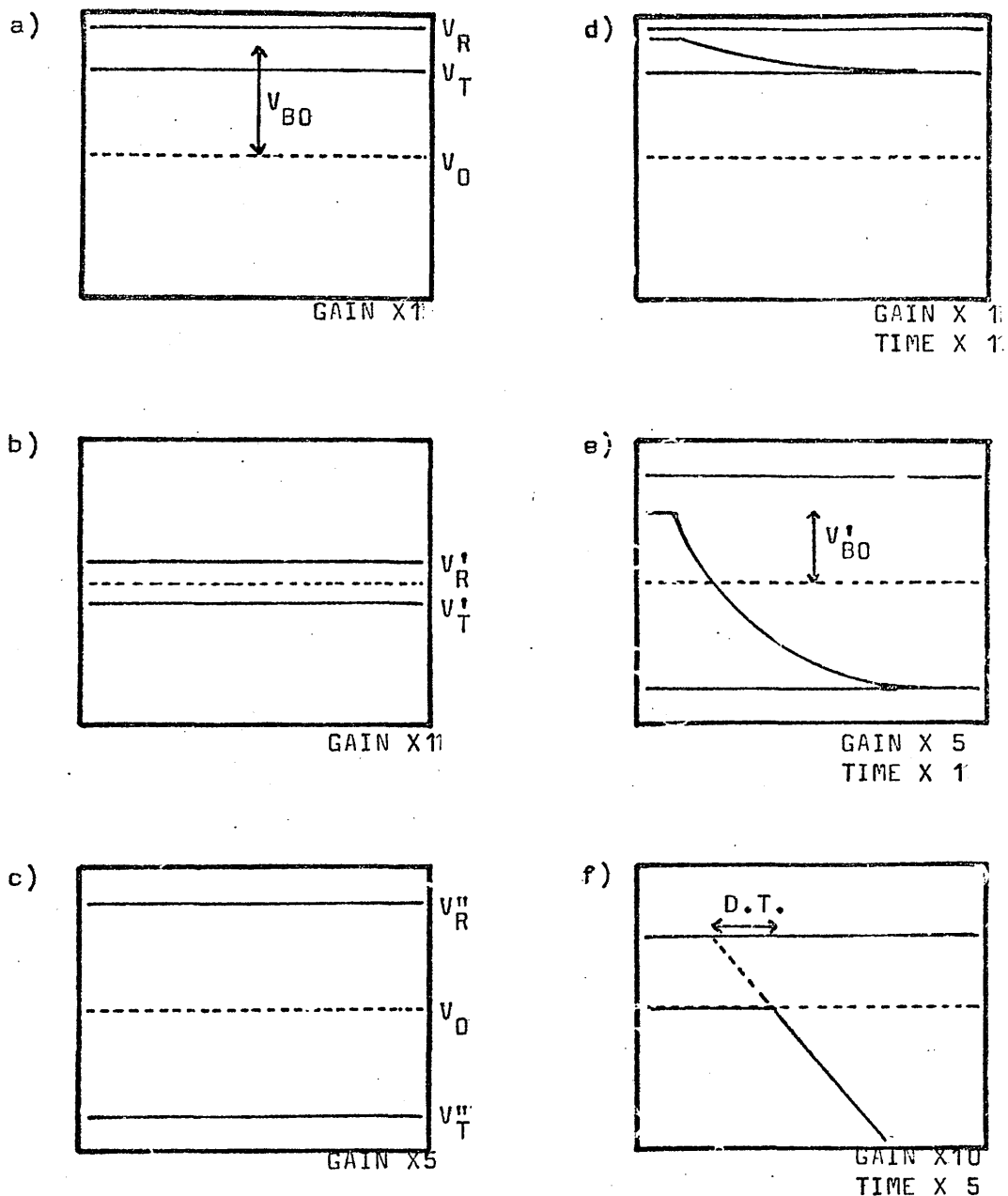
$$\text{O.D.} = \log_{10} \frac{V_o}{V} \quad 2.4$$

The amplified voltage from the photomultiplier tube may be displayed on the graduated oscilloscope screen as in figure 2.6a. The above assumption regarding photo-tube linearity was shown to hold experimentally since the optical density was found to be independent of the absolute value of V_o up to a value $V_o = 5$ volts. Only occasionally when the optical density was particularly small was a value of $V_o = 4$ volts exceeded.

The "Back-Off".

Measurement of optical densities using equation 2.4 with data of the type shown in figure 2.6a is practical only if the optical density is large; in this case 0.176. Many of the experiments in this work employed changes in optical density as small as 10^{-3} corresponding to a very small difference between V and V_o on the oscilloscope screen. Increasing the gain on the screen is impossible owing to the large absolute value of V_o .

The "back-off" and treatment of data.



V_0 = Ground voltage (zero volts)

V_R = Reference voltage

V_T = Test voltage

D.T. = Dead time

FIGURE 2.6

Consequently, a back-off voltage was used.

If a known but variable voltage $-V_{BO}$ is applied to the signal in figure 2.6a, the situation in figure 2.6b is obtained with

$$\begin{aligned} V_R &= V_{BO} + (V_R' - V_0) \\ V_T &= V_{BO} + (V_T' - V_0) \end{aligned} \quad 2.5$$

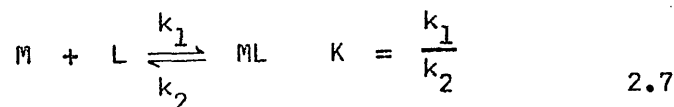
Increasing the gain, in this case by a factor of five is feasible giving figure 2.6c with

$$\begin{aligned} V_R &= V_{BO} + (V_R'' - V_0) \times \frac{1}{G} \\ V_T &= V_{BO} + (V_T'' - V_0) \times \frac{1}{G} \end{aligned} \quad 2.6$$

where G is the gain. With this system, changes in optical density as small as 10^{-5} could be detected.

Figure 2.6d shows a hypothetical reaction trace involving the formation of a coloured product from colourless reactants. Utilisation of the back-off facility allows amplification as in figure 2.6e, from which the optical density at any point in the reaction trace may be determined and the time course evaluated. A trace of the initial rate, figure 2.6f, is obtained by further increasing the backing-off voltage by an amount V_{BO}' . As mentioned previously, the dead time of the trace may be found by extrapolation of the trace to the reference time (corresponding to the mixed but unreacted solutions).

Instead of recording a reference line on the trace, a convenient approximation can be made when dealing with ligand substitution reactions of the type



where the reaction is followed by an increase in optical density due to the product ML .

The rate of complex formation is given by

$$\frac{d(\text{ML})}{dt} = k_1(\text{M})(\text{L}) - k_2(\text{ML}) \quad 2.8$$

at equilibrium,

$$k_1 [\text{M}][\text{L}] = k_2 [\text{ML}]$$

where round brackets refer to instantaneous concentration and square brackets to equilibrium concentration.

Hence

$$\frac{d(\text{ML})}{dt} = k_2 \frac{[\text{ML}]}{[\text{M}][\text{L}]} (\text{M})(\text{L}) - k_2 (\text{ML}) \quad 2.9$$

Assuming that M is constant excess so that $(\text{M}) \approx [\text{M}]$, then

$$\frac{d(\text{ML})}{dt} = k_2 \frac{[\text{ML}]}{[\text{L}]} (\text{L}) - k_2 (\text{ML}) \quad 2.10$$

Now,

$$(\text{L}) + (\text{ML}) = [\text{L}] + [\text{ML}] \quad 2.11$$

hence

$$\frac{(\text{L})}{[\text{L}]} = 1 + \frac{[\text{ML}] - (\text{ML})}{[\text{L}]} \quad 2.12$$

giving

$$\begin{aligned} \frac{d(\text{ML})}{dt} &= k_2 \{ [\text{ML}] - (\text{ML}) \} + k_2 \frac{[\text{ML}]}{[\text{L}]} \{ [\text{ML}] - (\text{ML}) \} \\ &= \{ k_2 + k_2 K [\text{M}] \} \{ [\text{ML}] - (\text{ML}) \} \end{aligned} \quad 2.13$$

And, since

$$\begin{aligned} \frac{d(\text{ML})}{dt} &= - \frac{d[\text{ML}]}{dt} - \frac{d(\text{ML})}{dt} \\ &= - d \left\{ \frac{[\text{ML}] - (\text{ML})}{dt} \right\} \end{aligned} \quad 2.14$$

an equation, first order in $[\text{ML}] - (\text{ML})$ is obtained.

A plot of $\log_e \{ [\text{ML}] - (\text{ML}) \}$ against time should be linear with gradient $\{ k_2 + k_1 [\text{M}] \}$

If the Beer-Lambert law is obeyed,

$$[ML] - (ML) = \text{O.D.}_s - \text{O.D.}_t \quad 2.15$$

$$\begin{aligned} \text{O.D.}_s - \text{O.D.}_t &= \log_{10} \frac{V_o}{V_s} - \log_{10} \frac{V_s}{V_t} \\ &= \log_{10} \frac{V_t}{V_s} \end{aligned} \quad 2.16$$

which is independent of V_o , the water line. The rate constant may thus be evaluated knowing only the voltage at equilibrium and its time dependence. Further, with a knowledge of the dead time, the optical density changes may be corrected using the expression,

$$\text{O.D.}_{\text{true}} = \text{O.D.}_{\text{apparent}} \exp(kt) \quad 2.17$$

where t is the dead time and k is the first order rate constant $\{k_2 + k_1[M]\}$.

All data obtained on the complex formation reactions of iron III (chapter 4) were amenable to this treatment and were treated accordingly. It was thus essential that the dead time was accurately known and, to minimise errors, as small as possible. Typical observed rate constants at 25°C for formation of iron (III) complexes were of the order of 10 s^{-1} introducing a 6% correction to the optical density for a dead time of six milliseconds.

Values of the voltages represented by traces on the oscilloscope screen were determined from photographs. The screen was calibrated in centimeter squares and a knowledge of the gain allowed the voltage difference between any two points on the reaction trace to be evaluated. A grid in divisions of 0.2 cms. was used to increase the precision of the measurements. In the case of the 564 oscilloscope, this grid was an integral part of the photograph, being scribed on a perspex plate placed in front of the oscilloscope screen while with the 5103^N it took the form of a flexible transparent sheet aligned accurately over the photograph itself. Use of the perspex plate produced a parallax error in the photographic record. Due account of this problem was taken in the computation of data. (Page 38)

```
01 PRINT "GAIN B.O. R.B.O. R.R."
02 LET C7=1
03 INPUT A1;
04 PRINT ,;
05 INPUT A2;
06 PRINT ,;
07 INPUT A3;
08 PRINT ,;
09 INPUT A4
10 PRINT "TIME",;
11 INPUT A5
12 LET A5=A5/2
13 PRINT "R.T. TIME O.D. LN(O.D.)"
14 GOTO 0016
15 LET D6=B2
16 INPUT A6;
17 IF A6=999 THEN GO TO 0052
18 LET A7=(A2*.005535)-(A1*A3)+(.041)
19 LET A8=A8+1
20 LET A9=A7+(A6*A1)
21 LET B1=A7+(A4*A1)
22 LET B2=(LOG(A9)-LOG(B1))/2.303
23 LET B2=ABS(B2)
24 LET B3=LOG(B2)
25 LET B4=A8*A5
26 PRINT ,B4,;B2,;B3,;
27 PRINT ""
28 LET B5=B5+1
29 IF B5=1 THEN GO TO 0015
30 IF B5=2 THEN GO TO 0016
31 IF B5=3 THEN GO TO 0034
32 GO TO 0040
33 PRINT ""
34 LET B6=B4
35 LET B7=B6*B6
36 LET B8=B3
37 LET B9=B8*B8
38 LET C1=B6*B8
39 GOTO 0016
40 LET C2=B4
41 LET B6=B6+C2
42 LET C3=C2*C2
43 LET B7=B7+C3
44 LET C4=B3
45 LET B8=B8+C4
46 LET C5=C4*C4
47 LET B9=B9+C5
48 LET C6=C4*C2
49 LET C1=C1+C6
50 LET C7=C7+1
```

```

51 GO TO 0016
52 LET C9=B6*B6
53 PRINT "    "
54 PRINT ,B6;,B7;,C1;,
55 PRINT "    "
56 PRINT ,B8;,B9;,C7;,
57 PRINT "    "
58 LET C8=((B6*B8)-(C7*C1))/(C9-(C7*B7))
59 LET D1=((C1*B6)-(B8*B7))/(C9-(C7*B7))
60 LET D2=(B9-(2*C8*C1)-(2*D1*B8)+(2*C8*DL*B6))
61 LET D2=D2+(B7*C8 2)+(C7*D1 2)
62 LET D2=D2/(C7-2)
63 LET D3=(C7*B7)-B6 2
64 LET D4=C7*D2/D3
65 LET D5=B7*D2/D3
66 LET D2=SQR(ABS(D2))
67 LET D4=SQR(ABS(D4))
68 LET D5=SQR(ABS(D5))
69 PRINT "    "
70 PRINT "GRADIENT & ERROR",C8,D4
71 PRINT "    "
72 PRINT "INTERCEPT & ERROR",D1,D5
73 PRINT "    "
74 PRINT "ROOT MEAN SQR ERROR",D2
75 LET D7=.0066
76 LET D8=D6*EXP(ABS(CB)*D7)
77 LET D9=(D8-D6)/D7
78 PRINT "    "
79 PRINT "O.D.O. & INIT. RATE.",D8,D9
80 END

```

03 Parallax error $A1 = 1.032 * A1$

75 Dead time = .0066 seconds

Calculations of optical density were made on a Nova 1200 (later 2000) dedicated computer using the programme shown on page 37. This programme calculates the optical density difference represented by any two points on the oscilloscope screen. Input data are of the form of distances (cms.) from the bottom of the oscilloscope screen to a particular point on the reaction trace. The absolute data may be calculated from a knowledge of the gain (volts cms.⁻¹), and the absolute voltage of a single point on the screen. This latter point is conveniently supplied by the position of the beam when the oscilloscope is grounded to earth, the absolute voltage being equal to the back-off, figure 2.6.

Output data are, the optical density difference ($OD_n - OD_t$) its natural logarithm and the unweighted least squares slope of the plot of this latter function against time. This affords the rate constant directly in the case when first order kinetics are followed.

Under typical conditions of usage, the errors involved in data processing are not excessive. The back-off could be determined to ± 1 back-off unit (0.0055 volts) giving a 1.6% error in an optical density of 6.86×10^{-2} when the absolute voltage was around 3.6 volts. Positions on the oscilloscope screen were estimated to ± 0.01 cms. although accuracy was probably in the region of ± 0.05 cms. Under the conditions stated above, this produced an error of less than 1% in the optical density.

Under favourable experimental conditions, reaction rate constants and optical density measurements could be reproduced to within 1%. The major factors limiting accuracy are thus not greatly affected by the techniques used in measurement, rather on the other factors such as the purity of materials, the preparation of solutions and possibly the temperature.

CHAPTER 3

Experimental Details; Preparation of Materials

Experimental Details: Preparation of Materials.

1. General

All glassware used in the course of this study was cleaned by prolonged immersion in a solution of Pyroneg followed by washing in dilute acid, repeated rinsing with tap water then distilled water. Non volumetric glassware was dried at 100°C in an oven while volumetric glassware was dried by rinsing with AnalaR grade acetone. Volumetric glassware, of B.S. grade A specification where possible (otherwise grade B) was used without further calibration. Solutions were prepared at room temperature which was reasonably uniform (20[±]5°C) throughout the period in which experiments were performed. All reagents were stored in glass containers to prevent contamination by metal ions.

2. Preparation of stock perchloric acid solution.

Perchloric acid (70%, Hopkin and Williams, AnalaR grade) was used without further purification and diluted with distilled water to approximately the required concentration. Standardisation of a solution ~ 0.5 M prepared by accurate dilution of the stock was achieved by titration against weighed amounts of disodium tetraborate (Hopkin and Williams, AnalaR grade) using methyl red as indicator.¹¹⁸ Only results reproducible to $\pm 0.2\%$ were considered acceptable.

3. Preparation of stock sodium perchlorate solutions.

The appropriate amount of crystalline sodium perchlorate (Fluka, puriss) was dissolved in distilled water and filtered to give a stock solution usually about 5M. in concentration. A sample was tested for the absence of chloride and sulphate impurities and the pH checked to ensure neutrality. (B.D.H. Universal Indicator Paper). Gravimetric standardisation was achieved by the evaporation of 2 ml. aliquots to dryness in an oven at 120°C for 24 hours, sufficient to decompose the monohydrate salt. Agreement with an ion exchange method was found to within $\pm 0.2\%$.

This method involved passing 2ml. aliquots of the stock solution through an ion exchange column (Amberlite IR-120(H)) in the acid form. The displaced H⁺ was then eluted

with distilled water (~ 200 mls.) until a pH 4-5 was reached (B.D.H. Universal Indicator Paper). The total eluent was then titrated with 0.1 M NaOH and the metal ion content of the original solution evaluated.

4. Preparation of stock lithium perchlorate solution.

Anhydrous lithium carbonate 500gms., (Hopkin and Williams, Reagent grade) was slowly added with continuous stirring to 1000mls. of conc. HClO_4 (70%, Hopkin and Williams, AnalaR grade), the temperature being maintained at 80°C . Small volumes of distilled water were added throughout the dissolution time to keep the LiClO_4 in solution.

On completion of the neutralisation, the pH was adjusted to ~ 5 (B.D.H. Universal Indicator Paper) by addition of a small amount of the appropriate reactant. The hot solution was then filtered through a sintered funnel and allowed to cool to room temperature slowly before further cooling to 0°C overnight. The solid LiClO_4 was then collected and dried as thoroughly as possible by suction.

Two further recrystallisations were effected as follows: The crystals were dissolved in distilled water at 80°C and the solution was filtered and allowed to cool slowly to room temperature then 5°C overnight. Crystals remaining after recrystallisation were dried as completely as possible and dissolved to give an almost saturated solution ($\sim 4\text{M}$) at room temperature. A sample was tested for the absence of chloride and sulphate and the solution was standardised gravimetrically as outlined with sodium perchlorate.

5. Preparation of stock iron III perchlorate solution.

Two sources of iron III solution were used in this work. Both preparations yielded solutions which exhibited identical spectrophotometric and kinetic properties.

(a) Iron III perchlorate (Fluka, purum) was recrystallised twice from perchloric acid solution as follows. The crystalline

salt (100 gms.) was dissolved in 500 mls. of distilled water to which perchloric acid was added until the resultant solution exhibited a purplish tinge.

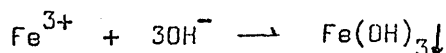
The mixture was filtered then heated and the perchloric acid-water azeotrope was allowed to evaporate slowly until the solution turned a deep reddish brown colour. Slow cooling to room temperature resulted in the formation of purple needles of the perchlorate salt.

(b) Iron III nitrate (Hopkin and Williams, General Purpose Reagent) was dissolved in water and the stirred solution was made basic by dropwise addition of aqueous ammonia (B.D.H., AnalaR grade). After the resultant precipitate of iron III hydroxide had settled, the supernatant liquid was siphoned off with the aid of a suction pump. This was followed by repeated washing and siphoning with distilled water until ammonia could no longer be detected. The precipitate was then dissolved in concentrated perchloric acid and recrystallised three times by the procedure outlined in (a).

The final crystals were collected in a glass sintered funnel and sucked as dry as possible to remove excess perchloric acid. Dissolution in distilled water yielded the required stock solution.

The iron III content of the solution was determined by reduction to iron II and standardisation¹¹⁹ with freshly prepared KMnO_4 solution. Reduction was achieved using a Jones reductor,¹¹⁹ care being taken to minimise the effects of aerial oxidation on the iron II solution. Comparison of this method of reduction with stannous chloride reduction¹¹⁹ yielded satisfactory agreement. The total iron III determination could be reproduced to within 0.3%.

Perchloric acid present in the iron III solutions was determined by titrating to $\text{pH} = 9$ with freshly prepared sodium hydroxide using phenolphthalein as indicator. During the titration, the reaction



occurs and due account was taken of this process in the calculations. The reddish colour of the precipitate did however interfere with the sharpness of the end point although with care, the same level

of reproducibility as in other determinations could be obtained. It was found that best results occurred when the indicator was added after the coagulation of the iron III. This latter process was accelerated by heating the solution during titration.

Analysis of the iron (III) content of dilute solutions was effected spectrophotometrically by the addition of excess ammonium thiocyanate. Comparison of the optical density obtained when test and known concentrations of iron III were used enabled the evaluation of the test concentration.

6. Preparation of a solution of iron II perchlorate.

A solution of iron III perchlorate ($\sim 0.5M$) in perchloric acid was reduced electrolytically under a nitrogen atmosphere using a mercury cathode and platinum anode. Although the presence of iron III could be detected by the red colour produced on the addition of ammonium thiocyanate, this method was found to yield iron II quantitatively.

The solution was standardised by titrating aliquots with freshly prepared potassium dichromate using barium diphenylamine sulphonate as indicator.¹²⁰ Similar aliquots passed through a Jones reductor yielded identical results indicating only trace concentrations of iron III ions. The hydrogen ion content was determined by titrating aliquots with standard base to $pH = 4$ using methyl orange as indicator. It was found that the end point was reproducible to only 2% due to aerial oxidation and the formation of an iron III hydroxide precipitate. This accuracy was however adequate for the relevant experiments.

7. Preparation of a stock solution of copper II perchlorate.

Excess copper II oxide (Hopkin and Williams, AnalaR grade) was dissolved in concentrated perchloric acid (Hopkin and Williams, AnalaR grade) by stirring for three days. After reaction was completed, the solution was filtered in a glass sintered funnel to remove the remaining oxide.

The copper II content was determined by titrating iodine, liberated on the addition of excess potassium iodide to a known

volume of solution, with sodium thiosulphate using starch as indicator.¹²¹ The thiosulphate was standardised using potassium iodate-potassium iodide as described elsewhere.¹²¹ Tests of the acidity (B.D.H., Universal Indicator Paper) indicated that the solution was neutral.

8. Mercaptocarboxylic acids.

Mercaptocarboxylic acids were obtained from various sources. Mercaptoacetic acid (Hopkin and Williams, Reagent grade), 2-mercaptopropionic acid (Koch-Light, pure), 2-mercaptoisobutyric acid (Koch-Light, pure), 3-mercaptopropionic acid (Koch-Light, puriss) and 2-mercaptopropionic acid (Evans Chemetics, 97%) were stored under an atmosphere of nitrogen and used without further purification. The purity of the ligands was checked by nuclear magnetic resonance spectroscopy. Only in the case of mercaptoacetic acid were small amounts of impurities observed, the most important of which was water. Samples of both mercaptoacetic acid and 2-mercaptopropionic acid, redistilled under vacuum, showed identical kinetic and spectrophotometric properties to those of the original solutions. Micro analysis showed that the purity of the mercaptoacetic acid was around 95% with 5% water.

Mercaptocarboxylic acids have been shown to be stable for long periods of time if stored in an atmosphere of nitrogen.¹²² The major decomposition under these conditions would appear not to be oxidation but the formation of H_2S and higher homologs of the thiols. This process is however slow and the amount of conversion low.¹²³

Cysteine (Koch-Light, pure) and penicillamine (Koch-Light, pure) were used without further purification.

9. 2-Hydroxyacetophenone (Koch-Light, pure) was redistilled under reduced pressure and analysed C 70.4%, H 5.91% (theory C 70.6%, H 5.9%) Dihydroxytolulene (Koch-Light, lab reagent) was recrystallised twice from ether to yield white platelets m.p. $87^\circ C$ (lit. $87^\circ C$). Analysis showed C 71.0%, H 6.1% (theory C, 70.6%, H, 5.9%).

10. Preparation of standard sodium hydroxide solutions involved the use of B.D.H. "Convol" ampoules made up with boiled out distilled water and standardised against accurately weighed samples of potassium hydrogen phthalate with phenolphthalein as indicator.¹²⁴

Solutions used in the experiments were prepared by accurate dilution of stock solutions with distilled water. In general, stock ligand solutions were prepared immediately before use to prevent aerial oxidation. Both metal-ion and ligand solutions were of the same hydrogen ion concentration and ionic strength to minimise the effects of diffusion in the stopped-flow devices.

Solutions were outgassed by freezing to 76°K, evacuating the flask and melting under reduced pressure. Besides reducing the concentration of dissolved gasses (specifically oxygen) to less than 10^{-6} M, this helped prevent cavitation. Where the effects of dissolved gasses were important as in the case of the reactions of copper II, the outgassing procedure was repeated and solutions were maintained under a nitrogen atmosphere by using a nitrogen bleed line connected to the evacuating system. In these circumstances, a modification of the stopped-flow reservoir syringes was required. A positive nitrogen pressure was maintained in the outgassing vessel from which solutions were withdrawn into polypropylene syringes (B-D, Plastipak) of suitable capacity using a close fitting teflon adaptor. These syringes could then be inserted directly into the apertures normally occupied by the reservoir syringes.

Conventional U.V. - visible spectra were obtained using a Unicam S.P. 800 spectrophotometer fitted with a thermostatted cuvette which could be flushed with nitrogen gas when required. Air sensitive solutions for experiments carried out on this apparatus were prepared in an inert atmosphere box.

Raman spectra were obtained on a Spex Ramalog 4 Laser Raman Spectrometer.

Data were processed using the University of Glasgow's KDF9 computer or the Nova computer described in chapter 2.

The following abbreviations have been used throughout this Thesis.

Mercaptoacetic Acid	MAA
2-Mercaptopropionic Acid	2-MPA
3-Mercaptopropionic Acid	3-MPA
2-Mercaptosuccinic Acid	2-MSA
2-Mercaptoisobutyric Acid	2-MIBA

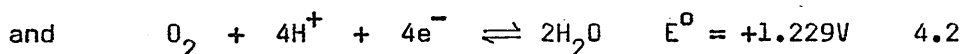
CHAPTER 4

Substitution Reactions of Iron III

Introduction

Iron is one of the most important elements. It occurs in many biological systems¹²⁵ and has wide industrial applications. The electronic structure of the neutral atom is (Ar) 3d⁶ 4s² and known oxidation levels range from -2 to + 6. Stabilities of the various states depend on many factors including electronic structure, ionisation potential, charge and ionic radius of the species but are best considered in relation to the solution environment. Negative oxidation levels require the stabilising properties of π -bonded ligands and are unknown in aqueous media. Consequently, only states +1 to +6, accessible in these conditions are considered.^{37, 126}

A satisfactory indication of the thermodynamic stability of a particular level in a given environment is given by its electrode potential E° . In a medium such as aqueous perchlorate, the limits of redox potential for thermodynamic stability lie between the reactions.^{127,128}



in acidic media or,



in basic solution.

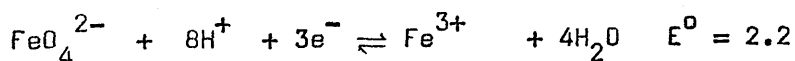
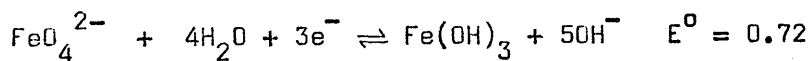
The existence of only the +2 and +3 ions as stable species is confirmed in acidic media,^{37,127} the relevant potentials being listed in table 4.1. The iron II/iron III couple is very sensitive to the effects of complexing ligands. This is best understood in terms of the properties of the individual ions.

Iron III is a hard acid with a small ionic radius (0.64Å⁰) and high charge. Its most common coordination number is six with octahedral geometry although the presence of bulky ligands such as Cl⁻ and Br⁻ can induce a geometrical change to form tetrahedral anions FeX₄⁻. Other geometries have been reported

TABLE 4.1

Reduction potentials of iron III couples.

	E° (Volts)	Conditions
$Fe^{3+} + e^{-} \rightleftharpoons Fe^{2+}$	0.77	
	0.77	1M HCl
	0.747	1M HClO ₄
	0.438	1M H ₃ PO ₄
	0.679	0.5M H ₂ SO ₄
$Fe(OH)_3 + e^{-} \rightleftharpoons Fe(OH)_2 + OH^{-}$	-0.56	
$Fe\ edta + e^{-} \rightleftharpoons Fe\ edta$	0.117	
$Fe(CN)_6^{3-} + e^{-} \rightleftharpoons Fe(CN)_6^{4-}$	0.69	
$Fe(phen)_3^{3+} + e^{-} \rightleftharpoons Fe(phen)_3^{2+}$	1.14	



edta = ethylenediaminetetraacetic acid

phen = o-phenanthroline

a - ref. 127,128

but are relatively rare.³⁷

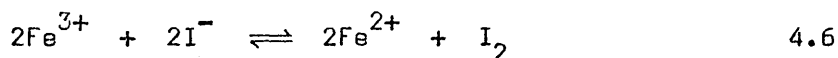
The most stable complexes are formed with first row p-block donors¹²⁹ in anionic ligands as reflected by the trend with the halogens.

$$F^- (170)^{130} > Cl^- (4.1)^{131} > Br^- (0.61)^{132} \quad 4.4$$

The figures in brackets are the values for the stability constants

$$K'_1 = \frac{[FeL^{2+}]}{[Fe^{3+}][L^-]} \quad 4.5$$

for the various monocomplexes, usually reported referring to conditions close to $T=25^\circ C$ at one molar ionic strength. Iodide (710)¹³³ appears anomalous in this respect although the value quoted is uncertain since the complex is unstable with respect to the redox reaction.



Iron III has its greatest affinity for ligands in which the donor atom is oxygen (HCO_2^- (1.26×10^3),¹³⁴ OH^- (6×10^{10}),¹³⁵ $C_6H_5O^-$ (1.7×10^8)¹³⁶). Large oxyanions such as periodate, perchlorate and nitrate which have poor donor qualities however and show little or no tendency to displace water from the inner coordination sphere although sulphate (170)¹³² does form a stable complex.

Nitrogen donors have no particular affinity unless they occur in the form of pseudo-halides N_3^- (0.51),¹³⁷ OCN^- (140),¹³⁸ SCN^- (130)¹³² or in chelate complexes. Simple amines show a preference for protons, eventually inducing hydrolysis of the metal ion.

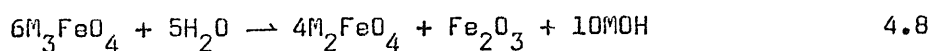
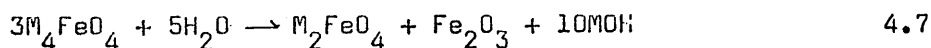
Of the remaining second row p-block donor atoms, there is evidence only for sulphur bonded complexes ($S_2O_3^{2-}$ (127),¹³⁹ SO_3^- (0.4)¹⁴⁰) in aqueous solution. As in the case of iodide, measurements are complicated by the tendency of the complexes to undergo a redox process.

Iron II forms complexes with virtually every stable anion.

It is similar to the higher oxidation state since it adopts an octahedral configuration in all but a few cases such as FeCl_4^{2-} . Although it has a lower charge and larger ionic radius (0.74 Å) than iron III, it too is a hard acid and forms similar complexes.³⁷ In general however, the stability constants are smaller in magnitude (SO_4^{2-} (10),¹⁴¹ SCN^- (6.8)¹⁴²).

Hard bases with their preference for the higher oxidation state, reduce the value of the reduction potential, whereas the converse is true for softer ligands. A further contributing factor concerns the electronic configuration of the ions. For octahedral geometry, high spin d^5 iron III (6A_1) has greater stability than the low spin configuration (2T_2) due to the factors involved in maximising the electron exchange energy. Iron II, d^6 , however obtains additional stability from spin pairing in the low spin state. With ligands which are high in the spectrochemical series therefore, the +2 state stability should be enhanced as in the case of the tris-phenanthroline complex.

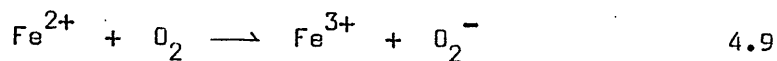
These and similar arguments may be extended to deal with less stable oxidation levels.¹⁴³ In highly alkaline media, the oxidising anion, FeO_4^{2-} , has been characterised.^{126,144} It reacts in acid solution with rapid evolution of oxygen. The +4 and +5 states are unstable¹⁴³ with respect to disproportionation to +6 and +3,



where M^+ is an alkali metal cation.

Bray and Gorin¹⁴⁵ proposed that the ferryl ion FeO^{2+} is formed as an intermediate in the catalytic decomposition of H_2O_2 and claimed that there was kinetic evidence for the same species in reactions with iodide, stannous ion and hydroxylamine. Since the appearance of this paper, several workers^{146,147} have inferred the presence of this ion and the pentavalent species,¹⁴⁸ mainly from kinetic dependences. Iron I has a similar status with kinetic evidence¹⁴⁹ in the autocatalytic oxidation of cysteine to support its formation.

Although iron II is thermodynamically more stable than iron III in aqueous solution, it is aerially oxidised¹⁵⁰



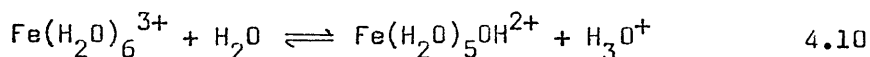
and unless the iron III formed has a readily accessible pathway for reconversion to iron II, it is kinetically stable under these conditions. Factors affecting this reaction are discussed in chapter 5.

High spin octahedral d^5 iron III has a 6A_1 ground state electronic structure. This is the only sextet level and thus all $d-d$ electronic transitions are intrinsically orbitally forbidden. Visible spectra of octahedral iron III complexes are thus of very low intensity.

Solutions of $\text{Fe}(\text{H}_2\text{O})_6^{3+}$ in acid solution are weakly coloured, exhibiting a violet tinge. Assignments¹⁵¹ of the bands in the spectrum are shown in table 4.2, substantiated by results obtained from crystal studies on ferric ammonium sulphate¹⁵² containing the octahedral hexaaquo iron III ion.

The presence of halides F^- , Cl^- , Br^- introduces a yellow colouration to the solution resulting from the tail of a red-shifted ligand to metal charge transfer band.¹⁵³ The shift increases in the order $\text{F}^- < \text{Cl}^- < \text{Br}^-$ and since the band is of high intensity, it obscures details of the $d-d$ absorptions. A similar explanation is offered for the yellowing of solutions on increasing the pH. Shifts in the charge transfer bands being accounted for by the formation of hydrolysed species.¹⁵⁴

The aqueous chemistry of iron III is dominated by hydrolysis equilibria.¹⁵⁵ The small, highly charged metal ion attracts electron density from the coordinated water, reducing the O — H bond strength relative to that in free water resulting in an acid-base reaction of the type



Sylva¹⁵⁵ has recently reviewed some aspects of the subject.

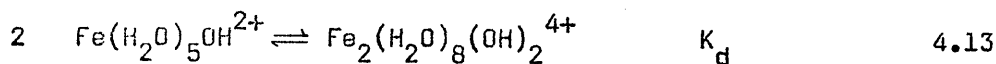
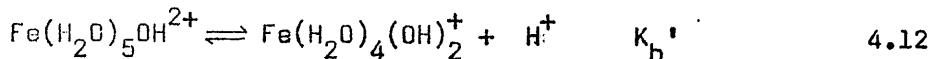
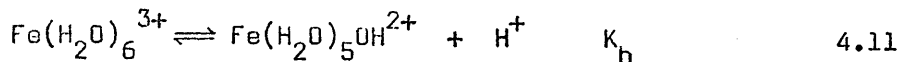
TABLE 4.2.Electronic transitions in the spectrum of $\text{Fe}(\text{H}_2\text{O})_6^{3+}$

ϵ^a $\text{M}^{-1}\text{cm}^{-1}$	λ nm.	Assignment	λ nm.	ϵ^b $\text{M}^{-1}\text{cm}^{-1}$
		${}^6\text{A}_1$		
0.1	794	${}^4\text{T}_1$	793	0.05
0.1	540	${}^4\text{T}_2$	549	0.01
0.4	411	${}^4\text{A}_1$	413	
			407	1.3
0.5	406	${}^4\text{E}$	394	
		${}^4\text{T}_2$	361	1

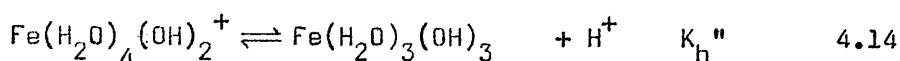
a ref. 151

b ref. 152

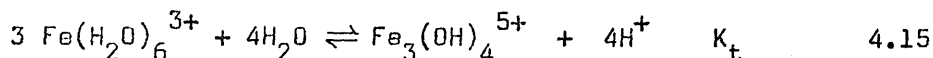
The results of various studies may conveniently be represented by the equilibria¹³⁴



Further equilibria^{156,157}



and



have also been suggested although they become important only at high pH. Values of the relevant equilibrium constants obtained by Millburn¹³⁴ under conditions similar to those used in this study are presented in table 4.3. It is obvious that even at high hydrogen ion concentrations, the presence of hydrolysed species in significant amounts is important.

Kinotically, the protolytic reactions 4.11 and 4.12 present little problem. The equilibria are established rapidly,¹⁵⁸ much more rapidly than the rate at which typical substitution reactions occur. On the timescale of iron III complex formation reactions therefore, they result in pre-equilibrium hydrogen ion dependences and while this does present a problem in terms of the "proton ambiguity" to be discussed later, it does not lead to complications in obtaining the rate data themselves. On the other hand, the rates associated with the dimerisation equilibria are comparable with those of ferric substitution reactions. To avoid this undesirable complication in kinetic and equilibrium studies, conditions of high acidity and low iron III concentrations are required.

As was pointed out by McBryde,¹⁵⁹ such conditions are unsuited to the study of complexes of weak organic acids (HL) as may be seen from equilibria of the type

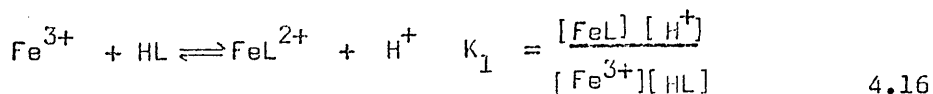


TABLE 4.3

Hydrolytic equilibria involving iron III in aqueous perchlorate solution $T = 25^{\circ}\text{C}$, $I = 1.0\text{M}^{\text{a}}$.

		ΔH kcal mole ⁻¹	ΔS cal K ⁻¹ mole ⁻¹
K_h	1.65×10^{-3}	10.2	21
K_d	700	-8.2	-14

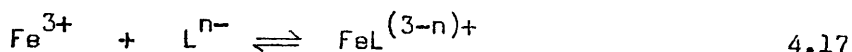
a ref. 134

where the release of the proton is generally taken to indicate a loss from the ligand rather than hydrolysis of the metal ion. In general $K_1 = K_1' / K_a$ is rather small and thus the degree of conversion to FeL^{2+} is low. For reasons discussed later in this chapter, spectrophotometric evaluation of K_1 and the extinction coefficient ϵ is frequently impossible. The situation is alleviated slightly since in many of these complexes in which the ligand has a suitable chromophore, the visible absorption spectra are enhanced allowing the range of experimental conditions to be extended with subsequently greater precision in the derivation of the parameters.

The nature of this enhancement is not at all clear. Bowen¹⁶⁰ has attributed it to a ligand to metal charge transfer band. Williams¹⁶¹ suggested however that the spectra are due to d - d transitions coupled with partial charge transfer to the cation. From the data then available, he noted that while electron donors shift the bands to longer wavelength, the intensities varied from less than 10^2 to more than $10^4 \text{ M}^{-1} \text{ cm}^{-1}$. If the absorption band were purely d - d he argued, then the extinction coefficients should not change markedly and always be less than $10^2 \text{ M}^{-1} \text{ cm}^{-1}$. He implied that the electron acceptor properties of the ferric ion must be greater in the excited state and are consistent with a partial vacation of a 3d level. The extent of this vacation determines the extinction. Holt and Dingle¹⁶² hold the view that although the spectra may be associated with d - d transitions, an exact assignment cannot be made. The 'allowedness' of the transition is a function of a spin-orbit coupling mechanism involving either a transition internal to the ligand or a charge transfer band.

Obviously, more information is required on the bonding in these complexes. Attempts to interpret trends in the stability constants of iron III complexes in terms of the bonding have met with limited success. Perhaps because of the versatility of phenolic ligands in terms of electron withdrawing and releasing properties, they have attracted most attention.

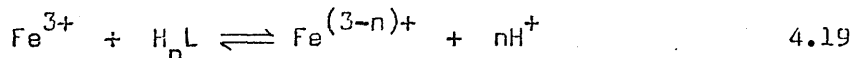
Linear free energy relationships between the constant for complex formation



and the overall acid dissociation constant,



have been discussed in terms of the "unity" of the correlating slope.¹⁶³⁻¹⁶⁵ Ambiguity arising from the inability to differentiate between contributions to the free energy changes from entropy and enthalpy of protonation¹⁶⁶ and complex formation¹⁶⁵ however have resulted in conflicting reports of the π -donor¹⁶⁵ and π -acceptor¹⁶¹ character of iron III. This problem was overcome by Millburn¹⁶⁴ who evaluated the thermodynamic parameters for a number of phenolic complexes. He described a unit slope in the enthalpy plots of the above equilibria and found that the entropy contributions were dominant. His results are consistent with changes in the degree of solvent release on varying the substituents on the phenolic ring.¹⁶⁴ The importance of these entropy contributions is most apparent in equilibria of the type.



in which the enthalpy changes are invariably positive. The feasibility of the reaction is thus governed by the entropy term.

Chelate complexes are generally more stable than the comparable complexes of unidentate ligands.¹⁶⁷ The criterion for identification of polydentate chelate formation is generally the overall number of protons released in the reaction although the possibility of protonated ligand donor sites and hydrogen bonding cannot be ruled out. Values^{133,167-170} for the association constants for complexes between iron III and some organic ligands are given in table 4.4. It is apparent that the constants K_1' reflect the basicities of the ligands, that weakly associated groups play at most a minor role in the bonding (cf. acetate¹⁶⁷ and 2-hydroxyacetate¹⁶⁹), and that five membered chelate rings are more stable than six member rings.¹⁶⁷

TABLE 4.4

Equilibrium constants for complexes of carboxylic acid derivatives with iron III under various conditions.

	T/°C	I/M	K _{1/M}	K' _{1/M} ⁻¹	ref.
HCO ₂ H	20	1.0	0.4	1260	a
CH ₃ CO ₂ H	20	1.0	0.050	1590	a
CH ₃ CO ₂ H	25	0.5	0.014	427	b
CH ₃ CH ₂ CO ₂ H	20	1.0	0.062	2820	a
(CH ₃) ₂ CHCO ₂ H	20	1.0	0.093	4000	a
ClCH ₂ CO ₂ H	20	1.0	0.32	126	a
HOCH ₂ CO ₂ H	25	0.5	0.019	795	c
HO ₂ CCO ₂ H	25	0.5	1150	3.6×10 ⁷	b
HO ₂ CCH ₂ CO ₂ H	25	0.5	0.83	2.9×10 ⁷	b
HO ₂ C(CH ₂) ₂ CO ₂ H	25	0.5	0.0082	7.6×10 ⁶	b
HO ₂ C(CH ₂) ₃ CO ₂ H	25	0.5	0.0074	6.0×10 ⁶	b
HO ₂ CCHOHCH ₂ CO ₂ H	20	0.1	0.135	1.35×10 ⁷	d
HO ₂ C(CHOH) ₂ CO ₂ H	20	0.1	0.54	3.1×10 ⁶	d
HO ₂ C(CHOH) ₂ CO ₂ H	25	1.0	0.23	5.4×10 ⁵	e
(HO ₂ CCH ₂) ₂ COHCO ₂ H	20	0.1	0.038	2.5×10 ¹¹	d

a ref 133

b ref 167

c ref 169

d ref 168

e ref 170

In common with the behaviour exhibited by the hexaquo ion, complexes with organic ligands show a marked tendency to oligomerise under conditions of high pH. Dimers, trimers and higher polymers have all been reported.^{168,170}

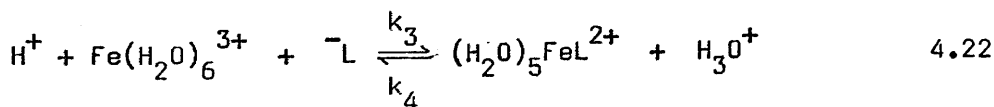
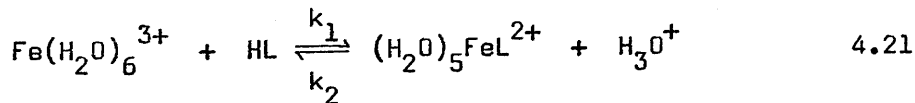
The mechanism by which equilibria of the type 4.19 are established has been the subject of a large number of investigations over the past twenty years. Kinetic studies yield information on both the rate of monocomplex formation and dissociation. Most discussion has centred on the former reaction since high spin d^5 iron III complexes are kinetically labile. By the principle of microscopic reversibility,¹⁷¹ however, both forward and backward reactions share the same transition state and assignment of a mechanism to one reaction automatically defines the other.

For reasons discussed earlier, the possibility of obtaining unambiguous data consistent with an associative or dissociative mechanism in reactions of iron III is unlikely. Consequently, early attempts¹⁷² to explain thermodynamic parameters of a single reaction have been discarded in favour of comparison of the relative rates of similar reactions. This approach has been thwarted however by ambiguous interpretations of acid dependent terms in the rate law.

In the general case, an anionic ligand L^- may be subject to a protolytic equilibrium



Reactions of $Fe(H_2O)_6^{3+}$ with both L^- and HL must therefore be considered

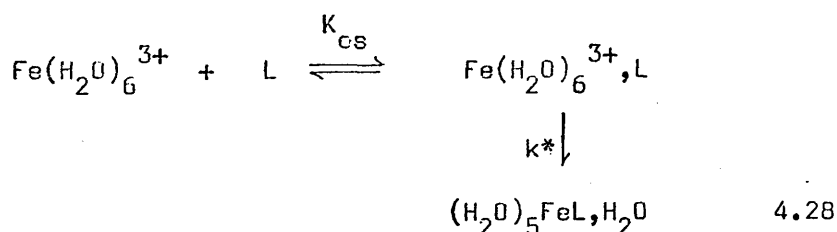


leading to a formation rate law of the type

$[(H_2O)_5FeOH, L^-]^+$ and not $[(H_2O)_4Fe(OH)_2, HL]^+$.

Eigen's hypothesis is consistent with the magnitude of the outer sphere association constants (table 1.1) which favour the formation of $[Fe(H_2O)_6^{3+}, L^-]$ rather than $[Fe(H_2O)_5OH^{2+}, HL]$. Although dissociative in nature since the rate determining step is loss of water from the hydroxocompound in the outer sphere complex, this mechanism shows a ligand dependence characteristic of an associative mechanism as a result of a variation in the extent of conversion of $[(H_2O)_5FeOH_2, L^-]^{2+}$ to $[(H_2O)_5FeOH, HL]^{2+}$ with ligand basicity.

Seewald and Sutin⁴⁴ reinterpreted the data in terms of reactions of $Fe(H_2O)_5OH^{2+}$ with HL for ligands of higher basicity where a significant amount of the protonated species exists in solution. Their results suggested that the rate constants for reaction with $Fe(H_2O)_6^{3+}$ all lie within the range $4 - 127 M^{-1} s^{-1}$ while those for $Fe(H_2O)_5OH^{2+}$ lie in the range $3 \times 10^3 - 3 \times 10^5 M^{-1} s^{-1}$ at 25°C, consistent with an I_d mechanism involving outer sphere complex formation and rate determining loss of water.



The rate constant $k = K_{os} k^*$ would be expected to exhibit a spread of around 10^2 by virtue of the fact that K_{os} changes by this amount on increasing the ligand charge. The second order rates for water exchange for $Fe(H_2O)_6^{3+}$ and $Fe(H_2O)_5OH^{2+}$ were quoted as $280 M^{-1} s^{-1}$ and $10^4 M^{-1} s^{-1}$ at 25°C in good agreement with this hypothesis.

These water exchange rates are however subject to variation with improving experimental technique and more accurate values have been reported (table 4.5).¹⁷³ Higher rates for water exchange in the hydroxocompound are expected for an I_d mechanism both from the point of view of electrostatic interaction and stabilisation of the I_d transition state by π -bonding to the hydroxyl ligand



TABLE 4.5

Water exchangerates for complexes of iron III in aqueous solution.
 T = 25°C.

Reagent	k_{-1} s ⁻¹	$M^{-1}k_{-1}^*s^{-1}$	ref.
Fe(H ₂ O) ₆ ³⁺	2 × 10 ⁶	3.6 × 10 ⁴	a
	2.4 × 10 ⁴	2.6 × 10 ³	b
	8.2 × 10 ³		
	1.5 × 10 ⁴	280	c
	3.0 × 10 ³	54	d
	1.5 × 10 ²	2.7	e
Fe(H ₂ O) ₅ OH ²⁺		10 ⁴	c
Fe(NCS) ₄ ⁻ (NCS ⁻ exchange)	1.0 × 10 ⁵		d
Fe(Cl ₂) ⁺ (Cl ⁻ exchange)		3 × 10 ⁵	f

- a. R.E. Connick in ref. 16, p.15
 R.E. Connick and R.E. Poulson, J. Chem. Phys., 1959, 30, 759.
- b. R.E. Connick and E.D. Stover, J. Phys. Chem. 1961, 65, 2075.
- e. M.R. Judkins, U.C.R.L.(1967) 17561, reported in ref. 173.
- c. R.E. Connick and E.E. Genser, reported in ref. 44.
- d. H.W. Dodgen, R. Murray and J.P. Hunt, Inorg. Chem., 1965, 4, 1820.
- f. Ref. 106.

(k* = k/55.5)

in a way similar to the dissociative conjugate base mechanism in reactions of pentaammine cobalt (III). It has been suggested that the trans water molecule would be especially labilised.¹⁷⁴

Accascina, Cavasino and d'Alessandro¹⁷⁵ extended the ideas of Seewald and Sutin to include a means of distinguishing pathways 4.22 and 4.24 based on the magnitude of the rate constants. Differentiation of equation 4.26 leads to

$$[H^+]_{\min} = \left\{ \frac{k_{13}K_hK_a}{k_1} \right\}^{\frac{1}{2}} \quad 4.30$$

where $[H^+]_{\min}$ indicates a minimum in the acidity dependence of the forward rate constant. The observation of a minimum thus provides a means of evaluating constants k_1 and k_{13} . Resolution of the composite term $(k_3 + k_{11}K_h/K_a)$ is however more difficult. Separation of the two constants can be made only if, by assuming one to be the sole pathway, it exceeds the diffusion controlled limit.

Subsequent studies extended the range of ligand basicity to include reactions where minima were observed¹⁷⁶⁻¹⁷⁸ and where the second requirement could be safely met.^{179,180} In the course of this latter study, it was suggested¹⁸⁰ that reactions with ligands of high basicity involved only $Fe(H_2O)_5OH^{2+}$ with the protonated ligand consistent with a mechanism in which proton transfer from the entering ligand to $Fe(H_2O)_5OH^{2+}$ occurred in the course of complex formation, accounting for their relatively low formation rates.¹⁸¹ Further studies¹⁸² reveal inconsistencies in this hypothesis.

When resolved by the methods outlined above, the rate constants do indeed generally fall within the limits outlined by Seewald and Sutin for reactions of $Fe(H_2O)_6^{3+}$ and $Fe(H_2O)_5OH^{2+}$. It may thus be argued¹⁸³ although with much less certainty that if the contribution to the composite rate constant, assuming either of the rate constants to be within these limits, is very small, then this pathway is of minor importance and the constant may be attributed solely to the alternative reaction. A further criterion which has been used to differentiate between reactions 4.22 and 4.24 depends on the higher reactivity of $Fe(H_2O)_6^{3+}$

with ligands of higher charge, consistent with table 1.1. If the pathway involving $\text{Fe}(\text{H}_2\text{O})_6^{3+}$ and HL exceeds that with L^- , then the assignment must be considered anomalous.¹⁷⁵

The possibility of rate determining ring closure has been examined in a number of studies with bidentate^{184,185} and polydentate ligands.^{186,187} In all cases however the rates have been in accordance with those found with monodentate ligands, implying that the rate determining step is the loss of the first coordinated water molecule. Other ligand effects include rate determining keto-enol tautomerism,^{187,188} protonation¹⁸⁹ and coordination isomerisation,¹⁹⁰ occurring only in ligands of unusual structure.

Rate constants and thermodynamic parameters for reactions of iron III with various ligands are presented in table 4.6 and are discussed later in this chapter.

TABLE 4.6

Formation rate constants of iron III monocomplexes.

A Reactions of $\text{Fe}(\text{H}_2\text{O})_6^{3+}$

Ligand	I/M	T/°C	$k_{M^{-1}s^{-1}}$	ΔH^*	ΔS^*	ref.
$\text{C}_6\text{H}_5\text{OH}$	0.1	25	25			a
<i>o</i> - $\text{OCHC}_6\text{H}_4\text{OH}$	0.2	25	24.6			b
<i>o</i> - $\text{OCHC}_6\text{H}_4\text{OH}$	1.0	25	2.6	17.3	0.9	c
<i>o</i> - $\text{OCC}_3\text{C}_6\text{H}_4\text{OH}$	1.0	25	3.04	22.1	17.7	d
<i>o</i> - $\text{HNCHC}_6\text{H}_4\text{OH}$	1.0	25	15	16.6	2.6	cc
<i>o</i> - $\text{HO}_2\text{CC}_6\text{H}_4\text{OH}$	1.0	25	3.0			e
$\text{C}_6\text{H}_5\text{CHOHCO}_2\text{H}$	0.35	25	4			f
$\text{CH}_3\text{CO}_2\text{H}$	0.5	25	27			g
$\text{CH}_3\text{CO}_2\text{H}$	1.0	20	4.8			h
$\text{CH}_3\text{CH}_2\text{CO}_2\text{H}$	1.0	20	5.7			h
$\text{ClCH}_2\text{CO}_2\text{H}$	1.0	20	2.2			h
acac E*	0.5	25	0.26	11	-16.9	i
acac E*	1.0	25	5.2			j
acac K*	1.0	25	0.29			j
tacac E*	1.0	25	1.4			k
HF	0.5	25	11.4	8.7	-24	l
HN_3	1.0	25	4.0			m
HN_3	1.0	25	2.6			n
H_3PO_2	1.0	25	35			o
<i>p,o</i> - $\text{SO}_3\text{HO}_2\text{CC}_6\text{H}_3\text{OH}^-$	1.0	25	1.5			p
$\text{HO}_2\text{CCO}_2^-$	1.0	25	860			q
$\text{HO}_2\text{CCO}_2^-$	0.5	25	1440	18	16	r
SCN^-	0.5	25	90			s
SCN^-	0.4	25	127	13	-5	t
SCN^-	0.1	25	132			u
SCN^-	0.5	25	130			v
SCN^-	0.5	25	150			w
Cl^-	1.0	25	9.4	16.6	2	x
Cl^-	0.5	25	1.1			y
Cl^-	1.0	25	50	12	-10	z
Cl^-	1.0	25	8.4			aa
Cl^-	3.0	25	10.8			aa
Cl^-	6.0	25	90			aa

Table 4.6 cont'd.

Ligand	I/M	T/ ^o C	$k_{M^{-1}S^{-1}}/\Delta H^*$	ΔS^*	ref.
Br ⁻	1.7	22	20		bb
Br ⁻	1.0	25	19	16	1 t
HSO ₃ ^{-*}	1.0	25	1.5		cc
HSO ₄ ⁻	1.2	25	38		dd
HSO ₄ ⁻	2.0	25	51		dd
SO ₄ ²⁻	0.5	25	4350		ee
SO ₄ ²⁻	0.5	25	4000	15	10 dd

Table 4.6 cont'd.

B Reactions of $\text{Fe}(\text{H}_2\text{O})_5\text{OH}^{2+}$

Ligand	I/M	T/°C	$10^{-3} k_{\text{M}^{-1} \text{s}^{-1}}$	H*	S*	ref.
8-OHQ ⁺	0.2	25	0.27	15		b
C ₆ H ₅ OH	1.0	25	0.72			a
C ₆ H ₅ OH	0.1	25	1.1	12.8	-5.4	ff
C ₆ H ₅ OH	0.1	25	1.5			gg
o-NH ₂ C ₆ H ₄ OH	0.1	25	110			a
o-HNCHC ₆ H ₄ OH	1.0	25	2.6	6.3	-22	c
o-CH ₃ C ₆ H ₄ OH	0.1	25		12.4	-8.1	ff
o-HO ₂ CC ₆ H ₄ OH	0.1	25	2.9	11		b
o-HO ₂ CC ₆ H ₄ OH	1.0	25	5.5	12	-2	e
o-OCCHC ₆ H ₄ OH	0.2	25	0.65	13		b
o-OCCHC ₆ H ₄ OH	1.0	25	1.37	6.8	-21	c
o-OCCH ₃ C ₆ H ₄ OH	1.0	25	1.39	9.7	-11.4	d
o-HOCH ₂ C ₆ H ₄ OH	1.0	25	1.0	7.3	-20.1	d
o-HOC ₆ H ₄ OH	0.1	25	3.1	9.6	-11.1	hh
o-ClC ₆ H ₄ OH	0.1	25	1.0	13.4	-4.0	ff
o-ClC ₆ H ₄ OH	0.1	25	0.35			gg
o-BrC ₆ H ₄ OH	0.1	25	1.9	11.3	-13.1	ff
m-CH ₃ C ₆ H ₄ OH	0.1	25	0.9	9.7	-16.3	ff
m-CH ₃ C ₆ H ₄ OH	0.1	25	1.6			gg
m-NO ₂ C ₆ H ₄ OH	0.1	25	0.7	14.6	0.3	ff
m-NO ₂ C ₆ H ₄ OH	0.1	25	0.59			ii
m-NO ₂ C ₆ H ₄ OH	0.1	25	0.80			gg
m-ClC ₆ H ₄ OH	0.1	25	1.3			gg
p-NO ₂ C ₆ H ₄ OH	0.1	25	0.8	14.5	-0.4	ff
p-NO ₂ C ₆ H ₄ OH	0.1	25	0.82			gg
p-NO ₂ C ₆ H ₄ OH	0.1	25	0.91			jj
p-ClC ₆ H ₄ OH	0.1	25	0.66			gg
p-ClC ₆ H ₄ OH	0.1	25	1.2	12.5	-2.5	ff
p-BrC ₆ H ₄ OH	0.1	25	0.7	11.1	-10.8	ff
C ₆ H ₅ CHOHCO ₂ H	0.35	25	2.56	6	-25	f
HO ₂ CCHC ₆ H ₅ CO ₂ H	0.1	25	5.4			kk
HO ₂ CCHC ₃ H ₆ CO ₂ H	0.1	25	3.3			kk
HO ₂ CCHC ₄ H ₉ CO ₂ H	0.1	25	2.6			kk
HO ₂ CCHCH ₃ CO ₂ H	0.1	25	4.3			kk
HO ₂ CCH ₂ CO ₂ H	0.1	25	6.2			kk

Table 4.6 cont'd.

Ligand	I/M	T/°C	$10^{-3} k_{-1} s^{-1}$	ΔH^*	ΔS^*	ref.
$ClCH_2CO_2H$	1.0	20	6.8			h
$CH_3CH_2CO_2H$	1.0	20	5.1			h
CH_3CO_2H	1.0	20	5.3			h
CH_3CO_2H	0.5	25	2.8	11.1	5.4	g
$HOCHCH_2CO_2HCO_2H$	1.0	20	4.5			ll
$HSCHCH_2CO_2HCO_2H$	1.0	25	11.5	10.2	-4	mm
$HSCH_2CO_2H$	1.0	25	40.6	10.5	-2.1	d
$HSCHCH_3CO_2H$	1.0	25	15.6	10.3	-4.7	d
$HSC(CH_3)_2CO_2H$	1.0	25	2.20	10.3	-8.7	d
H_2ida	1.0	25	2.5	6.1	-23	nn
H_3nta	1.0	25	15	9.9	-5	nn
H_4edta	1.0	25	30	7.3	-15	oo
H_5dtpa	1.0	25	53			oo
acac E*	0.5	25	2.52			i
acac E*	1.0	25	4.4			j
acac K*	1.0	25	0.0054			j
tacac E*	1.0	25	13			k
HF	0.5	25	3.1	10	-8	l
HN_3	1.0	25	6.8			m
HN_3	1.0	25	6.1			n
HN_3	0.1	25	7.4			pp
HOCN	1.0	2	.015			qq
H_3PO_2	1.0	25	21			o
$\rho, o -SO_3HO_2CC_6H_5OH^-$	0.1	25	5.7	15		b
$\rho, o -SO_3HO_2CC_6H_5OH^-$	1.0	25	5.5			p
$O_2CC_6H_4OH^-$	1.0	25	14	11	-3	e
$ClCH_2CO_2^-$	1.0	20	28			h
$HO_2CHCO_2^-$	0.1	25	130			kk
$HO_2CHCH_3CO_2^-$	0.1	25	120			kk
$HO_2CHC_3H_9CO_2^-$	0.1	25	100			kk
$HO_2CHC_3H_6CO_2^-$	0.1	25	110			kk
$HO_2CHC_6H_5CO_2^-$	0.1	25	100			kk
$HO_2CCO_2^-$	1.0	25	20			q
$HO_2CCO_2^-$	0.5	25	48			r
$Hida^-$	1.0	25	8.8	4.9	-22	nn
H_2nta^-	1.0	25	56	6.3	-16	nn
H_2nta^-	0.5	25	110			s

Table 4.6 cont'd.

Ligand	I/M	T/°C	$10^{-3}k_{M^{-1}s^{-1}}\Delta H^*$	ΔS^*	ref.	
H ₃ edta ⁻	1.0	25	110	5.7	-15	oo
H ₄ dtpa ⁻	1.0	25	160			oo
SCN ⁻	0.5	25	5.1			s
SCN ⁻	0.4	25	10	16	-7.6	t
SCN ⁻	0.1	25	4.2			u
SCN ⁻	0.5	25	1.3			v
SCN ⁻	0.5	25	27			w
N ₃ ⁻	1.0	25	10			m
Cl ⁻	1.0	25	11	13	4	x
Cl ⁻	3.0	25	2.1			y
Cl ⁻	1.0	25	41	6	-18	z
Cl ⁻	1.0	25	18.1			aa
Cl ⁻	3.0	25	23.8			aa
Br ⁻	1.7	22	10			bb
Br ⁻	1.0	25	11.5	11	-3	t
HSO ₄ ⁻			24			rr
HSO ₄ ⁻	0.5	25	145	5	-18	w
HCrO ₄ ⁻	1.0	25	21.2			ss
HSO ₃ ^{-*}	1.0	25	0.27			cc
P ₃ O ₁₀ ²⁻	1.0	25	12			p
SO ₄ ²⁻			240			rr
SO ₄ ²⁻	1.2	25	114			dd
SO ₄ ²⁻	2.0	25	78			dd
SO ₄ ²⁻	0.5	25	187			ee
SO ₄ ²⁻	0.5	25	231	11.3	4	dd
8-OHQ	-		8-hydroxyquinoline			
acac	-		acetylacetone			
tacac	-		theonyltrifluoroacetone			
H ₂ ida	-		iminodiacetic acid			
H ₃ nta	-		nitrilotriacetic acid			
H ₄ edta	-		ethylenediaminetetraacetic acid			
H ₅ dtpa	-		diethylenetriaminepentaacetic acid			
E	-		enol			
K	-		keto			
ΔH^*	-		kcal mole ⁻¹			
ΔS^*	-		cal ^o K ⁻¹ mole ⁻¹			

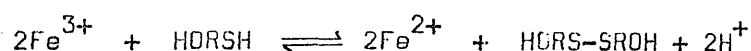
References to Table 4.6

- a. Ref. 182.
- b. P.G.T. Fogg and R.J. Hall, J. Chem Soc. A. 1971, 1365.
- c. Ref. 180.
- d. This work.
- e. G. Sani and E. Mentasti, Inorg. Chim. Acta., 1970, 4.
- f. A.D. Gilmour and A. McAuley, J. Chem Soc. A. 1971, 3176.
- g. Ref. 173.
- h. Ref. 176.
- i. Ref. 187.
- j. Ref. 188.
- k. Ref. 189.
- l. Ref. 172.
- m. Ref. 44.
- n. Ref. 270.
- o. J.H. Espenson and D.F. Dustin, Inorg. Chem. (1969) 8, 760.
- p. Ref. 178.
- q. E.B. Moorhead and N. Sutin, Inorg. Chem. 1966, 5, 1866.
- r. Ref. 185.
- s. S. Funahashi, S. Adachi and M. Tanaka, Bull. Chem. Soc. Jap., 1973, 46, 479.
- t. Ref. 105.
- u. Ref. 174.
- v. D.M. Goodall, P.W. Harrison, M.J. Hardy, and K.C. Jane, J. Chem. Ed., 1972, 12, 675.
- w. H. Wendt and H. Strehlow, Z. Electrochem., 1962, 66, 228.
- x. Ref. 106.
- y. R.J. Campion, T.J. Conocchioli and N. Sutin, J. Amer. Chem. Soc., 1964, 86, 4591.
- z. Y. Yasunga and S. Harrada, Bull. Chem. Soc. Jap., 1969, 42, 2165.
- aa. Ref. 227.
- bb. P. Matthies and H. Wendt, Z. Physik. Chem. (Frankfurt), 1961, 30, 137.
- cc. Ref. 190.
- dd. Ref. 177.
- ee. F.L. Baker and W. McF. Smith, Canad. J. Chem., 1970, 48, 3100.
- ff. Ref. 180.
- gg. Ref. 179.
- hh. E. Mentasti and E. Pelizzetti, J. Chem. Soc. Dalton, 1973, 2605.

- ii. Ref. 181.
- jj. Ref. 220.
- kk. Ref. 184.
- ll. Ref 326.
- mm. Ref. 197.
- nn. Ref. 186.
- oo. E.Mentasti, E. Pelizzetti and G. Saini, J. Chem. Soc. Dalton, 1974, 1944.
- pp. Ref. 175.
- qq. D.W. Carlyle and J.H. Espenson, J. Amer. Chem. Soc., 1969, 91, 599.
- rr. G. Davis and W. McF. Smith, Canad. J. Chem., 1960, 38, 569.
- ss. Ref. 183.

Substitution Reactions of Iron III with 2-Mercaptocarboxylic Acids.

The reaction between iron III and 2-mercaptocarboxylic acids in aqueous acidic conditions is characterised by the rapid formation and subsequent disappearance (figure 4.1) of a blue colour to yield a colourless solution containing iron II and the corresponding disulphide. This has been interpreted as the formation of a metal-ion complex which acts as an intermediate in the overall redox process.



where HORSH is the abbreviation used throughout this work to represent a mercaptocarboxylic acid.

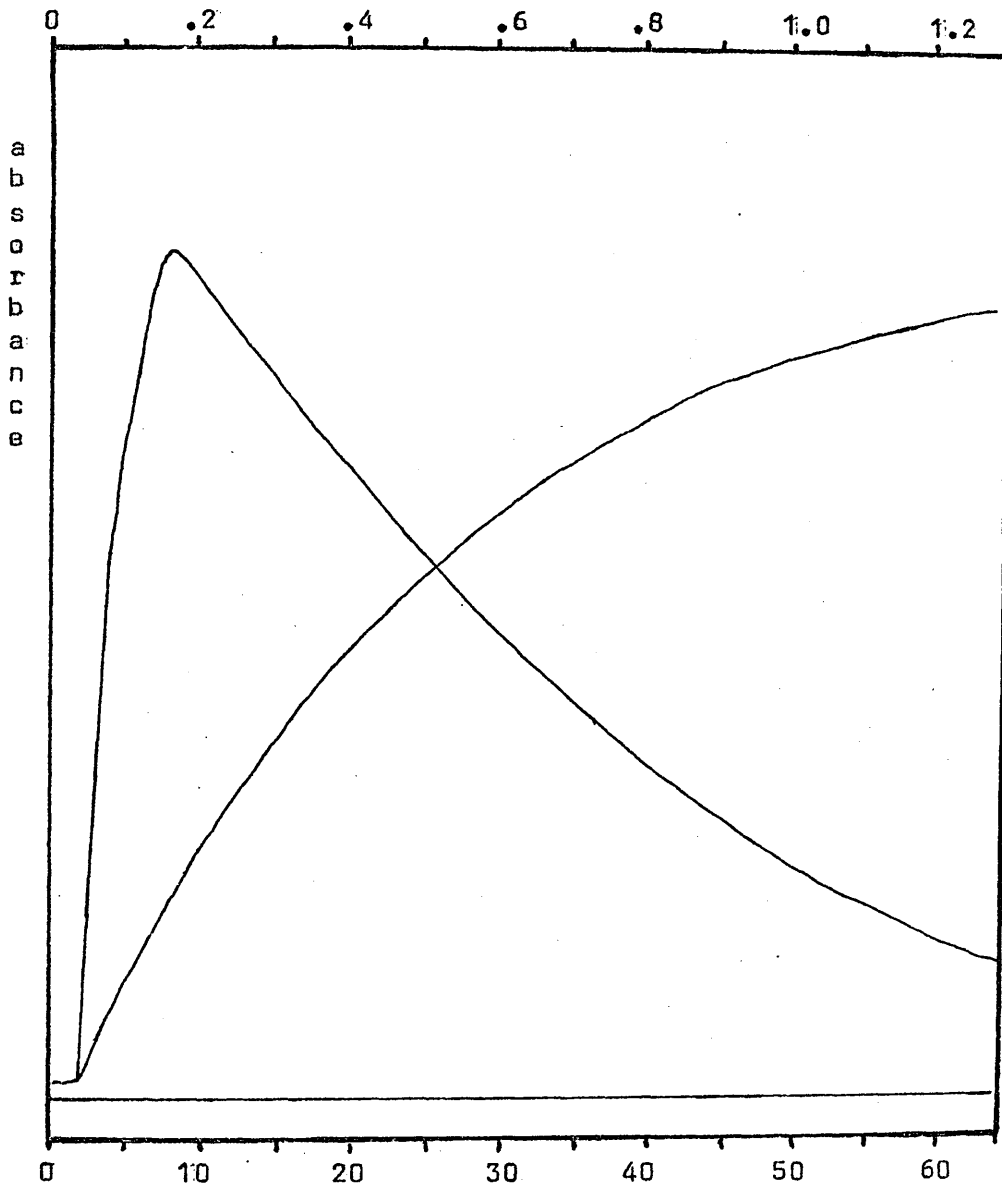
In this section data are presented for the characterisation and formation kinetics of the intermediate complex formed with mercaptoacetic acid (MAA), 2-mercaptopropionic acid (2-MPA) and 2-mercaptoisobutyric (2-MIBA). A discussion of the redox process may be found in chapter 5.

Experimental conditions were chosen to minimise the number of species required for detailed analysis of the reaction. An excess of metal ion was used to optimise the formation of only a monocomplex whilst high hydrogen ion concentration ($> 0.25M$) prevented hydrolysis and reduced the amount of dimeric iron III to negligible proportions. The ionic strength was maintained constant at 1.0M using perchlorate as the counter anion. In most experiments sodium was the supporting cation although some were repeated with lithium to investigate possible medium effects.

Over the temperature range studied (10° - 25°C), the reactions are rapid and, being kinetically complex, require the use of fast reaction techniques both in kinetic studies and in characterising the intermediate. Treatment of the data involved methods of successive approximation derived from an equilibrium situation in which no subsequent redox step takes place.

Typical trace of optical density against time for the reactions of 2-mercaptocarboxylic acids with iron III.

$\lambda = 600\text{nm}$. $[\text{H}^+] > 0.25\text{M}$.



Upper scale refers to complex (colour) formation trace, lower scale to the trace of the overall reaction. Both scales are in seconds.

FIGURE 4.11

Characterisation of the Intermediates.

The spectra of the intermediate complexes, shown in figure 4.2, were obtained from plots of optical density against time at wavelengths over the range 350-700 nm. Those shown were compiled from the point of maximum optical density observed in the reaction since this could be defined accurately. No changes in the form of the spectra were noted over the time course of the reaction (both formation and decay) or over the range of hydrogen ion concentrations used, consistent with the formation of a single complex, apparently not subject to significant hydrolysis. Hydrolysis constants of equivalent complexes, estimated¹⁸¹ to be in the region of 10^{-5} M may not however be discounted since the range of experimental conditions is limited. At the wavelengths of maximum absorbance of the complexes (table 4.7) neither of the reactants shows appreciable absorbance. It was therefore convenient to carry out the kinetic investigations at these wavelengths.

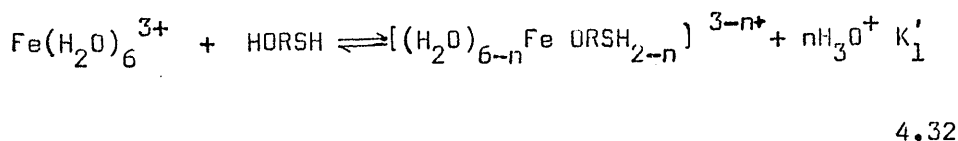
In conditions of high hydrogen ion concentration, the approximation may be made that

$$[\text{Fe}^{3+}]_0 = [\text{Fe}(\text{H}_2\text{O})_6^{3+}]$$

and

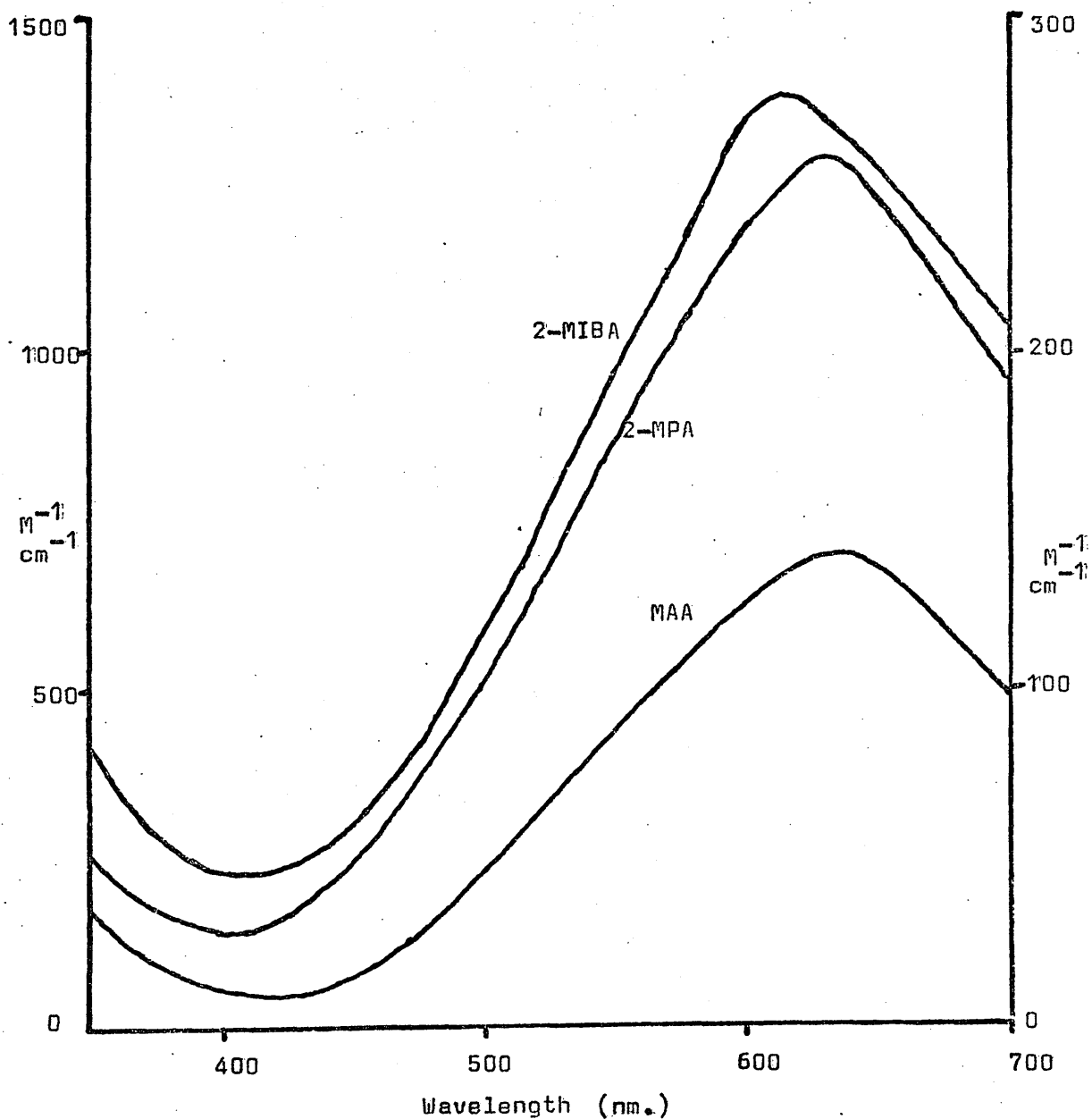
$$[\text{HORSH}]_0 = [\text{HORSH}] \quad 4.31$$

where the subscript 0 indicates the analytical concentration of the species. The concentrations of the various hydrolysed forms are small. Assuming the formation of a 1:1 complex, the equilibrium 4.32 may be written



Values for the equilibrium constants and extinction coefficients of the complexes $[(\text{H}_2\text{O})_{6-n}\text{Fe ORSH}_{2-n}]^{(3-n)+}$ may be determined from equilibrium optical density measurements using the Scott¹⁹¹ modification of the Benesi-Hildebrand¹⁹² procedure. Equation 4.34 may be derived from expansion of the equilibrium relationship

Absorption spectra of complexes of iron (III) with 2-mercaptocarboxylic acids.



Right hand ordinate refers to MAA and 2-MPA, left hand ordinate to 2-MIBA.

FIGURE 4.2

TABLE 4.7

Absorption maxima, extinction coefficients, equilibrium constants and related thermodynamic parameters for complexes of iron III with 2-mercaptocarboxylic acids.

LIGAND	$\lambda_{\max}/\text{nm.}$	$\epsilon/\text{M}^{-1}\text{cm}^{-1}$	$T^{\circ}\text{C}$	K_1/M
MAA	640 \pm 5	140 \pm 20	10	1.9 \pm 0.2
			15	2.2 \pm 0.2
			20	2.7 \pm 0.2
			25	3.2 ^a
			$\Delta H^b = 5.7 \pm 2.0$	
$\Delta S^c = 21.5 \pm 5.0$				
2-MPA	630 \pm 5	260 \pm 30	10	0.99 \pm 0.1
			15	1.19 \pm 0.1
			20	1.31 \pm 0.1
			25	1.48 ^a
			$\Delta H^b = 4.6 \pm 2.0$	
$\Delta S^c = 16.2 \pm 5.0$				
2-MIBA	615 \pm 5	1400 \pm 100	10	0.28 \pm 0.05
			15	0.33 \pm 0.05
			20	0.35 \pm 0.05
			25	0.43 \pm 0.05
			$\Delta H^b = 4.5 \pm 2.0$	
$\Delta S^c = 13.5 \pm 5.0$				
2-MSA ^d	615 \pm 5	350 \pm 20	10	1.65 \pm 0.2
			14	1.85 \pm 0.2
			20	2.30 \pm 0.2
			25	2.55 \pm 0.2
			$\Delta H^b = 5.1 \pm 1.4$	
$\Delta S^c = 20 \pm 5$				

a - calculated from thermodynamic parameters.

b - kcal mole⁻¹

c - cal K⁻¹ mole⁻¹

d - ref 197

Table 4.7 cont'd.

LIGAND	$\lambda_{\max}/\text{nm.}$	$\epsilon/\text{M}^{-1}\text{cm}^{-1}$	$T^{\circ}\text{C}$	K_1/M
3-MPA	600	75	20	0.05
cysteine ^e	606	300	20	0.058
penicillamine	595	600	20	0.10

a - calculated from thermodynamic parameters

b - kcal mole⁻¹

c - cal °K⁻¹ mole⁻¹

d - ref 197

e - ref 326

$$K_1' = \frac{K_1}{[H^+]^n} = \frac{[(H_2O)_{6-n}Fe(H_2O)_2(H_2O)_{2-n}]^{(3-n)+}}{[Fe(H_2O)_6^{3+}][H_2O]_n} \quad 4.33$$

at high hydrogen ion concentration, by assuming that the complex concentration at equilibrium is small and therefore that terms in its square may be neglected.

$$\frac{[Fe^{3+}]_0 [H_2O]_0}{O.D._{max}} = \frac{1}{K_1' \epsilon \ell} + \frac{1}{\epsilon \ell} [Fe^{3+}]_0 + [H_2O]_0 \quad 4.34$$

where $O.D._{max}$ is the equilibrium optical density, ϵ the extinction coefficient of the intermediate complex and ℓ the optical pathlength.

A plot of the left hand side of equation 4.34 against $[Fe^{3+}]_0 + [H_2O]_0$ should allow characterisation of the number of protons released in reaction 4.32 thus affording values for ϵ and K_1' .

Criticism of this general method has been voiced by many workers. Person¹⁹³ examined criteria involved in obtaining a slope of equation 4.34 of sufficient magnitude to allow separation of ϵ and K_1' . He pointed out that reliable equilibrium constants are obtained only when the complex concentration is comparable to that of the free ligand at equilibrium, with the metal in excess.

Deranleau¹⁹⁴ criticised the whole concept of Scott-Benesi-Hildebrand plots preferring instead numerical optimisation methods. By defining a saturation factor

$$S = \frac{[\text{complex}]}{[\text{ligand}]_0} \quad 4.35$$

he restated Person's conclusions in terms of $S = 0.2-0.8$ as the optimum range for determining K_1' and ϵ . If the range of S is small, Scott plots yield a straight line no matter the nature of the equilibrium. In order to accurately characterise the system, experiments must be performed over 75% of the optimum range, an impossible task using the Scott method if the inherent assumptions are to be valid.

Further inaccuracies in the method¹⁹⁵ are caused by deviations from Beer's law, solvent interaction, variation of activity coefficients and the formation of higher complexes. This latter aspect was criticised particularly by Johannsson.¹⁹⁶

In the present study, the range of saturation factors varies with ligand structure. For MAA 56%, 2-MPA 40% while for 2-MIBA 14%. While in no case are the above criteria wholly fulfilled, the ranges are sufficient to allow separation of K_1 and ϵ based on equations 4.34 and 4.33 in which the value of n is two indicating the release of two protons.

A more serious problem involved in these systems results from the approximation that the maximum optical density formed in the reaction approaches the true equilibrium value. The validity of this assumption varies markedly with the ligand involved. Fortunately, for all the ligands examined, interference from the redox step decreases with increasing hydrogen ion concentration such that in all cases, the approximation is valid at $[H^+] > 0.45M$.

A knowledge of the redox kinetic parameters enabled the deviation from equilibrium to be treated on a semi-quantitative basis. Using an average for the extinction coefficient from equation 4.34 at different acidities, the mean equilibrium constant K_1 was evaluated at each hydrogen ion concentration and a plot of K_1 against $[H^+]^{-4}$ yielded an intercept which was considered to be a better estimate of the true equilibrium constant. Recalculated values for the extinction coefficients using only optical density measurements at higher acidities were found to differ by not more than 10% from the original values. No trend in the extinction coefficient with temperature was noted and average values over the temperature range studied together with the final values for the equilibrium constants, are presented in table 4.7

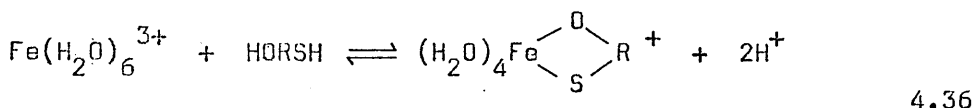
Systematic errors due to the interference from the redox reaction increase with the magnitude of the equilibrium constant as those associated with the inadequacies of the Benesi-Hildebrand treatment decrease. While it must be admitted that in spite of the ten fold range in K_1 and ϵ with structure, the product $K_1\epsilon$ remains approximately constant suggesting that the treatment is inadequate, the fact that the extinction coefficients are

temperature independent is pleasing.

Preliminary studies were also carried out with the ligands 3-mercaptopropionic acid and penicillamine. The relevant parameters and those obtained from other sources are also presented in table 4.7.

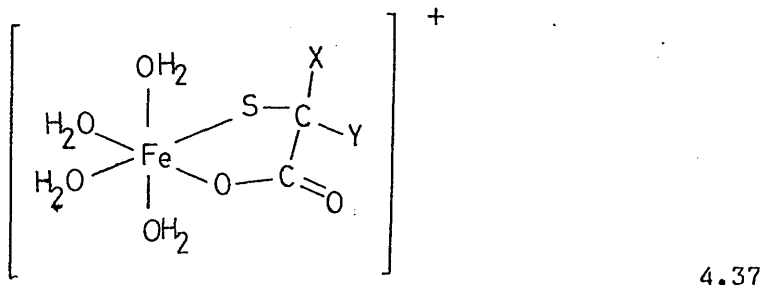
Thermodynamic parameters were calculated from plots of $\log_e K_1$ against T^{-1} ($^{\circ}K^{-1}$) using an unweighted least squares procedure. The errors quoted are derived from this treatment.

The results are consistent with the formation of a bidentate sulphur-oxygen bonded chelate.



Inclusion of sulphur in the bonding pattern is necessary to explain the marked changes in the visible absorption spectra when compared with such ligands as acetate¹⁶⁷ and 2-hydroxyacetate.¹⁶⁹

The ligands represent a series in which the number of methyl substituents on the carbon atom bonded to the sulphhydryl group increases from zero to two on going from MAA to 2-MIBA. It is apparent from the data in table 4.7 that the wavelength maxima exhibit a trend, decreasing with increasing methylation of the ligand possibly indicating that the electronic transition involves some metal to ligand charge transfer. More striking however is the dependence of the extinction coefficients on substituents X and Y.

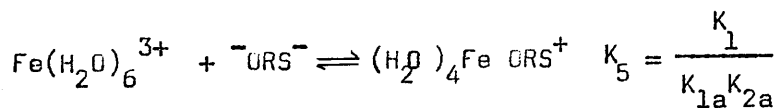


In the case of MAA where X=Y=H, little or no repulsion is expected between these atoms whereas in 2-MIBA where X=Y=CH₃,

construction of a model indicates considerable interaction leading to changes in the bond angles with some strain within the five membered ring. An intermediate value for 2-MPA indicates a larger interaction than in the case of MAA but much smaller than in the case of 2-MIBA and is similar to that for 2-MSA¹⁹⁷ (table 4.7) suggesting that the latter forms a five-membered ring complex with the group $-\text{CH}_2\text{CO}_2\text{H}$ as substituent. The corresponding six-membered ring chelate might be expected to have an extinction coefficient similar to that of 3-MPA. This latter value is also consistent with the proposed steric explanation for extinction changes since crowding is reduced in the six-membered ring.

It may be argued that since the complexes undergo subsequent oxidation-reduction reactions, the visible absorption spectra should reflect a mixture of d-d transitions and charge transfer from the ligand to the metal. The ease of this process should be revealed in the energy of the transition and the extinction coefficient. Methyl substituents promote such interactions and thus the spectrum of 2-MIBA should be shifted to longer wavelengths and the extinction coefficient should be increased relative to MAA. Only the latter parameter is consistent with this explanation.

Complex stability constants K_1 show the opposite trend to that shown by the extinction coefficients, decreasing with increasing methyl substitution. Interpretation of these data presents difficulties since sufficiently accurate values for the sulphhydryl dissociation constants of the various ligands in the present experimental conditions are lacking and, consequently, parameters relating to the equilibrium,



4.38

cannot be evaluated. Table 6.1 lists the known values for K_{1a} and K_{2a} which indicate that the complexes have a high thermodynamic

stability ($K_5 \approx 10^{14} \text{ M}^{-1}$) in contrast to the behaviour expected of hard iron III with a soft mercaptide group.¹⁹⁸ In this respect the results are in agreement with those proposed for iodide.¹³²

K_{1a} values (chapter 6) reveal no comparable trend with ligand structure and, based on the electron releasing properties of methyl substituents, the required explanation is contrary to predicted changes in the sulphhydryl ionisation K_{2a} .

Thermodynamic parameters relating to K_1 reveal that the reactions are endothermic and further, that within experimental error, the enthalpy changes are equal. The complex formation reactions are thus entropy controlled in a manner similar to that found by Millburn¹⁶⁴ with phenolic ligands.

The observed trend in K_1 would be expected if ring strain were the explanation for stability changes. This should however also be reflected in the enthalpy although a loss of conformational freedom in the five-membered ring due to methyl interactions might be consistent with the observations.

Entropy changes in complexation reactions are generally identified¹⁹⁹ with changes in solvation structure. The smaller change in the case of 2-MIBA relative to MAA is considered to indicate a decrease in the number of water molecules released in reaction 4.36 in accord with the hydrophobic nature of the methyl substituents.

Increasing the ring size has the effect of lowering the stability of the complex in keeping with previous results with iron III, although several studies have indicated greater stability of six membered sulphur-oxygen bonded chelates with other metals.²⁰⁰ No further discussion of this effect will be considered since the data are few.

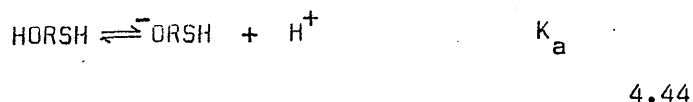
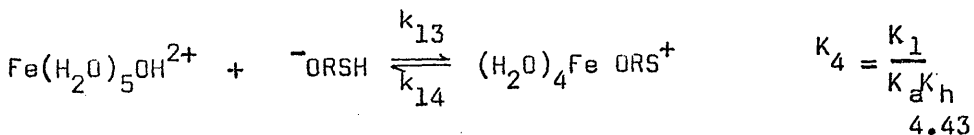
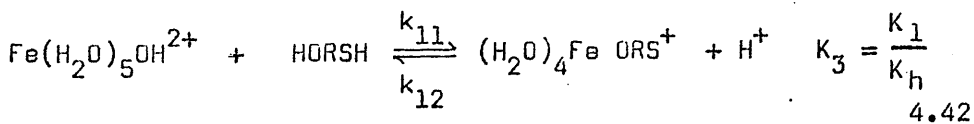
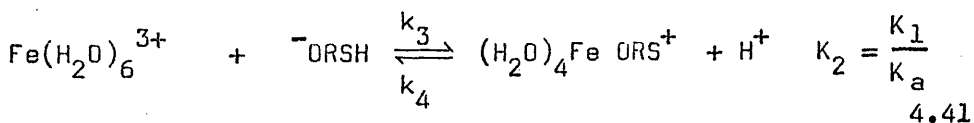
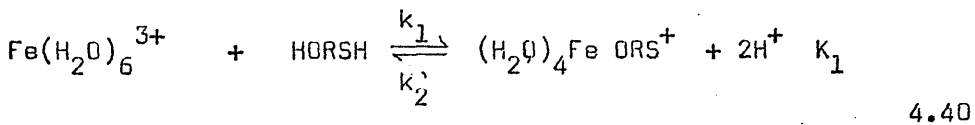
Kinetics and Mechanism of Complex Formation.

As a preliminary to kinetic investigation, initial rate studies were undertaken to identify the concentration dependences of the reactants. Correction of the rate for the dead time of the stopped-flow instrument was necessary since, under differing conditions, the proportion of the reaction occurring within this period varied significantly. The data, illustrated in figure 4.3, are consistent with an expression of the type

$$\text{Initial Rate} = k_{ir} \frac{[\text{Fe}^{3+}]_0 [\text{HORSH}]_0}{[\text{H}^+]_0} \quad 4.39$$

in all cases suggesting a common mechanism. The results of this study are presented in table 4.8

In studies of the overall complex formation reaction, consideration was given to all the forms of reactant in solution. The following rate scheme was proposed



Providing protolytic equilibria are rapid, under conditions of excess metal ion (> 4:1) and constant hydrogen ion concentration, the rate of complex formation may be described by the pseudo

Plots of initial rate of colour formation against concentration for the reaction between iron III and 2-mercaptopropionic acid.

$T=20^{\circ}\text{C}$, $I=1.0\text{M}$. pathlength = 0.5cm.

A:- $[\text{H}^+] = 0.4\text{M}$, $[\text{Fe}^{3+}] = 0.05\text{M}$, $[\text{HORSH}]$ variable.

B:- $[\text{H}^+] = 0.4\text{M}$, $[\text{Fe}^{3+}]$ variable, $[\text{HORSH}] = 0.0025\text{M}$.

C:- $[\text{H}^+]$ variable, $[\text{Fe}^{3+}] = 0.02\text{M}$, $[\text{HORSH}] = 0.005\text{M}$.

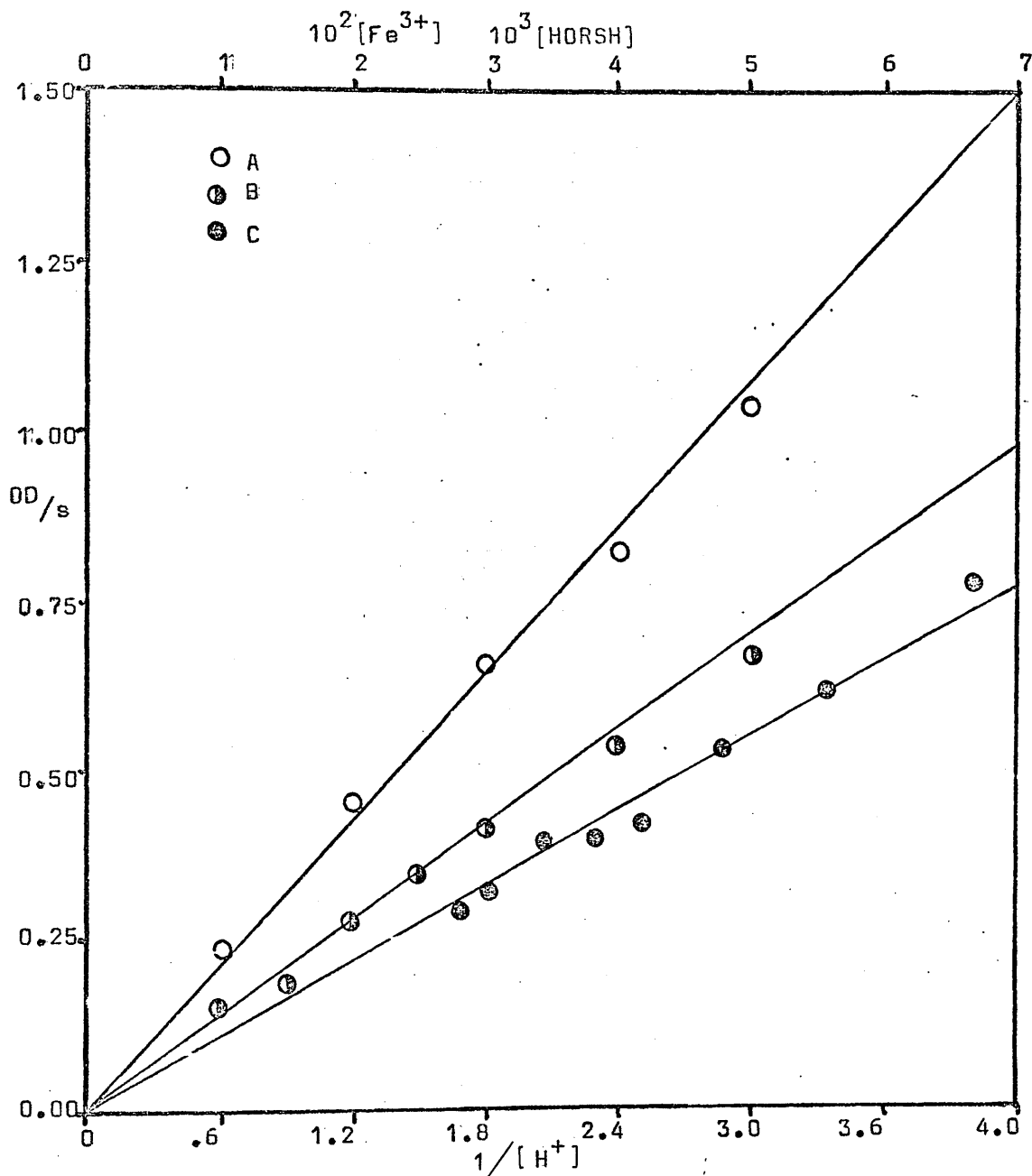


FIGURE 4.3

TABLE 4.8

Absorbance, initial rate data and pseudo-first order rate constants for reactions of 2-mercaptocarboxylic acids with iron III. $I = 1.0M$, pathlength = 0.5cm.

MAA.^a

$[H^+]/M$	$10^2 [Fe^{3+}]/M$	$10^3 [HORSH]/M$	$10^2 OD.$	k_{obs}/s^{-1}	$10^2 -ir/OD.s^{-1}$
T = 10°C.					
0.4	1.500	2.22	2.03	2.62	5.26
	2.000		2.55	3.18	7.97
	2.500		3.06	3.41	10.27
	3.000		3.70	3.41	12.40
	4.000		4.31	3.97	16.78
	5.000		4.85	4.12	19.59
0.45	1.375	2.43	1.75	2.91	5.02
	1.833		2.26	3.03	6.75
	2.292		2.64	3.31	8.60
	2.750		3.07	3.66	11.04
	3.667		3.77	3.92	14.51
	4.583		4.48	4.40	19.29
0.5	1.250	2.44	1.44	3.06	4.35
	1.667		1.83	3.25	5.83
	2.088		2.18	3.36	7.19
	2.500		2.57	3.57	9.00
	3.333		3.15	3.88	12.00
	4.175		3.66	4.31	15.46
T = 15°C					
0.4	1.500	2.29	2.48	4.56	11.06
	2.000		3.11	5.00	15.17
	2.500		3.67	5.44	19.44
	3.000		4.11	5.71	22.82
	4.000		5.11	6.35	31.47
	5.000		6.05	6.93	40.53
0.45	1.375	2.51	2.14	4.94	10.33
	1.833		2.64	4.89	12.60
	2.292		3.21	5.56	17.34
	2.750		3.61	5.71	20.03
	3.667		4.47	6.28	27.24
	4.583		5.19	7.17	35.89

Table 4.8 cont'd.

$[H^+]/M$	$10^2 [Fe^{3+}]/M$	$10^3 [HORSH]/M$	$10^2 OD.$	k_{obs}/s^{-1}	$10^2 -ir/OD.s^{-1}$
T = 15° C.					
0.5	1.250	2.44	1.63	4.90	7.81
	1.667		2.08	5.32	10.77
	2.088		2.47	5.45	13.08
	2.500		2.92	5.98	16.96
	3.333		3.56	6.34	21.88
	4.175		4.18	6.40	25.91
T = 20° C.					
0.3	1.167	2.56	3.71	6.76	24.24
	1.750		4.71	7.43	33.74
	2.333		5.82	9.03	50.23
	2.918		6.13	10.66	65.31
	3.500		7.96	11.12	83.82
	4.667		8.64	12.01	97.77
	5.835		10.32	15.98	152.43
0.4	1.000	2.52	1.87	6.48	11.73
	1.500		2.64	7.34	18.70
	2.000		3.25	7.68	23.99
	2.500		3.85	8.24	30.47
	3.000		4.50	9.06	39.01
	4.000		5.40	10.20	52.39
	5.000		6.50	10.40	64.23
0.45	.917	2.38	1.62	6.33	9.93
	1.375		2.35	8.14	18.36
	1.833		3.19	7.48	23.02
	2.292		3.56	9.38	31.86
	2.750		4.13	9.15	36.11
	3.667		5.09	11.05	53.27
	4.583		5.89	11.06	61.70
0.5	.833	2.25	1.31	6.7	8.50
	1.250		1.82	8.24	14.41
	1.667		2.24	8.08	17.36
	2.088		2.71	9.14	23.69
	2.500		3.12	9.89	29.37
	3.333		4.12	9.71	38.16
	4.175		4.64	9.30	41.21

Table 4.8 cont'd.

2 MPA^a
 $[H^+]_M$ $10^2 [Fe^{3+}]_M$ $10^3 [HORSH]_M$ $10^2 OD$ k_{obs}/s^{-1} $10^2 -ir/OD \cdot s^{-1}$
T = 10⁰ C.

0.4	1.500	2.70	2.87	1.71	4.86
	2.000		3.69	1.85	6.77
	2.500		4.64	1.97	9.05
	3.000		5.19	2.08	10.68
	4.000		6.48	2.24	14.36
	5.000		7.82	2.29	17.71
0.45	1.375	2.80	2.26	1.91	4.28
	1.833		2.89	2.01	5.75
	2.292		3.56	2.07	7.29
	2.750		4.14	2.09	8.57
	3.667		5.34	2.24	9.61
	4.583		6.37	2.33	14.66
0.5	1.250	2.52	1.59	2.11	3.32
	1.667		2.01	2.15	4.28
	2.088		2.48	2.17	5.33
	2.500		2.97	2.18	6.40
	3.333		3.85	2.36	8.97
	4.175		4.61	2.46	11.21

T = 15⁰ C.

0.4	1.500	2.62	3.27	3.01	9.68
	2.000		4.21	3.11	12.91
	2.500		5.04	3.33	16.50
	3.000		5.93	3.48	20.29
	4.000		7.39	3.79	27.48
	5.000		8.73	4.04	34.58
0.45	1.375	2.62	2.46	3.23	7.83
	1.833		3.19	3.28	10.30
	2.292		3.88	3.32	12.68
	2.750		4.51	3.57	15.81
	3.667		5.79	3.73	21.21
	4.583		6.94	4.05	27.54
0.5	1.250	2.52	1.77	3.52	6.13
	1.667		2.30	3.33	7.53
	2.088		2.95	3.62	10.47
	2.500		3.42	3.72	12.49
	3.333		4.31	4.00	16.91
	4.175		5.24	4.10	21.06

Table 4.8 cont'd.

$[H^+]_M$	$10^2 [Fe^{3+}]_M$	$10^3 [HORSH]_M$	10^2OD.	k_{obs}/s^{-1}	$10^2 -ir/\text{OD.}s^{-1}$
T = 20° C.					
0.3	1.167	2.76	4.50	4.01	17.69
	1.750		6.88	4.43	29.80
	2.333		8.55	5.01	41.78
	2.918		9.47	5.10	47.10
	3.500		11.49	5.69	63.54
	4.667		14.52	6.64	93.30
	5.835		16.53	7.44	118.53
	0.4		1.000	2.61	2.66
1.500		3.73	4.12		15.06
2.000		4.86	4.92		23.33
2.500		5.78	4.94		27.87
3.000		6.43	5.59		34.94
4.000		8.66	6.54		54.85
5.000		10.58	6.92		70.76
0.45	.917	2.89	2.07	5.03	10.16
	1.375		3.03	5.42	15.99
	1.833		4.01	5.24	20.50
	2.292		4.82	5.68	26.60
	2.750		5.64	5.95	32.57
	3.667		7.19	6.18	43.11
	4.583		9.01	6.76	58.91
0.5	.833	2.26	1.67	4.98	8.10
	1.250		1.77	6.83	11.68
	1.667		2.45	6.02	14.32
	2.088		2.83	6.08	16.69
	2.500		3.53	6.46	22.11
	3.333		4.45	6.36	27.40
	4.175		5.20	6.35	32.00

Table 4.8 cont'd.

2 MIBA^a

$[H^+]/M$	$10^2 [Fe^{3+}]/M$	$10^3 [HORSH]/M$	10^2OD.	k_{obs}/s^{-1}	$10^2 -ir/\text{OD.}s^{-1}$
T = 10 ⁰ C.					
0.3	1.167	2.25	5.47	0.568	3.10
	1.750		8.10	0.600	4.84
	2.333		10.62	0.610	6.46
	2.918		13.18	0.64	8.41
	3.500		15.36	0.64	9.80
	4.667		20.07	0.64	12.81
	5.835		24.56	0.71	17.38
0.4	1.000	2.09	2.51	0.80	2.00
	1.500		3.71	0.83	3.06
	2.000		4.85	0.83	4.01
	2.500		6.09	0.81	4.91
	3.000		7.23	0.81	5.83
	4.000		9.33	0.87	8.08
	5.000		11.56	0.88	10.13
0.5	.833	2.04	1.90	0.75	1.42
	1.250		2.71	0.84	2.27
	1.667		3.45	0.85	2.92
	2.088		4.30	0.88	3.77
	2.500		4.74	0.92	4.34
	3.333		6.25	0.92	5.72
	4.175		7.67	0.96	7.33
0.6	0.667	2.19	0.76	1.31	0.99
	1.000		1.19	1.17	1.38
	1.333		1.60	1.24	1.97
	1.667		1.92	1.22	2.33
	2.000		2.30	1.21	2.76
	2.667		3.10	1.19	3.66
	3.333		3.88	1.21	4.67
T = 15 ⁰ C.					
0.3	1.167	2.31	4.15	1.19	4.91
	1.750		6.18	1.26	7.73
	2.333		8.04	1.23	9.83
	2.918		10.35	1.19	12.25
	3.500		12.29	1.25	15.26
	4.667		17.35	1.33	22.92
	5.835		22.06	1.43	31.32

Table 4.8 cont'd.

$[H^+]_M$	$10^2 [Fe^{3+}]_M$	$10^3 [HORSH]_M$	$10^2 OD.$	k_{obs} / s^{-1}	$10^2 -ir / 00.s^{-1}$
T = 15 ⁰ C.					
0.4	1.000	2.27	3.01	1.29	3.86
	1.500		4.43	1.31	5.76
	2.000		5.92	1.35	7.94
	2.500		7.33	1.30	9.46
	3.000		8.67	1.33	11.46
	4.000		11.48	1.37	15.62
	5.000		14.06	1.51	21.08
0.5	.833	2.01	1.57	1.66	2.58
	1.250		2.34	1.57	3.65
	1.667		3.11	1.67	5.14
	2.088		3.88	1.61	6.70
	2.500		4.68	1.61	7.47
	3.333		5.98	1.68	9.97
	4.175		7.37	1.67	12.20
0.6	0.667	2.22	0.87	2.14	1.84
	1.000		1.36	1.97	2.65
	1.333		1.81	2.07	3.70
	1.667		2.21	2.00	4.37
	2.000		2.68	2.05	5.43
	2.667		3.58	1.96	6.94
	3.333		4.45	2.07	9.12
T = 20 ⁰ C.					
0.3	1.167	2.20	6.70	1.61	10.70
	1.750		9.77	1.85	17.91
	2.333		12.82	1.69	21.48
	2.918		15.06	1.86	27.75
	3.500		18.40	1.82	33.18
	4.667		23.87	2.01	47.50
	5.835		28.45	2.03	57.18
0.4	1.000	2.61	3.69	2.12	7.75
	1.500		5.64	2.22	12.39
	2.000		7.27	2.23	16.02
	2.500		9.27	2.28	20.90
	3.000		10.90	2.36	25.43
	4.000		14.23	2.34	32.91

Table 4.8 cont'd.

$[H^+]_M$	$10^2 [Fe^{3+}]_M$	$10^3 [HORSH]_M$	$10^2 OD.$	k_{obs}/s^{-1}	$10^2 -ir/OD.s^{-1}$
T = 20 ⁰ C.					
0.4	5.000	2.61	17.21	2.50	42.50
0.45	.917	2.42	2.62	2.27	5.88
	1.375		3.91	2.26	8.73
	1.833		5.10	2.33	11.74
	2.292		6.37	2.43	15.29
	2.750		7.51	2.46	18.25
	3.667		9.98	2.48	24.45
	4.583		12.22	2.53	30.52
0.5	.833	2.50	1.98	2.57	5.02
	1.250		2.99	2.68	7.90
	1.667		4.04	2.65	10.56
	2.088		4.98	2.69	13.21
	2.500		5.94	2.76	16.16
	3.333		7.67	2.73	20.65
	4.175		9.61	2.73	25.87
0.6	0.667	2.42	1.02	2.99	3.61
	1.000		1.58	3.14	4.90
	1.333		2.03	3.19	6.39
	1.667		2.60	3.08	7.87
	2.000		3.11	2.99	9.16
	2.667		4.09	3.31	13.31
	3.333		5.08	3.21	16.05
0.65	.580	2.29	0.67	3.25	2.15
	1.460		1.68	3.42	5.65
	2.920		3.41	3.47	11.63
0.7	.500	2.24	0.55	3.29	1.78
	1.250		1.52	3.77	5.61
	2.500		2.40	3.78	8.89
T = 25 ⁰ C.					
0.3	1.167	2.31	5.32	2.90	15.22
	1.750		8.00	3.42	26.91
	2.333		10.81	3.36	35.72
	2.918		13.53	3.47	46.13
	3.500		16.18	3.59	57.06
	4.667		21.92	3.68	79.20
	5.835		26.32	4.01	103.44

Table 4.8 cont'd.

$[H^+]_M$	$10^2 [Fe^{3+}]_M$	$10^3 [HORSH]_M$	$10^2 OD.$	k_{obs}/s^{-1}	$10^2 -ir/OD.s^{-1}$
T = 25° C.					
0.4	1.000	2.27	3.73	3.32	12.18
	1.500		5.46	3.45	18.52
	2.000		7.21	3.54	25.08
	2.500		8.81	3.52	30.48
	3.000		10.64	3.65	38.12
	4.000	2.06	12.79	3.81	47.80
	5.000		16.61	3.85	62.75
0.5	.833	1.95	1.97	3.90	7.54
	1.250		2.98	4.13	12.06
	1.667		3.88	4.23	16.09
	2.088		4.76	4.29	20.00
	2.500		5.86	4.44	25.47
	3.333		7.58	4.53	33.58
	4.175		9.23	4.54	40.95
0.6	0.667	2.14	1.25	5.40	6.57
	1.000		1.72	5.22	8.73
	1.333		2.25	5.33	11.70
	1.667		2.78	5.38	14.54
	2.000		3.41	5.34	17.74
	2.667		4.46	5.35	23.24
	3.333		5.59	5.52	30.03

Table 4.8 cont'd.

2 MIBA^b

$[H^+]/M$	$10^2 [Fe^{3+}]/M$	$10^3 [HORSH]/M$	$10^2 \theta_{00}$	k_{obs}/s^{-1}	$10^2 -ir/00.s^{-1}$
T = 20° C.					
0.3	1.167	2.46	6.64	1.78	
	1.751		9.93	1.87	
	2.333		13.01	1.93	
	2.918		16.02	1.94	
	3.500		18.89	2.00	
	4.667		24.85	2.07	
	5.833		29.98	2.18	
0.4	1.000	2.50	3.49	2.14	
	1.500		5.19	2.28	
	2.000		6.87	2.38	
	2.500		8.52	2.39	
	3.000		10.18	2.38	
	4.000		13.36	2.52	
	5.000		16.77	2.51	
0.5	0.833	2.37	1.73	2.82	
	1.250		2.56	2.88	
	1.667		3.43	2.91	
	2.088		4.37	2.85	
	2.500		5.18	2.86	
	3.333		6.94	2.95	
	4.167		8.67	2.99	
0.6	0.667	2.64	1.08	3.77	
	1.000		1.62	3.40	
	1.333		2.13	3.50	
	1.667		2.67	3.32	
	2.000		3.17	3.67	
	2.667		4.34	3.39	
	3.333		5.47	3.75	

a - NaClO₄b - LiClO₄

first order expression

$$\frac{d(\text{FeORS}^+)}{dt} = \{k_a [\text{Fe}^{3+}]_0 + k_b\} \{ [\text{FeORS}^+] - (\text{FeORS}^+) \} \quad 4.45$$

where

$$k_a = k_2 [\text{H}^+]^2 + (k_4 + k_{12}) [\text{H}^+] + k_{14} \quad K_1 / ([\text{H}^+]^2 + K_a [\text{H}^+]) \quad 4.46$$

and

$$k_b = k_2 [\text{H}^+]^2 + (k_4 + k_{12}) [\text{H}^+] + k_{14} \quad 4.47$$

Description of the data, table 4.8, by this expression is dependent on the approach of the reaction to true equilibrium. At higher acidities, all first order plots were linear to greater than three half lives. At lower acidities however, significant curvature was observed and apparent rate constants derived from the initial stages of the reaction were used. The deviation was such that these were enhanced relative to the true rate constants.

Plots of the observed rate constant $k_a [\text{Fe}^{3+}]_0 + k_b$ against $[\text{Fe}^{3+}]_0$ at constant $[\text{H}^+]$ should yield values for k_a and k_b . In general good linearity was found in all cases, including those using apparent rate constants. Values of k_a and k_b are reported in table 4.9.

Since the available range of iron III concentrations was small ($0.5 - 6 \times 10^{-2}$ M) and deviations from true equilibrium varied over the metal-ion range employed, the slopes k_a of equation 4.45 which might have been considered to yield rate constants were in fact not used. Instead, the intercepts k_b were derived to a greater degree of accuracy and were used to determine the kinetic parameters employing equation 4.47 and the relevant stability constants.

Using equation 4.47, a quadratic dependence of k_b on $[\text{H}^+]$ would be expected and, although complex acidity dependences were observed in most cases, the following rationalisation was employed.

TABLE 4.9

Variation of constants k_a and k_b with temperature ^a

LIGAND	$[H^+]/M$	$T^{\circ}C$	k_a	k_b
MAA ^b	0.4	10	45.0 \pm 6.0	2.00 \pm 0.15
	0.45		45.2 \pm 3.5	2.32 \pm 0.10
	0.5		43.6 \pm 1.7	2.49 \pm 0.04
	0.4	15	71.9 \pm 6.0	3.58 \pm 0.15
	0.45		59.5 \pm 6.5	4.16 \pm 0.12
	0.5		49.8 \pm 4.5	4.51 \pm 0.18
	0.3	20	181 \pm 22	4.71 \pm 0.63
	0.4		124 \pm 13	5.30 \pm 0.35
	0.45		131 \pm 15	5.82 \pm 0.45
	0.5		92 \pm 22	6.53 \pm 0.55
2-MPA ^b	0.4	10	20.3 \pm 2.5	1.43 \pm 0.06
	0.45		13.8 \pm 1.5	1.76 \pm 0.04
	0.5		13.8 \pm 1.8	1.92 \pm 0.05
	0.4	15	29.9 \pm 2.0	2.58 \pm 0.05
	0.45		26.9 \pm 2.0	2.82 \pm 0.05
	0.5		18.9 \pm 2.0	3.26 \pm 0.05
	0.3	20	74.4 \pm 4.0	3.15 \pm 0.15
	0.4		70.2 \pm 6.5	3.46 \pm 0.20
	0.45		43.6 \pm 3.5	4.66 \pm 0.13
	0.5		27.8 \pm 7.5	5.29 \pm 0.20

Table 4.9 cont'd.

LIGAND	[H ⁺]/M	T ^o C	k _a	k _b
2-MIBA ^b	0.3	10	2.2 ± 0.5	0.56 ± 0.02
	0.4		1.8 ± 0.8	0.79 ± 0.02
	0.5		2.2 ± 0.8	0.88 ± 0.01
	0.6		1.3 ± 1.0	1.21 ± 0.03
	0.3	15	4.6 ± 0.7	1.13 ± 0.02
	0.4		3.7 ± 0.7	1.26 ± 0.02
	0.5		2.9 ± 1.0	1.56 ± 0.03
	0.6		1.9 ± 2.0	2.00 ± 0.05
	0.3	20	8.6 ± 1.1	1.53 ± 0.04
	0.4		8.0 ± 0.8	2.10 ± 0.02
	0.45		7.3 ± 0.7	2.24 ± 0.02
	0.5		5.3 ± 0.9	2.60 ± 0.03
	0.6		4.5 ± 1.5	3.08 ± 0.03
	0.65		5.3 ± 4.0	3.34 ± 0.30
	0.7		3.7 ± 3.0	3.72 ± 0.20
	0.3		25	17.1 ± 2.0
	0.4	10.3 ± 1.0		3.33 ± 0.03
	0.5	16.7 ± 1.2		3.95 ± 0.03
0.6	7.5 ± 3.1	5.25 ± 0.07		
2-MIBA ^c	0.3	20	7.2 ± 0.4	1.73 ± 0.02
	0.4		5.9 ± 0.4	2.21 ± 0.02
	0.5		3.4 ± 0.3	2.85 ± 0.02
	0.6		1.0 ± 0.3	3.39 ± 0.02

a - Fe(III) = 5-12 × 10⁻³ M, HORSH = 2 × 10⁻³ M, I = 1.00M,
λ = 610 - 640 nm.

b - NaClO₄

c - LiClO₄

A linear plot of k_b against $[H^+]$ was obtained in the case of 2-MIBA as shown in figure 4.4. From this curve it is seen that the intercept k_{14} is zero within experimental error and there is apparently no higher order dependence on acidity. It would appear that the dissociation reaction proceeds by way of pathways 4.41 and 4.42, and in this respect, the data complement the initial rate studies where a linear acidity dependence was anticipated. 2-MIBA is exceptional among these thiols because the equilibrium constant K_1 is small and interference from the subsequent redox reaction is slight. In the case of the other two thiols, this interference was experienced and accounted for at lower acidities (figure 4.4). At higher acidities however, the data conform to the same pattern as was observed with 2-MIBA. Based on this and the more reliable initial rate data, values for all three thiols are described using a similar mechanism.

The slopes of k_b against $[H^+]$ plots yield the composite constant ($k_4 + k_{12}$) suggesting the two complex formation pathways via $Fe(H_2O)_6^{3+}$ and $Fe(H_2O)_5OH^{2+}$ respectively 4.41 and 4.42 which are kinetically indistinguishable. In this case the proton ambiguity was resolved using criteria suggested by Espenson¹⁸³ regarding the "reasonableness" of the rate constants.

The most recent value¹⁷³ for the water exchange rate parameter for $Fe(H_2O)_6^{3+}$ is $150s^{-1}$. Given a postulated rate constant of $10^3 M^{-1} s^{-1}$ for k_3 , viz. an order of magnitude greater than the rate for water exchange, it may be shown using the equilibrium constant k_2 , that k_4 contributes at most only 4% to the composite rate constant ($k_4 + k_{12}$). The percentage would fall proportionately if the assumed rate constant were reduced to a value comparable to that found in other studies. This observation strongly suggests that the only effective contributing pathway to the formation reaction is that in 4.42 and the rate constants derived using this model are presented in table 4.10. The parameters evaluated in this way are in good agreement with those from the initial rate data.

Plots of k_b against $[H^+]$ (equation 4.47) for reactions between iron III and 2-mercaptocarboxylic acids. $T=20^\circ C$
 $I=1.0M$.

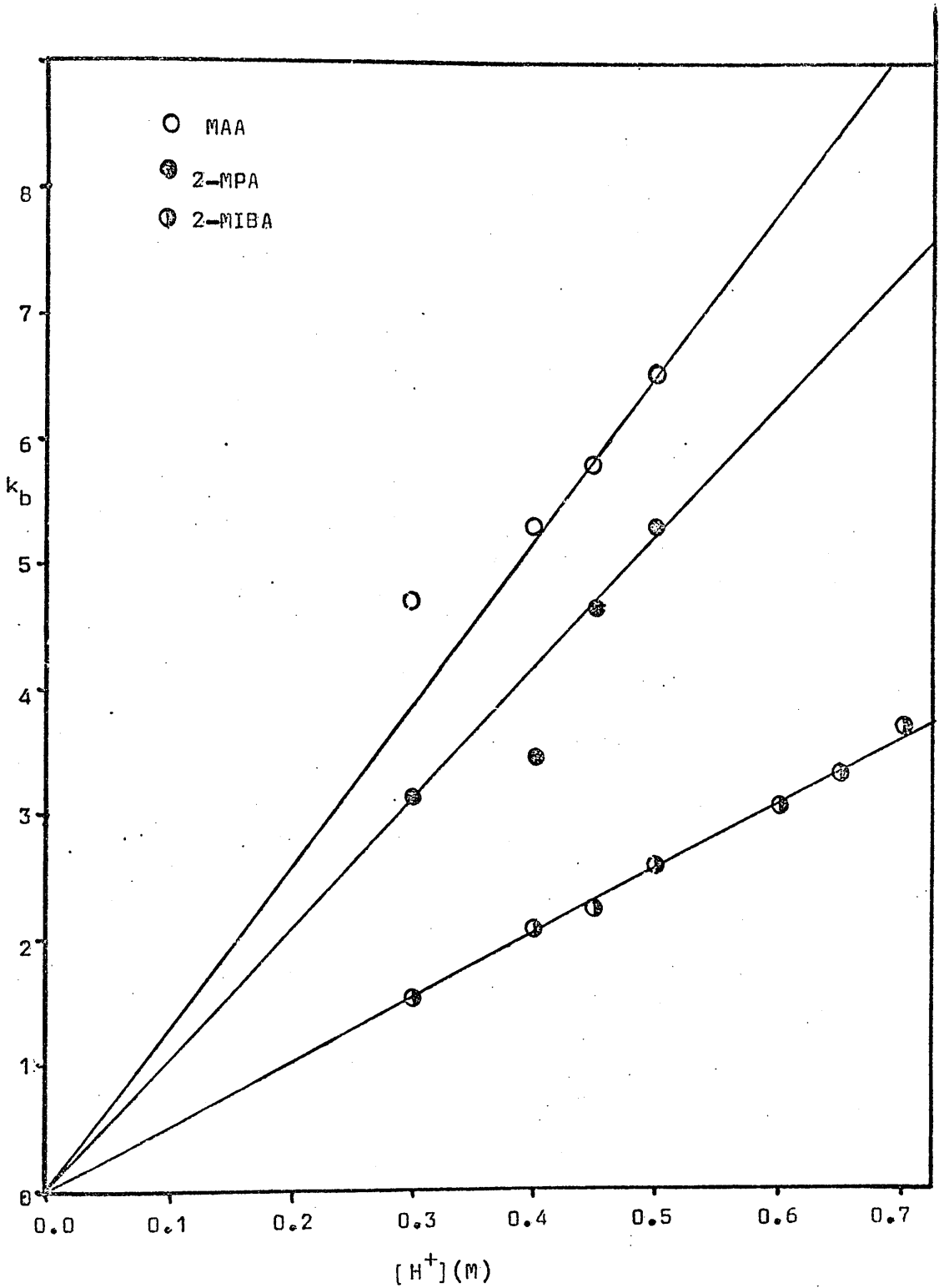


FIGURE 4.4

TABLE 4.10

Complex formation rate constants and activation parameters

T = 25°C I = 1.00

LIGAND	T°C	$k_{12} + k_4$ $M^{-1}s^{-1}$	$10^3 k_{11}$ $M^{-1}s^{-1}$ a	$10^3 k_{11}$ $M^{-1}s^{-1}$ b
MAA	10	5.05 ± 0.5	14.5 ± 1.5	15.6 ± 3
	15	9.10 ± 0.5	21.9 ± 2	20.8 ± 4
	20	13.0 ± 1.0	28.5 ± 3	27.6 ± 6
	25	22.4 ± 1.5	40.6 ± 4	
2-MPA	10	3.84 ± 0.5	5.75 ± 0.5	5.99 ± 1
	15	6.43 ± 0.5	8.33 ± 1.0	8.35 ± 2
	20	10.5 ± 1.0	11.2 ± 1.0	11.7 ± 2
	25	16.7 ± 1.5	15.6 ± 1.5	
2-MIBA	10	1.89 ± 0.2	0.80 ± 0.05	0.85 ± 0.2
	15	3.18 ± 0.3	1.10 ± 0.10	1.07 ± 0.2
	20	5.15 ± 0.5	1.50 ± 0.15	1.43 ± 0.3
	25	8.35 ± 0.7	2.20 ± 0.20	2.02 ± 0.4
2-MSA ^c	10	1.80 ± 0.5	4.47 ± 1.0	
	14	2.68 ± 0.5	5.75 ± 1.0	
	20	5.00 ± 1.0	9.33 ± 2.0	
	25	7.78 ± 1.0	12.00 ± 2.0	

a - derived from k_{12} , K_1 , K_h b - derived from k_{11} , ϵ , K_h

c - recalculated from ref.197

Further support for this line of reasoning is provided by the absence of any evidence for equilibrium 4.43 and by the fact that since the dissociation constants of the carboxylic acids in the ligands are $10^{-4}M$ (chapter 6), in the concentration range used ($\sim 10^{-3}M$), the amounts of dissociated acid present in solution are very small indeed.

This interpretation of a common mechanism allows for re-evaluation of the complex acidity dependence observed in the reaction with 2-mercaptosuccinic acid. Relevant values for the rate constants in this case are also presented in table 4.10.

The rate constants for reaction 4.42 are in accord with the limits proposed by Seewald and Sutin for comparable processes. It is difficult however to reconcile the large variation in rate constants for such similar ligands with an I_D mechanism. Indeed, using the free energy relationship suggested in chapter 1 (equations 1.4 and 1.5), a slope of approximately 0.5 was obtained (figure 4.5) indicative of an I_a mechanism. If changes in the value of K_1 reflect the varying nucleophilicity of the sulphhydryl group, then the results certainly do conform to the pattern expected of an I_a mechanism. There is however no reason to suppose that a sulphhydryl group adjacent to two electron releasing methyl groups should be less nucleophilic than in the absence of substituents. If anything, on electronic grounds, the opposite would be predicted. An argument based on steric reduction of the rate constant caused by bulky methyl substituents would also be consistent with an associative mechanistic interpretation of the data.

The variation in the rates of an associative reaction are generally reflected in changes in the enthalpy of activation. Activation parameters for the reactions discussed in this section were evaluated from a non-linear least squares Arrhenius treatment and are presented in table 4.11. They reveal that the trend in k_{11} with increasing methyl substitution results from the entropy of activation, enthalpy values being equal within experimental error. Thus although some associative

Plot of $\log_e k_{12}$ against $\log_e K_{11}$ for the reactions between iron III and MAA, 2-MPA and 2-MIBA. $T=25^\circ\text{C}$, $I=1.0\text{M}$.

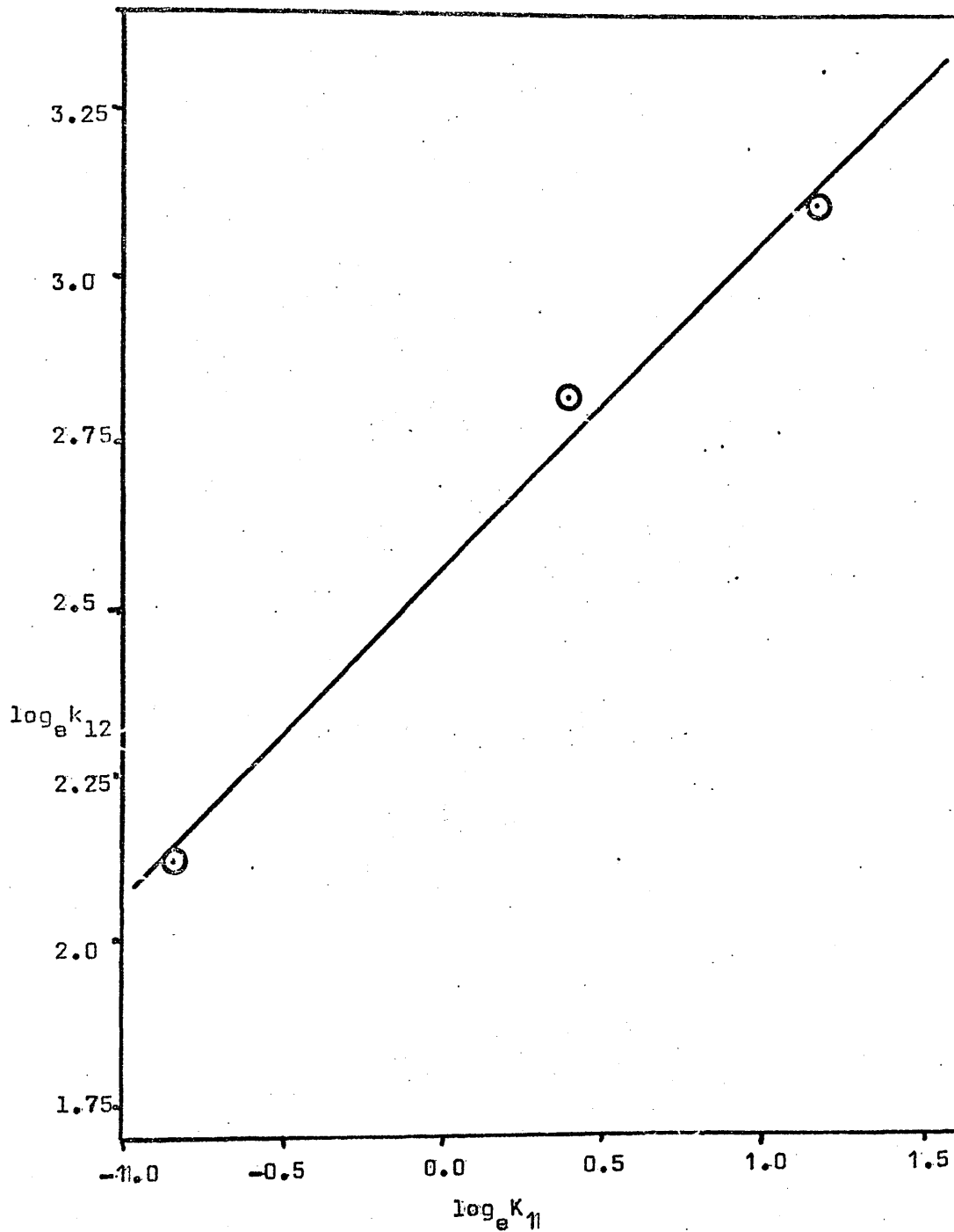


FIGURE 4.5

TABLE 4.11

Rate Constants and Activation Parameters for the Reaction between Iron III and 2-mercaptocarboxylic Acids.

LIGAND	$10^3 k_{11}/M^{-1}s^{-1}$		$k_{12}/M^{-1}s^{-1}$
MAA	40.6 ± 4		22.4 ± 1.5
ΔH^{*a}	10.5 ± 2	(11.3)	15.0 ± 2
ΔS^{*b}	-2.1 ± 3		-2.2 ± 3
2-MPA	15.6 ± 1.5		16.7 ± 1.5
ΔH^{*a}	10.3 ± 2	(10.7)	15.9 ± 2
ΔS^{*b}	-4.7 ± 3		$+0.5 \pm 3$
2-MIBA	2.20 ± 0.20		8.35 ± 0.7
ΔH^{*a}	10.3 ± 2	(9.2)	16.0 ± 2
ΔS^{*b}	-8.7 ± 3		-0.8 ± 3
2-MSA	12.1 ± 2		7.78 ± 1
ΔH^{*a}	10.8 ± 2		15.9 ± 2
ΔS^{*b}	-3.7 ± 2		0.32 ± 3

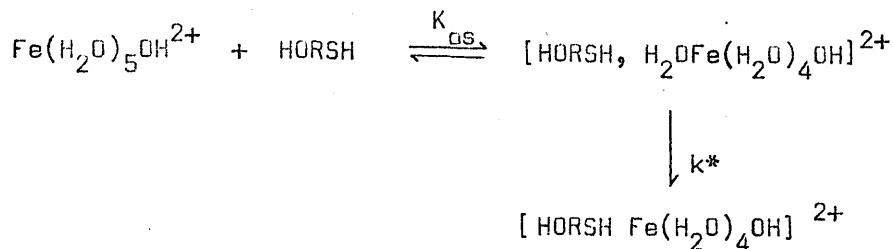
Figures in brackets are calculated from studies of the initial rate of reaction.

a - kcal mole⁻¹

b - cal °K⁻¹ mole⁻¹

character cannot be excluded, an alternative explanation is considered more likely.

In an I_d mechanism, the rate determining step is the dissociative loss of water from an outer sphere complex.



4.48

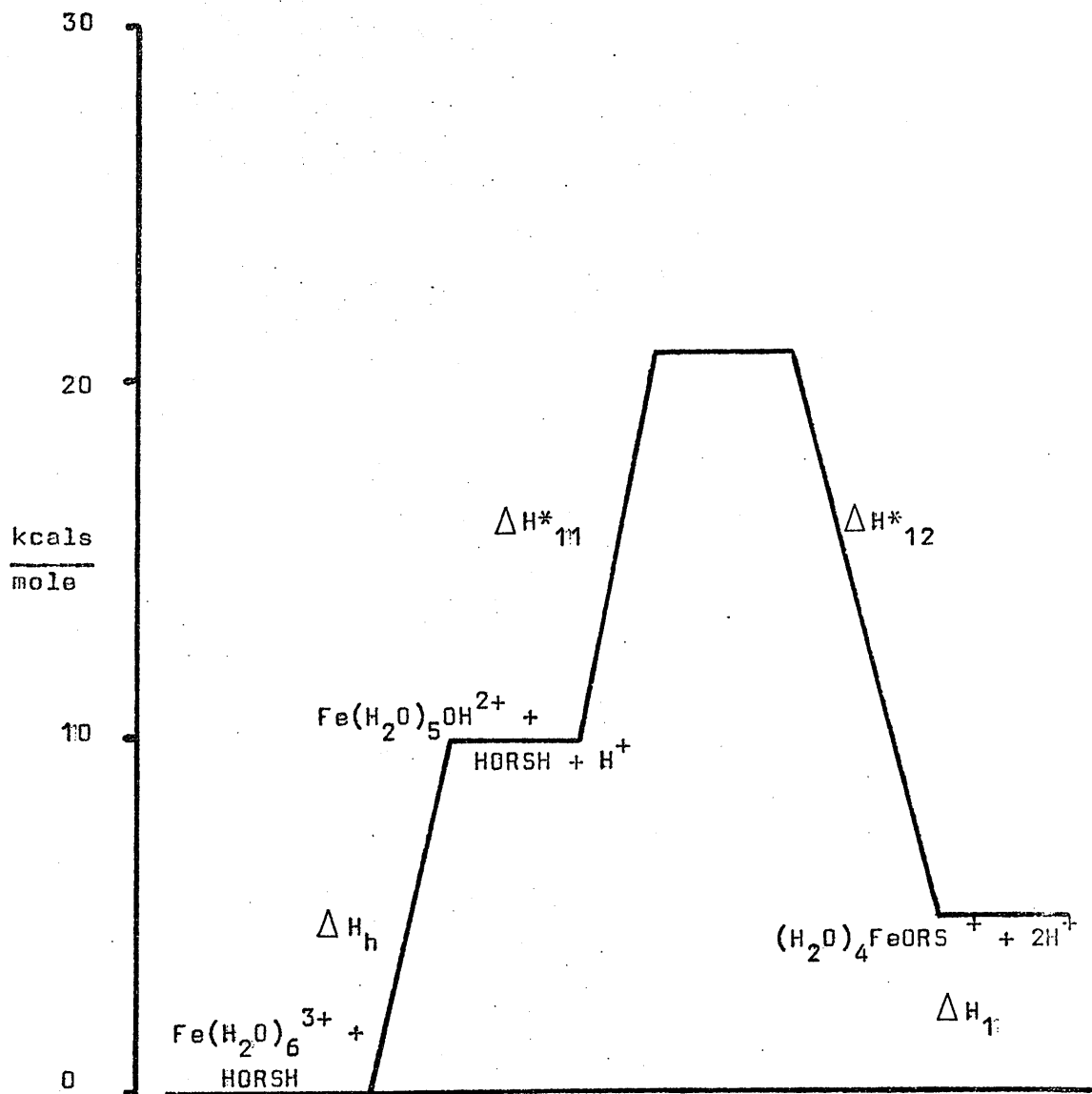
The trend in $k_{11} = K_{os} k^*$ could thus be attributed to either a change in K_{os} or k^* . Variations in the thermodynamic parameters associated with the terms k_{11} and K_1 show a similar trend with ligand structure and it is not unreasonable to suggest a common source for this effect. Since both outer and inner sphere complexes may have similar steric requirements, it is concluded that the variation in k_{11} may be attributed to the K_{os} term. Again, solvation effects apparently dominate the molecular processes.

Data for all three ligands are consistent with the enthalpy scheme 4.1 where the initial hydrolysis reaction has a accompanying enthalpy change of 10kcal mol^{-1} . The fact that this treatment holds for all three thiol acids with extinction coefficients and equilibrium constants varying by an order of magnitude would appear to justify the treatment of all reactions by a single mechanism. The thermodynamic parameters for the complex formation reaction are similar to those observed in other reactions of FeOH^{2+} with unchanged species (table 4.6).

Implicit in the formation of the blue colour is the formation of the chelate ring. The possibility of rate determining ring closure, considered because of the high basicity of the mercaptide group, is ruled out since the reaction with acetic acid proceeds at a rate slower than that observed with mercaptoacetic acid. Thus either the sulphhydryl group initiates the reaction and rate determining ring closure is unlikely or, again outer sphere associations dominate.

Assuming that the sulphhydryl group is the first to be incorporated

SCHEME 4.1.

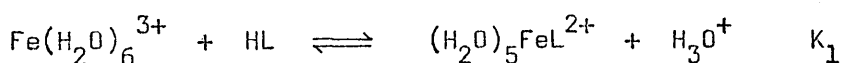


into the inner sphere, if as Nakamura et al,¹⁸⁰ suggest proton transfer to the coordinated hydroxyl takes place, the ring closure will proceed at a rate determined by water exchange in $\text{HORSFe}(\text{H}_2\text{O})_5^{2+}$ which might be comparable with that of hexaquo-iron III. This is incompatible with the findings since, in contrast to the rates obtained with some phenolic species, the reactions discussed in this thesis are not anomalously slow, if anything the opposite is true.

Substitution Reactions of Iron III with Phenolic Ligands.

The reactions of 2-hydroxyacetophenone and dihydroxytolulene with iron III were studied to complete an investigation in progress into the effects of ortho substituents in phenol substitution reactions. Experimental conditions were chosen identical to those in the previous section although lithium perchlorate was used as supporting electrolyte.

Spectra of the complexes were obtained using conventional visible spectrophotometry since redox reactions of these ligands with iron III are extremely slow. The forms of the spectra and absorption maxima (table 4.12) are similar to those reported previously for related phenols. Attempts to apply the Scott-Benesi-Hildebrand treatment to the optical density data were unsuccessful due to the small range of saturation factor which was accessible. In both cases, it was deduced that a single proton is released on complexation



4.49

A value for the extinction coefficient of 2-hydroxyacetophenone complex reported by Agren²⁰¹ from combined conductometric-spectrophotometric measurements relating to slightly different conditions was used to evaluate the equilibrium constant K_1 . In the case of dihydroxytolulene an extinction coefficient of $2000 \pm 500 \text{ M}^{-1} \text{ cm}^{-1}$ was estimated from consideration of values for similar phenolic ligands. Values for the extinction coefficients, equilibrium constants and related thermodynamic parameters are presented in tables 4.12 and 4.13. Initial rate studies (table 4.14) indicated a formation rate law of the form.

$$\text{Initial rate} = \left\{ k_{ir1} + \frac{k_{ir2}}{[\text{H}^+]_0} \right\} [\text{Fe}^{3+}]_0 [\text{HL}]_0 \quad 4.50$$

with a negligible k_{ir1} term for dihydroxytolulene. The overall rate was treated using the scheme on page 57 yielding a pseudo first order rate expression of the type,

TABLE 4.12

Absorption maxima, extinction coefficients and equilibrium constants for iron III-phenolate complexes $T = 25^{\circ}\text{C}$ $I = 1.00$

LIGAND	λ_{max} n.m.	ϵ_{max} $\text{M}^{-1}\text{cm}^{-1}$	K_1	ref.
2-hydroxyacetophenone	530 ± 10	$1300 \pm 300^{\text{a}}$	0.76	
Dihydroxytoluene	560 ± 10	2000 ± 500	0.045	
Salicylic acid	530	1620	7.4	b
Salicylaldehyde	550	1200	1.13	c
Salicylamide	525	1500	15	c
Phenol	556	1950	0.017	d

a - ref. 201

b - Z.L. Ernst and F.G. Herring, Trans. Farad Soc., 1963, 59, 2838.

c - J.P. McCann, Ph.D. Thesis, University of Glasgow, 1975.

d - ref. 136,164.

TABLE 4.13

Equilibrium constants and thermodynamic parameters for the reaction between iron III and phenolic ligands.

I = 1.00M

LIGAND	T ^o C	K ₁	ΔH kcal mole ⁻¹	ΔS cal °k ⁻¹ mole ⁻¹
2-hydroxyacetophenone	10	0.49		
	15	0.55		
	20	0.65		
	25	0.76	4.9 ± 0.4	16.1 ± 2
dihydroxytolulene ^a	10	0.030		
	15	0.030		
	20	0.042		
	25	0.045	5.2 ± 1.5	11.6 ± 5
phenol ^b	25	0.017	5.6	-2.8

a - calculated on the basis of $\epsilon = 2000\text{M}^{-1}\text{cm}^{-1}$

b - ref. 136,164.

errors:-- 2-hydroxyacetophenone K₁ ± 0.1 at all T

dihydroxytolulene K₁ ± 0.02 at all T

TABLE 4.14

Absorbance, initial rate data and pseudo-first order rate constants for reactions of phenolic ligands with iron III.

I = 1.0M, pathlength = 0.2cm.

2-Hydroxyacetophenone

$[H^+]_M$	$10^2 [Fe^{3+}]_M$	$10^3 [HL]_M$	$10^2 OD.$	k_{obs}/s^{-1}	$10^2 -ir/OD.s^{-1}$
T = 10° C.					
0.3	1.458	2.48	3.85	1.10	4.3
	2.917		7.86	1.13	8.6
	4.375		11.25	1.14	12.7
	5.833		14.60	1.17	16.7
0.4	1.250	2.63	1.77	1.10	1.9
	2.500		5.21	1.15	5.9
	3.750		7.53	1.16	8.7
	5.000		9.95	1.20	11.7
0.5	1.042	2.59	1.83	1.23	2.2
	2.083		3.35	1.27	4.2
	3.125		4.75	1.22	5.8
	4.167		6.67	1.22	8.0
0.6	0.833	2.60	1.14	1.17	1.3
	1.667		2.13	1.34	2.8
	2.500		3.26	1.25	4.0
	3.333		4.32	1.30	5.5
T = 15° C.					
0.3	1.458	2.40	3.96	1.73	6.7
	2.917		7.74	1.83	13.8
	4.375		11.00	1.82	19.7
	5.833		14.30	1.94	27.3
0.4	1.250	2.96	3.21	1.93	6.1
	2.500		6.38	1.91	11.5
	3.750		9.44	2.03	18.7
	5.000		12.20	2.05	24.4
0.5	1.042	2.54	1.88	2.08	3.8
	2.083		3.64	2.05	7.3
	3.125		5.37	2.08	10.9
	4.167		7.07	2.11	14.6

Table 4.14 cont'd.

$[H^+]_M$	$10^2 [Fe^{3+}]_M$	$10^3 [HL]_M$	10^2OD.	k_{obs}/s^{-1}	$10^2 -ir/\text{OD.}s^{-1}$
T = 15 ^o C.					
0.6	0.833	2.46	1.43	2.10	2.9
	1.667		2.52	2.13	5.2
	2.500		3.80	2.18	8.7
	3.333		5.05	2.18	10.7
T = 20 ^o C.					
0.3	1.458	2.66	2.26	2.99	6.7
	2.917		4.37	3.02	13.1
	4.375		6.41	3.09	19.8
	5.833		8.43	3.36	28.0
0.4	1.250	3.01	1.66	3.06	5.0
	2.500		3.22	3.26	10.4
	3.750		3.35	3.35	15.8
	5.000		6.14	3.28	19.9
0.5	1.042	2.78	1.00	3.40	3.6
	2.083		2.00	3.37	6.7
	3.125		2.90	3.40	9.7
	4.167		3.89	3.33	12.8
0.6	0.833	2.90	0.65	3.60	2.3
	1.667		1.38	3.62	5.0
	2.500		2.03	3.62	7.4
	3.333		2.72	3.47	9.4
T = 25 ^o C.					
0.3	1.458	2.40	2.38	5.02	11.6
	2.917		4.63	5.00	23.0
	4.375		6.88	5.23	34.7
	5.833		8.65	5.42	45.6
0.4	1.250	2.96	1.92	4.90	8.8
	2.500		3.80	5.17	18.7
	3.750		5.40	5.21	27.1
	5.000		7.15	5.38	37.5
0.5	1.042	2.54	1.12	5.21	5.7
	2.083		2.41	5.06	11.8
	3.125		3.10	5.69	16.9
	4.167		4.45	5.35	22.4
0.6	0.833	2.46	0.81	6.42	5.1
	1.667		1.49	6.30	10.3
	2.500		2.29	6.00	12.5
	3.333		6.21	5.68	34.3

Table 4.14 cont'd.

Dihydroxylolulene

$[H^+]/M$	$10^2 [Fe^{3+}]/M$	$10^3 [HL]/M$	$10^2 OD.$	k_{obs}/s^{-1}	$10^2 -ir/OD.s^{-1}$	
T = 10° C.						
0.3	2.917	6.14	1.94	10.5	17.9	
	4.375		2.81	10.9	26.7	
	5.833		3.86	10.2	34.8	
0.4	5.833	6.93	2.20	9.1	17.9	
	2.500		6.01	1.24	11.7	11.6
	3.750			1.84	11.3	18.0
0.5	5.000		2.27	11.1	22.0	
	3.125	6.04	1.26	12.1	13.2	
	4.167		1.63	11.7	16.6	
0.6	3.333	6.01	1.09	12.7	11.7	
	3.333	3.44	0.63	12.9	6.9	
T = 15° C.						
0.3	2.917	6.14	5.79	16.3	77.5	
	4.375		6.00	16.5	81.0	
	5.833		4.77	19.0	72.1	
0.4	2.500	6.01	1.21	20.9	23.1	
	3.750		2.41	19.4	34.0	
	5.000		2.56	20.6	41.2	
0.5	4.167	6.04	1.97	19.6	30.4	
0.6	3.333	6.01	1.93	22.3	33.2	
T = 20° C.						
0.3	2.917	6.14	1.02	23.6	22.4	
	4.375		1.81	23.9	21.2	
	5.833		2.15	25.3	29.3	
0.4	2.500	6.01	0.65	24.3	13.9	
	3.750		0.95	24.1	21.2	
	5.000		1.17	27.2	29.3	
0.5	2.083	6.04	0.45	25.4	10.5	
	3.125		0.63	25.7	15.0	
	4.167		0.95	26.4	23.1	
0.6	3.333	3.44	0.36	25.0	8.4	
	3.333	6.01	0.59	26.5	14.5	

Table 4.14 cont'd.

$[H^+]_M$	$10^2 [Fe^{3+}]_M$	$10^3 [HL]_M$	$10^2 OD.$	k_{obs}/s^{-1}	$10^2 -ir/OD.s^{-1}$
T = 25° C.					
0.3	2.917	6.14	1.72	35.2	52.0
	4.375		1.20	36.7	50.0
	5.833		2.23	36.5	76.0
0.4	2.500	5.90	0.68	33.7	27.0
	3.750		0.91	36.7	30.0
	5.000		1.35	39.3	52.0
0.5	3.125	6.04	0.67	33.8	21.0
	4.167		0.87	36.5	28.0
0.6	3.333	6.01	0.64	37.0	26.0

$$\frac{d[(H_2O)_5FeL^{2+}]}{dt} = \left\{ k_a [Fe^{3+}]_0 + k_b \right\} \left\{ [FeL^{2+}] - (FeL^{2+}) \right\} \quad 4.51$$

in which

$$k_a = k_1 + \frac{k_3 K_a}{[H^+]} + \frac{k_{11} K_h}{[H^+]} + \frac{k_{13} K_h K_a}{[H^+]^2} \quad 4.52$$

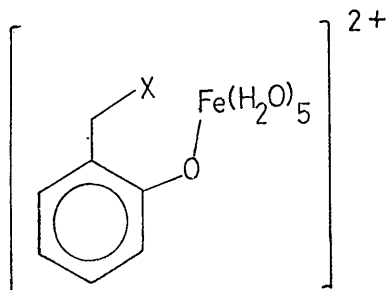
and

$$k_b = \left\{ k_1 [H^+] + k_3 K_a + k_{11} K_h + \frac{k_{13} K_a K_h}{[H^+]} \right\} \frac{1}{K_1} \quad 4.53$$

The variance of the observed rate constant with iron III, table 4.14, is very small consistent with the magnitude of the equilibrium constant. As in the preceding section, reaction rates were evaluated from the intercepts k_b and the relevant equilibrium constants. Plots of k_b against $[H^+]$ figure 4.6 were linear with finite intercepts. In the case of dihydroxytolulene, the slope was zero within experimental error in agreement with the initial rate findings.

The slopes of these plots may be related unambiguously to the rate constant k_1 for reaction between $Fe(H_2O)_6^{3+}$ and the protonated phenol using the equilibrium constant K_1 . Intercepts however correspond to the kinetically indistinguishable pathways 4.22 and 4.24. As with the mercaptocarboxylic acids, the high ligand basicity allows assignment of the forward rate solely to pathway 4.24 involving reaction between $Fe(H_2O)_5OH^{2+}$ and the protonated ligand. Values for the derived rate constants and corresponding thermodynamic parameters are presented in table 4.15, together with relevant data for related ligands.

The equilibrium data may be interpreted in terms of monodentate complexes



4.54

Plots of k_b against $[H^+]$ (equation 4.53) at various temperatures for the reaction between iron III and 2-hydroxyacetophenone. $I=1.0M$.

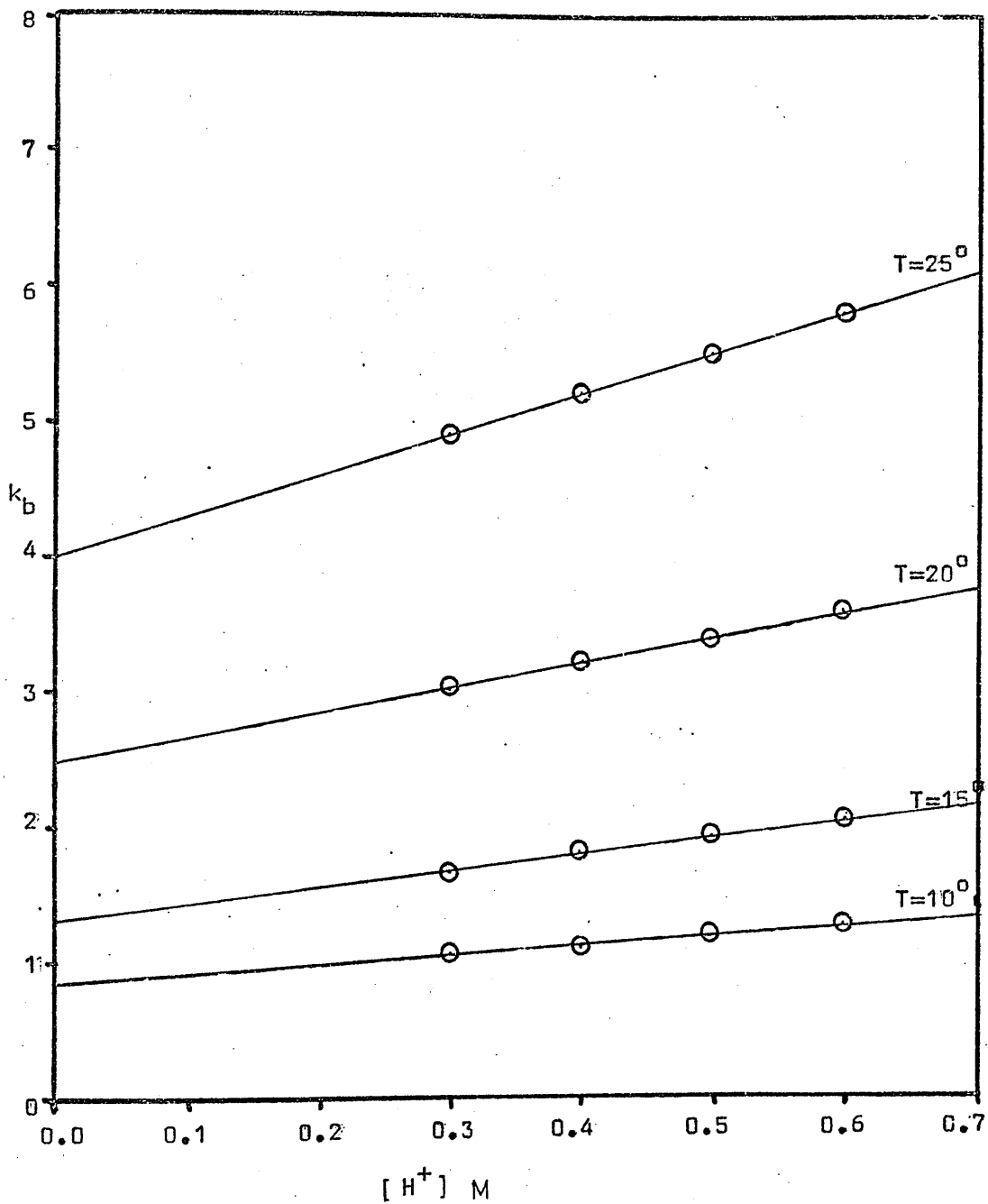


FIGURE 4.6

TABLE 4.15

Rate constants and thermodynamic parameters for complex formation reactions between iron III and phenolic ligands.

I = 1.0M.

LIGAND	T °C	$k_{11}/M^{-1}s^{-1}$	$k_{21}/M^{-1}s^{-1}$	$10^3 k_{11}$ $M^{-1}s^{-1}$	k_{12}/s^{-1}
hap	10	0.42 ± 0.1	0.69 ± 0.1	0.64 ± 0.2	0.85 ± 0.2
	15	0.72 ± 0.2	1.23 ± 0.2	0.79 ± 0.3	1.31 ± 0.3
	20	1.63 ± 0.4	1.80 ± 0.4	1.33 ± 0.4	2.51 ± 0.4
	25	3.04 ± 0.5	3.00 ± 0.5	1.84 ± 0.5	4.01 ± 0.5
ΔH*		22.1 ± 3.0	16.1 ± 1.4	11.8 ± 1.2	17.2 ± 1.0
ΔS*	25	17.7 ± 4.0	-4.4 ± 2.0	-4.0 ± 3.0	1.9 ± 2.0
dht	10			0.50 ± 0.3	11.0 ± 4
	15			0.66 ± 0.3	20.1 ± 4
	20			0.85 ± 0.4	25.0 ± 4
	25			1.00 ± 0.4	35.9 ± 5
ΔH*			7.3 ± 1.0	12.1 ± 1.0	
ΔS*	25			-20.1 ± 6	-10.9 ± 3
sal ^a	25	3.0		5.5	
ΔH*				12	
ΔS*	25			-2	
saa ^b	25	2.61		1.37	
ΔH*		17.3 ± 4.0		6.8 ± 1.0	
ΔS*	25	0.9 ± 2.0		-21.4 ± 4.0	
sam ^b	25	14.9		2.4	
ΔH*		16.6 ± 3.0		6.3 ± 3.0	
ΔS*	25	2.6 ± 3.0		-21.6 ± 6.0	

ΔH* - kcal mole⁻¹

ΔS* - cal °K⁻¹ mole⁻¹

hap - 2-hydroxyacetophenone

dht - dihydroxytolulene

sal - salicylic acid

saa - salicylaldehyde

sam - salicylamide

a - 178

b - J.P. McCann, Ph.D. thesis, University of Glasgow, 1975.

in which the group x is capable of an additional weaker interaction. Because of the uncertainties involved in their evaluation, the absolute magnitude of the constants merits little discussion. It is apparent however that the constant for 2-hydroxyacetophenone is similar to values found previously²⁰¹ in different conditions while that of dihydroxytolulene is smaller and of the order of magnitude of reported for unsubstituted phenol.¹⁶⁴ In this respect, the values probably reflect the basicities of the phenolic protons with a minor contribution from the ortho interaction.

In the values of the rate constants also, there is little variation with changing ortho substituent and the parameters comply with the limits suggested by Seewald and Sutin⁴⁴ for an I_d mechanism. Any effects due to the ortho substituents are minor and may be adequately accounted for by the variation in the outer sphere complex stability constants.

General Discussion.

A summary of the available rate data and activation parameters for reactions of iron III with various ligands is presented in table 4.6. Studies at constant acidity have been excluded. Eliminating reagents which are capable of exhibiting special effects, the constants for reactions of $\text{Fe}(\text{H}_2\text{O})_6^{3+}$ show a spread at 25°C over the range 1 to $4000\text{M}^{-1}\text{s}^{-1}$ while those for $\text{Fe}(\text{H}_2\text{O})_5\text{OH}^{2+}$ cover the range 2×10^2 to $2 \times 10^5\text{M}^{-1}\text{s}^{-1}$. This has been interpreted^{13,39,45} as evidence for some associative character in reactions of the hexaaquo ion while a dissociative conjugate base mechanism is operative in the case of the hydroxoion. It is however worthwhile examining these claims.

If it is assumed that both I_a and I_d mechanisms involve the formation of an outer sphere complex as the initial step, then the following situation arises.

I_a :— In the outer sphere complex, the ligand acts as a nucleophile assisting the loss of water from the metal ion. A trend in nucleophilicity, reflected in the activation enthalpy should therefore be expected. The data with $\text{Fe}(\text{H}_2\text{O})_6^{3+}$ are too diverse to afford many conclusions. It is apparent however that a major part of the rate variation is derived from the entropy contribution ($+16 \rightarrow -24\text{cal}^\circ\text{K}^{-1}\text{mole}^{-1}$) together with an enthalpy variation of $12 \rightarrow 26\text{k cal,mole}^{-1}$. With the hydroxocompound, the range of activation enthalpies is smaller $5 \rightarrow 15\text{k cal mole}^{-1}$ but again the variation in the entropy is extremely large ($-25 \rightarrow +5\text{cal}^\circ\text{K}^{-1}\text{mole}^{-1}$). In the light of Edwards' comments on the reliability of thermodynamic parameters, it is unwise to speculate on the meaning of these values.¹¹

Diebler³⁹ and Swaddle¹³ consider that the spread of rate constants is a sufficient criterion to implicate an I_a mechanism in the case of $\text{Fe}(\text{H}_2\text{O})_6^{3+}$ but that a dissociative conjugate base mechanism may be operative in the case of $\text{Fe}(\text{H}_2\text{O})_5\text{OH}^{2+}$. It can be seen however that the range of thermodynamic parameters is similar in each case. While Sykes⁴⁵ also favours a mechanism with some associative character for the hexaaquo ion, he suggests that the activation enthalpies are not sufficiently small nor entropies sufficiently large to draw conclusions.

I_d :- Variations in the rate constants may also be explained by an I_d mechanism. Changes in both the solvent exchange rate in an outer sphere complex and the outer sphere complexation constant itself can occur. Even if the former parameter is assumed to be the same as in free water (table 4.5), changes in the latter leave sufficient scope for the observed variations. It should however be noted that if the presence or absence of a proton can cause a rate variation of the order of 10^2 then the effects of ligands of differing proton affinity in the outer sphere complex might also have a critical effect on the solvent exchange rate. Whether this type of interaction is termed associative or not is a matter of opinion. The activation step remains metal-solvent bond breaking, a dissociative process.

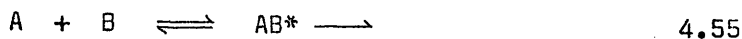
A point in favour of an I_d mechanism is the fact that the rates fall within a fairly narrow range with both ions and further, these rates are of similar orders of magnitude to the respective water exchange rates. In the original papers, where significant variations in the rate constants are observed, most authors have chosen to interpret their data in terms of changes in the outer sphere association constant, usually with valid reasons.

Although volumes of activation, important in differentiating between an I_a and an I_d mechanism with other metal ions, have so far proved unsuccessful²⁰² in the case of iron III, studies in dimethylsulphoxide^{203,204} where no proton ambiguity arises are consistent with a dissociative pathway. It is not unreasonable to suppose that the nature of the mechanism will be the same in aqueous solution.

The various rate constants are subject to errors, not only from direct measurements but also from inaccuracies in the various equilibrium and hydrolysis constants required for their evaluation. Difficulties in interpretation caused by the "proton ambiguity" are a further source of uncertainty. In particular, variations in the ionic strength and the composition of the medium are known²⁰⁵ to cause changes in the hydrogen ion activity. Outer sphere complex formation constants are also susceptible to ionic strength variations. It is hardly surprising therefore that a factor of five or even ten between the rate constants for the same complexation reaction may result from medium effects.³² Entropies of activation are normally the "scapegoat" for such effects.

The Solution Composition.

Choice of the reaction medium is dictated largely by the requirements of working with charged species. Transition state theory³ predicts that the rate constant for the process



with reactants A and B in equilibrium with the activated complex AB* is given by the relationship,

$$k = k_0 \frac{\gamma_A \gamma_B}{\gamma_{AB^*}} \quad 4.56$$

where γ_i is the activity coefficient of the i^{th} species and k_0 is the rate constant at infinite dilution. The rate will thus be influenced by changes in the ionic environment. Selection of a suitable medium for reaction depends on the requirement that either the function $\gamma_A \gamma_B / \gamma_{AB^*}$ be calculable to provide a means of evaluating k_0 from k or, be invariant within the range of conditions used in a particular study to yield a truly constant value for k .²⁰⁶

The former approach²⁰⁷ in its simplest form yields an expression of the type

$$\log_{10} k = \log_{10} k_0 + f(z_A, z_B, I) \quad 4.57$$

where z_i is the charge on the i^{th} species and I the ionic strength. Calculated values of the function $f(z_A, z_B, I)$ are however restricted to the limits of extended Debye-Huckel calculations, usually acceptable to an ionic strength of 0.1M.

While the evaluation of k_0 is the most fundamental approach and affords most information, it is generally unsuited to kinetic studies involving highly charged transition metal ions due to their large contribution to the ionic strength. Extrapolation of k to infinite dilution is thus impossible and the factor $\gamma_A \gamma_B / \gamma_{AB^*}$ must be maintained constant.

The most common method of achieving this constancy is to employ an ionic medium whose composition remains sensibly constant although the reactant concentrations may be varied. This generally involves the addition of an inert supporting electrolyte. Ideally this electrolyte should not interact with the reactant species and for this purpose, alkali metal perchlorates are employed. In all cases under consideration in this chapter, the ligands are present in solution mainly in their unionised forms and as such are unlikely to be affected directly by alkali metal cations. Attention must however be given to the possibility of complex formation between the highly charged iron III cation and the weakly coordinating perchlorate anion. Johansson²⁰⁸ in his recent review, suggests that if a species such as FeClO_4^+ is formed, its association constant is small. Present data are unable to distinguish between a weak complex and medium effects. In view of this uncertainty, the possibility of complex formation is usually treated as a medium effect.

The perchlorate ion is also a strong oxidising agent¹²⁷ but the rates of oxidation in aqueous solution are in general slow since the anion is kinetically stable.²⁰⁹ Oxidations from this source may be neglected on the timescale of the reactions under consideration here.

Two formulations are at present used to maintain constant activity coefficients in solutions of high ionic concentration,

$$(a) \text{ Constant ionic strength } I = 0.5 \sum_i c_i z_i^2$$

$$(b) \text{ Constant total ionic charge } C = 0.5 \sum_i c_i z_i$$

where c_i is the concentration of the i th species. There is no theoretical foundation for either concept in conditions of high ion concentrations and there has been recently much criticism^{210,211} of both. Although it may be shown experimentally^{212,213} that use of the latter formulation affords more constancy in activity coefficients under some conditions, use of constant ionic strength is more general and must be preferred for the purposes of comparison of rate data. In common with most other studies in the field therefore, an ionic strength of 1.0M was used in this

work. Since the hydrogen ion concentration, maintained greater than 0.25M to prevent hydrolysis, was varied over the range 0.25 to 0.75M and the iron III concentration varied over half the range available to maintain a constant ionic strength of 1.0M with either lithium or sodium perchlorate as the background electrolyte, it is evident that this study suffers to the extent of the experimentalist's inability to ensure a sensibly constant ionic composition.

Considerable effects deriving from this might be expected. The variation in the mean activity coefficients in different single electrolyte solution at the same ionic strength as illustrated by the data in table 4.16 suggests that when dealing with mixed electrolytes, the activity coefficient of each species changes with substantial changes in composition of the medium.²¹⁴ In view of this, an attempt was made to estimate the magnitude of possible errors involved. The most obvious method of accomplishing this is the calculation of activity coefficients for the various species in solution.

Activity coefficients of the components of mixed electrolyte solutions may be accounted for by Harned's rule²¹⁵ that the activity coefficient of one electrolyte in a mixture is dependent on the concentration of the other components. There is however no method for obtaining the parameters required for calculations of this nature except by direct experimental measurement. Many approximations based on single electrolyte solution data have however been suggested.²¹⁶⁻²¹⁸

The approach used in this work is that outlined by Reilly et al.²¹⁸ using both single and binary electrolyte data. Activity coefficients may however be adequately represented²¹⁸ by single electrolyte data using the equation

$$\frac{z_L}{z_1 z_L} \ln \gamma_{\pm 1L} = \sum_{i=1}^n \frac{E_i}{E_L} \left[\frac{z_{1L}}{z_1 z_L} \left\{ 1 - \beta_{1L}^0 + \ln \gamma_{1L}^0 \right\} + \frac{z_{iL}}{z_i z_L} \left\{ 1 - \beta_{iL}^0 + \ln \gamma_{iL}^0 \right\} - \frac{z_{iL}}{z_i z_L} \left\{ \left[1 + \frac{z_{1L} E_L}{2I} \right] \left[1 - \beta_{iL}^0 \right] + \ln \gamma_{iL}^0 \right\} \right]$$

4.58

TABLE 4.16

Parameters used in the calculation of mixed electrolyte activity coefficients.^a

Electrolyte	I M	$\frac{r_{n+}}{R}$	γ_{\pm}	β^0
HClO ₄	1.0		0.823	1.041
LiClO ₄	1.0	0.68	0.887	1.072
NaClO ₄	1.0	0.97	0.629	0.913
Ga(ClO ₄) ₃	1.0	0.62	1.150	1.661
Fe(ClO ₄) ₃	1.0	0.64	-	-
Zn(ClO ₄) ₂	1.0	0.74	0.909	1.328
Fe(ClO ₄) ₂	1.0	0.74	-	-

a - ref. 205

for an n component mixture with a common anion L where

$$\begin{aligned} z_{iL} &= z_i - z_L \\ E_i &= z_i c_i \\ E_L &= -z_L c_L \end{aligned} \quad 4.59$$

and γ_{+iL} , γ_{iL}^0 and ϕ_{iL}^0 are respectively the mean activity coefficient of species iL in the mixture, the mean single electrolyte activity coefficient and the single electrolyte osmotic coefficient.

There are no single electrolyte data reported for iron III perchlorate. If activity coefficients depend on the nature of the ionic atmosphere surrounding the ion, then for ions of similar radius and charge the coefficients should be similar. Reference to table 4.16 reveals that the ions Fe^{3+} and Ga^{3+} are similar and thus the single electrolyte data for gallium III perchlorate²¹⁹ were substituted for those of iron III perchlorate in the treatment. Representative results are presented in table 4.17 and show that the activity coefficients of all species in solution vary significantly over the range of experimental conditions. Also, the differences are smaller in the case of lithium perchlorate presumably due to the similarity of the single electrolyte coefficients of LiClO_4 and HClO_4 , those of NaClO_4 being substantially different.²¹⁴

Effects of this nature have been observed experimentally in a number of studies of reactions of iron III. Variations in rate²²⁰⁻²²³ and equilibrium constants²²⁴⁻²²⁶ on changing from one supporting cation to another have been explained in terms of specific interaction with the perchlorate anion²²⁴ and changes in the activity coefficients.²²² The effects of varying the ionic strength have also been examined.^{227,228}

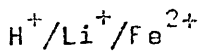
In the present study, differences in the rate constants between Na^+/H^+ and Li^+/H^+ mixed electrolytes are tentatively ascribed to medium effects. Figure 4.7 shows a plot of k_D against the hydrogen ion concentration for the reaction between iron III and

TABLE 4.17

Activity coefficients calculated using equation 4.58
for mixed electrolyte solutions. $T = 25^{\circ}\text{C}$ $I = 1.0\text{M}$ (perchlorate)

 $\text{H}^+/\text{Na}^+/\text{Fe}^{3+}$

$[\text{H}^+]$ M	$[\text{Fe}^{3+}]$ M	γ_{H^+}	$\gamma_{\text{Fe}^{3+}}$
0.3	0	1.097	1.157
	0.01167	1.115	1.272
	0.02333	1.151	1.399
	0.03500	1.188	1.539
	0.04667	1.227	1.693
	0.05833	1.266	1.862
0.4	0	1.148	1.350
	0.01000	1.159	1.465
	0.02000	1.191	1.590
	0.03000	1.224	1.725
	0.04000	1.258	1.872
	0.05000	1.293	2.031
0.5	0	1.201	1.576
	0.00833	1.207	1.687
	0.01667	1.234	1.806
	0.02500	1.262	1.933
	0.03333	1.292	2.069
	0.04167	1.322	2.215
0.6	0	1.257	1.840
	0.00667	1.258	1.943
	0.01333	1.280	2.052
	0.02000	1.304	2.166
	0.02667	1.329	2.288
	0.03333	1.354	2.416
0.7	0	1.316	2.148
	0.0050	1.314	2.237
	0.0100	1.331	2.331
	0.0150	1.350	2.428
	0.0200	1.369	2.529
	0.0250	1.389	2.634



$[\text{H}^+]$ M	$[\text{Fe}^{3+}]$ M	γ_{H^+}	$\gamma_{\text{Fe}^{3+}}$
0.3	0	1.174	1.419
	0.01167	1.189	1.530
	0.02333	1.219	1.648
	0.03500	1.249	1.776
	0.04667	1.281	1.914
	0.05833	1.313	2.063
0.4	0	1.217	1.609
	0.01000	1.226	1.716
	0.02000	1.252	1.829
	0.03000	1.279	1.950
	0.04000	1.307	2.080
	0.05000	1.335	2.217
0.5	0	1.261	1.824
	0.00833	1.266	1.924
	0.01667	1.287	2.030
	0.02500	1.311	2.141
	0.03333	1.334	2.259
	0.04167	1.359	2.383
0.6	0	1.308	2.068
	0.00667	1.308	2.158
	0.01333	1.325	2.253
	0.02000	1.349	2.351
	0.02667	1.365	2.454
	0.03333	1.385	2.561
0.7	0	1.355	2.345
	0.00500	1.354	2.421
	0.01000	1.367	2.500
	0.01500	1.382	2.581
	0.02000	1.397	2.665
	0.02500	1.413	2.752

Activity coefficient correction for plots of k_D against $[H^+]$ for the reaction of iron (III) with 2-MIBA. $T=20^\circ\text{C}$, $I=1.0M$.

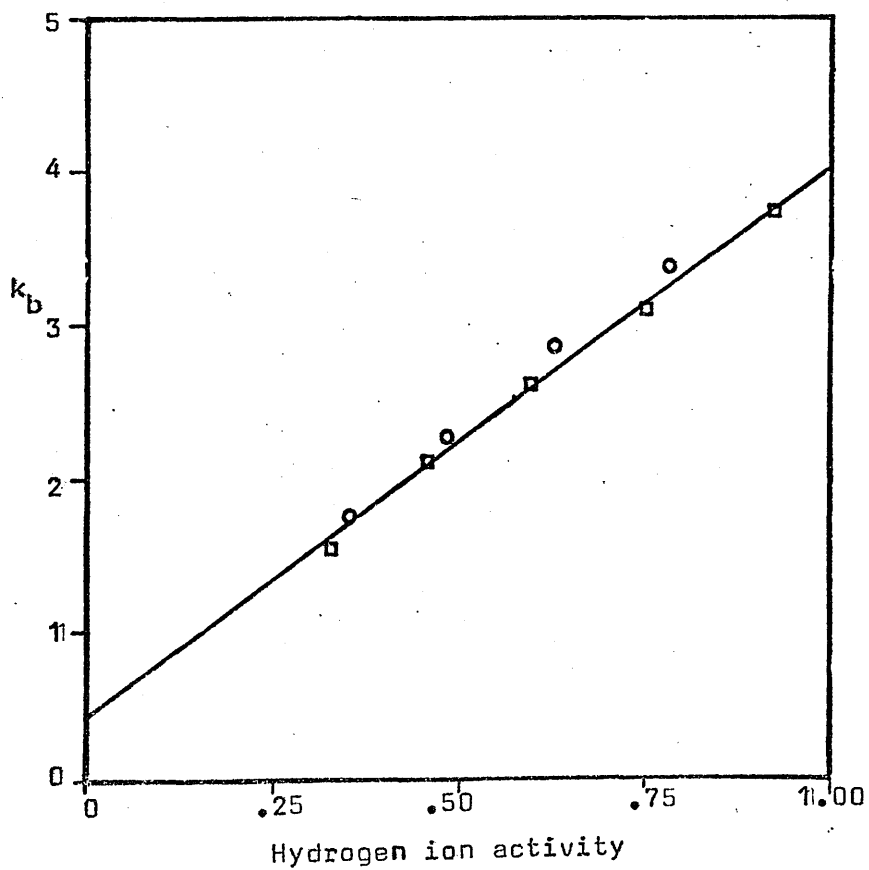
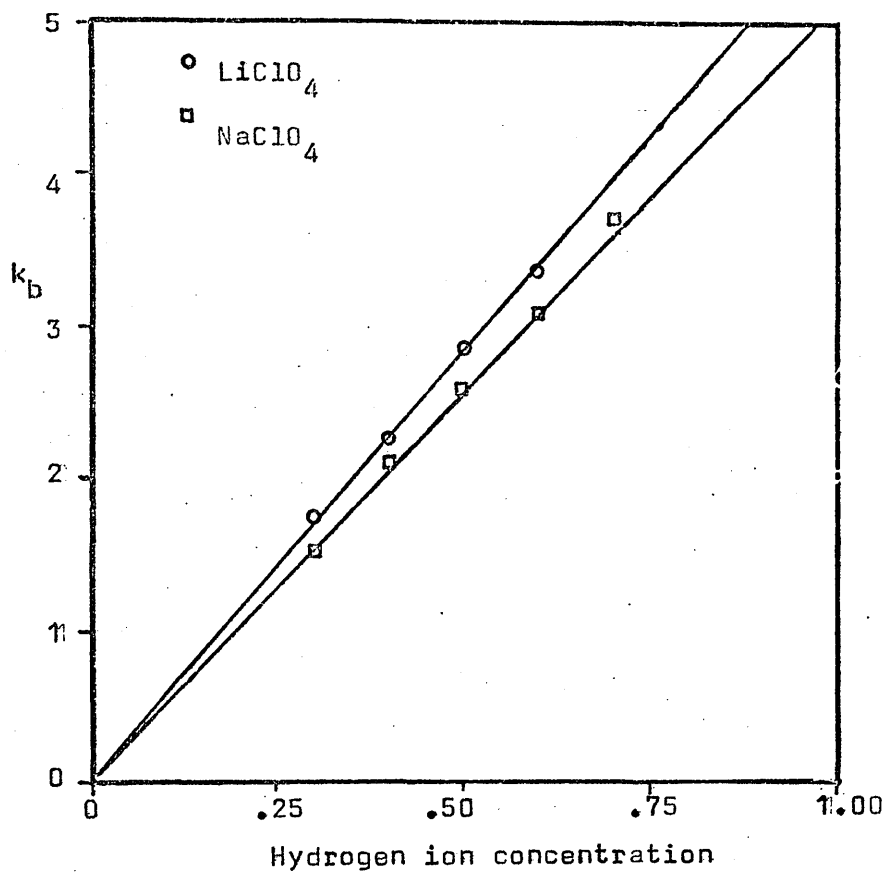


FIGURE 4.7

2-MIBA in the different media. The significant differences largely disappear when the hydrogen ion activity is used, as shown in figure 4.7. Further, an acid independent pathway is revealed.

That such results can be obtained from a crude model is surprising and may be somewhat fortuitous. They are however encouraging and their implications far reaching in regard to the interpretation of the proton ambiguity. Obviously, this aspect requires much more detailed examination.

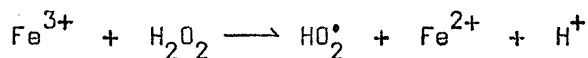
CHAPTER 5

Oxidation of Mercaptocarboxylic Acids.

Oxidation of Non-Metallic Substrates by Iron III.

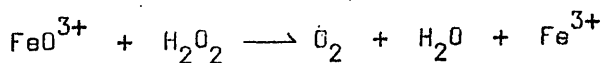
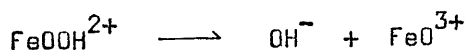
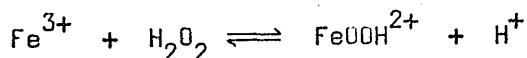
Iron III is a moderately strong one electron oxidant^{229,230} and a large number of its reduction processes have been examined. With non-metallic substrates, the reactions are kinetically complex and the rates vary markedly due to their dependence not only on the properties of the aquo metal ion, but also on the specific nature of the ligand, products and the stability of possible free radical intermediates. As an illustration, in this section, a few of the more detailed mechanistic studies are reviewed.

One of the most complex and controversial reactions is that between iron III and hydrogen peroxide. Barb et al²³¹ proposed a mechanism involving a radical chain reaction initiated by the step



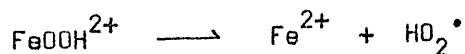
5.1

Kremer and Stein^{232,233} however envisaged a process in which metal complexes serve as templates for the cleavage of the O-O bond.



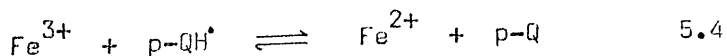
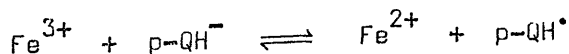
5.2

Although this mechanism is supported by Brown et al,²³⁴ more recent work is consistent with the Barb mechanism involving HO_2^\bullet ²³⁵ and HO_2^\bullet ²³⁶ radicals and incorporating initiation by spontaneous decay of a complex²³⁶

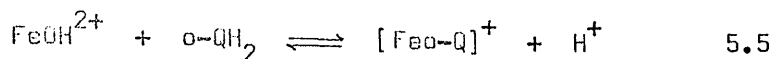


5.3

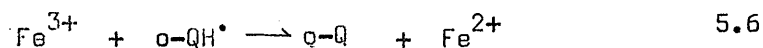
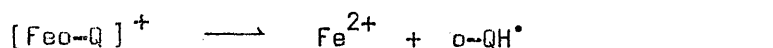
The oxidations of hydroquinones, QH_2 , have also provided interest. With the para isomer, no metal-ion complex is invoked,²³⁷



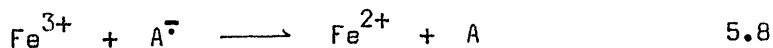
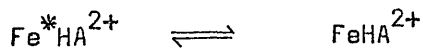
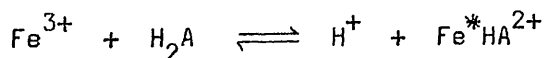
Formation of the semiquinone $p\text{-Q}^{\cdot-}$, stabilised by the benzene ring, is the initial process. Oxidation of the ortho isomer on the other hand proceeds through a well characterised intermediate,²³⁸



which decomposes spontaneously²³⁹ to yield the semiquinone radical (Pathway 5.6) and the quinone in the presence of an excess of iron III,²⁴⁰ by a metal ion catalysed pathway 5.7, both $\text{Fe}(\text{H}_2\text{O})_6^{3+}$ and $\text{Fe}(\text{H}_2\text{O})_5\text{OH}^{2+}$ being involved.

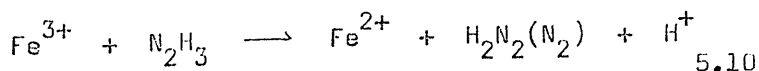
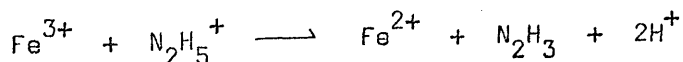


Ascorbate A^{2-} oxidation involves²⁴¹ a similar mechanism although two different forms of a complex are apparently involved,



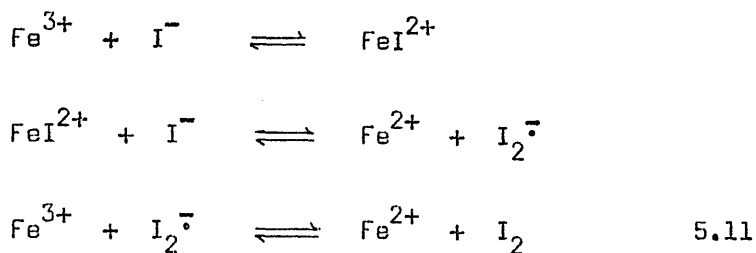
While complexes are probable intermediates²⁴² in the reaction with acetoin, the kinetics are complicated by keto-enol tautomerism.²⁴³ Again however the formation of radicals in a spontaneous decomposition is the initial step.²⁴⁴

Hydrazine has promoted much study^{229,230} because of its value in distinguishing between one and two electron oxidants. The mechanism^{61,75,245}



explains most experimental details, variable stoichiometry being attributed^{229,230} to different contributions of pathways 5.9 and 5.10 under different conditions.

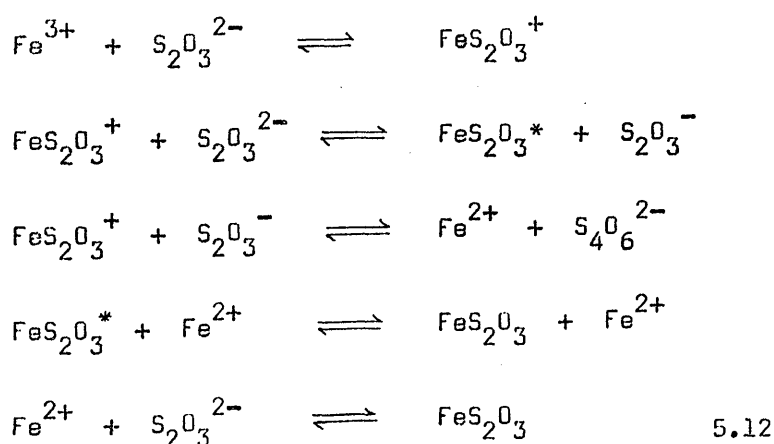
With iodide, the product is dimeric and pathways involving the more stable $I_2^{\cdot-}$ radical ion have been proposed,^{246,247} the reactants being I^- and either an inner²⁴⁶ or outer²⁴⁷ sphere complex.



Hydroxylamine is also oxidised to a dimeric product N_2O and while no definite conclusions can be made from the form of the rate law, it is probable²⁴⁸ that the mechanism involves the formation of a binuclear intermediate containing hydroxylamine bridges.

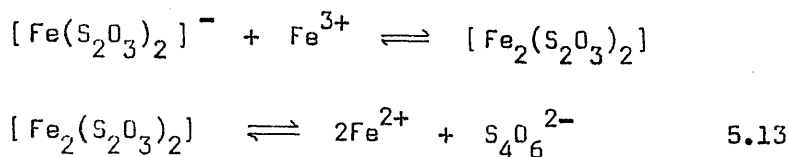
The sulphite reaction exemplifies a system where there is the possibility of either dimeric or monomeric products.⁷⁶ Although the detailed mechanistic interpretation^{249,250} varies from author to author, spontaneous breakdown of an iron III-sulphite complex which may be sulphur bonded¹⁹⁰ is probably involved.

Sulphur bonding is also invoked in the reaction with thiosulphate which proceeds by the following mechanism²⁵¹

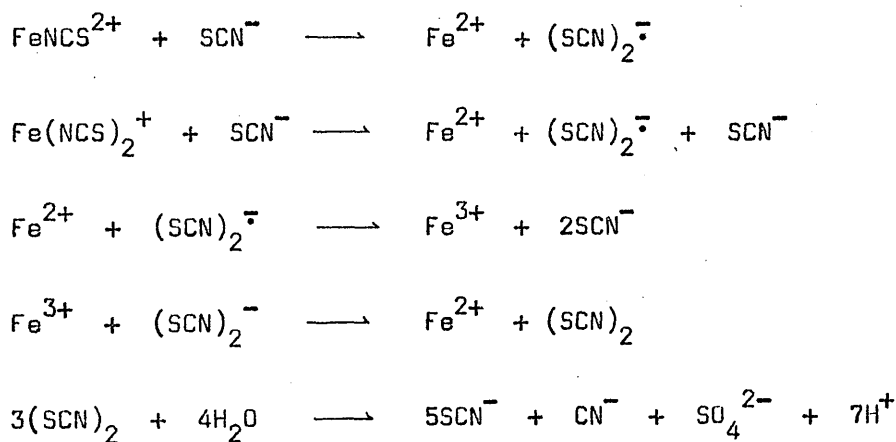


in which further intermediates $FeS_2O_3^*$ and $S_2O_3^-$ are invoked to

explain the complex kinetic behaviour. The reaction is accompanied by the rapid formation and subsequent decay of a purple colour which is attributed ²⁵²⁻²⁵⁴ to the complex FeS_2O_3^+ . In a previous attempt ²⁵⁵ to explain the kinetics, the complex $[\text{Fe}(\text{S}_2\text{O}_3)_2]^-$ was postulated, formation of the dimeric product occurring by the mechanism,



Betts and Dainton ²⁵⁶ examined the oxidation of the predominately N-bonded iron III-thiocyanate complex and found that the decomposition is ligand catalysed, consistent with the formation of $(\text{SCN})_2^{\cdot-}$ radical ion as a primary product.



5.14

In conditions of very high acidity however, the nitrogen is protonated and a transient purple sulphur bonded complex is produced. ²⁵⁷ Oxidation of this form is considerably faster. A similar observation has been made on solutions containing iron III and thiourea.

In many of the above reactions, iron III has an inhibitory role, in some cases because the redox equilibria are directly reversible ²³⁷⁻ ^{239,256} while in others there is competition between iron II and iron III for complexing with the reductant. ²⁵¹ Catalysis by other metal ions, principally copper, ^{248,249} is also common.

Reaction Between Iron III and Mercaptocarboxylic Acids.

The oxidation of mercaptocarboxylic acids to the corresponding disulphides has been the subject of scientific investigation²⁵⁸⁻²⁶¹ ever since the biological importance of cysteine was recognised. Indeed, early attempts to isolate the pure mercaptides were hampered by rapid aerial oxidation to disulphide. It was noted at an early date that the presence of metal ions, particularly iron and copper produce highly coloured complexes which are important in the oxidation process.²⁶²

Mathews and Walker²⁶³ are credited with the first satisfactory explanation of the autocatalytic role of these complexes in the oxidation process. Further evidence for their reaction scheme was furnished by Harris²⁶² although his hypotheses show minor differences in the nature of the complexes. Studies were extended by Warburg and Sakuma²⁶⁴ and later Harrison²⁶⁵ to include an investigation of the rate of oxygen uptake of solutions of mercaptocarboxylic acids containing metal ions. It was apparent however that the nature of the complexes under study varies markedly in the different experimental conditions.

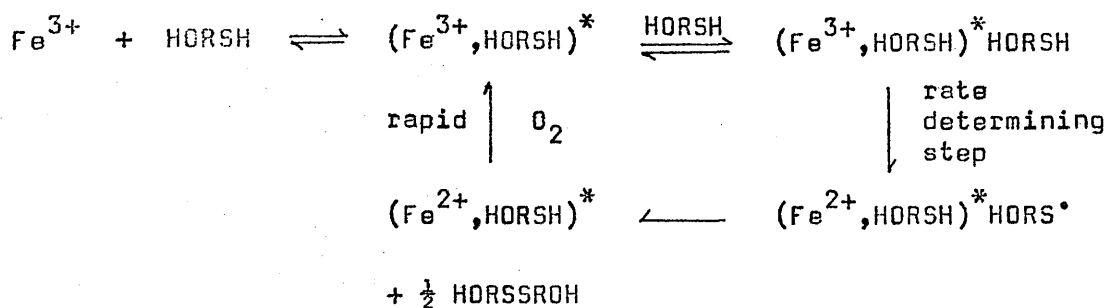
In a detailed study in 1929, Cannan and Richardson²⁶⁶ highlighted this confusion. They described two complex types in the reaction between iron III and mercaptoacetic acid: a deep red coloured species formed at $\text{pH} > 6$ which is autocatalytically active and, at $\text{pH} < 4$, a transient blue complex having no catalytic activity but which is freely autoxidisable to yield a solution containing iron II and disulphide. Preliminary studies indicated complex kinetic behaviour in the case of the red coloured species while the reactions of the blue complex were too rapid for investigation by the techniques then available.

In the same year, Michaelis, Schubert and their co-workers²⁶⁶⁻²⁶⁹ embarked on an investigation of the reactions of iron with mercaptocarboxylic acids using complexes of cobalt²⁶⁸ as models. They succeeded in isolating two solids containing iron II and mercaptoacetic acid and provided structural details of possible intermediate complexes in the autocatalytic cycle.²⁶⁹ Their ideas were later developed by Martell and Calvin.²⁹⁰

The understanding of what is an extremely complex reaction had thus reached the stage summarised in scheme 5.1 by the middle

SCHEME 5.1

The nature of the autocatalytic cycle



$(\text{Fe}^{n+}, \text{HORSH})^*$ is the catalytically active complex.

of the present century. Controversy arising from the composition of the intermediate complexes and the interrelating steps however remained unresolved. Although much of the work since then has involved both the biologically important mercaptoaminoacids as well as simpler mercaptocarboxylic acids, the systems show similar behaviour, dominated by the mercaptide group, with little direct evidence for the incorporation of the amino group. It is convenient therefore to treat both types of studies on a complementary basis.

Gerwe²⁷¹ showed in 1939 that although cysteine oxidises spontaneously to give cystine, it oxidises at a very slow rate in the absence of metal ions. Several workers²⁷²⁻²⁷⁴ have examined the mercaptide/disulphide redox couples and their results are summarised in table 5.1. With iron III in aqueous perchloric acid, the free energy change for the reaction



is of the order of $-33.9\text{kcal mole}^{-1}$ for MAA and $-33.5\text{kcal mole}^{-1}$ for 2-MPA. An unknown factor is the moderation of the redox potential on complex formation.

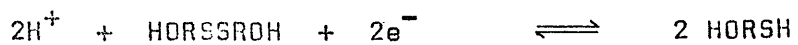
Reactions of the Red Complexes.

A. Reaction at High pH in Anaerobic Conditions.

Employing anaerobic conditions to interrupt the autocatalytic cycle, Leussing, Kolthoff and their co-workers²⁷⁵⁻²⁷⁸ examined the species responsible for the red colour in buffered solutions (pH 8.4-10.1) of iron III and mercaptocarboxylic acids. With mercaptoacetic acid, the major species was considered²⁷⁵ to be $\text{Fe}^{\text{III}}\text{OH}(\text{ORS})_2^{2-}$ while an additional complex $\text{Fe}^{\text{III}}(\text{ORS})_3^{3-}$ predominated in the case of cysteine.²⁷⁶ The following mechanism was proposed to explain the rate law of the bleaching reaction.²⁷⁷⁻²⁷⁸

TABLE 5.1

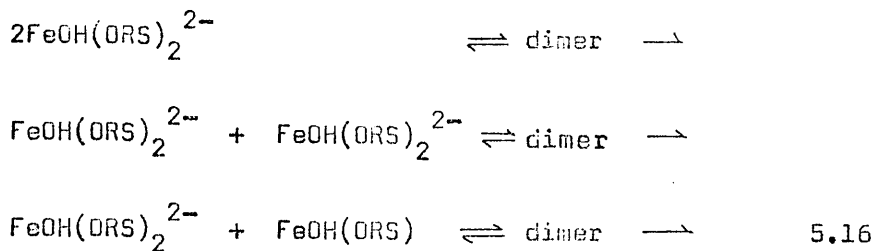
Reduction potentials for mercaptide-disulphide system
(T = 25°C)



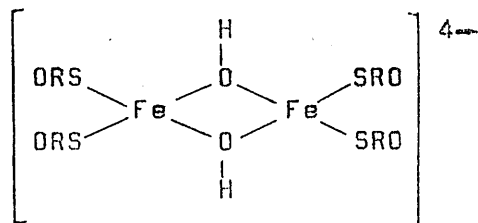
	E^0 volts	ref.
MAA	0.073	a
2-MPA	0.09	b
cysteine	0.02	b
	0.074	a

a ref 272

b ref 273



where the complexes $\text{Fe(OH)}_2(\text{ORS})^-$ and FeOH(ORS) are in equilibrium with the major species in solution. Leussing²⁷⁷ rationalised the mechanism by noting that in each proposed dimer structure

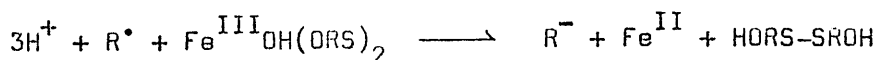


5.17

two sulphur atoms occupy positions on the same metal ion providing the possibility for simultaneous two electron transfer to the other iron III through a hydroxyl bridge. At higher temperatures, two radicals formed anywhere on the dimer might react to form the disulphide.

B. Reactions at High pH in Aerobic Conditions.

Lamfrom and Nielsen²⁷⁹ tested the possibility of the anaerobic reaction as the rate determining step in the aerobic cycle with mercaptoacetic acid (pH4.6-5.8), and showed that such a hypothesis is inconsistent with the experimental observations, proposing instead a mechanism involving free radicals. Leussing and Tischer²⁸⁰ extended the study (pH7.5-8.2) and concluded that although radicals are involved, the facilitation of two electron transfer through co-ordination remains important. On reaction of $\text{Fe}^{\text{III}}\text{OH(ORS)}_2^{2-}$ with a radical R



iron III and the radical are reduced as the disulphide is formed. A further study²⁸¹ contested the composition of the species in solution (pH~11), proposing an iron:mercaptoacetate ratio of 1:3 as had been observed²⁸² in the case of cysteine.

Gilmour and McAuley²⁸³ investigated the subsequent oxidation of solutions containing iron II and cysteine, (pH6-10) proposing a reaction between iron II-cysteine complexes and molecular oxygen to explain the change in rate law from that found with iron II alone.¹⁵⁰ Both 1:1 and 1:2 complexes are involved and it was shown conclusively that this step is not rate limiting in the autocatalytic cycle.

Solids of composition $\text{Fe}^{\text{II}}(\text{ORS})$ and $\text{Fe}^{\text{II}}(\text{ORS})_2$ had already been isolated and characterised by several investigators^{269,275,276,284} and their formulation as polymeric species has recently been confirmed by x-ray crystallographic²⁸⁵ and magnetic²⁸⁶ measurements.

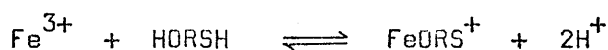
To explain an unusual rate law in the iron III catalysed oxidation of cysteine, Taylor et al¹⁴⁹ proposed the spontaneous decomposition of $\text{Fe}^{\text{III}}(\text{ORS})_3$ to yield one mole of disulphide and an iron I cysteine complex which undergoes subsequent rapid oxidation. Guzzi & Gal²⁸¹ showed that although the reaction may be conveniently halted after the formation of disulphide, in conditions of excess oxidant, further oxidation produces sulphide.

It is apparent that much controversy concerning the nature of the aerobic process remains. The reaction in the absence of oxygen is however fairly well characterised apart from uncertainties regarding the exact nature of the reactant complexes. This aspect was examined by Tomita et al²⁸⁸ who identified a red 1:2 and violet 1:3 oxygen-sulphur (O,S) bonded chelate with cysteine in alkaline media. These assignments were questioned by McKenzie and co-workers²⁸⁹ who studied similar complexes with penicillamine and cysteamine-N-acetic acid, favouring instead 1:2 stoichiometry in both cases. These workers also described a marked stabilisation of the iron III-sulphur chromophore of these two amino acids compared with the cysteine species. A similar observation by Stadtherr and Martin²⁹⁰ was ascribed to inhibition of redox and oligomerisation reactions by the addition of methyl substituents.

Reactions of the Blue Complexes.

As was noted in chapter 4, the reaction between iron III and mercaptocarboxylic acids in aqueous acid solution is characterised by the rapid formation and subsequent disappearance of a blue colour, attributed to a 1:1 S,O-bonded chelate. Lack of catalytic activity of such complexes may be understood in terms of the low rate of aerial oxidation of iron II in solution of mercaptocarboxylic acids at low pH.^{150,283} Instead, the reaction is irreversible with the formation of iron II and the corresponding disulphide.²⁶⁶

Page²⁹¹ obtained visible spectra of the blue complexes with mercaptoacetic acid and cysteine using capacity flow. In a later paper,²⁸² he characterised the equilibrium



with cysteine. Lamform and Nielsen²⁷⁹ assigned the structure $\text{Fe}^{\text{III}}_2(\text{OH})_2(\text{ORS})_3^{2-}$ to the complex and proposed that it acted as an intermediate in reactions of the red complex discussed above. They found that the disappearance of the colour followed first order kinetics.

Tomita et al²⁸⁸ used Job's method of continuous variation²⁹² to characterise the complex as 1:1 in 90% ethanol. Their results are consistent with S,O-bonding although no information is available on the coordination number and other coordinating ligands. Lack of optical activity of the absorption band suggests a weak complex.

Stadtherr and Martin²⁹⁰ reached a similar conclusion from their results with penicillamine and presented further evidence for the bonding in the species.

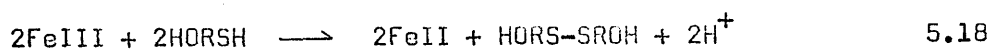
Ellis and McAuley¹⁹⁷ found that the reaction with 2-MSA was also consistent with a bidentate chelate²⁹³ and the reaction kinetics are typical of those found in the formation of octahedral complexes of iron III. A similar result is found with the ligands MAA, 2-MPA and 2-MIBA, presented in chapter 4.

Kinetics and Mechanism of the Redox Reaction between Iron III and Mercaptocarboxylic Acids in Aqueous Acidic Media.

The experimental conditions were chosen to be identical to those used in the complex formation reaction (chapter 4). Additional experiments were however performed to investigate the rate dependence on the reaction products and on dissolved oxygen.

Characterisation of the Products.

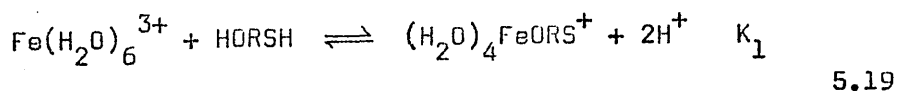
The stoichiometry of the reaction (table 5.2) was measured by the decrease in iron III immediately after the blue colour due to the intermediate complex had been discharged. Under conditions of excess metal ion, this indicates the conversion of all the mercaptocarboxylic acid to the corresponding disulphide,



the remaining iron III being determined spectrophotometrically by adding excess thiocyanate to the solution. Oxidation of the disulphide product by excess iron III is probable but this reaction appears slow enough to be neglected in the present study. Iron II was detected as a product of the reaction by the appearance of a red colour on addition of o-phenanthroline. The other major products were isolated and identified as the corresponding disulphides (table 5.2). This confirms the results of earlier investigators.²⁶⁶

Kinetics and Mechanism.

The complex formation reactions may be expressed as



In the electron transfer reaction, the instantaneous rate of disappearance of colour ($\Delta \text{O.D.} / \Delta t$) was found to be independent of $[\text{H}^+]_0$, $[\text{Fe}^{\text{III}}]_0$, $[\text{HORSH}]_0$, $[\text{Fe}^{\text{II}}]_0$ and $[\text{O}_2]$ suggesting a reaction of the complex $(\text{H}_2\text{O})_4\text{FeORS}^+$ alone. Plots of \log_{10} (instantaneous rate) against $\log_{10}(\text{O.D.})$ were found to be linear with a gradient

TABLE 5.2

Stoichiometric ratios of the reactants.^a

LIGAND	FeIII : HORSH
MAA	1.12 \pm 0.17
2-MPA	0.88 \pm 0.10
2-MIBA	0.91 \pm 0.10
2-MSA ^b	0.93 \pm 0.05

a - based on determination of residual iron III after reaction

b - ref. 12.

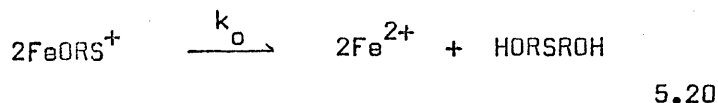
Characterisation of disulphide products.

MERCAPTIDE	$\nu_{S-S} \text{ cm}^{-1}$ (raman spectrum)
2-MPA	520, 535
2-MIBA	515, 534

E.J. Bastian and R.B. Martin, J. Phys Chem., 1973, 77, 1129.

between 2 and 3, the exact value depending on the particular ligand involved. Whilst a mechanism might be postulated involving a bimolecular reaction of the complex, a termolecular process is considered unlikely and the observation of an order greater than two is explained by consideration of the nature of the pre-equilibrium.

If it is assumed that a bimolecular mechanism is operating, then since the conditions are such that the mono-complex is the sole reactant in appreciable concentration, equation 5.20 may be written



Water molecules are omitted for the sake of clarity. The initial reactant concentrations may be expressed in the form

$$\begin{aligned} [\text{Fe}^{3+}]_o &= [\text{Fe}^{3+}] + [\text{FeORS}^+] + [\text{Fe}^{2+}] \\ [\text{HORSH}]_o &= [\text{HORSH}] + [\text{FeORS}^+] + [\text{Fe}^{2+}] \end{aligned} \quad 5.21$$

assuming no added iron II and that hydrolysed species may be regarded as having negligible concentration under the conditions used in the study hence

$$[\text{Fe}^{3+}]_o - [\text{HORSH}]_o = [\text{Fe}^{3+}] - [\text{HORSH}] \quad 5.22$$

After the initial induction period (formation of complex), since equilibrium 5.19 is adjusted more rapidly than the rate at which the redox reaction proceeds, from 5.19 and 5.22 the following equations may be derived.

$$K_1[\text{Fe}^{3+}] \left\{ [\text{Fe}^{3+}] - [\text{Fe}^{3+}]_o + [\text{HORSH}]_o \right\} = [\text{FeORS}^+][\text{H}^+]^2 \quad 5.23$$

and

$$[\text{Fe}^{3+}] = \frac{[\text{Fe}^{3+}]_o - [\text{HORSH}]_o + \sqrt{\left([\text{Fe}^{3+}]_o - [\text{HORSH}]_o\right)^2 + \frac{4[\text{FeORS}^+][\text{H}^+]^2}{K_1}}}{2}$$

From equation 5.21

$$[\text{Fe}^{2+}] = [\text{Fe}^{3+}]_0 - [\text{Fe}^{3+}] - [\text{FeORS}^+] \quad 5.25$$

and from 5.24 the expression 5.26 may be obtained

$$[\text{Fe}^{2+}] = [\text{Fe}^{3+}]_0 - \frac{[\text{Fe}^{3+}]_0 - [\text{HORSH}]_0}{2} - \frac{[\text{Fe}^{3+}]_0 - [\text{HORSH}]_0}{2} + \frac{4[\text{FeORS}^+][\text{H}^+]}{K_1} - [\text{FeORS}^+] \quad 5.26$$

The rate law may be written as (equation 5.20)

$$\frac{d[\text{Fe}^{2+}]}{dt} = 2k_o [\text{FeORS}^+]^2 \quad 5.27$$

and by differentiating 5.26 and substituting into 5.27, it may be shown that

$$\frac{-d[\text{FeORS}^+]}{dt} = 2k_o \left\{ \frac{K_1^2 [\text{Fe}^{3+}]_0 - [\text{HORSH}]_0}{[\text{H}^+]^4} + \frac{4K_1 [\text{FeORS}^+]}{[\text{H}^+]^2} \right\}^{\frac{1}{2}} [\text{FeORS}^+]^2 \quad 5.28$$

$$1 + \left\{ \frac{K_1^2 [\text{Fe}^{3+}]_0 - [\text{HORSH}]_0}{[\text{H}^+]^4} + \frac{4K_1 [\text{FeORS}^+]}{[\text{H}^+]^2} \right\}^{\frac{1}{2}}$$

Plots of instantaneous rate immediately after the induction period for complex formation against the function on the right hand side of equation 5.28, using values of K_1 and ϵ reported in chapter 4 yielded constant values of k_o .

Integrating equation 5.28 gives the expression

$$\left\{ \frac{[H^+]^2 \left\{ 1 + \frac{4[H^+]^2 [FeORS^+]}{K_1 ([Fe^{3+}]_0 - [HORSH]_0)^2} \right\}^{\frac{1}{2}}}{K_1 ([Fe^{3+}]_0 - [HORSH]_0)} + 1 \right\} \frac{1}{[FeORS^+]}$$

$$+ \frac{2[H^+]^4}{K_1^2 ([Fe^{3+}]_0 - [HORSH]_0)^3} \log_e \left\{ \frac{\frac{1+4[H^+]^2 [FeORS^+]}{K_1 ([Fe^{3+}]_0 - [HORSH]_0)^2} - 1}{\frac{1+4[H^+]^2 [FeORS^+]}{K_1 ([Fe^{3+}]_0 - [HORSH]_0)^2} + 1} \right\}$$

$$+ Q = 2k_0 t$$

5.30

where the constant Q is given by

$$Q = \left\{ \frac{[H^+]^2 \left\{ 1 + \frac{4[H^+]^2 [FeORS^+]_0}{K_1 ([Fe^{3+}]_0 - [HORSH]_0)^2} \right\}^{\frac{1}{2}}}{K_1 ([Fe^{3+}]_0 - [HORSH]_0)} + 1 \right\} \frac{1}{[FeORS^+]_0}$$

$$- \frac{2[H^+]^4}{K_1^2 ([Fe^{3+}]_0 - [HORSH]_0)^3} \log_e \left\{ \frac{1 + \frac{4[H^+]^2 [FeORS^+]_0}{K_1 ([Fe^{3+}]_0 - [HORSH]_0)^2} - 1}{1 + \frac{4[H^+]^2 [FeORS^+]_0}{K_1 ([Fe^{3+}]_0 - [HORSH]_0)^2} + 1} \right\}$$

5.31

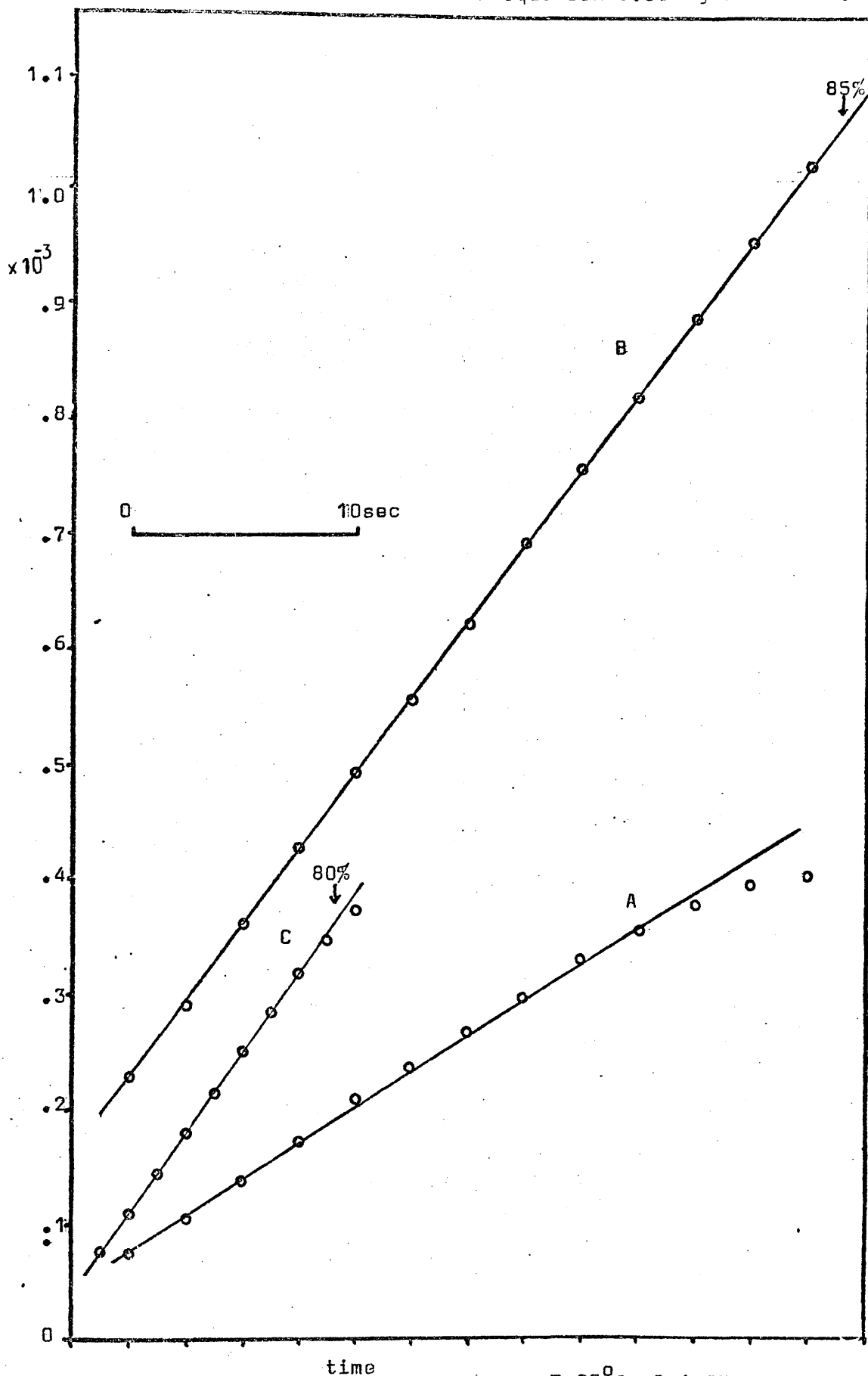
and $[FeORS^+]_0$, the complex concentration extrapolated to zero time may be approximated by the equilibrium expression

$$[FeORS^+]_0 = \frac{\left\{ [Fe^{3+}]_0 + [HORSH]_0 + \frac{[H^+]^2}{K_1} \right\} - \left\{ [Fe^{3+}]_0 + [HORSH]_0 + \frac{[H^+]^2}{K_1} \right\}^2 - 4[Fe^{3+}]_0 [HORSH]_0}{2}$$

5.32

Plots of the left hand side of equation 5.30 against time show good linearity in all cases and where the errors involved in the parameters ϵ and K_1 are small, this extends to greater than 80% reaction (figure 5.1). Excellent agreement was observed between the values of k_0 obtained by this method and those obtained using the method of instantaneous rates (equation 5.28), the data under various

Plots of the left hand side of equation 5.30 against time.



Conditions:-

 $T=25^{\circ}\text{C}$, $I=1.0\text{M}$ $[\text{Fe}^{3+}] = 0.05\text{M}$, $[\text{H}^{+}] = 0.3\text{M}$, A, [2-MIBA] = 0.0025M.

B, [2-MPA] = 0.0029M.

C, [MAA] = 0.0025M.

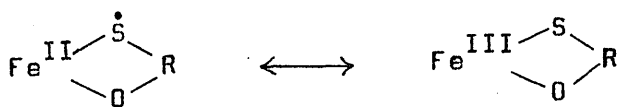
FIGURE 5.1

conditions being presented in table 5.3. In view of the uncertainties involved, the substantial constancy of the values of k_0 on variation of $[Fe^{3+}]_0$, $[HORSH]_0$, $[Fe^{2+}]_0$ and $[O_2]$ confirms rate equation 5.27. Mean values of k_0 for each ligand at various temperatures are presented together with the corresponding thermodynamic parameters in table 5.4. Simulated reaction curves were obtained using the relevant values of k_0 , K_1 and E in a modified form of equation 5.30 and are compared with the experimental results in figure 5.2.

The extreme simplicity of the rate law suggests that a bimolecular reaction mechanism is operative in these systems and as such the reactions are comparable with those observed in more basic conditions in the absence of oxygen. Lack of any significant dependence on the product iron II might be predicted both from consideration of the overall free energy change and the low affinity of the reactant mercaptocarboxylic acids for iron II.

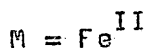
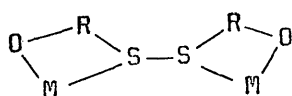
The mechanism is considered to be a modified form of that proposed by Leussing²⁷⁷. Whereas Leussing's original postulate requires two sulphur atoms on adjacent sites on the same metal ion, in this case, both reactants are monocomplexes. There are numerous plausible mechanisms which are consistent with a second order rate law, each differing in the intimate nature of the interaction.

(a) If the complex is considered to be in a state of indeterminate valence.



5.33

acting as a radical stabiliser, then the process may be envisaged as a radical dimerisation reaction



5.34

TABLE 5.3

Rate constants, k_o , for various ligands at differing hydrogen ion concentrations, $I = 1.0M$

LIGAND	T/°C	[H ⁺]/M	[HORSH] _o /M	[Fe ^{III}] _o /M	$k_o/M^{-1}s^{-1}$
MAA	10	0.3	0.00258	0.025	99
				0.050	104
		0.4	0.00256	0.025	89
	0.050			100	
	15	0.3	0.00397	0.025	122
				0.050	117
		0.4	0.00256	0.025	132
	0.050			134	
	20	0.3	0.00258	0.002267	138
				0.0175	147
				0.023333	138
		0.4	0.00210	0.05	153
				0.02918	149
				0.0350	138
	25	0.3	0.00258	0.05833	141
0.025				164	
0.4		0.00256	0.050	161	
	0.025		168		
2-MPA	10	0.3	0.00294	0.050	171
				0.025	53
		0.4	0.00256	0.025	48
	0.050			62	
	15	0.3	0.00303	0.025	76
				0.050	83
		0.4	0.00256	0.025	82
	0.050			88	

a

Table 5.3 cont'd.

LIGAND	T/°C	[H ⁺]/M	[HORSH] ₀ /M	[Fe ^{III}] ₀ /M	k ₀ /M ⁻¹ s ⁻¹		
2-MPA	20	0.3	0.00262	0.01167	103	a	
				0.0175	98		
				0.02333	104	a	
				0.02917	98	a	
				0.0350	96		
				0.04667	101		
				0.05833	100		
				0.00264	0.025	102	b
				0.050	97	b	
				0.025	96	c	
				0.050	100	c	
	0.00254	0.01458	97				
	0.02917	102	d				
	0.04375	100	d				
	0.05833	119	d				
	0.02917	102					
	0.04375	102	a				
	0.05833	101					
	0.4	0.00210	0.050	98			
	0.25	0.00248	0.025	100	a		
	0.3			103			
	0.4			101			
	0.45			115			
0.50			99				
0.60			110				
25	0.3	0.00294	0.025	124			
			0.050	128			
			0.4	0.00256	0.025	136	
			0.050	129			
2-MIBA	10	0.3	0.00248	0.025	33	a	
				0.050	18	a	
	15	0.3	0.00258	0.025	25	a	
				0.050	17	a	
	20	0.3	0.00277	0.0175	45	a	
				0.02918	41	a	
			0.0350	28	a		

Table 5.3 cont'd.

LIGAND	T/°C	[H ⁺]/M	[HORSH] ₀ /M	[Fe ^{III}] ₀ /M	k ₀ /M ⁻¹ s ⁻¹		
2-MIBA	20	0.3	0.00277	0.04667	31		
				0.05835	28	a	
	25	0.4	0.00195	0.050	36		
				0.025	44	a	
		0.3	0.00248	0.050	47		
2-MSA ^d	10	0.3	0.00257	0.025	27		
				0.050	28		
		0.4	0.00251	0.025	27		
				0.050	28		
	15	0.3	0.00271	0.025	38		
				0.050	41		
		0.4	0.00251	0.025	40		
				0.050	41		
			0.3	0.004	0.0422	56	
					0.0317	61	
	20	0.4	0.004	0.0264	57		
				0.0211	53		
		0.5	0.0158	0.0106	0.0158	54	
					0.0106	54	
0.0053			0.0053	0.0053	56		
2-MSA	20	0.4	0.004	0.053	59		
				0.042	58		
				0.037	60		
				0.036	54		
				0.032	57		
				0.026	55		
				0.021	52		
		0.5	0.011	60			
			0.005	60			
			0.04	55			
			0.035	61			
			0.030	56			
			0.025	56			
			0.020	56			
0.015	55						
0.010	65						
0.005	56						

Table 5.3 cont'd.

LIGAND	T/°C	[H ⁺]/M	[HORSH] ₀ /M	[Fe ^{III}] ₀ /M	k ₀ /M ⁻¹ s ⁻¹	
2-MSA	20	0.6	0.004	0.037	55	
				0.0317	57	
				0.0264	56	
				0.0211	55	
				0.0158	59	
				0.0106	62	
	25	0.3	0.00257	0.025	68	
				0.050	66	
				0.025	72	
		0.4		0.00251	0.025	72
				0.050	67	
				0.050	67	

a) - from instantaneous rates

b) - [Fe^{II}]₀ = 0.00321

c) - [Fe^{II}]₀ = 0.00642

d) - with rigorous oxygen exclusion.

TABLE 5.4

Redox rate constants and thermodynamic parameters ^a

LIGAND	T ^o C	k_o M ⁻¹ s ⁻¹	ΔH^* b kcal mole ⁻¹	ΔS^* b cal ^o K ⁻¹ mole ⁻¹
MAA	10	96.1 ± 12.2	5.3 ± 1.4	-30.7 ± 5.4
	15	126.4 ± 11.0		
	20	139.0 ± 11.8		
	25	166.9 ± 17.6		
2-MPA	10	53.3 ± 10.6	9.1 ± 2.2	-18.4 ± 3.4
	15	82.2 ± 8.2		
	20	101.1 ± 5.8		
	25	130.2 ± 10.2		
2-MIBA	10	24.0 ± 26.2 ^c	13.6 ± 3.9	-5.2 ± 1.3
	15	20.5 ± 20.4		
	20	33.9 ± 13.0		
	25	47.2 ± 8.0		
2-MSA	10	27.3 ± 4.4	10.1 ± 1.6	-16.0 ± 2.1
	15	40.1 ± 3.8		
	20	57.0 ± 1.6		
	25	67.7 ± 7.4		

a - error limits quoted are two standard deviations

b - derived from an unweighted least squares procedure

c - value excluded in calculation of thermodynamic parameters.

Comparison of observed (dots) and calculated (full line) traces of concentration against time for the redox reaction between iron III and 2-mercaptosuccinic acid. $T=20^{\circ}\text{C}$, $I=1.0\text{M}$.

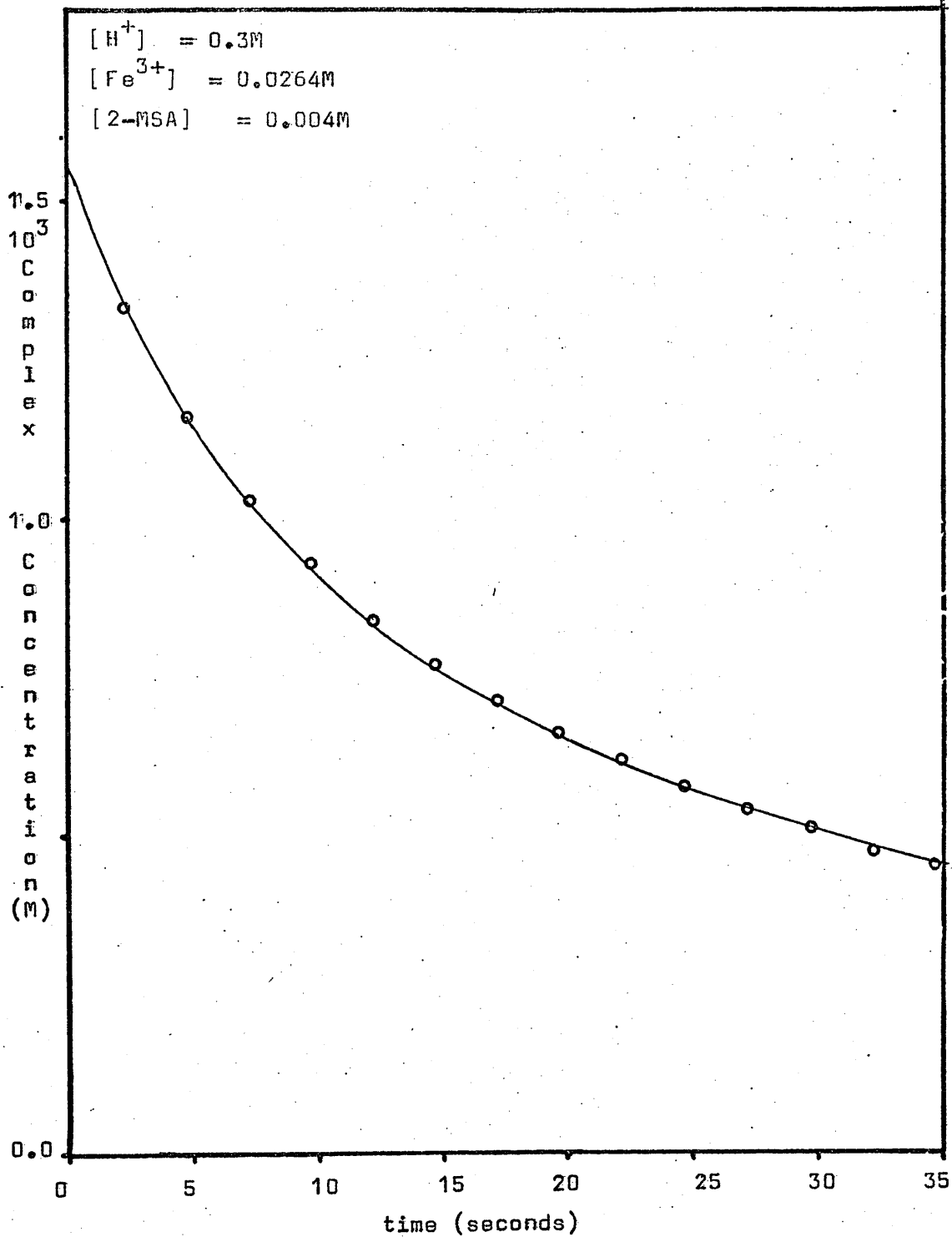
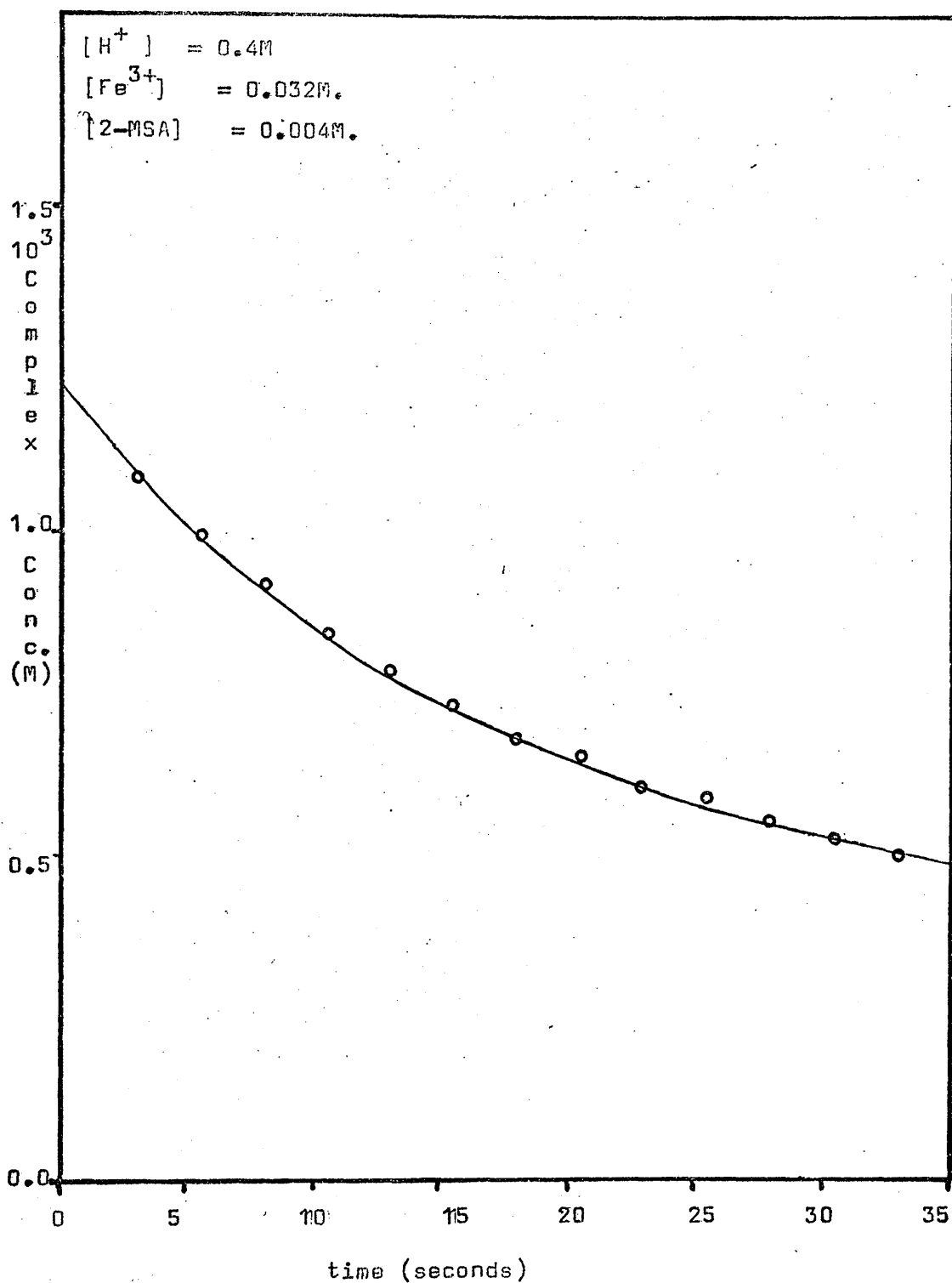


FIGURE 5.2

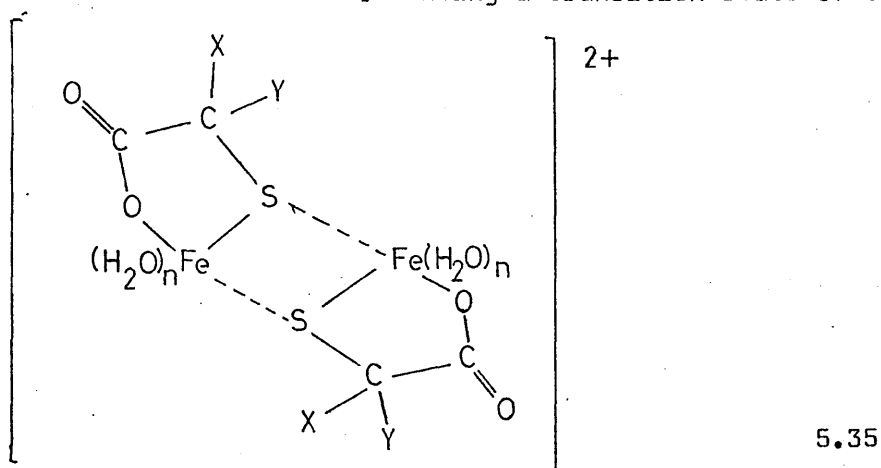


(Time axis is displaced because of induction period.
 Complex concentration calculated from the optical density
 using the appropriate values for the extinction coefficient
 and path length.)

FIGURE 5.2

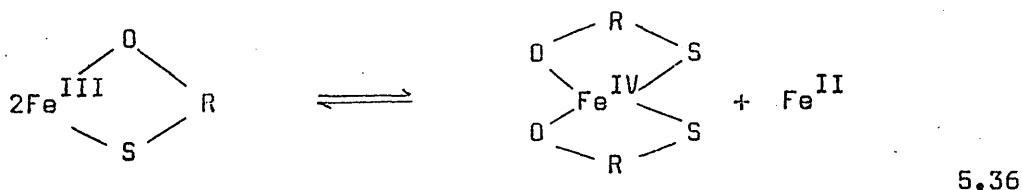
with subsequent dissociation of the disulphide to form two moles of iron II. Such a mechanism is operative in the case of uncoordinated radical species⁷⁸ and an intermediate of type 5.34 has been observed²⁹⁴ with chromium III where reduction of the metal is unfavourable.

(b) The expected lability of these monocomplexes suggests that an inner sphere electron transfer involving a transition state of the type



is possible. Since the reaction rates are one to two orders of magnitude greater than the overall acid catalysed aquation reactions and since the redox step exhibits no acid catalysis, metal-ligand cleavage is not expected to take place and the reaction rates may be governed either by rate determining substitution at coordinated sulphur or by the increased rate of solvent exchange in the complex.

An alternative formulation of this mechanism utilising the unique electron transfer properties of bridging sulphur²⁹⁵ to incorporate a higher oxidation state



with subsequent reductive elimination to give disulphide is considered unlikely on energetic grounds.

Addition of acrylonitrile to a rigorously deoxygenated solution containing excess iron III and 2-mercaptosuccinic acid produced a white polymeric precipitate after 24 hours. This evidence is

suggestive of a mechanism involving free or coordinated radical species. Although such a mechanism cannot be ruled out, since no polymer is produced immediately after the disappearance of the blue colour and since there is the possibility of over oxidation, interpretation of the result is ambiguous.

A mechanism involving spontaneous radical formation



5.37

might be expected to involve rate law dependences on iron III, iron II and O_2 and is considered unlikely in view of the effect of substituents on the rate constants and thermodynamic parameters. The ease of a spontaneous process might be expected to increase with increasing methylation contrary to the observed trend.

The effects of substituents on the reactions are consistent with an associative dimerisation mechanism where increasing the bulk of the group next to the sulphur introduces steric hindrance which reduces the rate of dimerisation. If the effect were electronic in origin, acceleration of the rate by methyl substituents would be expected. The variation in activation enthalpies in these reactions would also tend to support this assignment as would the negative activation entropies. Comparison of the data with other dimerisation reactions of iron III (table 5.5) reveals that the rates are similar in magnitude but gross differences in structure preclude any meaningful interpretation.

Increasing methylation in mercaptoaminoacids has previously been observed^{289,290} to retard the overall rate of electron transfer. The transient intermediate found in the case of 2-MIBA is longer lived by a factor of around 10^2 over the intermediate in the case of MAA as shown in figure 5.3. Consideration of the overall mechanism, scheme 5.2, reveals that the redox rate k_0 varies by only a factor of three and that the effects may be attributed more to the thermodynamic stabilities of the complexes. By changing by a factor of ten, these result in a hundred-fold change in the overall rate by affecting the concentration available for reaction.

TABLE 5.5

Dimerisation and Related Reactions of Complexes of Iron III.

T = 25°C (Various ionic strengths).

Reaction	$k/M^{-1}S^{-1}$	ref.
$Fe(H_2O)_6^{3+} + Fe(H_2O)_5OH^{2+}$	4	a
$+ Fe(CN)_6^{3-}$	800	b
$Fe(H_2O)_5OH^{2+} + Fe(H_2O)_5OH^{2+}$	250	ac
$Fe(H_2O)_5Cl^{2+}$	100	c
$Fe(H_2O)_5SCN^{2+}$	85	c
$Fe(H_2O)_5SO_4^+$	110	c
$Fe(CN)_6^{3-}$	3.6×10^4	b
$FeedtaOH_2 + FeedtaOH$	2×10^4	de
$FeHedtaOH_2 + FeedtaOH$	6×10^4	d
$FecyctaOH_2 + FecyctaOH$	100	d
$FeedtaOH + FeedtaOH$	600	d
$FeHedtaOH + FeHedtaOH$	900	d
$FecyctaOH + FecyctaOH$	90	d

a. H.N. Po and N. Sutin, *Inorg. Chem.*, 1971, 10, 428.B.A. Sommer and D.W. Margerum, *Ibid.*, 1970, 9, 2517.T.J. Connocchioli, E.J. Hamilton and N. Sutin, *J. Amer. Chem. Soc.*, 1965, 87, 926.B. Lutz and H. Wendt, *Ber. Bunsenges. Phys. Chem.*, 1970, 74, 372.b. R.G. Walker and K.O. Watkins, *Inorg. Chem.*, 1968, 7, 885.D.L. Singleton and J.H. Swinehart, *Ibid.*, 1967, 6, 1536.c. H. Wendt, *Z. Electrochem.*, 1962, 66, 235.d. R.G. Wilkins and R.E. Yelin, *Ibid.*, 1969, 8, 1470.e. A.D. Gilmour and A. McAuley, *Inorg. Chim. Acta.*, 1970, 4, 158.

edta = ethylenediaminetetraacetic acid.

cycta = cyclohexyldiaminetetraacetic acid.

Traces of optical density against time for reactions of iron (III) with 2-mercaptocarboxylic acids.

$T = 25^{\circ}\text{C}$ $I = 1.0\text{M}$

$[\text{H}^+]_0 = 0.4\text{M}$, $[\text{Fe}^{3+}]_0 = 0.05\text{M}$, $[\text{HORSH}]_0 = 0.0025\text{M}$.

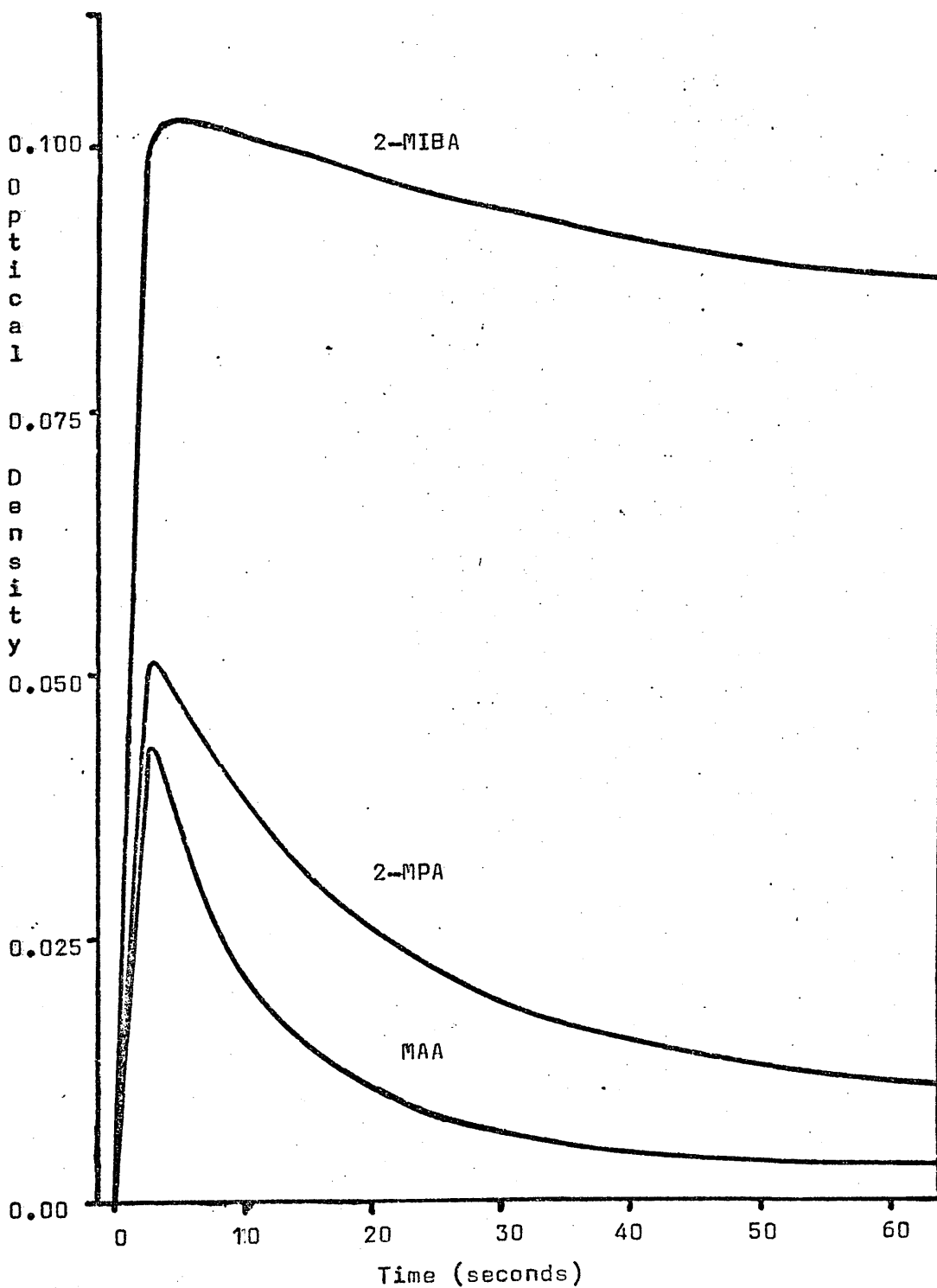
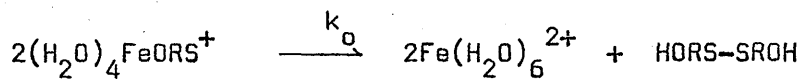
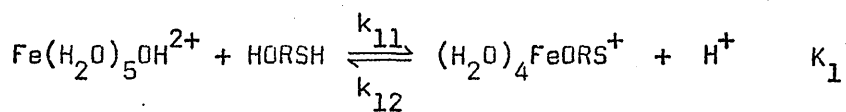
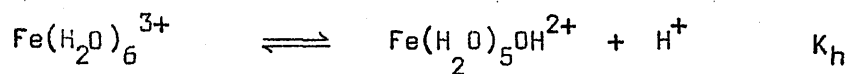
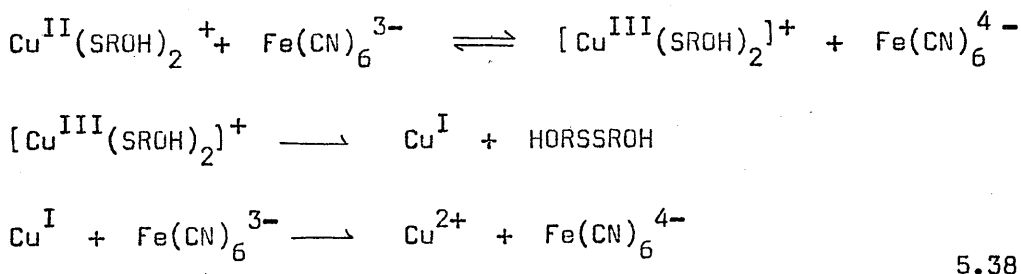


FIGURE 5.3

SCHEME 5.2

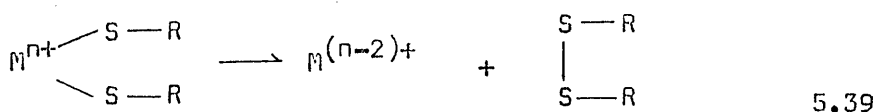
While the exact nature of the interaction between two monocomplexes remains uncertain, it is likely that the driving force must be to allow the two iron III centres to act as a concerted two-electron oxidant in the proximity of two mercaptide groups with resultant disulphide formation, eliminating the need to invoke high energy radical species. If the thermodynamic aspects of disulphide bond formation are important then the reactions of metal-sulphur bonded species might show some resemblance to reactions of organometallic complexes which are governed in many instances by carbon-carbon bond formation without the formation of unfavourable radical intermediates.²⁹⁶

Second order reactions are found in the oxidation of mercapto-carboxylic acids by $\text{Fe}(\text{CN})_6^{3-}$ and complex radical mechanisms have been proposed.²⁹⁷⁻²⁹⁹ The observation of copper ion catalysis³⁰⁰ has however led to the formulation of a mechanism³⁰¹ in which thermodynamic aspects of disulphide formation appear to be important



A less well defined example of metal ion cooperative effects has been noted³⁰² in the catalytic oxidation of cysteine by ferriporphyrin IX in which the addition of polybases known to stack the porphyrin rings, increases the catalytic effect.

Concerted two electron transfer pathways are also dominant in the corresponding reactions of $\text{Cr}(\text{VI})$ ³⁰³ and $\text{V}(\text{V})$ ³⁰⁴ both of which proceed by way of a 1:2 complex yielding disulphide directly



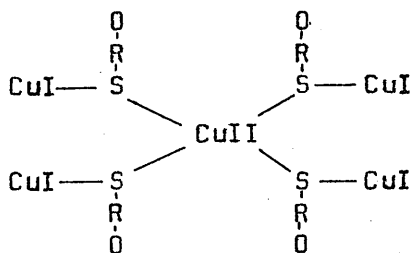
This mechanistic type is however by no means general and spontaneous redox processes are reported in reactions of Co(III)³⁰⁵, Ce(IV)³⁰⁶ and Np(VI)³⁰⁷. In the case of the oxidation of coordinated thiols by the latter reagent, the lability of the metal-sulphur bond is apparently important.³⁰⁸

Reaction between Copper II and Mercaptosuccinic Acid.

Consideration of the possibility of copper ion catalysis in the reaction of mercaptocarboxylic acids with iron III, prompted a study of some aspects of the corresponding reaction with copper II. This reaction has been the subject of many previous investigations because of its biological and medical importance and reports of the nature of the system are varied and contradictory.

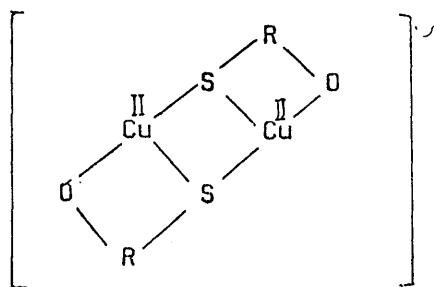
The copper II/copper I redox couple has a value of 0.158 volts¹²⁷ but, like that of iron III/iron II, it is susceptible to large variations on complexation. Although copper II like iron III is a hard acid, copper I is soft and is formed only in the presence of a suitable valence specific reagent. Such a species is the soft mercaptide group and it therefore serves a dual role in the reaction, acting both as a reductant and a complexing agent.³⁰⁹ The result of this valence specificity is that the products of the reaction between copper II and mercaptocarboxylic acids vary on changing the reaction conditions with a highly coloured purple complex formed in excess metal and a yellow complex in other circumstances. Although the latter is well characterised as a linear Cu(I)-mercaptide macromolecular species,^{309,310} the purple complex has been the subject of much discussion.

In the case of 2-MSA, Klotz et al³¹¹ considered it to be a polynuclear mixed valence complex of the type



5.40

and his conclusions have been substantiated³¹²⁻³¹⁶ by studies with other ligands. Hemmerich³¹⁷ and Hill³¹⁸ independently however obtained a 1:1 stoichiometry for the complex and the former proposed a structure³¹⁹



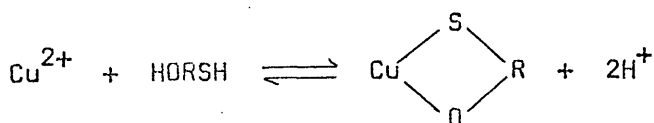
5.41

Both purple and yellow complexes are susceptible to reaction with molecular oxygen³¹⁸ and studies of the rate and amount of oxygen uptake have been reported.^{320,321} As yet however, there has been little attempt to describe the relationship between the complexes.

A study of the reaction between copper II and 2-mercaptosuccinic acid was carried out using both stopped flow and conventional spectrophotometry. Experimental measurements were made at 25°C on rigorously deoxygenated solutions over the concentration ranges $[H^+] = 0.01 \rightarrow 1.0M$, $[Cu^{2+}] = 2 \times 10^{-2} \rightarrow 2 \times 10^{-4}M$ and $[HORSH] = 10^{-1} \rightarrow 10^{-4}M$ at 1.0M ionic strength with lithium perchlorate as background electrolyte. Although these reactions are too complex to allow kinetic treatment at present, intermediate complexes were observed and initial rate measurements were made to allow a qualitative description of the reaction.

By analysis of time dependent U.V.-visible spectra, three species (figure 5.4) were identified as participating in the reaction. The first detectable intermediate exhibits an absorption maximum in the region of 350nm and is formed in conditions of both excess metal and ligand. The formation is within the time of mixing consistent with a copper II complex formation reaction and its decomposition could be observed only at $[H^+] \neq 0.01M$ since the rate law is strongly acid dependent.

These facts may be explained by a 1:1 chelate complex of the type.



5.42

in which participation of sulphur is proposed to account for the red shift in the spectrum. The geometry of the complex is considered to be square planar or tetragonally distorted octahedral

Absorption spectra of species involved in the reaction between copper II and 2-mercaptosuccinic acid. $T=25^{\circ}\text{C}$, $I=1.0\text{M}$.

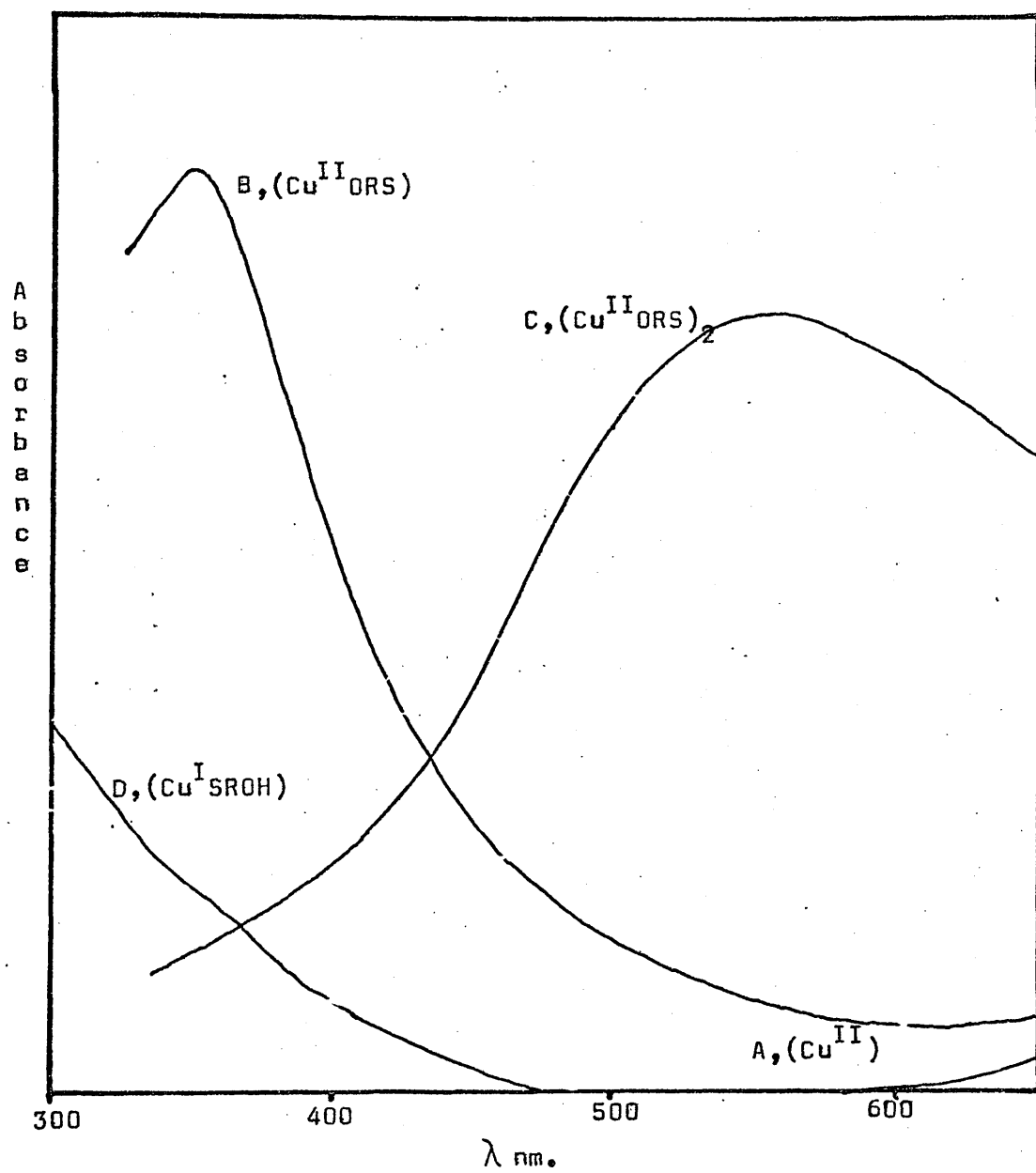
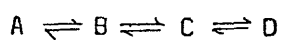


FIGURE 5.4

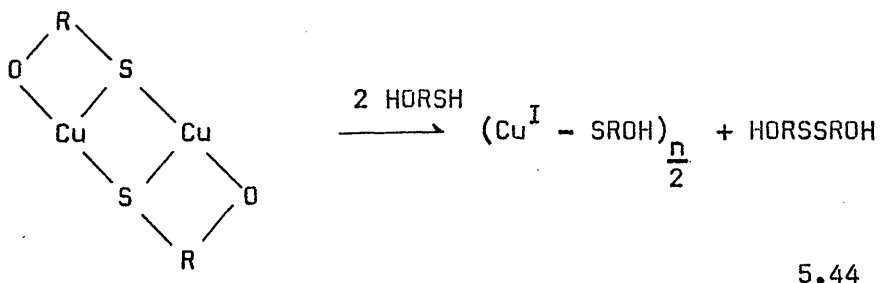
as found in other copper II complexes.³²²

This species undergoes a transformation to yield the purple intermediate complex. Studies of the initial rate of appearance of the purple colour were found, figure 5.5, to conform to the rate law

$$\text{Initial Rate} = k_{ir} \frac{[\text{Cu}^{2+}]_0^2 [\text{HORSH}]_0^3}{[\text{H}^+]_0^4} \quad 5.43$$

consistent with a pre-equilibrium and reaction of copper-mercaptocarboxylate complexes. The conversion of the first intermediate to the purple compound ($\lambda_{\text{max}} 525\text{nm.}$) is kinetically complex and although isosbestic behaviour (430nm.) is observed up to 50% reaction, deviations thereafter suggest that perhaps an oligomerisation process is taking place.

The dimeric structure proposed by Hemmerich³¹⁹ for this species involves copper in a state of indeterminate valence accounting for its intense colour and lack of electron paramagnetic resonance spectrum. It is stable only because the release of disulphide leads to the formation of copper I, a thermodynamically unfavourable process. In the presence of an excess of ligand however, a redox equilibrium is set up between the purple complex and the yellow stabilised copper I macromolecular species



5.44

A ratio of $[\text{Cu}^{\text{II}}]_0 : [\text{HORSH}]_0$ of 1:2 is therefore required for maximum formation of the yellow species as shown in figure 5.6.

In conditions of excess ligand ($>2:1$), detection of the purple complex is not possible presumably because of ligand

Plots of \log_{10} (initial rate, OD/s) against \log_{10} (concentration) for the formation of the purple coloured copper II - 2-mercapto-succinate complex. Absolute scales on the co-ordinate axes are displaced for convenience. $T=25^{\circ}\text{C}$, $I=1.0\text{M}$, $\lambda=525\text{nm}$.

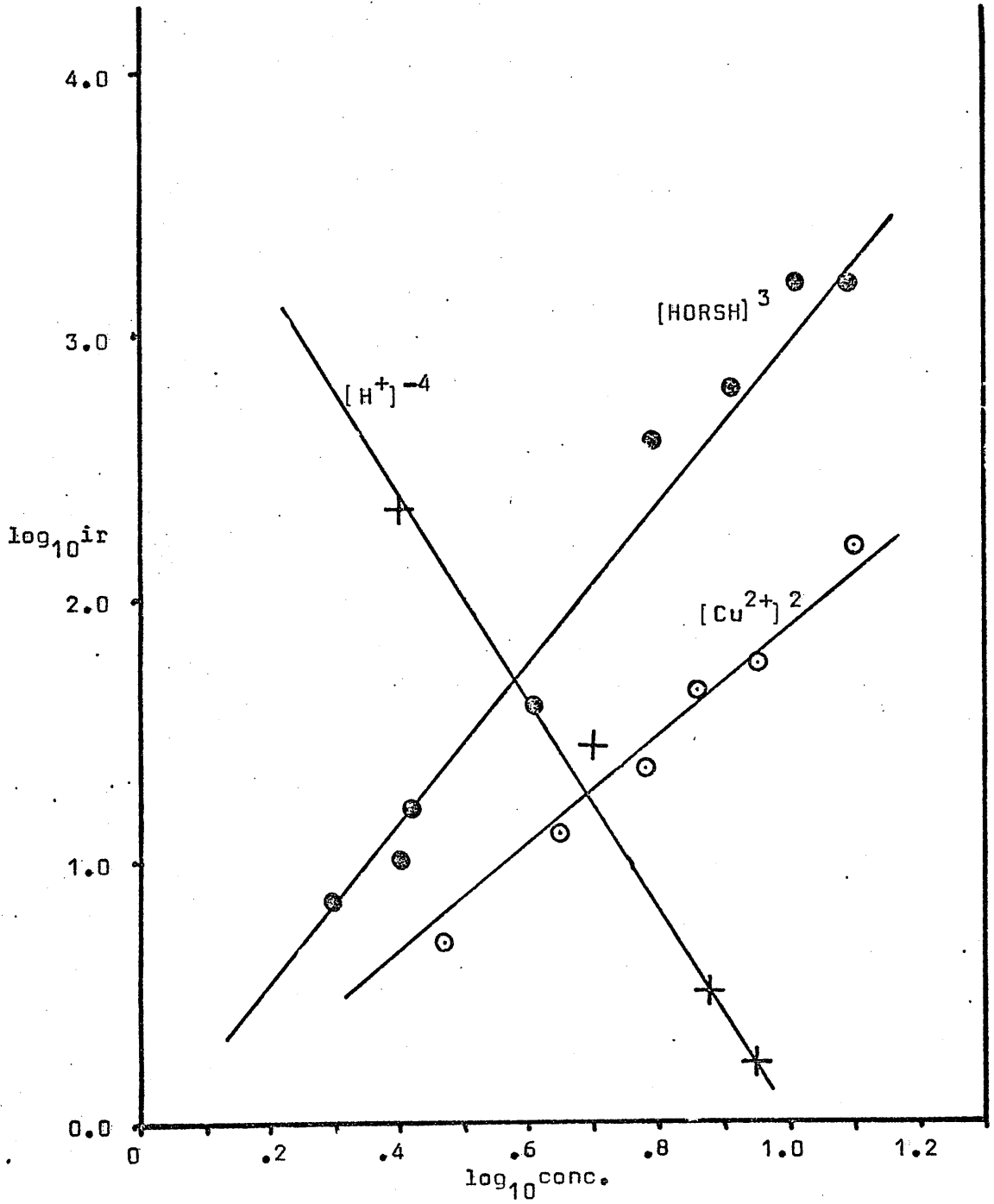


FIGURE 5.5

Spectrophotometric titration of the products of the reaction between copper II and 2-mercaptosuccinic acid under an atmosphere of nitrogen. $T=25^{\circ}\text{C}$, $I=1.0\text{M}$, $\lambda=350\text{nm}$. $l = 1.0\text{cm}$.

A; 5mls $[\text{Cu}^{2+}]$ + xmls[HORSH] } total volume 25mls.
 B; xmls $[\text{Cu}^{2+}]$ + 5mls[HORSH]

$[\text{Cu}^{2+}] = [\text{HORSH}] = 0.03\text{M}$. $[\text{H}^+] = 0.5\text{M}$.

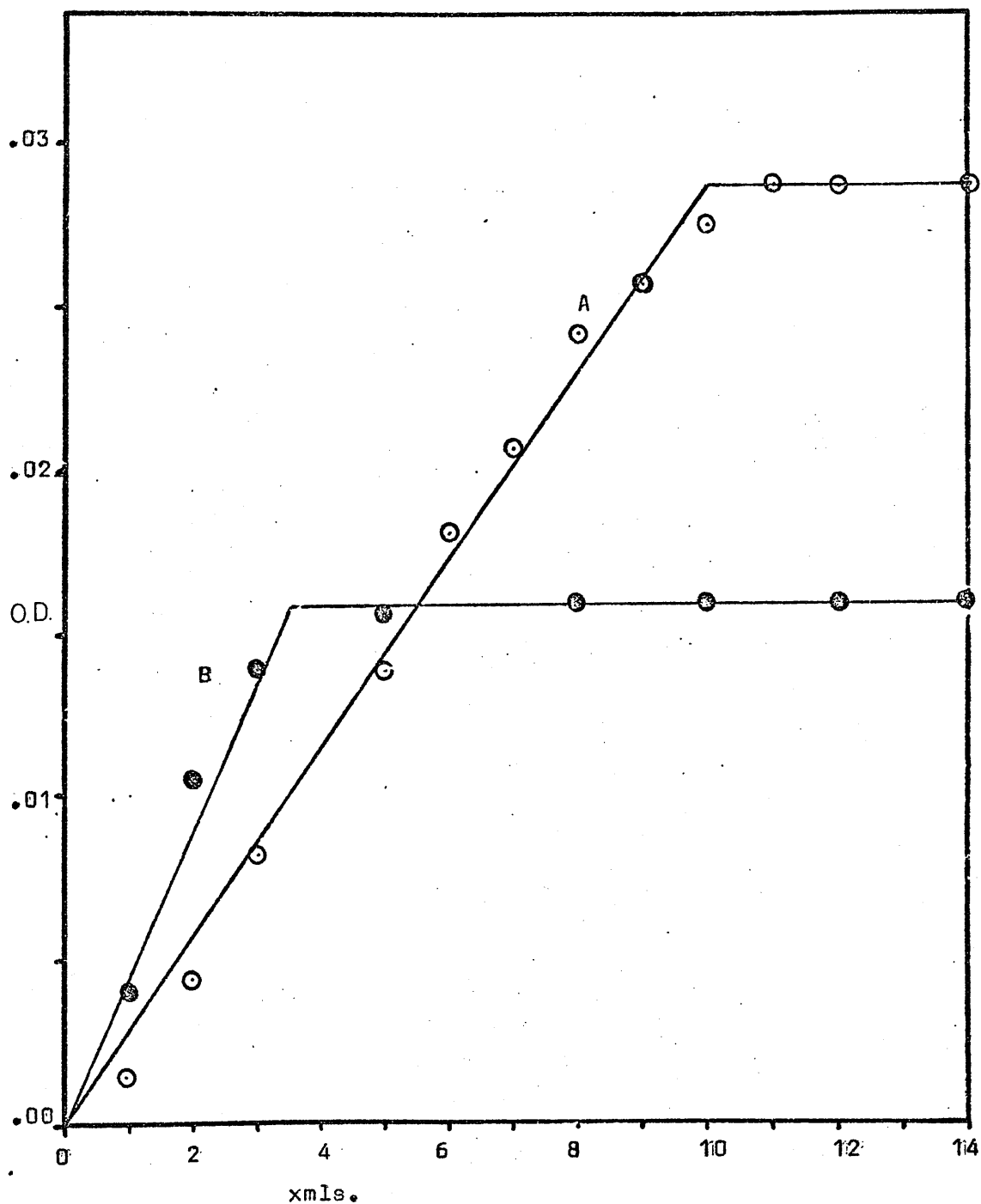
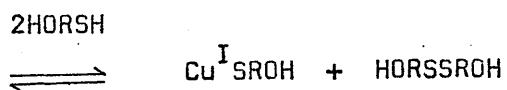
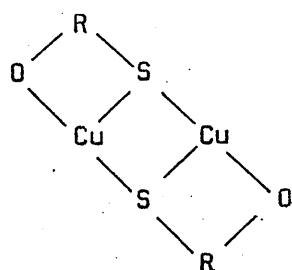
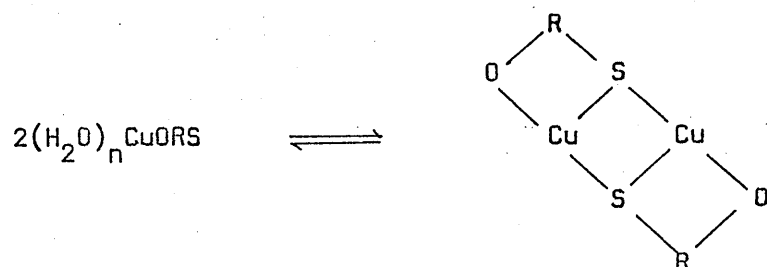
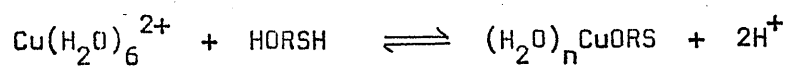


FIGURE 5.6

catalysis in reaction 5.44. At high acidity, even in conditions of excess metal, a balance is set up between the purple and yellow products possibly due to an unfavourable free energy change in equilibrium 5.42, preventing binding of all the free ligand and therefore allowing a contribution from equilibrium 5.44. At lower acidities however, with excess metal, the ligand is completely bound to copper II in the form of 5.42 preventing further reaction and thus stabilising the purple complex.

The proposed mechanism of the reaction, scheme 5.3, is thus apparently analagous to the one proposed in the case of the oxidant iron III. Stabilisation of the dimeric intermediate as a result of the instability of the copper I product is however a determining factor. Choice of a suitable ligand such as 2-MIBA³²³ may thus provide a means of moderating the equilibria involved and allow kinetic treatment and the evaluation of a detailed mechanism. A larger effect of structure on the equilibria involved with the copper II reaction might be expected in view of the related bio-medical phenomena in the treatment of Wilson's disease.³²⁴

SCHEME 5.3



CHAPTER 6

Acid Dissociation Constants of
Mercaptocarboxylic Acids.

Introduction

In the previous chapters, the mechanisms of several reactions of 2-mercaptocarboxylic acids have been described. In order to define more accurately the major equilibria and reaction pathways in these reactions, a knowledge of the ligand ionisation constants important in the pH range used is required. While values of these constants have been obtained under various conditions of temperature and ionic strength,³²⁵ only in the case of 2-MSA³²⁶ have results been reported at the same ionic strength and over the temperature range used in the kinetic experiments. Accordingly, it was decided to carry out a similar study on the other ligands of interest; MAA, 2-MPA and 2-MIBA. In view of the differences in the interaction of these ligands with iron (III), an examination of the thermodynamics of the ionisation process might aid the interpretation of effects specific to the ligands.

The ionisation of a weak acid HA in the presence of a base B may be represented by the protolytic reaction



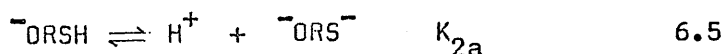
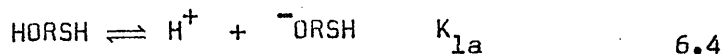
which is quantified by the equilibrium constant

$$K_a = \frac{a_{\text{HB}} a_{\text{A}}}{a_{\text{HA}} a_{\text{B}}} \quad 6.2$$

where a_x is the activity of species x and charges are omitted for clarity. In the studies considered in this chapter, attention is confined to dilute solutions of HA in B in which case the activity of the solvent in solution is virtually constant and equal to the activity of the pure solvent. Hence 6.2 may be reduced to

$$K_a = \frac{a_{\text{HB}} a_{\text{A}}}{a_{\text{HA}}} \quad 6.3$$

2-Mercaptocarboxylic acids are weak dibasic acids and rigorous treatment involves consideration of two equilibria



where

$$K_{1a} = \frac{a_{\text{H}^+} a_{\text{ORSH}^-}}{a_{\text{HORSH}}}$$

and

$$K_{2a} = \frac{a_{\text{H}^+} a_{\text{ORS}^{2-}}}{a_{\text{ORSH}^-}} \quad 6.6$$

Previously reported values of K_a (table 6.1) indicate that the acidity constants are widely separated with the sulphhydryl proton much more tightly bound than the carboxylic acid proton. Consequently in aqueous acid media, the concentration of the species $^-ORS^-$ may be considered negligible and in the determination of the acidity constants, provided measurements are restricted to $pH < 7$, equilibrium 6.5 may be ignored and the acid treated as monobasic.

The equilibrium may be rewritten

$$K_a = \frac{[H^+] [^-ORS^-]}{[HORSH]} \frac{Y_{H^+} Y_{^-ORS^-}}{Y_{HORSH}} \quad 6.7$$

where Y_x is the activity coefficient of x . Activity coefficients have been shown to depend on the ionic strength^{213,327} for a 1:1 electrolyte and may be held constant by working in a medium of virtually constant composition. By incorporating the activity coefficients into the thermodynamic ionisation constant, the concentration constant may be obtained

$$K_a = \frac{[H^+] [^-ORS^-]}{[HORSH]} \quad 6.8$$

At high ionic strength, there exists no fully satisfactory theory to predict activity coefficients and so this latter constant is the most useful although its application is strictly limited to specific conditions. It is the determination of this constant in 1M sodium perchlorate which has been undertaken. While there is no assurance that the same constant is of value in mixed electrolytes (sodium perchlorate - ferric perchlorate - perchloric acid) at the same ionic strength, any differences should be small since the concentration of the counter anion is virtually the same.²¹³

The use of potentiometry to determine the activity of hydrogen ions was reported as early as 1897³²⁸ and has been used extensively ever since. The methods depend on either the redox properties of the proton

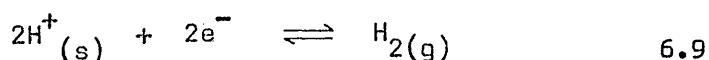


Table 6.1

Mercaptocarboxylic Acid Dissociation Constants Reported in the Literature.

Temperature (°C)	Medium (M)	$10^4 K_{1a}$ M	$10^{11} K_{2a}$ M	ref.
<u>1. Mercaptoacetic Acid.</u>				
0	0.10 KCl	3.8	3.3	a
15	0.10 KCl	2.8	4.5	a
20	0	2.76		b
	0.05 NaCl	2.76		b
	0.10 NaClO ₄	6.72	8.40	c
	0.10 NaClO ₄	3.89		d
	0.10 NaCl	3.08		b
	0.10 KCl	6.84		e
	0.20 NaCl	3.54		b
	0.30 NaCl	4.11		b
25	0	2.5	2.8	f
	0	3.83	6.35	g
	0	2.5	2.8	h
	0	3.54		b
	0	3.6	7.6	i
	0		7.91	j
	0	2.1	2.1	k
	0	6.02	10.0	l
	0.10 KCl	3.3	7.6	a
	0.10 KCl	2.8	6.0	i
	0.15 KNO ₃	6.20	0.4	m
	0.50 NaNO ₃	3.3	0.12	n
	0.00 KCl		8.88	o
30	0.10 KCl	6.45		p
31	0		8.74	j
35	0.10 KCl	2.6	8.5	a
40	0.10 KCl	2.2	11.2	a
60	0	0.85		b
	0	2.5	18	i
	0	3.3	24	i

Temperature (°C)	Medium (M)	$10^4 K_{1a}$ M	$10^{11} K_{2a}$ M	ref.
<u>2. 2-Mercaptopropionic Acid</u>				
20	0.1 NaClO ₄	5.73	8.22	q
	0.1 KCl	5.93		e
30	0.1 NaClO ₄	5.43	8.45	q
40	0.1 NaClO ₄	4.99	10.00	q
<u>3. 3-Mercaptopropionic Acid</u>				
25	0	7.86	6.5	k,r
	0	7.6	7.6	p
30	0.1 KCl	8.14		s
<u>4. 2-Mercaptoisobutyric Acid</u>				
?	?	5.93		t
<u>5. 2-Mercaptosuccinic Acid^z</u>				
20	0.10 KCl	8.34		e
		51.0		
	0.10 KCl	8.22		e
		62.9		
25	0	8.0	5.63	u
		69.0		
	0.10 KNO ₃	5.63	7.66	v
		56.4		
	0.10 KNO ₃	8.00	5.64	w
		12.9		
	1.00 KNO ₃	0.661	0.463	v
		72.5		
30	0.10 KCl	8.59		p
		52.1		
31	0.10 NaClO ₄	8.98		x
		62.0		
45	0	0.11		x
		71.8		
	0.10 KNO ₃	5.01	2.23	y
		11.48		

References for Table 6.1

- a. D.L. Leussing, R.E. Laramy and G.S. Alberts, J. Amer. Chem. Soc., 1960, 82, 4826.
- b. D. Urdonez and A. Garrido, Ion (Madrid), (1971), 31, 121, 158 (C.A. (1971), 75, 48241e).
- c. D.D. Perrin and I.G. Sayce, J. Chem. Soc. A., (1967), 82.
- d. J.E. Powell, R.S. Kolat and G.S. Paul, Inorg. Chem., (1964), 3, 518.
- e. E.R. Clark, J. Inorg. Nucl. Chem., (1963), 25, 353.
- f. D.G. Bush quoted in D.L. Leussing and I.M. Kolthoff, J. Amer. Chem. Soc., (1953), 75, 3904.
- g. D.L. Leussing, J. Amer. Chem. Soc., (1958), 80, 4180.
- h. D.G. Bush quoted in D.L. Leussing and I.M. Kolthoff, J. Electrochem. Soc., (1953), 100, 334.
- i. W. Lund and E. Jacobsen, Acta. Chem. Scand., (1965), 19, 1783.
- j. R.E. Benesch and R. Benesch, J. Amer. Chem. Soc., (1955), 77, 5877.
- k. E.Z. Larsson, Z. Anorg. Chem., (1928), 172, 375.
- l. R.K. Cannan and B.C.J.G. Knight, Biochem J., (1927), 21, 1384.
- m. N.C. Li and R.A. Manning, J. Amer. Chem. Soc., (1955), 77, 5225.
- n. D.L. Leussing, J. Amer. Chem. Soc., (1956), 78, 552.
- o. W.P. Jencks and K. Salvesen, J. Amer. Chem. Soc., (1971), 93, 4433.
- p. M. Cefola, A.S. Tompa, A.V. Celiano and P.S. Gentile, Inorg. Chem., (1962), 1, 290.
- q. R.S. Saxena and P. Singh, Z. Phys. Chem. (Leipzig), (1971), 247, 250.
- r. J.T. Spence and H.H.Y. Chang, Inorg. Chem., (1963), 25, 319.
- s. C.E. Cheney, Q. Fernando and H. Frieser, J. Phys. Chem., (1959), 63, 2055.
- t. J.R.A. Pollok and R. Stevens, eds., "Dictionary of Organic Compounds," 4th edition, Eyre and Spottiswoode, London, 1965.
- u. Q. Fernando and H. Frieser, J. Amer. Chem. Soc., (1958), 80, 4928.
- v. G.R. Lenz and A.E. Martell, Inorg. Chem., (1965), 3, 378.
- w. R.S. Saxena, K.C. Gupta and M.L. Mittal, Canad. J. Chem., (1968), 46, 311.
- x. S. Ramamoorthy and M. Santappa, Bull. Chem. Soc. Jap., (1968), 41, 1330.
- y. R.S. Saxena, K.C. Gupta and M.L. Mittal, Austral. J. Chem., (1959), 63, 2055.
- z. Values reported are - K_{1a}/K_{2a} First Column
 K_{3a} Second Column

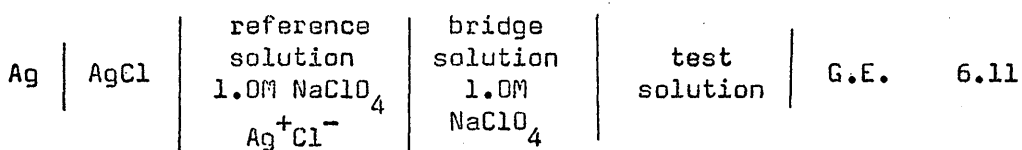
or one some membrane process involving a surface reversible to protons.



where subscripts s, g and m refer to solution, gas and membrane respectively. Of the latter type the glass electrode developed from the observations of Cremer³²⁹ is probably the most useful and versatile. Modern glass electrodes provide an accurate and rapid method for the determination of the hydrogen ion activity of solutions³³⁰

Apparatus

The first acidity constants of the mercaptocarboxylic acids were calculated from E.M.F. measurements on the cell.



G.E. -- glass electrode

The test solution was contained in a titration cell which was a modified 500 ml. three necked flask (figure 6.1) with an additional inlet in the base to allow oxygen free nitrogen (British Oxygen Co. Ltd.) previously saturated with water by passage through distilled water and 1.0M sodium perchlorate solution, to be bubbled through the solution continuously. This aided the mixing of the solution and ensured the exclusion of both O₂ and CO₂. The acid concentration in the cell was measured by means of a CTF 28 glass electrode (Russell pH Ltd.) using a model 46A "Vibret" pH meter (Electronic Instruments Ltd.). The reference electrode was silver-silver chloride and a "Wilhelm" bridge (figure 6.2) of the type described by Forsling et al.³³¹ was used to form the liquid junction.

The bridge was supported on an aluminium frame and the titration cell, reference electrode, bridge and dreschel bottles for pre-saturating the nitrogen gas were immersed in a water bath of

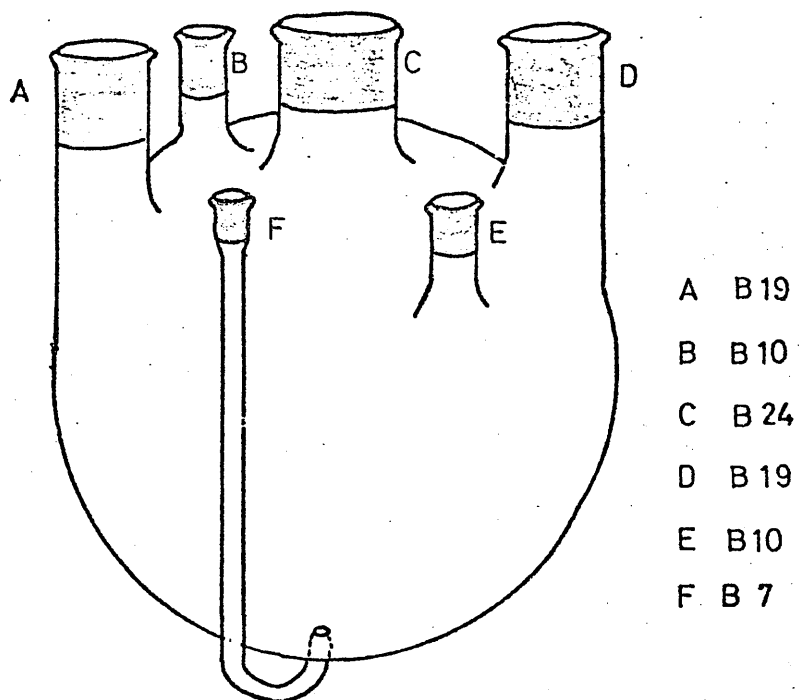
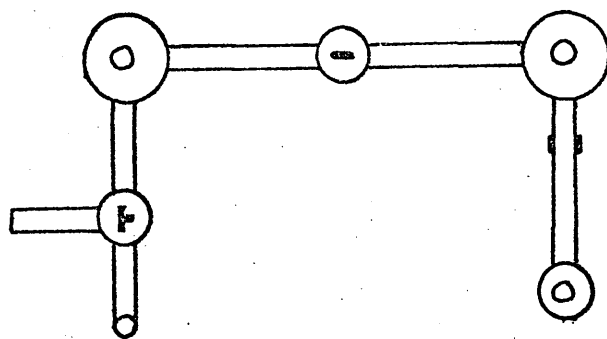
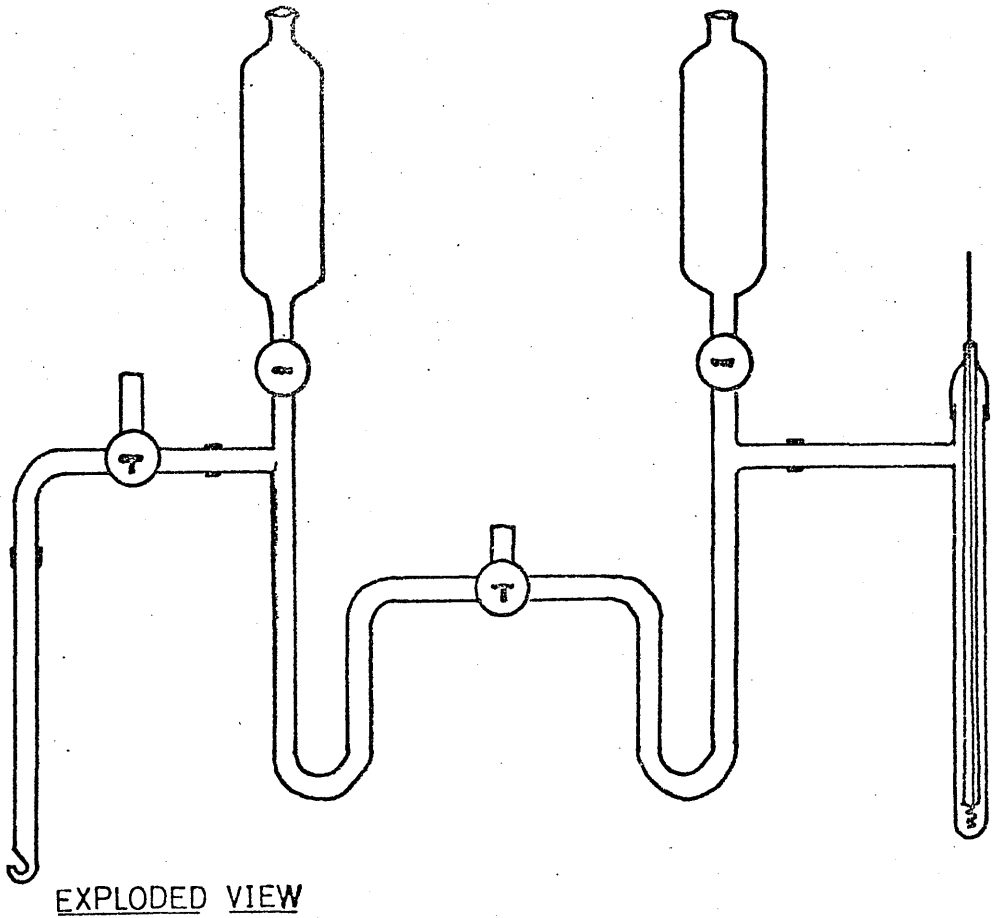


FIGURE 6.1 TITRATION CELL

The "Wilhelm" bridge.



-  2-way taps
-  3-way taps

PLAN

FIGURE 6.2

forty five litres capacity. The temperature of the bath was controlled by a Shandon circotherm Thermomix II thermoregulator (B. Braun, Melsungen) and a Tecam refrigeration unit (Techne (Cambridge) Ltd.) to obtain temperatures lower than room temperature and increase the sensitivity of control. The temperature was monitored using Zecol 0-50°C thermometers and it was found that it could be held constant to $\pm 0.1^\circ\text{C}$.

The Silver-Silver Chloride Electrode;

This was of the thermal electrolytic type described by Harned³³² The electrode was prepared by sealing a piece of platinum wire 1 mm. diameter, 2 cms. long in the form of a helix 3 mm. diameter in the end of a hollow pyrex glass tube to the other end of which was attached a B 10 quickfit cone. The platinum-glass seal was perfected by placing a few grains of Araldite powder at the junction of the platinum and glass. The helix was covered with a thick paste of silver oxide (Koch-Light, 99.99%) in distilled water. After drying in an oven at 120°C, this was placed in a muffle furnace and the temperature gradually raised to 400°C at which value it was retained until the decomposition of the silver oxide was complete. The process of coating the electrode was repeated until no cracks appeared on the dull silver surface.

Chloridisation was achieved by electrolysis of the electrode in 0.1M HCl at a current of 0.1 amps for one hour using a platinum wire helix as cathode. The electrode was then conditioned by heat treatment in distilled water at 50°C for two hours and stored in the dark in nitrogen saturated distilled water for one month until ready for use. When in use, the electrode was coated with dark P.V.C. tape to prevent spurious effects from its interaction with light. The level of illumination was virtually constant during the period when measurements were being made, and no effects attributable to the interaction of light with either the silver-silver chloride or glass electrodes were noted.

Experiments were performed at high constant ionic strength which permits the exclusion of activity coefficients from calculations and the stoichiometric dissociation constants are obtained. Theory predicts, however, that the response of the cell described above will be proportional to the hydrogen ion activity but calibration of the apparatus with solutions of known hydrogen ion

concentration allows a relationship between E.M.F. and $-\log_{10} [H^+]$ to be derived. Furthermore, under these conditions, the liquid junction potential of the cell may be ignored. ²¹²

The Hydrogen Ion Concentration Dependence of the Cell

Free energy changes in an open chemical system consisting of m species can be expressed by

$$dG = VdP - SdT + \sum_{i=1}^m \tilde{\mu}_i dn_i \quad 6.12$$

where dG , dP and dT are respectively the overall free energy change, pressure change and temperature change for the system and the electrochemical potential $\tilde{\mu}_i$ of the i^{th} species is defined by

$$\tilde{\mu}_i = \frac{\partial G}{\partial n_i} \quad T, P, n_1, \dots, n_m \quad 6.13$$

where n_i is the number of moles of the i th species.

At constant temperature and pressure, 6.12 may be reduced to

$$dG_{T,P} = \sum_{i=1}^m \tilde{\mu}_i dn_i \quad 6.14$$

The electrochemical potential μ of a species can be written as a function of the chemical potential μ and the charge z on the species

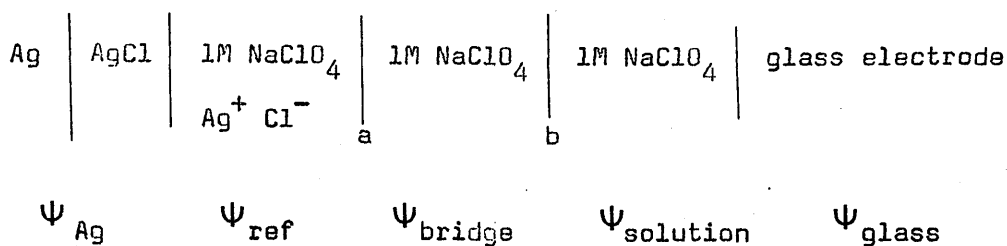
$$\begin{aligned} \tilde{\mu}_i &= \mu_i + z_i F \Psi \\ &= \mu_i^\circ + RT \ln a_i + z_i F \Psi \end{aligned} \quad 6.15$$

Where μ_i is the standard chemical potential of the i th species, R is the gas constant, F the faraday and Ψ is the electric potential of the phase containing the i th species.

If a system is at equilibrium, $dG = 0$ and hence

$$\sum_{i=1}^m \mu_i dn_i = 0 \quad 6.16$$

Consider the application of this relationship to each phase boundary in cell 6.11 at equilibrium.



6.11

The glass electrode is reversible to hydrogen ions and so one may write

$$\mu_{\text{H}^+_{\text{sol}}} = \mu_{\text{H}^+_{\text{glass}}}$$

expanding to

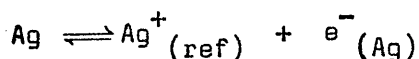
$$\mu_{\text{H}^+} + RT \ln a_{\text{H}^+} + F \Psi_{\text{sol}} = \mu_{\text{H}^+_{\text{glass}}} + F \Psi_{\text{glass}}$$

$$F (\Psi_{\text{glass}} - \Psi_{\text{sol}}) = (\mu_{\text{H}^+} - \mu_{\text{H}^+_{\text{glass}}}) + RT \ln a_{\text{H}^+}$$

and since $\mu_{\text{H}^+} - \mu_{\text{H}^+_{\text{glass}}}$ is a constant, this may be written

$$(\Psi_{\text{glass}} - \Psi_{\text{sol}}) = E_{\text{glass/sol}}^0 + \frac{RT}{F} \ln a_{\text{H}^+} \quad 6.17$$

At the reference electrode, the reaction is



$$\text{hence } \mu_{\text{Ag}} = \mu_{\text{Ag}^+} + RT \ln a_{\text{Ag}^+} + F \Psi_{\text{ref}} - F \Psi_{\text{Ag}}$$

$$F (\Psi_{\text{ref}} - \Psi_{\text{Ag}}) = (\mu_{\text{Ag}} - \mu_{\text{Ag}^+}) - RT \ln a_{\text{Ag}^+}$$

but since AgCl is sparingly soluble, if the solution is saturated

$$K_{\text{sp}} = a_{\text{Ag}^+} a_{\text{Cl}^-}$$

where K_{sp} is the solubility product of AgCl. Hence,

$$(\Psi_{ref} - \Psi_{Ag}) = \frac{\mu_{Ag} - \mu_{Ag^+}}{F} - \frac{RT}{F} \ln K_{sp} + \frac{RT}{F} \ln a_{Cl^-}$$

$$(\Psi_{ref} - \Psi_{Ag}) = E^{\circ}_{ref/Ag} + \frac{RT}{F} \ln a_{Cl^-} \quad 6.18$$

The overall E.M.F. of cell 6.11 may be written

$$E.M.F. = \Psi_{glass} - \Psi_{Ag} = (\Psi_{glass} - \Psi_{sol}) + (\Psi_{sol} - \Psi_{bridge}) +$$

$$(\Psi_{bridge} - \Psi_{ref}) + (\Psi_{ref} - \Psi_{Ag})$$

$$6.19$$

Substituting equations 6.17 and 6.18 in 6.19,

$$E.M.F. = E^{\circ}_{glass/sol} + \frac{RT}{F} \ln a_{H^+} + E^{\circ}_{ref/Ag} + \frac{RT}{F} \ln a_{Cl^-} +$$

$$(\Psi_{sol} - \Psi_{bridge}) + (\Psi_{bridge} - \Psi_{ref})$$

$$6.20$$

If the ionic strength, temperature and chloride ion concentration are maintained constant, $(\Psi_{bridge} - \Psi_{ref})$ may be considered constant such that

$$E.M.F. = E' + (\Psi_{sol} - \Psi_{bridge}) + \frac{RT}{F} \ln [H^+] \quad 6.21$$

where E' is a constant depending on temperature, ionic strength and electrode characteristics.

The problem of the solution-bridge liquid-junction potential may be overcome by calibrating the E.M.F. of the cell versus $\log[H^+]$ using solutions of known hydrogen ion concentration. The reverse process then allows the determination of hydrogen ion concentration from the E.M.F. of the test solution. A linear dependence of E.M.F. on $\log [H^+]$ was observed (figure 6.3) in agreement with Biedermann and Sillen²¹² who suggested an expression of the type,

$$(\Psi_{sol} - \Psi_{bridge}) = A \log \left(1 + \frac{B[H^+]}{I} \right) \quad 6.22$$

Typical "Wilhelm" bridge calibration plot of E.M.F. against $\log[H^+]$. $I=1.0M$, $T=15^\circ C$.

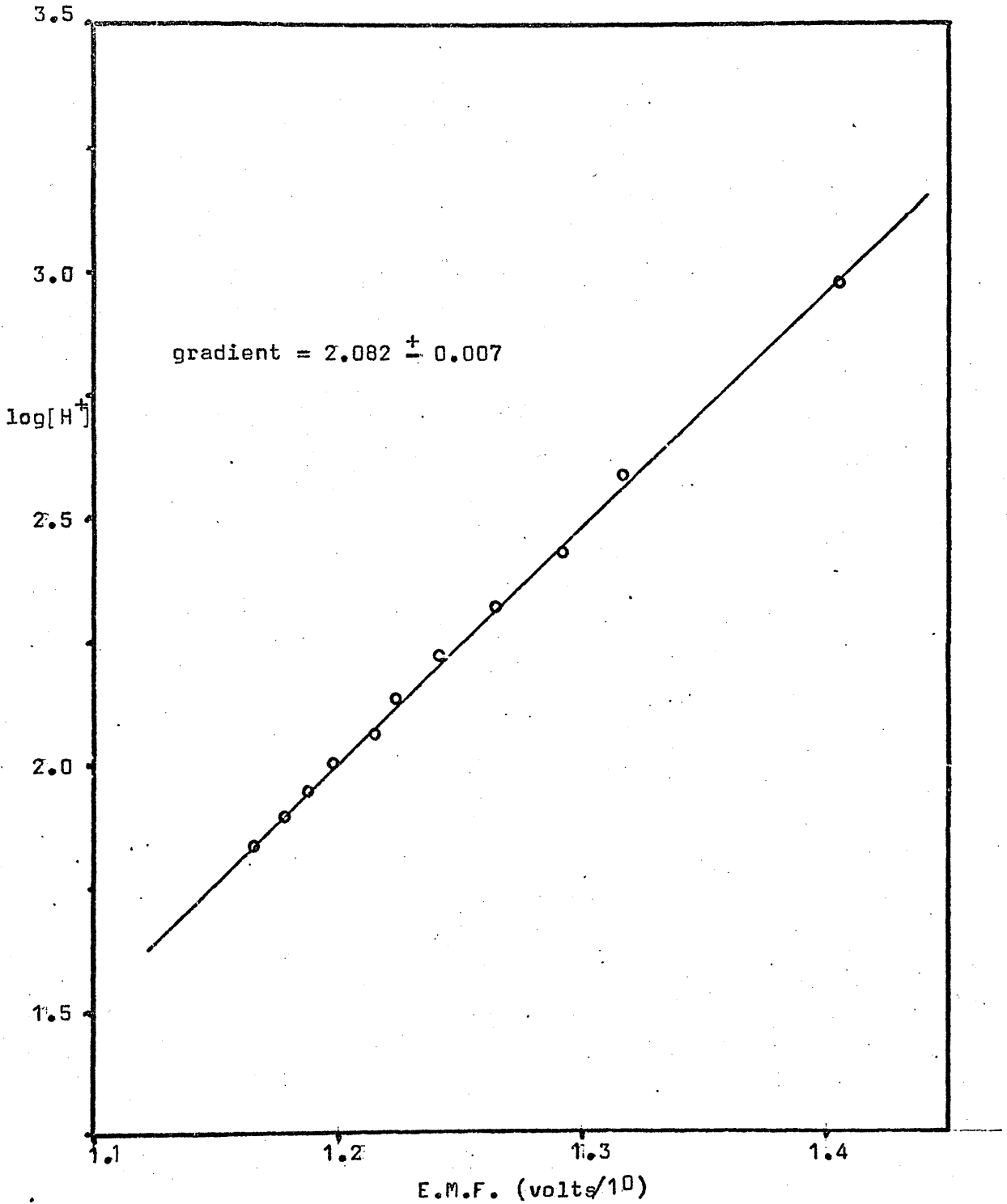
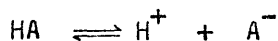


FIGURE 6.3

where A and B are constants and I is the ionic strength, to describe the solution-bridge liquid-junction potential in a "Wilhelm" bridge at high ionic strength.

The acid dissociation constant can then be evaluated from a knowledge of the hydrogen ion concentration and the total amounts of base and test acid in the solution.

Consider a weak acid HA in equilibrium with its dissociated species A^-



$$K_a = \frac{[H^+][A^-]}{[HA]}$$

If a = total number of moles of HA added to the solution.

b = number of moles of NaOH added

v = original volume of solution

v' = volume of NaOH added

h = hydrogen ion concentration

Then

$$[HA] + [A^-] = a/(v + v')$$

and by electroneutrality

$$[Na^+] + [H^+] = [OH^-] + [A^-]$$

Neglecting OH^- at pH 7,

$$b/(v + v') + h = [A^-]$$

and hence

$$K_a = \frac{h(h + b/(v + v'))}{(a/(v + v') - h - b/(v + v'))}$$

6.23

Preparation of Materials

1. Preparation of Carbonate Free Sodium Perchlorate Solution.

A stock solution of sodium perchlorate was prepared by dissolving the crystalline solid (Fluka, puriss) in distilled water and filtering to give a solution around 7M. This solution was then boiled, cooled under a stream of nitrogen gas (British Oxygen Co. Ltd.) and standardised gravimetrically as described in chapter 3. Carbonate free distilled water was prepared by a similar treatment of heating and cooling under a stream of nitrogen gas.

2. Preparation of Carbonate Free Sodium Hydroxide at 1M Ionic Strength.

A saturated solution of sodium hydroxide (roughly 20M) was prepared by dissolving approximately 80 grams of sodium hydroxide pellets (BDH, AnalaR grade) in 100mls. of distilled water in a 250ml. conical flask. The flask was sealed and shaken and the resulting precipitate of sodium carbonate allowed to settle before aliquots of the solution were removed and the base concentration found by titration with a standard hydrochloric acid solution using methyl red as indicator. Sufficient stock solution to prepare one litre of 0.15M sodium hydroxide was then added to the required amount of carbonate free sodium perchlorate solution to give one molar ionic strength when the mixture was diluted to one litre using boiled out distilled water. The base content was then determined by titration against weighed amounts of potassium hydrogen phthalate (BDH, AnalaR grade) using phenolphthalein as indicator.

3. Preparation of Carbonate Free Hydrochloric Acid Solution at 1M Ionic Strength.

Stock solutions of hydrochloric acid (0.1M) were prepared by adding "Convolve" ampoules (BDH, AnalaR grade) to the required amount of carbonate free sodium perchlorate to give one molar ionic strength and the mixture diluted to the required volume using boiled out distilled water as above. The acid content of the solutions was then determined by titration against weighed amounts of di-sodium tetraborate (BDH, AnalaR grade) using methyl red as indicator.

4. Preparation of Stock Mercapto-carboxylic Acid Solutions.

These compounds were obtained and stored as described in Chapter 3. Stock solutions were prepared immediately before use by dissolving accurately weighed quantities of the acid in one molar carbonate free sodium perchlorate solution (prepared by accurate dilution of the sodium perchlorate stock with boiled-out water). The concentrations as the acids were checked by titration of aliquots against standard base.

When portions of stock solution were removed from storage flasks, water saturated nitrogen gas was bubbled through the

solution for a short time to prevent absorption of carbon dioxide. Solutions were thus stored under an atmosphere of nitrogen.

Procedure

Solutions in the titration cell were prepared by transferring the required amount of acid stock at 1M ionic strength by pipette and diluting with a known volume of 1M sodium perchlorate. At least one hour was allowed to achieve thermal equilibrium and nitrogen gas was bubbled continuously through the solution during this and the subsequent period of titration. Titrations were performed using a 10ml. burette graduated in divisions of 0.02mls. Base was added in increments of 0.1ml. to 0.5ml. and five minutes were allowed between each delivery to ensure thermal equilibration and complete mixing. A fine glass rod was used to transfer any drops of base remaining on the tip of the burette to the solution. The absorption of carbon dioxide by the base was prevented by attaching a drying tube containing soda lime to the open end of the burette.

The liquid junction was renewed at the beginning of each titration and the 3-way taps were opened as in figure 6.2 only during the measurement of the E.M.F. in order to prevent excessive diffusion. When not in use, the glass electrode was stored in distilled water and on being transferred from one solution to another, the electrode was rinsed with distilled water and the stem dried with a paper tissue.

Typical conditions for the experiments were as follows

Calibration:- 10mls. of a solution of 0.1M HCl in 0.9 NaClO₄ with 250mls. of 1M NaClO₄ were titrated with 0.15M NaOH in 0.85M NaClO₄.

Ionisation constant determination:- 25mls. of 0.04M mercapto-carboxylic acid in 1M NaClO₄ with 250mls. of 1M NaClO₄ were titrated with 0.15M NaOH in 0.85M NaClO₄.

Calibration titrations were performed before and after each ionisation constant determination and the relationship between E.M.F. and $-\log_{10}[\text{H}^+]$ was found not to differ significantly between successive calibrations. The slopes of plots of E.M.F. versus $-\log_{10}[\text{H}^+]$ were of the order of magnitude of the theoretical value

of $\frac{2.303RT}{F}$. The slopes were calculated using an unweighted least squares procedure on a Nova 2000 computer.

Results

Representative data from titration results are shown in table 6.2 and figure 6.4. The values of the acid dissociation constants calculated using equation 6.23 are presented in table 6.3 for the various temperatures studied together with the corresponding values for 2-MSA.³²⁶ It can be seen from the data that these constants exhibit complex dependences on temperature, in some cases showing a maximum in the value of K_a . This behaviour has been noted with many weak electrolytes³³³ and there is much discussion in the literature as to the exact nature of the empirical equation to describe the variation although Harned and co-workers^{333,334} have employed an expression of the type.

$$\ln K_a = A/T + B + CT \quad 6.24$$

which is generally agreed to³³⁵ describe the behaviour of most weak electrolytes within the limits of experimental error.

Thermodynamic parameters may be obtained by the use of the appropriate functions

$$\Delta G = RT \ln K_a = -R (A + BT + CT^2) \quad 6.25$$

$$\Delta H = RT^2 \frac{\partial \ln K_a}{\partial T} = R (CT^2 - A) \quad 6.26$$

$$\Delta S = \frac{\Delta H - \Delta G}{T} = R (B + 2CT) \quad 6.27$$

$$\Delta C_p = \frac{\partial \Delta H}{\partial T} = 2 CRT. \quad 6.28$$

The temperature T_θ at which K_a exhibits a maximum value is given by

$$T_\theta = \sqrt{A/C} \quad 6.29$$

$$\ln K_{a\theta} = B - 2\sqrt{AC} \quad 6.30$$

A least squares analysis of the data in table 6.3 was performed using a standard programme on the University of Glasgow's KDF9 computer

Table 6.2

Representative Data Used in the Determination of Acid Dissociation Constants at $T = 20^{\circ}\text{C}$, $I = 1.00\text{M}$.

MAA = 1.125 m.moles. $[\text{OH}^-] = 0.149\text{M}$. Initial Total Volume = 275mls.

Base Added (mls.)	E.M.F. (mv)	$10^4 K_a$ (M)
0.2	156.8	1.818
0.4	158.2	1.870
0.6	160.1	1.842
0.8	161.8	1.850
1.0	163.7	1.831
1.2	165.2	1.870
1.4	166.4	1.949
1.6	168.2	1.945
1.8	170.3	1.905
2.1	173.3	1.869
2.4	176.2	1.850
2.7	179.4	1.801
3.0	182.4	1.779

Ave. 1.860 ± 0.05

2-MPA 1.102 m.moles $[\text{OH}^-] = 0.149\text{M}$. Initial Total Volume = 275mls.

Base Added (mls.)	E.M.F. (mv)	$10^4 K_a$ (M)
0.00	154.4	2.685
0.2	155.9	2.684
0.4	157.5	2.664
0.6	158.5	2.798
0.8	162.2	2.672
1.0	160.2	2.763
1.2	163.9	2.656
1.4	165.4	2.684
1.6	167.2	2.657
1.8	168.4	2.747
2.1	171.7	2.612
2.4	174.2	2.629
2.7	177.0	2.604

Ave. 2.601 ± 0.06

2-MIBA = 0.982 [OH⁻] = 0.149M Initial Total Volume = 275mls.
m.moles.

Base Added (mls.)	E.M.F. (mv)	$10^4 K_a$ (M) ^a
0.0	156.7	1.203
0.1	157.9	1.185
0.3	159.9	1.200
0.5	161.7	1.238
0.7	163.8	1.244
0.9	165.5	1.289
1.1	167.9	1.267
1.3	169.9	1.281
1.5	172.0	1.286
1.7	174.1	1.291
2.1	178.4	1.290
2.4	182.1	1.254
2.7	185.8	1.222
3.0	189.1	1.221
3.3	192.6	1.209
3.6	196.6	1.171

Ave. 1.241 ± 0.04

Plot of E.M.F. against mls. of base for the data on page 185.
 $T = 20^{\circ}\text{C}$, $I = 1.0\text{M}$.

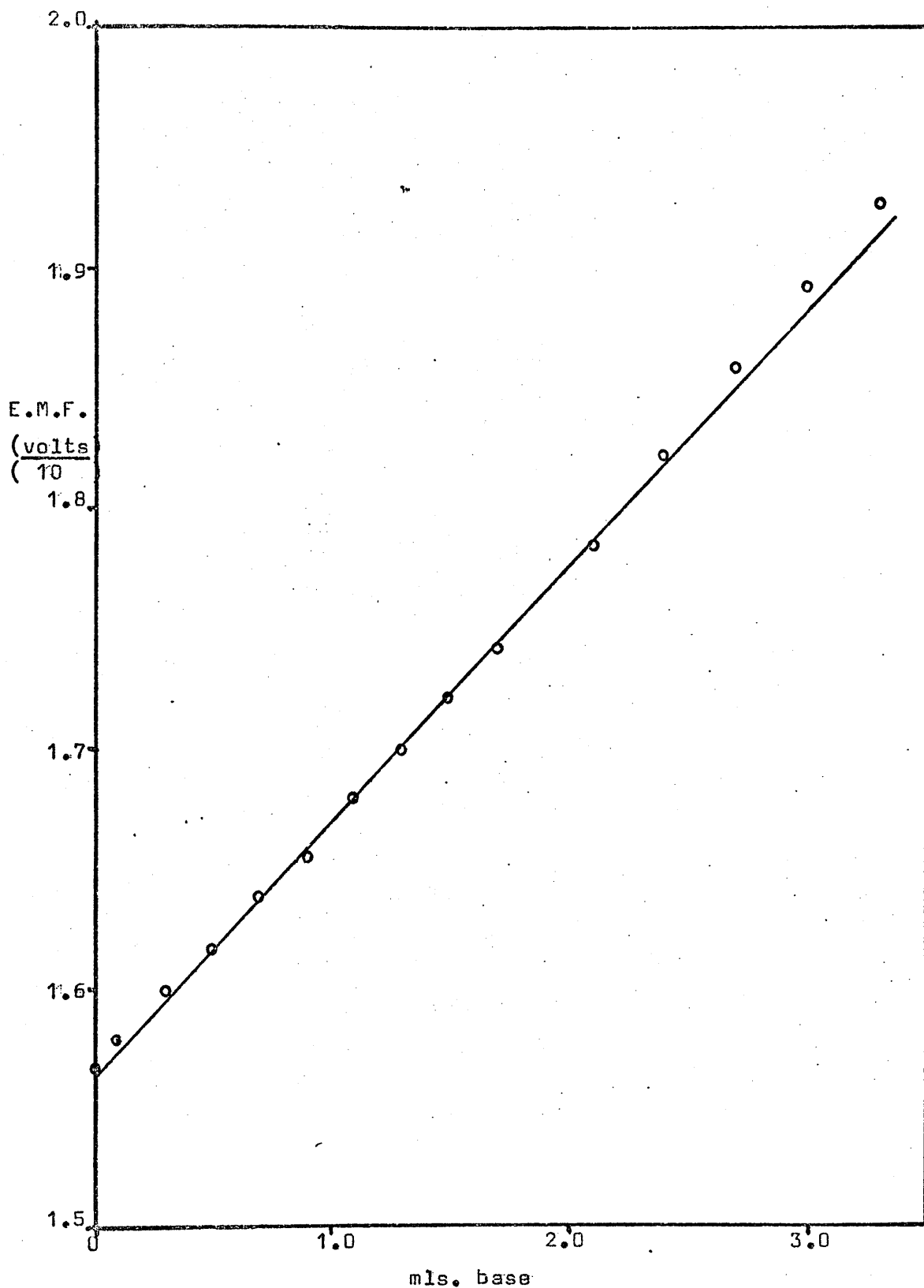


FIGURE 6.4

TABLE 6.3

Values of the concentration acidity constants for MAA, 2-MPA, 2-MIBA and 2-MSA in aqueous solution at one molar ionic strength.

T/°K	$10^4 K_a / M$				
	MAA	2-MPA	2-MIBA	2-MSA (1) ^a	2-MSA (2) ^a
273	-	-	-	7.35 ± .48	0.303 ± .018
	0.83	1.54	1.24	7.29	0.296
278	-	-	-	8.46 ± .21	0.373 ± .018
	1.09	2.01	1.27	8.54	0.384
283	2.29 ± .03 ^b	2.35 ± .04	1.32 ± .06	9.42 ± .44	0.429 ± .008
	1.36	2.42	1.29	9.38	0.451
288	1.61 ± .02	2.87 ± .10	1.23 ± .04	-	-
	1.62	2.69	1.28	9.71	0.481
293	1.86 ± .05	2.68 ± .06	1.24 ± .04	9.27 ± .29	0.475 ± .008
	1.84	2.79	1.26	9.49	0.468
298	1.98 ± .05	2.05 ± .05 ^b	1.28 ± .03	9.13 ± .27	0.433 ± .024
	2.00	2.70	1.23	8.78	0.417
303	-	-	-	7.58 ± .22	0.327 ± .014
	2.08	2.45	1.18	7.71	0.342
308	2.09 ± .04	2.10 ± .03	1.10 ± .03	-	-
	2.09	2.09	1.12	6.45	0.260

first rows are observed constants, second rows are calculated from the data in table 6.4 using equation 6.24. Errors quoted are root mean square errors.

a - ref. 326

b - outwith acceptable error limits and excluded in calculations.

to fit $\ln K_a$ versus T to the third power. The parameters obtained are those in equation 6.24 and are presented in table 6.4. The curves 6.24 are shown in figure 6.5 together with the experimental points. Derived thermodynamic parameters 6.25 - 6.30 are given in table 6.5.

Errors

The standardisation of solutions could be reproduced to better than 0.2%. It was estimated that in the experiments, solutions used were accurate to within 1% and that the volume of liquid in the titration cell was known to 2%. E.M.F. measurements were taken as accurate to ± 1 mv, although it was obvious from the data that the reproducibility was somewhat better.

From these estimates, it may be calculated that the maximum error in determining the hydrogen ion concentration by this potentiometric method is around 4% while the final error in the K_a value is typically about 5%. The root mean square errors quoted are within this figure so that the spread of values is not as large as the error might suggest. Using the IUPAC classification for accuracy³³⁶ this study is described as "approximate".

Discussion

The values of the acidity constants K_a are seen to be in reasonable agreement with most of the data in table 6.1. There is, however, such a spread of values reported that no real conclusions can be drawn.

To explain the results obtained, two factors require to be considered;

- (1) The effect of temperature on K_a .
- and
- (2) The effect of substituents on K_a .

Both of these points are interdependent and the overall situation is extremely complex. Thus while MAA is a weaker acid than either 2-MPA or 2-MIBA at temperatures less than 281^oK, it is stronger than 2-MIBA and above 308^oK, stronger than both 2-MPA and 2-MIBA.

Table 6.4

Parameters for the Equation $-\ln K_a = A/T + B + CT$ for 2-Mercaptocarboxylic Acids I = 1.00 NaClO₄.

Acid	A	B	C
MAA	2.19134×10^4	-1.34875×10^2	2.34424×10^{-1}
2-MPA	3.45760×10^4	-2.27739×10^2	4.02444×10^{-1}
2-MIBA	6.50202×10^3	-3.67420×10^1	8.02983×10^{-2}
2-MSA (1) ^a	2.7393×10^4	-1.8301×10^2	3.2928×10^{-1}
2-MSA (2) ^a	4.3711×10^4	-2.9262×10^2	5.2357×10^{-1}

a reference 326

Variation of the first acid dissociation constants of 2-mercaptocarboxylic acids with temperature. $I=1.0M$.

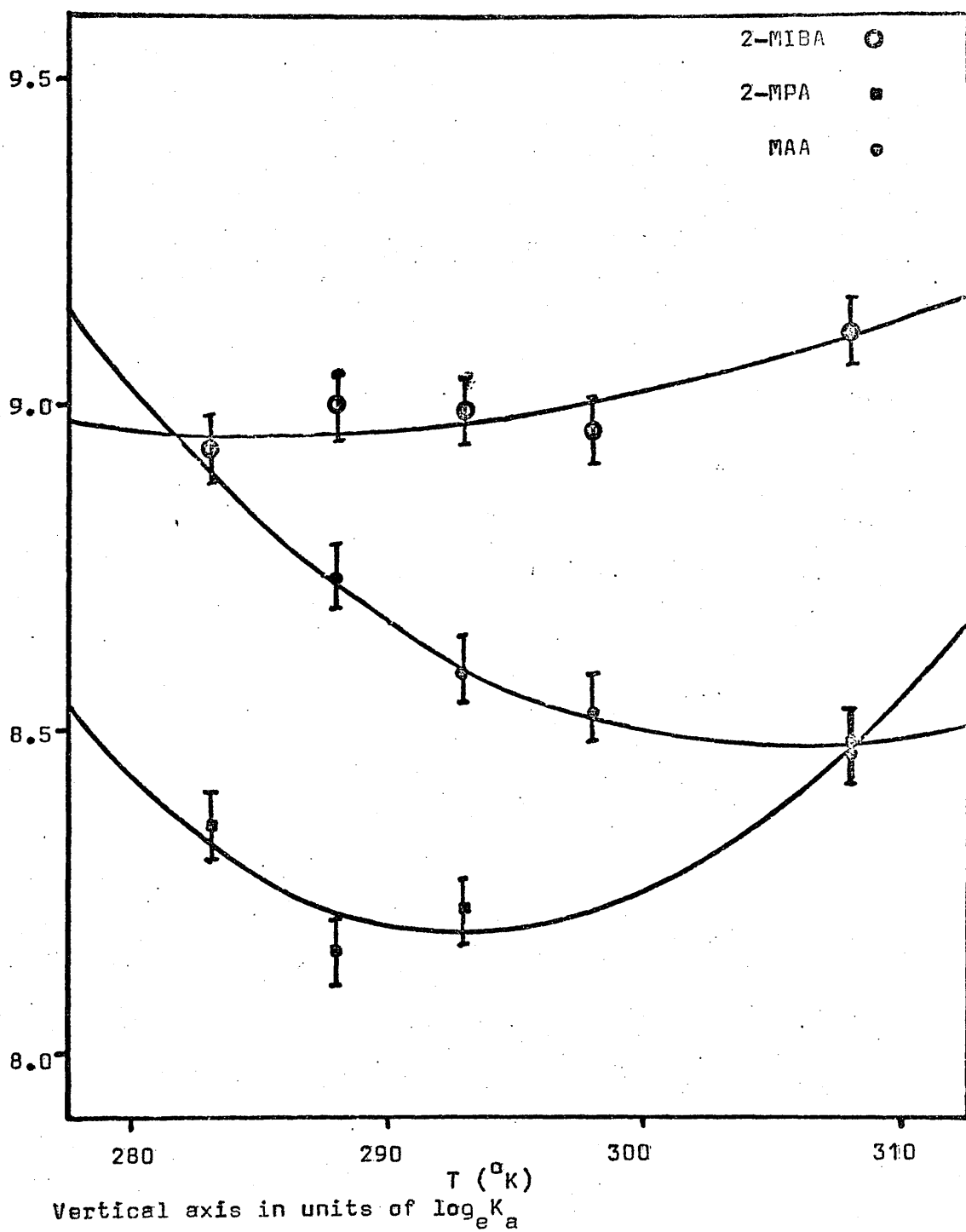


FIGURE 6.5

Table 6.5

Thermodynamic Variables for Acidity Constants Calculated Using Equation 6.24.

	Temperature °K	ΔG kcal mole ⁻¹	ΔH kcal mole ⁻¹	ΔS cal °K ⁻¹ mole ⁻¹
MAA	273	5.09	8.83	13.7
	278	5.04	7.54	9.0
	283	5.00	6.24	4.4
	288	4.99	4.91	-0.3
	293	5.01	3.55	-5.0
	298	5.04	2.18	-9.6
	303	5.10	0.78	-14.3
	308	5.19	-0.65	-18.9
2-MPA	273	4.76	9.11	15.9
	278	4.70	6.90	7.9
	283	4.68	4.66	-0.1
	288	4.70	2.38	-8.1
	293	4.76	0.05	-16.1
	298	4.86	-2.31	-24.1
	303	5.01	-4.71	-32.1
	308	5.19	-7.16	-40.1
2-MIBA	273	4.88	1.03	-14.1
	278	4.95	0.95	-15.7
	283	5.04	0.14	-17.3
	288	5.13	-0.31	-18.9
	293	5.23	-0.78	-20.2
	298	5.33	-1.25	-22.1
	303	5.45	-1.73	-23.7
	308	5.57	-2.22	-25.3

Table 6.5 Contd.

	Temperature °K	ΔG kcal mole ⁻¹	ΔH kcal mole ⁻¹	ΔS cal °K ⁻¹ mole ⁻¹
2-MSA ^a ₍₁₎	273	3.92	5.67	6.4
	278	3.90	3.86	-0.1
	283	3.92	2.03	-6.7
	288	3.97	0.16	-13.2
	293	4.05	-1.74	-19.8
	298	4.17	-3.67	-26.3
	303	4.32	-5.64	-32.9
	308	4.50	-7.64	-39.4
2-MSA ^a ₍₂₎	273	5.66	9.32	13.4
	278	5.62	6.45	3.0
	283	5.64	3.53	-7.4
	288	5.69	0.56	-17.8
	293	5.80	-2.46	-28.2
	298	5.97	-5.53	-38.6
	303	6.19	-8.66	-49.0
	308	6.46	-11.84	-59.4

Values of T_g (°K)

MAA	305.7
2-MPA	293.1
2-MIBA	284.6
2-MSA ₍₁₎	288.4
2-MSA ₍₂₎	288.9

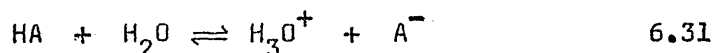
a reference 326

Most discussion on the effect of substituents on acidity constants has been restricted to a single temperature and while this is not serious if the acid strength varies markedly it is obvious from the above results that great caution must be employed in attaching significance to small changes in acidity constants.

For comparative purposes therefore, one must look beyond this behaviour at the gross differences observed on varying the structure. The most significant of these are the change in T_{θ} , the temperature at which K_a exhibits a maximum and the variation in the curve shape. The interdependence of equations 6.24 to 6.30 suggests that these features reflect significant changes in the thermodynamics of ionisation.

While there exists no satisfactory theoretical treatment for the temperature-structure dependence of ionisation constant, of weak electrolytes, it is proposed to discuss the current theories on temperature dependence and superimpose on this framework the effects of structure. In this way, qualitative information about the processes taking place may be obtained.

In 1938, Gurney³³⁷ proposed a model later developed by Baughan³³⁸ which accounted for most of the observed behaviour. Briefly, he proposed³³⁷ that the free energy change in the equilibrium

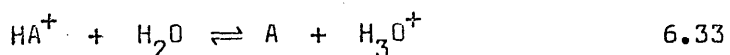


could be divided into two parts

$$\Delta G = \Delta G_{\text{ext}} + \Delta G_{\text{int}} \quad 6.32$$

Where ΔG_{ext} , dependent on the environment, may be equated with the electrical work required to form two charges of opposite sign, while ΔG_{int} , independent of the environment is concerned mainly with the chemical effects of bond making and breaking.

Consideration of the isoelectric process



in which the contribution from ΔG_{ext} should be of minor importance,

allows an examination of the properties of ΔG_{int} . To a first approximation, the temperature dependence of 6.33 may be expressed by

$$\ln K = A + BT \quad 6.34$$

from which it may be deduced that $\Delta C_{p,int} \approx 0$ and that ΔH_{int} is constant.

The standard free energy change for formation of opposite charges may be approximated³³⁸ by Born's³³⁹ equation

$$\Delta G_{ext} = \frac{Ne^2}{2\epsilon} \left(\frac{1}{r_+} + \frac{1}{r_-} \right) \quad 6.35$$

where N is Avogadro's number, e is the electronic charge, r_+ and r_- the respective ionic radii and ϵ is the dielectric constant of the medium. Thence,

$$\Delta G = \Delta G_{int} + \frac{Ne^2}{2\epsilon} \left(\frac{1}{r_+} + \frac{1}{r_-} \right) \quad 6.36$$

$$\ln K = \ln K_{int} - \frac{Ne^2}{2\epsilon RT} \left(\frac{1}{r_+} + \frac{1}{r_-} \right) \quad 6.37$$

The internal free energy change may be defined as the free energy change at infinite dielectric strength³³³ giving

$$\ln K = \ln K_{\epsilon=\infty} - \frac{Ne^2}{2\epsilon_0 RT} \left(\frac{1}{r_+} + \frac{1}{r_-} \right) \quad 6.38$$

The variation of dielectric constant with temperature may be approximated by $\epsilon = \epsilon_0 e^{-T/\theta}$ where θ is a temperature characteristic of the solvent (214°K for H₂O) so that

$$\ln K = \ln K_{\epsilon=\infty} - \frac{Ne^2}{2\epsilon_0 R} \left(\frac{1}{r_+} + \frac{1}{r_-} \right) \frac{e^{T/\theta}}{T} \quad 6.39$$

and with $D = \frac{Ne^2}{2\epsilon_0} \left(\frac{1}{r_+} + \frac{1}{r_-} \right)$,

$$\frac{\partial \ln K}{\partial T} = \frac{\partial \ln K_{\epsilon=\infty}}{\partial T} - \frac{D}{R} \left(\frac{1}{T\theta} e^{T/\theta} - \frac{1}{T^2} e^{T/\theta} \right) \quad 6.40$$

i.e.

$$\Delta H = \Delta H_{\epsilon=\infty} - D \left(\frac{T}{\theta} e^{T/\theta} - e^{T/\theta} \right) \quad 6.41$$

At the temperature T_{θ} , $\Delta H = 0$ and equation 6.41 may be rearranged to give

$$T_{\theta}^2 = \theta^2 \left(1 + \frac{H_{\epsilon=\infty}}{D} \right)$$

and since $\Delta S_{\epsilon=\infty} \approx 0$

i.e.

$$T^2 = \theta^2 \left(1 + \frac{\Delta G_{int}}{\Delta G_{ext_{\epsilon=\epsilon_0}}} \right) \quad 6.42$$

The temperature T_{θ} is thus seen to depend only on the ratio $\Delta G_{int}/\Delta G_{ext_{\epsilon=\epsilon_0}}$ and to be independent of the magnitude of K_a . While Baughan's theory³³⁸ extends this interpretation to obtain quantitative information, Harned and Owen³³³ rightly point out that the approximations embodied in equations 6.34 and 6.35 make his conclusions doubtful. Despite the observation³³⁵ that Gurney's theory "stumbles over too many hard and irreducible facts", some qualitative conclusions may be drawn. The observed order of value of T_{θ} 2-MIBA < 2-MPA ~ 2-MSA (K_{al}) < MAA implies that either the trend in ΔG_{int} should be

$$MAA > 2-MPA \sim 2-MSA > 2-MIBA \quad 6.43$$

and/or that for ΔG_{ext} should be

$$2-MIBA > 2-MPA \sim 2-MSA > MAA \quad 6.44$$

King³³⁵ notes that relative to acetic acid, carboxylic acids with bulky alkyl groups and those with highly polar substituents have T_{θ} at lower temperatures while neutral polar acids have T_{θ} at higher temperatures. A discussion of the implications of sequences 6.43 and 6.44 will be held over until later in this chapter.

Gurney³³⁷ uses a hypothetical ionic model for comparative purposes. Most other workers have however preferred to use real

systems as standards and since this immediately involves substituent effects, a brief discussion on the various lines of approach to this problem is required.

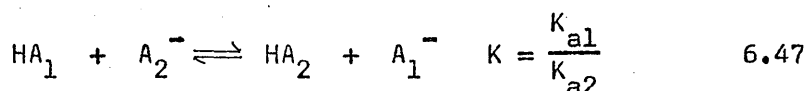
If one considers as a reference, the unsubstituted acid HA_1



and an acid HA_2 of similar structure but varying only by a substituent



then the effect of the substituent on the acidity constant can be defined by the equilibrium



$$\Delta G = \Delta G_{int_1} + \Delta G_{ext_1} - \Delta G_{int_2} - \Delta G_{ext_2} \quad 6.48$$

Bjerrum³⁴⁰ proposed that with acids of similar structure, $\Delta G_{int_1} \approx \Delta G_{int_2}$ and that the effect of a polar substituent can be considered in terms of an electrostatic model. If the substituent carries a point charge ze at distance r from the proton in a linear homogeneous isotropic medium of dielectric constant ϵ then

$$RT \ln \frac{K_{a1}}{K_{a2}} = \frac{Nze^2}{\epsilon r} \quad 6.49$$

where N is Avogadro's number. The theory can also be used where the substituent is represented by a point dipole μ inclined at an angle ξ to the line joining it to the proton.

$$RT \ln \frac{K_{a1}}{K_{a2}} = \frac{N\mu e \cos \xi}{\epsilon r^2} \quad 6.50$$

Eucken³⁴¹ however pointed out that Bjerrum's theory could not be used when the substituents, like $-CH_3$, were only moderately polar and suggested that the bulk dielectric constant be replaced by an effective constant to take account of variations in the former in close proximity to the acid. In an effort to extend this line of

thought, Kirkwood and Westheimer³⁴² separated the dielectric constant into two regions, the bulk dielectric and a cavity enclosing the molecule in which the effective dielectric is that of liquid paraffin. Depending on the shape of the molecule, the cavity is either spherical or ellipsoidal³⁴³ and Bjerrum's equation is replaced by an equation describing the change in the charge of the cavity on equilibrium 6.47.

Despite the success of the theory of Kirkwood and Westheimer both qualitatively and quantitatively, the assumptions involved require large differences in K_{a1} and K_{a2} for significant information to be derived. Its artificial nature also excludes the possibility of solvent-solute interaction and gives no satisfactory explanation of the temperature variation.

The use of the protolytic reaction 6.47 is preferable to the proton transfer 6.45 because of the possibility of isolating specific effects by matching one acid carefully against another³³⁵ Further, since there is no change in the overall number of particles or the distribution of charge, the thermodynamic parameters for reaction 6.47 are not swamped by factors introduced by the formation of ions as in 6.45. If Gurney's suggestion³³⁷ of internal and external effects is applied to the equilibrium, the change in acidity due to the intrinsic structural features of the acid and its conjugate base will comprise the internal part and the external effects may then be identified with the effect of structure on solvation³³⁵

Thus

$$\Delta G = \Delta G_{int} + \Delta G_{ext} \quad 6.51$$

$$\Delta H = \Delta H_{int} + \Delta H_{ext} \quad 6.52$$

$$\Delta S = \Delta S_{int} + \Delta S_{ext} \quad 6.53$$

Hepler and others^{166,344} have shown that for similar acids $\Delta S_{int} \approx 0$ so that the observed thermodynamic properties in solution are largely determined by ΔH_{int} and changes in solution. Evidence³⁴⁵ that solution processes afford a partial compensation of ΔH by $T\Delta S$ leads to an expression.

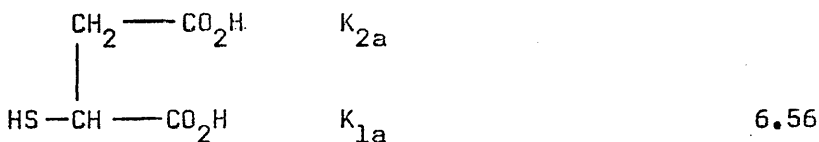
$$\Delta H_{ext} = \beta \Delta S_{ext} \quad 6.54$$

giving
$$\Delta G = \Delta H_{int} + (\beta - T)\Delta S \quad 6.55$$

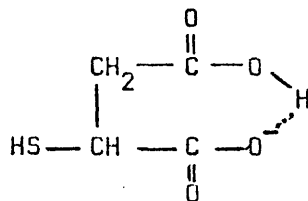
The fact that $\beta \approx 300K^{\circ 166,345}$ for aqueous solutions near room temperature leads to the suggestion that ΔH_{int} may be identified more closely with ΔG than ΔH ³⁴⁶ Observed trends in ΔH_{int} with structure in aliphatic carboxylic acids can be readily explained by inductive and resonance effects ³⁴⁷

Thus electron withdrawing and positively charged substituents stabilise the conjugate base relative to the acid while electron donating and negatively charged substituents have the opposite effect. Groups capable of exhibiting resonance forms complicate this model depending on whether resonance is more important in the ionised or neutral form of the acid. These latter effects are not however relevant to the present discussion. Specific effects such as internal hydrogen bonding can also play an important role in determining the relative stabilities. Fortunately, the small size of the protons implies that steric factors are largely unimportant although they should contribute to changes in solvation and are best discussed in terms of this. ³³⁵

The sulphhydryl group should be more electron withdrawing than a proton and so should increase the acidity of the acids with respect to acetic acid as is observed. One would thus expect that in 2-MSA

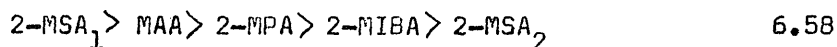


the acidity constants would refer to the groups as shown in 6.56 and this assumption will be employed in the following discussion. Methyl groups are electron donating and, while there is no real justification for expecting additivity in inductive effects it is reasonable to expect that two methyl groups are more electron donating than a single group. Comparison of the inductive effect of $-\text{CH}_2\text{CO}_2\text{H}$ relative to $-\text{CH}_3$ would lead to the expectation that the former is slightly electron withdrawing. More important however is the possibility of stabilisation of the anion by internal hydrogen bonding in the case of 2-MSA.



6.57

The second ionisation of the acid would be reduced by the charge. The order of acidity constants would thus be expected to be



which is consistent with 6.43 for the three acids in the centre but 2-MSA₁ where additional effects are operative, is out of sequence.

In order to attempt to quantify this observation the data have been treated using reaction 6.47 with MAA as reference. Evaluation for these equilibria are given in table 6.6. It is obvious that $\Delta H_{\text{int}} \approx 0$ for the effect of methyl substituents and that the data for 2-MSA_{1,2} are consistent with 6.58. This implies that the explanation for the variation in T_{θ} is contained largely in 6.44 and that the reactions are best discussed in terms of changes in solvation.

The effect of hydrophobic methyl substituents has been discussed by several workers^{348,349} and has been used to account for the acid strength of substituted ammonium ions. Besides providing a volume of low dielectric strength in the proximity of the carboxyl group, it also reduces the number of solvating water molecules. In electrostatic terms the overall effect is a reduction in the effective dielectric constant and as such can explain trend 6.44.

King³³⁵ suggests that the effect on an anion might be greater than on the neutral molecule, the resulting solvent exclusion giving rise to positive enthalpy and entropy changes. Table 6.6 however shows that both these properties vary markedly with temperature and without a knowledge of the relative degrees of solvation of the reference and substituted acids, their conjugate bases and the effect of temperature on them, further discussion of this is not justified. It may however be of significance that the heat capacity and change in ΔS with temperature for 2-MIBA are positive while those for the other acids are negative (figure 6.6). If,

TABLE 6.6

Thermodynamic parameters of 2-mercaptocarboxylic acids relative to mercaptoacetic acid ($I = 1.00(\text{NaClO}_4)$).

T(°K)	ΔG^b	ΔH^b	ΔS^c
2-MPA			
273	-0.33	+0.28	+2.2
278	-0.34	-0.64	-1.1
283	-0.32	-1.58	-4.5
288	-0.29	-2.53	-7.8
293	-0.25	-3.50	-11.1
298	-0.18	-4.49	-14.5
303	-0.09	-5.49	-18.2
308	-0.00	-6.51	-21.2
2-MIBA			
273	-0.21	-7.80	-27.8
278	-0.09	-6.95	-24.7
283	+0.04	-6.10	-21.7
288	+0.14	-5.22	-18.6
293	+0.22	-4.33	-15.2
298	+0.29	-3.43	-12.6
303	+0.35	-2.51	-9.4
308	+0.36	-1.57	-6.4
2-MSA(1) ^a			
273	-1.17	-3.16	-7.3
278	-1.14	-3.68	-9.1
283	-1.08	-4.21	-11.1
288	-1.02	-4.75	-12.9
293	-0.96	-5.29	-15.8
298	-0.87	-5.85	-16.7
303	-0.78	-6.42	-18.3
308	-0.61	-6.99	-20.5

Table 6.6 contd.

T(°K)	ΔG^b	ΔH^b	ΔS^c
2-MSA(2) ^a			
273	+0.57	+0.59	-0.3
278	+0.58	-1.09	-6.0
283	+0.63	-2.71	-11.8
288	+0.70	-4.35	-17.5
293	+0.79	-6.01	-25.2
298	+0.93	-7.71	-29.0
303	+1.09	-9.44	-34.7
308	+1.25	-11.19	-40.5

a - ref. 326

b - kcal mole⁻¹

c - cal^o K⁻¹ mole⁻¹

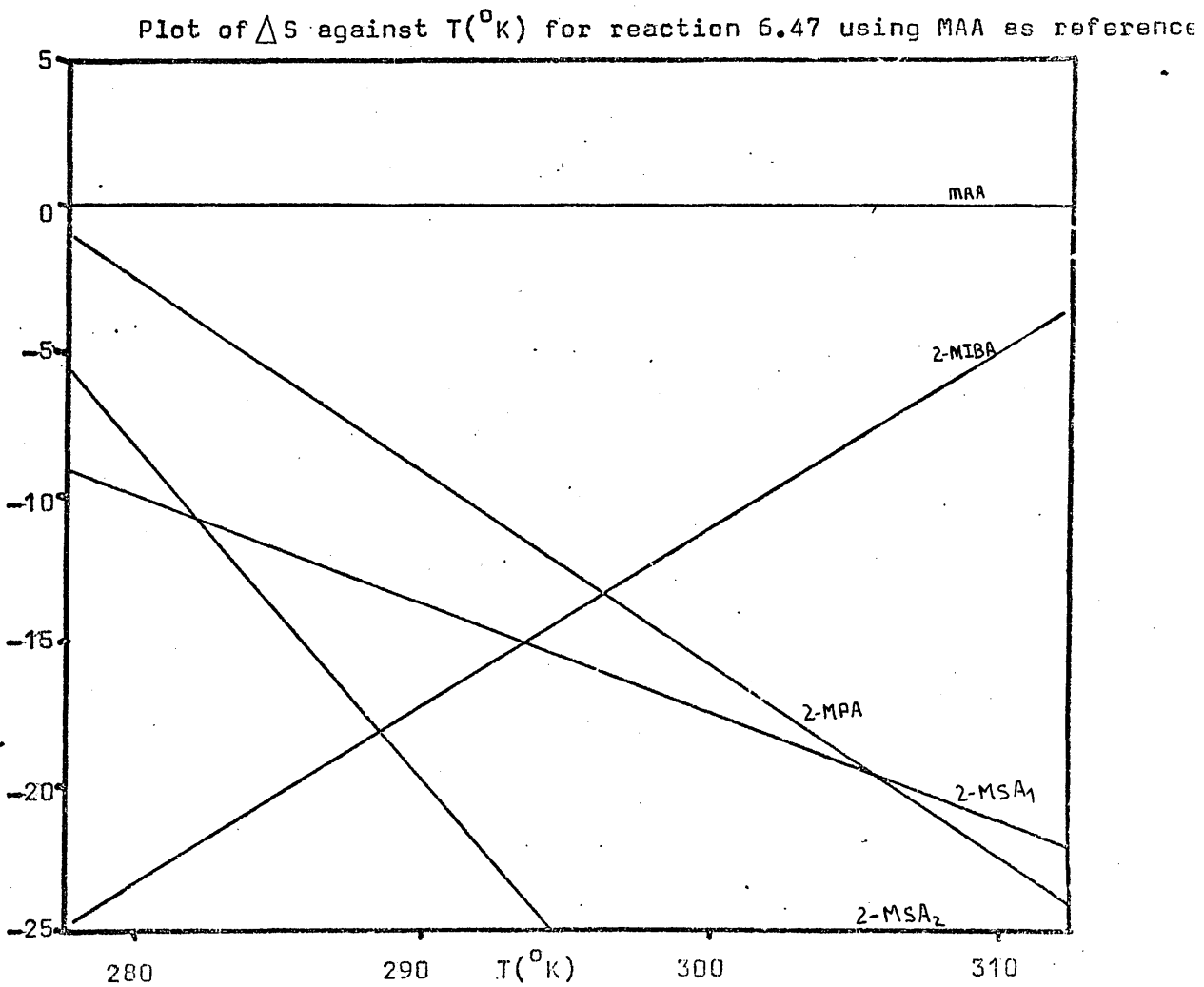
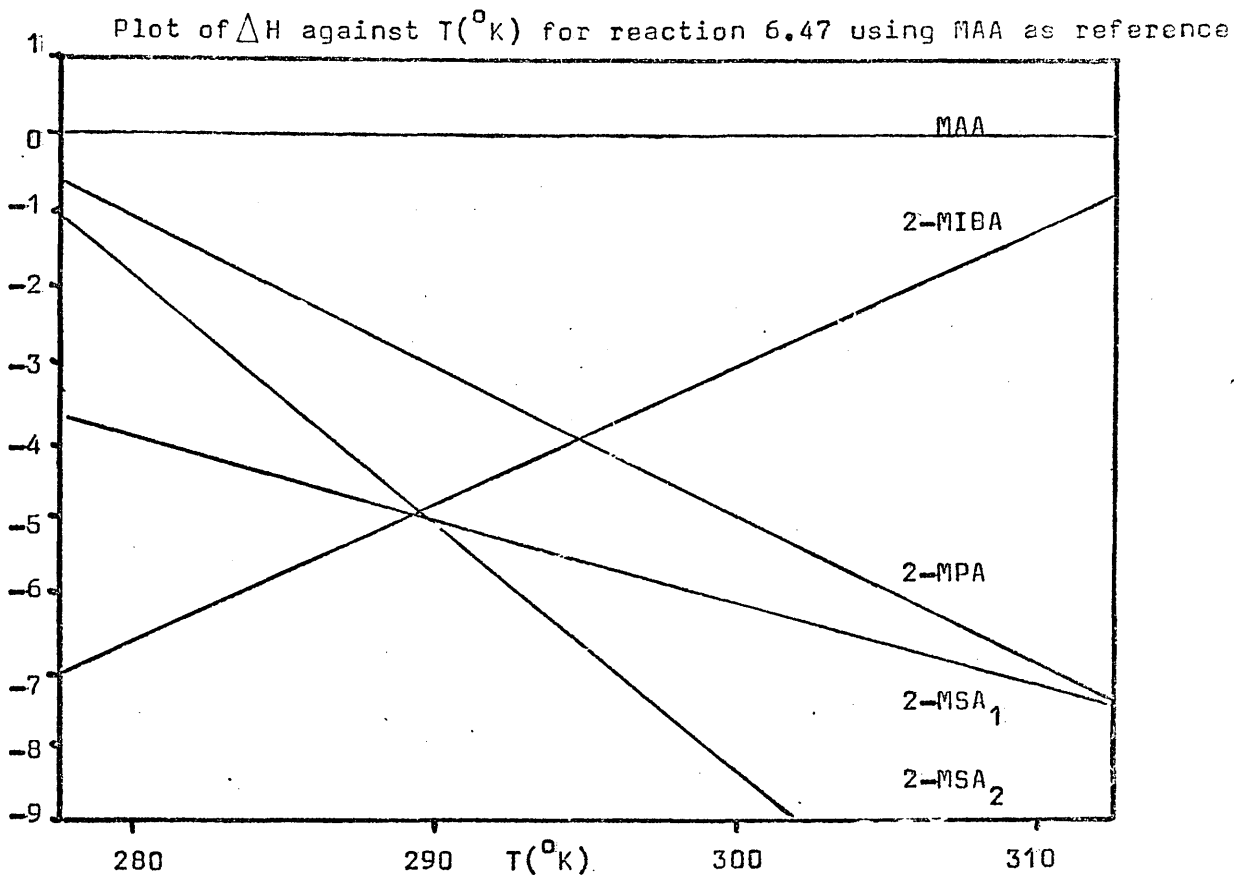
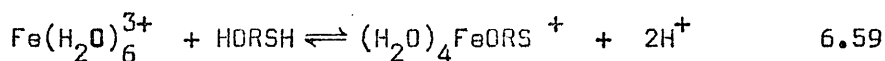


FIGURE 6.6

as King suggests, ΔS should be positive in these reactions, it is hard to conceive of a situation where ΔS increases from negative to positive with temperature and so the data for 2-MIBA are considered anomalous. Possibly in this case, the solvation of the neutral acid is dominant. While they must obviously play an important part, solvation effects in 2-MSA₁ are partially masked by internal hydrogen bonding discussed earlier. The similarity of the ΔH_{ext} values to those of 2-MPA is however particularly noteworthy.

Finally, to summarise, while internal substituent effects are noted in the case of 2-MSA, the main factor governing differences in the properties of these acids in solution appears to be the degree of solvation. This observation is relevant to the reactions with iron (III)



(HORSH = mercaptocarboxylic acid)

where the variation in stability of the complexes with ligand structure is largely determined by the entropy. Entropy changes in complexation reactions are due mainly to changes in the number of particles and hence depend markedly on solvation.¹⁹⁹ For the series of ligands studied, differences in the entropy can thus be considered in terms of the change in solvation of the free acid relative to the proximity of a highly charged metal ion. If variation in the solvation of the complex is considered negligible, ΔS for equilibrium 6.59 reflects the solvation of the mercaptocarboxylic acid. ΔS becomes more positive in the order 2-MIBA < 2-MPA < 2-MSA < MAA which is the predicted order of solvation. Since the stabilities of the complexes largely determine the overall rate of the redox reactions of the complexes, the solvating nature of the medium is thus a dominant feature of the whole reaction.

References.

1. D.N. Hague, "Fast Reactions", Wiley-Interscience, London, 1971.
2. C.H. Langford, in S. Petrucci, Ed., "Ionic Interactions", Vol.2, Academic Press, New York, 1971, p.1.
3. S. Glasstone, K.S. Laidler and H. Eyring, "The Theory of Rate Processes", McGraw-Hill, New York, 1941.
4. C.H. Langford and H.B. Gray, "Ligand Substitution Processes", Benjamin, New York, 1965.
5. A. McAuley, Coord. Chem. Rev., 1970, 5, 245.
6. E. Chaffee and J.O. Edwards, in J.O. Edwards, "Inorganic Reaction Mechanisms", Wiley-Interscience, New York, 1969, p.205.
7. F. Basolo and R.G. Pearson, "Mechanisms of Inorganic Reactions," 2nd Edition, J. Wiley and Sons, New York, 1967, Ch.3.
8. Ibid., Ch.6.
9. J.P. Hunt, "Metal Ions in Aqueous Solution", Benjamin, New York, 1963.
10. R.A. Horne, Survey of Progress in Chemistry, 1968, 4, 1.
11. J.O. Edwards, F. Monacelli and G. Ortaggi, Inorg. Chim. Acta., 1974, 11, 47.
12. A. McAuley and J. Hill, Quart. Rev., 1969, 23, 18.
13. T.W. Swaddle, Coord. Chem. Rev., 1974, 14, 217.
14. J.O. Edwards, "Inorganic Reaction Mechanisms", Benjamin, New York, 1965, Ch.4-6.
15. R.G. Wilkins, "The Study of Kinetics and Mechanism of Reactions of Transition Metal Complexes", Allyn and Bacon, Boston, 1974, Ch. 4.
16. M. Eigen, in S. Kirschner, "Advances in the Chemistry of the Coordination Compounds", MacMillan, New York, 1961, p.371.
17. P. Debye, Trans. Electrochem. Soc., 1942, 82, 265.
18. D.C. McCain and R.J. Myers, J. Phys.Chem., 1968, 72, 4115.
19. H.B. Gray and R.J. Olcott, Inorg. Chem., 1962, 1, 481.
20. F. Basolo, J. Chatt, H.B. Gray, R.G. Pearson and B.L. Shaw, J. Chem. Soc., 1961, 2207.
21. R.G. Pearson and D.A. Sweigart, Inorg. Chem., 1970, 19, 1167.
22. A. Peloso, Coord. Chem. Rev., 1973, 10, 123.
23. R.G. Pearson, C.R. Boston and F. Basolo, J. Amer. Chem. Soc. 1953, 75, 3089.
24. C.H. Langford, Inorg. Chem., 1965, 4, 265.
25. T.W. Swaddle and G. Guastalla, Inorg. Chem., 1968, 7, 1915.
26. M. Eigen and R.G. Wilkins, Advances in Chemistry, 40, 1965, 55.

27. N.V. Duffy and J.E. Earley, J. Amer. Chem. Soc., 1967, 89, 272.
28. M.B.H. Campbell, M.R. Wendt and C.B. Monk, J. Chem. Soc. Dalton, 1972, 1714.
29. D.W. Watts, Rec. Chem. Progr., 1968, 29, 131.
30. R.N. Fuoss, J. Amer. Chem. Soc., 1958, 80, 5059.
31. D.B. Rorabacher, Inorg. Chem., 1966, 5, 1891.
32. K. Kustin and J. Swinehart, in ref. 6, 107.
33. M.T. Beck, Coord. Chem. Rev., 1968, 3, 91.
34. M.G. Evans and G.H. Nancollas, Trans. Farad. Soc., 1953, 49, 363.
35. R.D. Archer, Coord. Chem. Rev., 1969, 4, 243.
36. A. Haim, Inorg. Chem., 1970, 9, 426.
37. F.A. Cotton and G. Wilkinson, "Advanced Inorganic Chemistry", 3rd Edition, Wiley Interscience, New York, 1972, Ch.25.
38. V.S. Sharma and D.L. Leussing, Inorg. Chem., 1972, 11, 138.
39. H. Diebler, Proc. XVth I.C.C.C., Dublin, 1974, S.13.
40. T.S. Roche and R.G. Wilkins, J. Amer. Chem. Soc., 1974, 96, 5082.
41. M. Eigen., Ber. Bunsenges. Phys. Chem., 1963, 67, 753.
42. D.B. Rorabacher and D.W. Margerum, Inorg. Chem., 1964, 3, 382.
43. R.G. Pearson and R.D. Lanier, J. Amer. Chem. Soc., 1964, 86, 765.
44. D. Seewald and N. Sutin, Inorg. Chem., 1963, 2, 643.
45. Y. Sasaki and A.G. Sykes, J. Chem. Soc. Dalton, 1975, 1048.
46. R.C. Patel and H. Diebler, Ber. Bunsenges, Phys. Chem., 1972, 76, 1035.
47. S.B. Tong and T.W. Swaddle, Inorg. Chem., 1974, 13, 1538.
48. J.H. Espenson, Inorg. Chem., 1969, 8, 1554.
49. T.W. Swaddle, Inorg. Chem., 1971, 10, 1566.
50. G.A. Nelson and R.G. Wilkins, J. Chem. Soc., 1962, 4208.
51. K. Kustin and R.F. Pasternack, J. Amer. Chem. Soc., 1968, 90, 2085.
52. J.P. Jones and D.W. Margerum, J. Amer. Chem. Soc., 1970, 92, 470.
53. S.C. Chan and G.M. Harris, Inorg. Chem., 1971, 10, 1317.
54. D.H. Huchital and H. Taube, Inorg. Chem., 1965, 4, 1660.
55. M. Anbar, in ref. 26, p.126.
56. J. Halpern, Quart. Rev., 1961, 15, 207.
57. H. Taube, J. Amer. Chem. Soc., 1953, 75, 4118, *ibid.*, 1954, 76, 2103.
58. R.A. Marcus, J. Chem. Phys., 1965, 44, 679.
59. R.A. Marcus, Dis. Farad. Soc., 1960, 29, 21.
60. A.G. Sykes in H.J. Emeleus and A.G. Sharpe (Eds.), Advances in Inorganic Chemistry and Radiochemistry, 1967, 10, 153.

61. A. Brown and W.C.E. Higginson, *J. Chem. Soc. Dalton*, 1972, 166.
62. J. Halpern, *J. Chem. Ed.*, 1969, 45, 372.
63. A. McAuley in *Specialist Periodic Reports*, Vol. 1, J. Burgess Ed. Chem. Soc. London, 1971, p.3.
64. J.P. Birk, *J. Chem. Ed.*, 1970, 47, 805.
65. G. Davies and K.O. Watkins, *Inorg. Chem.*, 1970, 9, 2735.
66. S. Benson, *J. Chem. Phys.*, 1952, 20, 1605.
67. C. Capellor and B.H.J. Bielsky, *Kinetic Systems*, Wiley-Interscience, New York, 1972.
68. K.J. Laidler, *Canad. J. Chem.* 1955, 33, 1614.
69. P.A. Adams and J.G. Sheppard, *J. Chem. Soc. Faraday 1*, 1974, 70, 30.
70. K. Ohkubo, H. Sakamoto and K. Tsuchihashi, *Bull Chem. Soc. Jap.*, 1974, 47, 2141.
71. J.E. Earley in Ref. 6, 243.
72. H. Taube, "Electron Transfer Reactions of Complex Ions in Solution", Academic Press, New York, 1970.
73. G.S. Hammond, *J. Amer. Chem. Soc.*, 1955, 77, 334.
74. J. Veprek-Siska, D.M. Wagnerova and K. Eckschlager, *Coll. Czech. Chem. Comm.*, 1966, 31, 1248.
75. A. Brown and W.C.E. Higginson, *Chem. Comm.*, 1967, 725.
76. W.C.E. Higginson and J.W. Marshall, *J. Chem. Soc.*, 1957, 447.
77. Prof. W.C.E. Higginson, personal communication.
78. J.W. Purdie, H.A. Gillis and N.V. Klassen, *Canad. J. Chem.*, 1973, 51, 3132. M.Z. Hoffman and E. Hayon, *J. Phys. Chem.*, 1973, 77, 990.
79. W.C.E. Higginson, D.R. Rosseinsky, J.B. Stead and A.G. Sykes, *Discus. Farad. Soc.*, 1960, 29, 49.
80. F. Hasan and J. Rocek, *J. Amer. Chem. Soc.*, 1972, 94, 3181.
81. Refs. 56, 60.
82. Ref. 63, vol. 2, 1972.
83. Ref. 63, vol. 3, 1974.
84. G. Davies and B. Warnqvist, *Coord. Chem Rev.*, 1970, 5, 349.
85. G. Davies, *Ibid.*, 1969, 4, 199.
86. G. Davies and K. Kustin, *Trans. Farad. Soc.*, 1969, 65, 1630.
87. G. Davies and K.O. Watkins, *J. Phys. Chem.*, 1970, 74, 3388
88. A. Olatunji and A. McAuley, *J. Chem. Soc., Dalton*, 1975. 682.
89. L. Treindl and H. Dubravorova, *Coll. Czech. Chem. Comm.*, 1971 36, 2022.
90. G. Davies and K. Kustin, *Inorg. Chem.*, 1969, 8, 1197.

91. Weissberger, Ed., *Technique of Organic Chemistry*, Vol. VIII, part II, 2nd. Ed. Wiley-Interscience, New York, 1963.
92. Weissberger, Ed., *Ibid.*, Vol. VI, part II, 3rd. Ed., Wiley-Interscience, New York, 1974.
93. E.F. Caldin, "Fast Reactions in Solution", Blackwell Oxford 1964.
94. Discussions of the Faraday Society, 1954, 17.
95. Chance et al., ed., "Rapid Mixing and Sampling Techniques in Biochemistry", Academic Press, New York, 1964.
96. M.H. Davies, J.R. Keefe and B.H. Robinson, *Ann. Rep. A.* 1973, 70, 123.
97. M. Eigen and L. de Maeyer in Ref. 91, p.895.
98. H. Hartridge and F.J.W. Roughton, *Proc. Roy. Soc., London*, 1923, A104, 376.
99. K. Dalziel, *Biochem. J.* 1953, 55, 79.
100. B. Chance, *J. Franklin Inst.* 1940, 229, 455, 613, 737.
101. B. Chance, *Rev. Sci. Instr.*, 1951, 22, 619.
102. F.J.W. Roughton, *Proc. Roy. Soc.*, 1934, 115B, 473.
103. Q.H. Gibson, *J. Physiol.*, 1952, 117, 491.
104. Q.H. Gibson, ref. 94, p.137.
105. J.F. Below, R.E. Connick, C.P. Coppel, *J. Amer. Chem. Soc.*, 1958, 80, 2961.
106. R.E. Connick, C.P. Coppel, *Ibid.*, 1959, 81, 6389.
107. R.L. Berger and R.L. Bowman in ref. 95, p.57.
108. K.G. Denbigh and F.M. Page in ref. 94, p.145.
109. F.M. Page, *Trans. Farad. Soc.* 1953, 49, 1033.
110. J. Hill and A. McAuley, *J. Chem. Soc. A*, 1968, 156.
111. A. McAuley and R. Shanker, *J. Chem. Soc. Dalton*, 1973, 2321.
112. J.M. Sturtevant in ref. 95,
113. G. Dulz and N. Sutin, *Inorg. Chem.*, 1963, 2, 917.
114. D. Dubois, *J. Biol. Chem.* 1941, 137, 123.
115. B. Chance in ref. 95, 39.
116. B. Chance in ref. 92, 26.
117. F.J.W. Roughton in ref. 91, 716.
118. A.I. Vogel, "Quantitative Inorganic Analysis", 3rd Edition Longmans, London 1961, p.238.
119. Ref. 118, p.287.
120. Ref. 118, p.309.
121. Ref. 118, p.349, 358.

122. S.B. Sant and B.R. Sant, *Anal. Chem.*, 1959, 31, 1879.
123. D.L. Leussing and I.M. Kolthoff, *J. Electrochem. Soc.*, 1953., 100, 334.
124. Ref. 118, p.243.
125. G.L. Eichhorn, Ed., "Inorganic Biochemistry", Elsevier, New York, 1973.
126. S.A. Cotton, *Coord. Chem. Rev.* 1972, 8, 185.
127. W.M. Latimer, "The Oxidation States of the Elements and their Potentials in Solution," 2nd Ed., Prentice-Hall, New Jersey, 1952.
128. G. Charlot, *Selected Constants* 8, Pergamon Press, London, 1958.
129. A.E. Martell and L.G. Sillen, *Stability Constants*, The Chemical Society, London, 1964, 1971.
130. J.B. Walker and G.R. Choppin, *Advances in Chemistry*, 1967, 71, 127.
131. G.W. Brady, M.B. Robin and J. Varimbi, *Inorg. Chem.* 1964, 3, 1168.
132. M.W. Lister and D.E. Rivington, *Canad. J. Chem.*, 1955, 33, 1572.
133. R.I. Novoselov and B.V. Ptitsyn, *Zhur. Neorg. Khim.*, 1965, 10, 2282.
134. D.D. Perrin, *J. Chem. Soc.*, 1959, 1710.
135. R.M. Millburn, *J. Amer. Chem. Soc.*, 1957, 79, 537.
136. Z.L. Ernst and F.G. Herring, *Trans. Farad. Soc.*, 1965, 61, 454.
137. D.W. Carlyle and J.H. Espenson, *Inorg. Chem.*, 1967, 6, 1370
138. A. Lodzinska, *Rocz. Chem.*, 1966, 40, 1595.
139. Ref. 253.
140. Ref. 190.
141. C.F. Wells and M.A. Salam, *J. Chem. Soc.. A.*, 1968, 308.
142. T.J. Conocchioli and N. Sutin, *J. Amer. Chem. Soc.*, 1967, 89, 282.
143. W. Levason and C.A. McAuliffe, *Coord. Chem. Rev.*, 1974, 12, 151.
144. R.H. Wood, *J. Amer. Chem. Soc.*, 1958, 80, 2038.
145. W.C. Bray and M.H. Gorin, *J. Amer. Chem. Soc.*, 1942, 51, 2124.
146. A.F. Cahill and H. Taube, *Ibid.*, 1952, 74, 3212.
147. Ref. 231.
148. Ref. 233.
149. J.E. Taylor, J.F. Yan and J. Wang, *J. Amer. Chem. Soc.*, 1966, 88, 1663.
150. P. George, *J. Chem. Soc.*, 1954, 4349.

151. C.K. Jorgenson, *Acta. Chem. Scand.*, 1954, 8, 1502.
152. H.B. Gray in *Bioinorganic Chemistry, Advances in Chemistry*, 1971, 100, 365.
153. R.J. Myers, D.E. Metzler and E.H. Swift, *J. Amer. Chem. Soc.*, 1950, 72, 3767.
154. L.N. Mulay and P.W. Selwood, *J. Amer. Chem. Soc.*, 1955, 77, 2693.
155. R.N. Sylva, *Rev. Pure and Appl. Chem.*, 1972, 22, 115.
156. B.O.A. Hedstrom, *Arkiv. Kemi.*, 1953, 5, 457.
157. R. Arnek and K. Schlyter, *Acta. Chem. Scand.*, 1968, 22, 1327.
158. R.P. Bell, "The Proton in Chemistry", 2nd Ed., Chapman and Hall, London, 1973, Ch.7.
159. W.A.E. McBryde, *Canad. J. Chem.*, 1968, 64, 2384.
160. E.J. Bowen, *Quart. Rev.*, 1950, 4, 236.
161. R.J.P. Williams, *J. Chem. Soc.*, 1955, 137.
162. S. Holt and R. Dingle, *Acta. Chem Scand.*, 1968, 22, 1091.
163. R.M. Millburn, *J. Amer. Chem. Soc.*, 1955, 77, 2064, R.M. Millburn and K.E. Jabalpurwala, *Ibid.*, 1966, 88, 3224.
164. R.M. Millburn, *Ibid.*, 1967, 89, 54. A.G. Desai and R.M. Millburn, *Ibid*, 1969, 91, 1958.
165. Z.L. Ernst and F.G. Herring, *Trans. Farad. Soc.*, 1963, 59, 2838.
166. L.G. Hepler, *J. Amer. Chem. Soc.*, 1963, 85, 3089.
167. M. Deneux, R. Meilleur and R.L. Eenoit, *Canad. J. Chem.*, 1968, 46, 1383.
168. C.F. Timberlake, *J. Chem. Soc.*, 1964, 1229.
169. E. Bottari, A Liberti, M. Vicedomini, *Gazz. Chim. Ital.*, 1973, 103, 859.
170. E. Bottari, and M. Vicedomini, *Ibid.*, 1974, 104, 523.
171. A.A. Frost and R.G. Peason, "Kinetics and Mechanism", 2nd. Ed. Wiley-International, New York, 1961, p.189.
172. D. Pouli and W. McF. Smith, *Canad. J. Chem.*, 1960, 38, 567.
173. R.N. Pandey and W. McF. Smith, *Canad. J. Chem.*, 1972, 50, 194.
174. F.P. Cavasino and M. Eigen, *Ricerca. Sci.*, 1964, A, 4, 509.
175. F. Accascina, F.P. Cavasino and S. D'Alessandro, *J. Phys. Chem.*, 1967, 71, 2474.
176. F. Accascina, F.P. Cavasino and E. DiDio, *Trans. Farad. Soc.*, 1969, 65, 489.
177. F.P. Cavasino, *J. Phys. Chem.*, 1968, 72, 1378.

178. G. Saini and E. Mentasti, *Inorg. Chim. Acta.*, 1970, 4, 210.
179. F.P. Cavasino and E. Di Dio, *J. Chem. Soc. A*, 1970, 1151.
180. K. Nakamura, T. Tsuchida, A. Yamagishi and M. Fujimoto, *Bull. Chem. Soc. Jap.*, 1973, 46, 456.
181. K. Tamura, *Ibid.*, 1581.
182. S. Gouger and J. Stuehr, *Inorg. Chem.*, 1974, 13, 379.
183. J.H. Espenson and S.R. Helzer, *Ibid.*, 1969, 8, 1051.
184. F.P. Cavasino and E. Di Dio, *J. Chem. Soc. (A)*, 1971, 3176.
185. R.F. Bauer and W. McF. Smith, *Canad. J. Chem.*, 1965, 43, 2763.
186. E. Mentasti, E. Pellizzetti and G. Saini, *Gazz. Chim., Ital.*, 1974, 104, 201.
187. W.K. Ong and R.H. Prince, *J. Chem. Soc. A*, 1966, 458.
188. D.P. Fay, A.R. Nichols and N. Sutin, *Inorg. Chem.*, 1971, 10, 2096.
189. M.R. Jaffe, D.P. Fay, M. Cefola and N. Sutin, *J. Amer. Chem. Soc.*, 1971, 93, 2878.
190. D.W. Carlyle, *Inorg. Chem.*, 1971, 10, 761.
191. R.L. Scott, *Rec. Trav. Chem.*, 1956, 75, 787.
192. H.A. Benesi and J.H. Hildebrand, *J. Amer. Chem. Soc.*, 1949, 71, 2703.
193. W.B. Person, *Ibid.*, 1965, 87, 167.
194. D.A. Deranleau, *Ibid.*, 1969, 71, 4044.
195. S.D. Christian, E.H. Lane and F. Garland, *J. Phys. Chem.*, 1974, 78, 557.
196. L. Johansson, *Acta. Chem. Scand.*, 1971, 25, 3569.
197. K.J. Ellis and A. McAuley, *J. Chem. Soc. Dalton*, 1973, 1533.
198. R.G. Pearson, *J. Amer. Chem. Soc.*, 1963, 85, 3533.
199. S. Ahrland, *Coord. Chem. Rev.*, 1972, 8, 21.
200. M. Cefola, A.S. Tompa, A.V. Celiano and P.S. Gentile, *Inorg. Chem.*, 1962, 1, 290.
201. A. Agren, *Acta. Chem. Scand.*, 1955, 9, 39.
202. K.R. Brower, *J. Amer. Chem. Soc.*, 1968, 90, 5401.
203. C.H. Langford and M.L. Chung, *Ibid.*, 1968, 90, 4485.
204. D.H. Devia and D.W. Watts, *Inorg. Chim. Acta.*, 1973, 7, 691.
205. R.A. Robinson and R.H. Stokes, "Electrolyte Solutions", 2nd Ed. Butterworths, London, 1959, Chapter 15.
206. C.H. Rochester, *Prog. React. Kinet.* 1971, 6, 144.
207. J.N. Bronsted, *Z. Phys. Chem.*, 1927, 102, 169.
208. L. Johansson, *Coord. Chem. Rev.*, 1974, 12, 241.
209. Ref. 6.
210. B. Perlmutter-Hayman, *Prog. React. Kin.*, 1971, 6, 240.

211. A.D. Pethybridge and J.E. Prue in J.O. Edwards, Ed., "Inorganic Reaction Mechanisms", Wiley-Interscience, New York, 1973.
212. G. Biedermann and L.G. Sillen, Arkiv. Kemi., 1953, 5, 425.
213. H. Ohtaki and G. Biedermann, Bull. Chem. Soc. Jap., 1971, 44, 1515.
214. R.M. Rush and J.S. Johnson, J. Phys. Chem., 1968, 72, 767.
215. H.S. Harned and B.B. Owen, "The Physical Chemistry of Electrolytic Solutions", Reinhold, New York, 3rd. Ed., 1958, chapter 14.
216. D.R. Rosseinsky and R.J. Hill, J. Electroanal Chem., 1971, 30, app.7.
217. C.F. Wells and M.A. Salam, J. Chem Soc. A, 1968, 24.
218. P.J. Reilly, R.H. Wood and R.A. Robinson, J. Phys. Chem., 1971 75, 1305.
219. C.S. Patterson, S.V. Tyree and K. Knox, J. Amer. Chem. Soc., 1955, 77, 2195.
220. D.W. Carlyle and J.H. Espenson, Inorg. Chem., 1967, 6, 1370
221. W.J. Gelsema, C.L. De Ligny and A.G. Remijnse, Rec. Trav. Chim., 1970, 89, 1133.
222. W.J. Gelsema and H.A. Vink, Ibid, 1971, 90, 165.
223. R. Koren and B. Perlmutter-Haymann, Inorg. Chem., 1972, 11, 3055.
224. A.R. Olson and T.R. Simonson, J. Chem. Phys., 1949, 17, 348, 1167, 1322.
225. D. Scatchard, "Electrochemical Constants", N.B.S. Circular 524, Washington, 1953, 185.
226. P.A. Zagorets and G.P. Bulgakova, Zh. Fiz. Khim., 1965, 39, 289.
227. J.K. Rowley and N. Sutin, J. Phys. Chem., 1970, 74, 2043.
228. W.K. Ong and R.H. Prince, J. Chem. Soc. A, 1966, 458.
229. W.C.E. Higginson, D. Sutton and P. Wright, J. Chem. Soc., 1953, 1380.
230. W.C.E. Higginson and D. Dutton, Ibid, 1402.
231. W.G. Barb, J.H. Baxendale, P. George and K.R. Hargrave, Trans. Farad. Soc., 1951, 47, 591.
232. M.L. Kremer and G. Stein, Ibid., 1959, 55, 959.
233. M.L. Kremer, Ibid., 1963, 59, 2535.
234. S.B. Brown, P. Jones and A. Suggett, Ref. 6, 159.
235. H.L. Chum and M.L. de Castro, J. Amer. Chem. Soc., 1974, 96, 5278.
236. C. Walling and A. Goosen, Ibid., 1973, 95, 2987.

237. J.H. Baxendale, H.R. Hardy and L.H. Sutcliffe, *Trans. Farad. Soc.* 1951, 47, 963.
238. E. Mentasti and E. Pelizzetti, *J. Chem Soc. Dalton*, 1973, 2605.
239. E. Mentasti, E. Pelizzetti and G. Saini, *Ibid*, 2609.
240. E. Pelizzetti, E. Mentasti, E. Pramauro and G. Saini, *Ibid*, 1940.
241. G.S. Laurence and K.J. Ellis, *Ibid.*, 1972, 1667.
242. P.K. Adolf and G.A. Hamilton, *J. Amer. Chem. Soc.*, 1971, 93, 3420.
243. A.M.H.P. van der Besselaar, J. Lubach and W. Drenth, *Rec. Trav. Chem.*, 1974, 93, 108.
244. J.K. Thomas, G. Trudel and S. Bywater, *J. Phys. Chem.*, 1960, 64, 51.
245. J.W. Cahn and R.E. Powell, *J. Amer. Chem Soc.*, 1954, 76, 2568.
246. A.J. Fudge and K.W. Sykes, *J. Chem. Soc.*, 1952, 119.
247. G.S. Laurence and K.J. Ellis, *Ibid.*, Dalton, 1972, 2229.
248. G. Bengtsson, *Acta. Chem. Scand.*, 1973, 27, 1717.
249. D.G. Karraker, *J. Phys. Chem.*, 1963, 67, 871.
250. D.W. Carlyle and G.F. Zeck, *Inorg. Chem.*, 1973, 12, 2978.
251. F.M. Page, *Trans. Farad. Soc.*, 1960, 56, 398.
252. H. Schmid, *Z. Phys. Chem. (Leipzig) Abt. A*, 1930, 148, 321.
253. F.M. Page, *Trans. Farad. Soc.*, 1953, 49, 635, *Ibid*, 1954, 50, 120.
254. I. Baldea and G. Niac, *Proc. IXth. I.C.C.C. St. Moritz, Switzerland*, 1966, 272.
255. V.J. Holluta and A. Martini, *Z. Anorg. Chem.*, 1924, 140, 206.
256. R.H. Betts and F.S. Dainton, *J. Amer. Chem. Soc.*, 1953, 75, 5721.
257. H.N. Po, W-K. Wong, K.D. Chen., *J. Inorg. Chem.*, 1974, 36, 3872.
258. R. Andreasch, *Ber.*, 1879, 12, 1391.
259. E. Baumann, *Zeits fur Physiol. Chem.*, 1883, VIII, 304.
260. K. Loven, *J. Prakt. Chem.*, (2), 1884, XXIX, 336.
261. R. Andreasch, *Nonatsh. fur. Chem.*, 1885, VI, 835.
262. L.J. Harris, *Biochem. J.*, 1922, 16, 739.
263. A.P. Mathews and S. Walker, *J. Biol. Chem.*, 1909, 6, 299.
264. O. Warburg and S. Sakuma, *Pfluger's Arch. ges. Physiol.*, 1923, 200, 203.
265. D.C. Harrison, *Biochem, J.* 1924, 18, 1009.
266. R.K. Cannan and G.M. Richardson, *Biochem. J.*, 1929, 23, 1248.
267. L. Michaelis and E.S.G. Barron, *J. Biol. Chem.*, 1929, 83, 191.
L. Michaelis, *Ibid.*, 1929, 84, 777.
268. M.P. Schubert, *J. Amer, Chem. Soc.*, 1931, 53, 3851.
269. M.P. Schubert, *Ibid.*, 1932, 54, 4077.
270. A.E. Martell and M. Calvin, "Chemistry of the Metal Chelate Compounds", Prentice-Hall, New York, 1952.

271. E.G. Gerwe, J. Biol. Chem., 1931, 92, 399.
272. H. Borsook, E.L. Ellis and H.M. Huffman, J. Biol. Chem., 1934, 106, 667.
273. I.M. Kolthoff, W.S. Stricks and N. Tanaka, J. Amer. Chem. Soc., 1955, 77, 4739.
274. W.M. Clark, "Oxidation-Reduction Potentials of Organic Systems," Bailliere, Tindall and Cox, London, 1960.
275. D.L. Leussing and J. M. Kolthoff, J. Amer. Chem. Soc., 1953, 75, 3904.
276. N. Tanaka, I.M. Kolthoff and W. Stricks, 1955, 77, 1996.
277. D.L. Leussing and L. Newman, Ibid., 1956, 78, 552.
278. D.L. Leussing, J.P. Mislán and R.J. Goll, J. Phys. Chem., 1960, 64, 1070.
279. H. Lamfrom and S.O. Nielsen, J. Amer. Chem. Soc., 1957, 79, 1966.
280. D.L. Leussing and T.N. Tischer, Advances in Chemistry, 37, 1963, 216.
281. C. Michon-Saucet and J-C. Merlin, Bull. Soc. Chim. France, 1965, 1905.
282. F.M. Page, Trans. Farad. Soc., 1955, 51, 919.
283. A.D. Gilmour and A. McAuley, J. Chem. Soc. A, 1970, 1006.
284. A. Tomita, H. Hirai and S. Makishima, Inorg. Chem., 1967, 6, 1746.
285. S. Jeannin, Y. Jeannin and G. Lavigne, J. Organomet. Chem., 1972, 40, 187.
286. K.S. Murray and P.J. Newman, Aust. J. Chem., 1975, 28, 773.
287. L. Guczi and D. Gal, Z. Physik. Chem., 1959, 212, 235.
288. A. Tomita, H. Hirai and S. Makishima, Inorg. Chem., 1968, 7, 760.
289. C.M. Bell, E.D. McKenzie and J. Orton, Inorg. Chem. Acta., 1971, 5, 109.
290. L.G. Stadtherr and R.B. Martin, Inorg. Chem., 1972, 11, 92.
291. F.M. Page, Spectrochim. Acta, 1957, 11, 549.
292. P. Job, Ann. Chim., 1928, 9, 113, 1936, 6, 97.
293. K.J. Ellis and A. McAuley, J. Inorg. Nucl. Chem., 1975, 37, 567.
294. E. Cotte, H. Diaz, A. Miralles and E.L. Bertha, Acta. Cient. Venez., 1971, 22, 93.
295. R.H. Lane and L.E. Bennett, J. Amer. Chem. Soc., 1970, 92, 1089.
296. P.S. Braterman and R.J. Cross, Chem. Soc. Rev. 1973, 2, 271.
297. J.J. Bohning and K. Weiss, J. Amer. Chem. Soc., 1960, 82, 4724.
298. E.J. Meehan, I.M. Kolthoff and H. Kakiuchi, J. Phys. Chem., 1962, 66, 1238.

299. R.C. Kapoor, O.P. Kachhwalā and B.P. Sinha, *Ibid*, 1969, 73, 1627.
300. G. Gorin and W.E. Godwin, *J. Catalysis*, 1966, 5, 279.
301. G.J. Bridgart, M.W. Fuller and I.R. Wilson, *J. Chem. Soc., Dalton*, 1973, 1274.
302. G. Blauer and B. Zvilichovsky, *Biochim et Biophys. Acta.*, 1965, 110, 215.
303. J.P. McCann and A. McAuley, *J. Chem. Soc. Dalton*, 1975, 783.
304. W.F. Pickering and A. McAuley, *Ibid*, A, 1968, 1173.
305. J. Hill and A. McAuley, *Ibid*, 1968, 2405.
306. D.K. Levallee, J.C. Sullivan and E. Deutsch, *Inorg. Chem.*, 1973, 12, 1440.
307. C.J. Weschler, J.C. Sullivan and E. Deutsch, *Ibid*, 1974, 13, 2360.
308. C.J. Weschler, J.C. Sullivan and E. Deutsch, *J. Amer. Chem. Soc.*, 1973, 95, 2720.
309. P. Hemmerich in J. Peisach, P. Aisen and W.E. Blumberge, "The Biochemistry of Copper", Academic Press, London, 1966, 15.
310. T. Ottersen, L.G. Warner and K. Seff, *Inorg. Chem.*, 1974, 13, 1904.
311. I.M. Klotz, G.H. Czerlinski and H.A. Friess, *J. Amer. Chem. Soc.* 1958, 80, 2920.
312. Y. Sugiura and H. Tanaka, *Chem. Pharm. Bull.*, 1970, 18, 368.
313. H. Sakurai, A. Yokoyama and H. Tanaka, *Ibid.*, 1970, 18, 2373.
314. H. Sakurai, A. Yokoyama and H. Tanaka, *Ibid.*, 1971, 19, 1416.
315. E.W. Wilson and R.B. Martin, *Archiv. Biochem and Biophys.*, 1971, 142, 445.
316. S.K. Srivistava, K.B. Pandeya and H.L. Nigam, *Inorg. Nucl. Chem. Letters*, 1975, 11, 196.
317. P. Hemmerich, H. Beinert and T. Vannyard, *Angew. Chem.*, 1966, 78, 449.
318. J. Hill, Phd. Thesis, University of Strathclyde, 1968
319. P. Kroneck, C. Naumann and P. Hemmerich, *Inorg. Nucl. Chem. Letters*, 1971, 7, 659.
320. B. Robert, *Bull. Ste. Chim. Biol.*, 1954, 36, 253.
321. A. Hanaki and H. Kamide, *Chem. Pharm. Bull.*, 1971, 19, 1006.
322. J.A. Thich, D. Mastropaolo, J. Potenza and H.J. Schugar, *J. Amer. Chem. Soc.*, 1974, 96, 726.
323. C. Neagley and J.K. Muster, 167th American Chem. Soc. Meeting, 1974, INOR,034.
324. J.M. Walshe in ref. 109,475.

325. Table 6.1
326. K.J. Ellis, unpublished results.
327. P. Debye and E. Huckel, Phys. Z., 1923, 24, 305.
328. W. Bottger, Z. Phys. Chem. (Leipzig), 1897, 24, 253.
329. M. Cremer, Z. Biol., 1906, 47, 562.
330. M. Dole, "The Glass Electrode", J. Wiley, New York, 1941.
331. W. Forsling, S. Hietanen and L.G. Sillen, Acta. Chem. Scand., 1952, 6, 901.
332. H.S. Harned, J. Amer. Chem. Soc., 1929, 51, 416.
333. H.S. Harned and B.B. Owen, ref. 215, chapter 15.
334. H.S. Harned and R.A. Robinson, Trans. Farad. Soc., 1940, 36, 973 and ref. 333.
335. E.L. King, "Acid Base Equilibria", Pergamon, 1965, chapter 8.
336. G. Kortum, W. Vogel and K. Androssow, "Dissociation Constants of Organic Acids in Aqueous Solution", Butterworths, London 1961, 1972.
337. R.W. Gurney, J. Chem. Phys., 1938, 6, 499, "Ionic Processes in Solution", McGraw-Hill, New York 1953, Chapter 7.
338. E.C. Baughan, J. Chem. Phys., 1939, 7, 951.
339. M. Born, Sci. Abs. 1918, 21A, 384.
340. N. Bjerrum, Z. Phys. Chem., 1923, 105, 219.
341. A. Eucken, Angew. Chemie, 1932, 45, 203.
342. J.G. Kirkwood and F.H. Westheimer, J. Chem. Phys., 1938, 6, 506.
343. J.G. Kirkwood and F.H. Westheimer, Ibid., 513.
344. L.G. Hepler and W.F. O'Hara, J. Phys. Chem. 1961, 65, 811.
J.W. Larson and L.G. Hepler, J. Org. Chem. 1968, 33, 3961.
345. M.G. Evans and M. Polanyi, Trans. Farad. Soc., 1936, 32, 1333.
346. P.D. Bolton and L.G. Hepler, Quart. Rev., 1971, 25, 525.
347. L.P. Hammett, "Physical Organic Chemistry", McGraw-Hill, New York, 1940.
348. A.G. Evans and S.D. Hamann, Trans. Farad. Soc., 1951, 47, 34.
349. A.F. Trotman-Dickenson, J. Chem. Soc., 1949, 1296.

